Investigating Adrenoceptor Regulation of the Astroglial Glycogen Reserve

Thesis submitted for the degree of Doctor of Philosophy

at the University of Leicester

By

Xianguo Jiang

Department of Molecular and Cell Biology

University of Leicester

June 2017

Abstract

There is increasing evidence that astrocytes can play crucial roles in signalling within the central nervous system. In particular, astrocytes can communicate with each other and also with neurons, the latter interaction giving rise to the concept of the "tripartite synapse". Thus, as well as astrocytes playing a homeostatic role to maintain an optimal extracellular environment within the brain, this cell-type may play roles in an array of CNS processes, including neurotransmission and synaptic activity. Astrocytes appear to be unique within the CNS in that they can store glucose in the form of glycogen. This constitutes the only energy reserve of the brain, and has been shown to play an important role not only at times of metabolic crisis, but also in supporting normal physiological brain function, including higher functions, such as learning and memory.

Primary rat cerebral cortex (and cerebellar) astrocytes have been studied to advance our understanding of how cell-surface receptors control glycogen turnover, focusing on the roles played by the key neurotransmitter, noradrenaline. Evidence is presented for the presence of multiple adrenoceptor subtypes in astrocytes, including β_1-, α_1- and α_2-adrenoceptors. β_1-adrenoceptor activation resulted in robust accumulation of adenosine 3',5'-cyclic-monophosphate (cAMP), with $\leq 5\%$ of the maximal cAMP response elicited by noradrenaline being sufficient to activate near-maximally glycogenolysis. The observed cAMP response to noradrenaline in astrocytes is the sum of stimulatory β_1-adrenoceptor-, and inhibitory α_2-adrenoceptor-mediated effects. Because of the amplification of signal observed between cAMP and glycogenolysis, the inhibitory α_2-adrenoceptor-mediated effect is only observed at the level of the glycogenolytic response over a small concentration range that may nevertheless coincide with the physiological range for noradrenaline effects on astrocytic function. Interestingly, α_2-adrenoceptor activation also appears to increase the rate of glycogen re-synthesis and to have a "glycogen-loading" effect on astrocytes, increasing resting glycogen concentrations in cells. In contrast, while noradrenaline also stimulated a robust increase in intracellular Ca^{2+} concentration ($[Ca^{2+}]_i$), no evidence was found of this α_1-adrenoceptor-mediated effect being able to contribute to the glycogenolytic response. Thus, while the sarco/endoplasmic reticular Ca^{2+}-ATPase inhibitor, thapsigargin, and membrane depolarization (by increasing $[K^+]_o$) could each evoke increases in $[Ca^{2+}]_i$ and stimulate glycogenolyis, addition of α_1-adrenoceptor-selective agonists did not. These data increase our understanding of how the neurotransmitter, noradrenaline exerts its actions in astrocytes to regulate glycogenolysis, as well as a variety of other signal transduction pathways.

Acknowledgements

Abbreviations

AA	Arachidonic acid
AC	Adenylyl cyclase
AD	Alzheimer's disease
AR	Adrenoceptor
ATP	Adenosine 5'-triphosphate
BAPTA-AM	1,2-Bis(2-aminophenoxy)ethane-N,N,N',N'-tetraacetic acid tetrakis(acetoxymethyl ester)
BBB	Blood-brain-barrier
BSA	Bovine serum albumin
βARK	The β-adrenergic receptor kinase
βARK-ct	The carboxyl-terminal peptide of βARK
$β_1AR$	$β_1$-adrenoceptor
$β_2AR$	$β_2$-adrenoceptor
cDNA	Complementary DNA
CaM	Calmodulin
cAMP	Adenosine 3',5'-cyclic monophosphate
$[Ca^{2+}]_i$	Cytosolic Ca^{2+} concentration
CBF	Cerebral blood flow
CNS	Central nervous system
CREB	cAMP response element binding
DAB	1,4-dideoxy-1,4-imino-D-arabinitol hydrochloride
DAG	Diacylglycerol
DDA	2',5'-dideoxyadenosine
DEX	Dexmedetomidine
DHPG	(*S*)-3,5-dihydroxyphenylglycine

DIV	Days *in vitro*
DMEM	Dulbecco's modified Eagle`s medium
DMSO	Dimethyl sulphoxide
DNA	Deoxyribonucleic acid
dNTP	Deoxyribonucleotide triphosphate
DTT	Dithiothreitol
EBSS	Earle's balanced salt solution
EC_{50}	Concentration giving 50% of the maximal response
EDTA	Ethylenediaminetetraacetic acid
EGF	Epidermal growth factor
ER	Endoplasmic reticulum
ERK	Extracellular signal-regulated kinase
FBS	Fetal bovine serum
FK	Forskolin
Fluo-4-AM	Fluo-4-acetoxymethylester
G1P	Glucose 1-phosphate
G6P	Glucose 6-phosphate
Gα/Gβγ	α and βγ subunits, respectively, of G proteins
GABA	γ-Aminobutyric acid
GAPDH	Glyceraldehyde 3-phosphate dehydrogenase
GDP	Guanosine 5'-diphosphate
GECIs	Genetically-encoded Ca^{2+} indicators
GEF	Guanine nucleotide exchange factor
GFAP	Glial fibrillary acidic protein
GFP	Green fluorescent protein
GLUT	Glucose transporter
GP	Glycogen phosphorylase

GPCR	G protein-coupled receptor
G protein	Guanine-nucleotide binding protein
GRK2	G protein-coupled receptor kinase 2
GS	Glycogen synthase
GTP	Guanosine 5'-triphosphate
HB-EGF	Heparin-binding EGF-like growth factor
HRP	Horseradish peroxidase
IBMX	Isobutylmethylxanthine
IC_{50}	Concentration at which 50% of maximal inhibition occurs
ICC	Immunocytochemistry
ICI118551	erythro-DL-1(7-methylin-dian-4-yloxy)-3-isopropylaminobutan-2-ol
IP3	Inositol 1,4,5-trisphosphate
ISO	Isoprenaline
KHB	Krebs-Henseleit buffer
LC	Locus coeruleus
LCC	L-type voltage-dependent calcium channel
MAPK	Mitogen-activated protein kinase
MAPKK	Mitogen-activated protein kinase kinase
MAPKKK	Mitogen-activated protein kinase kinase kinase
MCT	Monocarboxylate transporter
mGluR	Metabotropic glutamate receptor
MMP	Matrix metalloproteinase
mRNA	Messenger RNA
NA	Noradrenaline
NBC	Na^+/HCO_3^- cotransporter
NCX	Na^+/Ca^{2+} exchanger
NKA	Na^+/K^+ ATPase

NKCC	$Na^+/K^+/2Cl^-$ cotransporter
NO	Nitric oxide
PACAP	Pituitary adenylate cyclase-activating polypeptide
PBS	Phosphate-buffered saline
PCR	Polymerase chain reaction
PDBu	Phorbol-12,13-dibutyrate
PDE	Phosphodiesterase
PDGF	Platelet-derived growth factor
pEC_{50}	Negative logarithm of the concentration giving 50% of the maximal response
PhK	Phosphorylase kinase
PIP_2	Phosphatidylinositol 4,5-bisphosphate
PKA	cAMP-dependent protein kinase
PKC	Protein kinase C
PLC	Phospholipase C
PLCβ	β isoform of phospholipase C
PP1	Protein phosphatase 1
PP2	Src-family kinase inhibitor
PTX	Pertussis toxin
RTK	Receptor tyrosine kinase
sAC	Soluble adenylate cyclase
SDS	Sodium dodecyl sulphate
S.E.M.	Standard error of the mean
SOCE	Store-operated calcium entry
SERCA	Sarcoplasmic/endoplasmic reticulum Ca^{2+}-ATPase
SH2	Src-homology-2
SH3	Src-homology-3

STIM1	Stromal interacting molecule-1
TCA	Tricarboxylic acid
TEMED	N, N, N`, N -tetramethylethylendiamine
UTP	Uridine 5'-triphosphate
TG	Thapsigargin
TRP	Transient receptor potential

Contents

CHAPTER 1
Introduction

It is well known that the term neuroglia, usually named as glial cells, or simply as "glia", originated, in the 19th Century, from a Greek word meaning "glue". This non-neuronal cell-type accounts for ≥50% of total cell number in human brain (Allen and Barres, 2009b), however, little attention was paid to glial neurophysiological functions until relatively recently. Like neuronal cells, which possess distinctive anatomical characteristics, such as axons and dendrites, glial cells also have their own distinct morphological features. In the past, neuroscientists considered glial cells to play a less important role in central nervous system (CNS) compared to neurons, functioning within the 3-dimensional environment as chemical and physical insulators; for example, defining brain architecture, participating in extracellular homeostasis, supporting and protecting neurons, and generally enabling neurons to carry out their diverse functions (Kimelberg, 2007).

In recent decades, glial cells have attracted more and more scientific attention. Although glial cells do not participate directly in synaptic connectivity and electrical signalling, it has become increasingly evident that all types of glia can 'sense' functional activity in CNS and influence the transmission of information in several ways. For example, by maintaining the extracellular ionic milieu of nerve cells, glia can modulate the rate of nerve signal propagation, synaptic actions by controlling the uptake of neurotransmitters, fulfilling a scaffolding function for some aspects of neural development, and facilitating recovery following neuronal injury. With respect to these diverse functions, G protein-coupled receptors (GPCRs), expressed by glia, have been acknowledged as playing important roles, via a diverse array of intracellular signalling cascades, in responding to incoming information to help shape the glial contribution to CNS homeostasis (Agulhon et al., 2008).

Glial cells, comprising astrocytes, oligodendrocytes and microglia in the mature central nervous system (Figure 1.1), are involved in nearly every aspect of brain function, including brain development, homeostasis, information processing, neurological disease and psychiatric illness:

(i)   Astrocytes, which are restricted to the brain and spinal cord, have elaborate local processes that give these cells a star-like ('stellate') appearance. Astrocytes, the predominant glial cell-type, are considered as macroglia, together with

oligodendrocytes, and their major function is to maintain, in a variety of ways, an appropriate chemical environment for neuronal signalling (Khakh and Sofroniew, 2015).

(ii)   Oligodendrocytes, which are also restricted to the central nervous system, form the insulating myelin that ensheaths axons. Myelin has important effects on the speed of action potential conduction. This function is equivalent to that performed by Schwann cells in the peripheral nervous system. Pathological changes to oligodendrocytes can lead to a process of demyelination, which is the main cause of multiple sclerosis (Barres, 2008).

(iii)   Microglia, the smallest glial cells, are considered to play a role as resident macrophages or scavenger cells and perform an immune-policing function to remove cellular debris from sites of injury in CNS, which participate in inflammatory responses (Madry and Attwell, 2015).
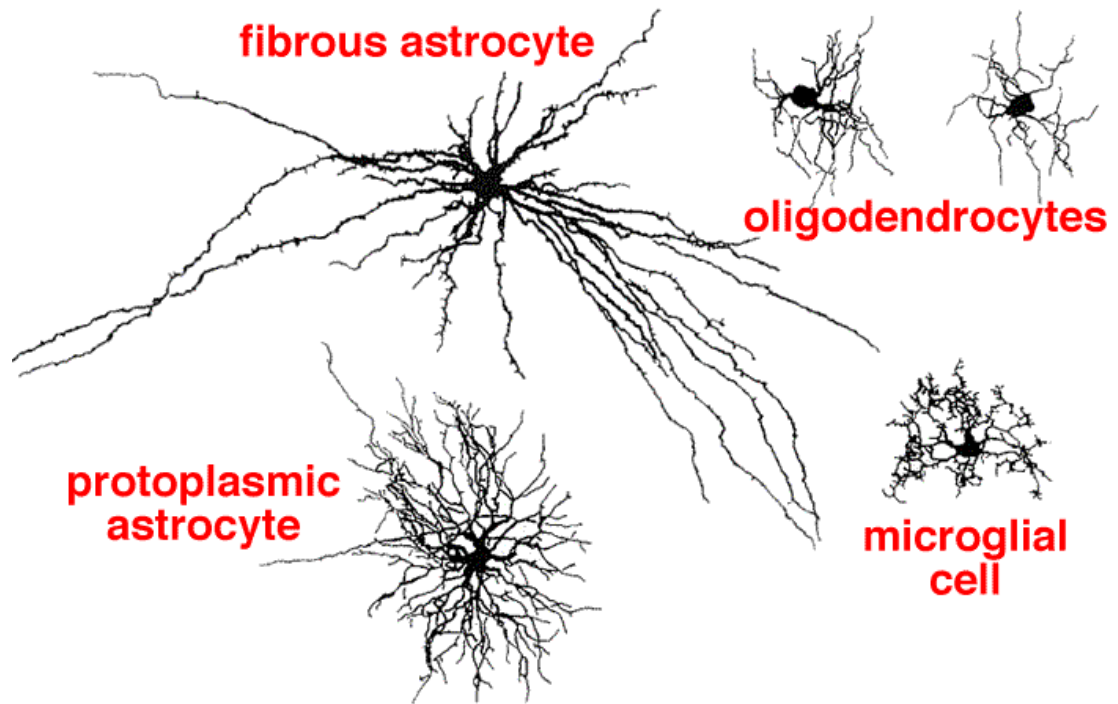
Figure 1.1 Schematic representation of three types of glial cells in the CNS. **Astrocytes** have two principal subtypes, protoplasmic astrocytes, which have more complex arbours of shorter cytoplasmic extensions; and fibrous astrocytes, which are relatively longer and have less complex branching of processes. **Oligodendrocytes**, having fewer processes than astrocytes and are relatively smaller; they wrap around neuronal axons to create an insulating barrier called the myelin sheath. **Microglia** are the smallest glia cell-type, are relatively rare in normal CNS and function as resident macrophages/phagocytes. Image taken from: http://vanat.cvm.umn.edu/neurHistAtls/pages/glia1.html.

1.1. Astrocyte Morphology

Astrocytes have been estimated to comprise approaching half of the volume of the adult mammalian brain and can be subdivided into two main groups, protoplasmic and fibrous astrocytes, on the basis of their distinct morphology and localization (Allen and Barres, 2009b, Matyash and Kettenmann, 2010, Sofroniew and Vinters, 2010b). Some other subtypes, such as Müller glia in the retina, Bergmann glia in the cerebellum, perivascular astrocytes, tanycytes and ependymal glia are also classified within the astrocyte sub-class, because of their expression of the glial cell-specific marker, glial fibrillary acidic protein(GFAP)(Emsley and Macklis, 2006, Pinto and Gotz, 2007). Protoplasmic astrocytes, the most common type of astrocyte, exhibit a complex morphology characterized by numerous and intricate processes associated with neurons and synapses, are found throughout all grey matter and are considered to play an important role through their intimate, contiguous interactions with synapses and other cell-types in the brain and spinal cord. Conversely, fibrous astrocytes, which are located predominantly within white matter, have relatively fewer organelles and display longer, less elaborate cytoplasmic projections, through which they can contact neurons at nodes of Ranvier and/or capillary walls (Sofroniew and Vinters, 2010b).

1.1.1 Astrocyte molecular markers

Intermediate filament (IF) proteins are cytoskeletal components found in most vertebrate cells, which can be regulated in the process of cell development and differentiation. There are two main IF proteins, vimentin and glial fibrillary acidic protein (GFAP), which have been found in glial cells, especially in astrocytes (Chiu et al., 1981). In the process of astrocytic development, vimentin is the major IF protein expressed in the neonatal brain or immature astrocytes, while GFAP expression progressively increases and replaces vimentin through a transition in the expression of IF genes during the period of astrocyte maturation (Middeldorp et al., 2010). It has been suggested that increased GFAP transcription during aging is an indication of reactive gliosis, a process that has been shown to be closely related to brain damage and aging (Nichols et al., 1993); for example, in response to many CNS pathologies, such as stroke, trauma, growth of a tumour or neurodegenerative disease, astrocytes become activated (so called reactive gliosis). Besides the up-regulation of GFAP by reactive astrocytes, the morphological character of astrocytes also undergoes moderate to marked changes, usually displaying hypertrophy of cellular processes, which can be

characterised by distinctive GFAP staining (Gomes et al., 1999). In this way, studies on GFAP regulation have been shown to be useful to understand not only brain physiology, but also neurological disease (Hol and Pekny, 2015, Middeldorp and Hol, 2011). Although GFAP expression has been regarded as one of most sensitive and reliable markers of astrocytes, it is important to note that many immature astrocytes, or even some mature astrocytes in healthy CNS tissue, do not express detectable levels of GFAP (Sofroniew, 2009). In addition, at the single-cell level, GFAP expression is not necessarily present throughout all the cytoplasm in astrocytes, with GFAP expression localized to the main stem astrocyte processes, rather than in the finely branching processes. As a consequence, GFAP staining cannot be used to define the true extent ('territory') of astrocytes, since it will inevitably underestimate astrocytic fine branching (Sofroniew and Vinters, 2010a, Bushong et al., 2002).

1.2. Pathophysiology of Astrocytes

It is increasingly appreciated that glial cells, especially astrocytes, are not merely "support" cells, but play key roles in the development and regulation of the mature CNS (Allen and Barres, 2009b) through a variety of intercellular chemical signals to communicate with each other and with neurons. Networks of astrocytes, linked via gap junctions, have been shown to function as a syncytium, by which ions and other small signalling molecules can spread from cell to cell (Giaume and Venance, 1998). Astrocytes also regulate the ionic and water content of the intercellular space to maintain a constant and optimal extracellular milieu (Simard and Nedergaard, 2004). Besides this, astrocytes also communicate by releasing trophic substrates to neurons, which may include neurotransmitters (e.g. ATP, glutamate, GABA and D-serine) that neurons use for synaptic transmission, to modulate neuronal signalling and to maintain a suitable physiological environment for neurons to function (Parpura et al., 2012, Li et al., 2013).

The ability of astrocytes to release and to respond to biogenic substances has led to the coining of the term "gliotransmission" (Gallagher and Salter, 2003). This recognition of a bidirectional communication between neurons and astrocytes at the synapse has also led to the concept of the "tripartite synapse" (Araque et al., 1999) (Figure 1.2). Moreover, astrocytes (along with pericytes) participate in the formation and maintenance of blood-brain barrier (BBB), which positions astrocytes to control nutritional support for neurons through their close association with small blood vessels via astrocytic processes called "end

feet" that surround blood vessels (Figure 1.3). The local regulation of blood-flow is also the basis for functional brain imaging using functional magnetic resonance imaging (fMRI), which has suggested dysfunctional regulation of blood flow by astrocytes as potential mechanisms contributing to migraine and stroke (DosSantos et al., 2015, Fabjan et al., 2015).
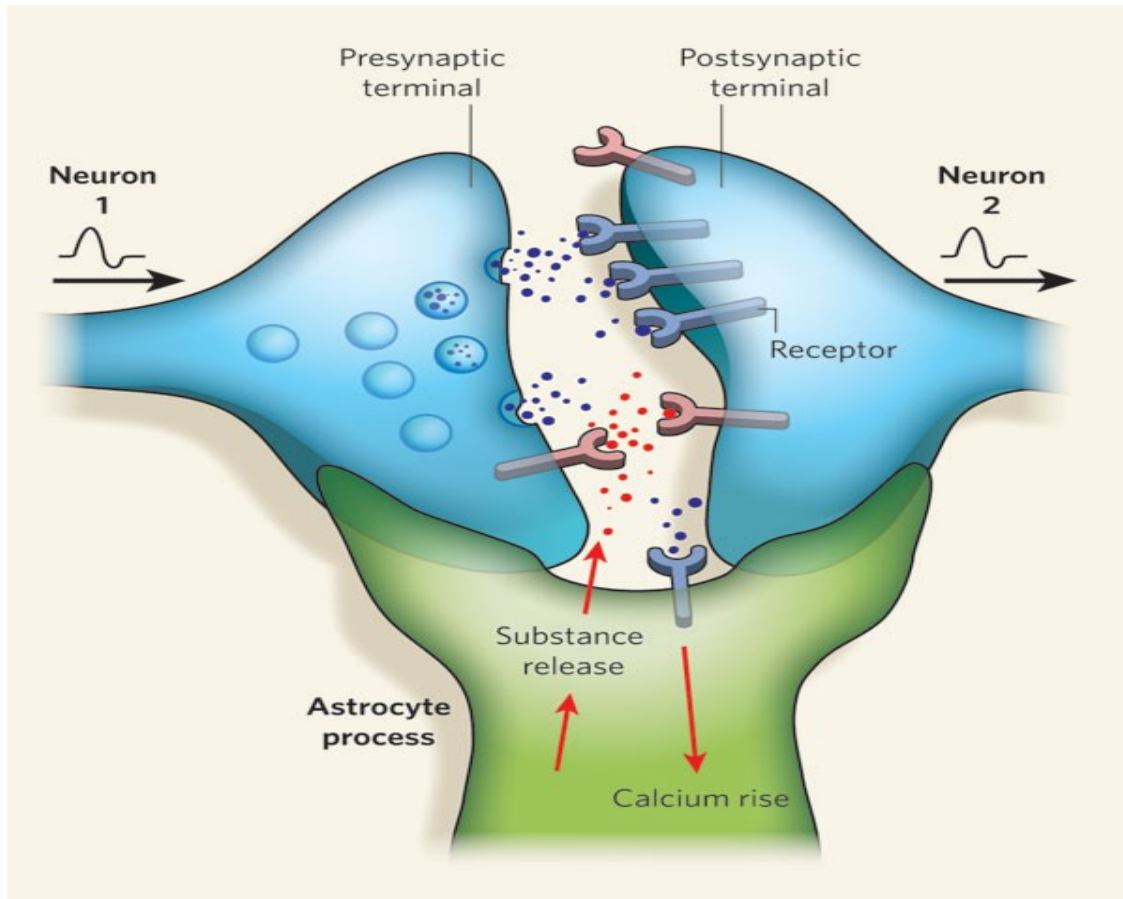
Figure 1.2 Schematic representation of a 'tripartite' synapse in the central nervous system. The diagram shows the functional integration and physical proximity of the presynaptic membrane, postsynaptic membrane, and their intimate association with a surrounding astrocytes process. The astrocyte is able to detect (and regulate through uptake) neurotransmitters and other signal molecules released from neurons at the synapse, and can also release gliotransmitters to modify neuronal excitability (e.g. through changes in intracellular Ca^{2+} concentration). Schematic taken from (Allen and Barres, 2009a).
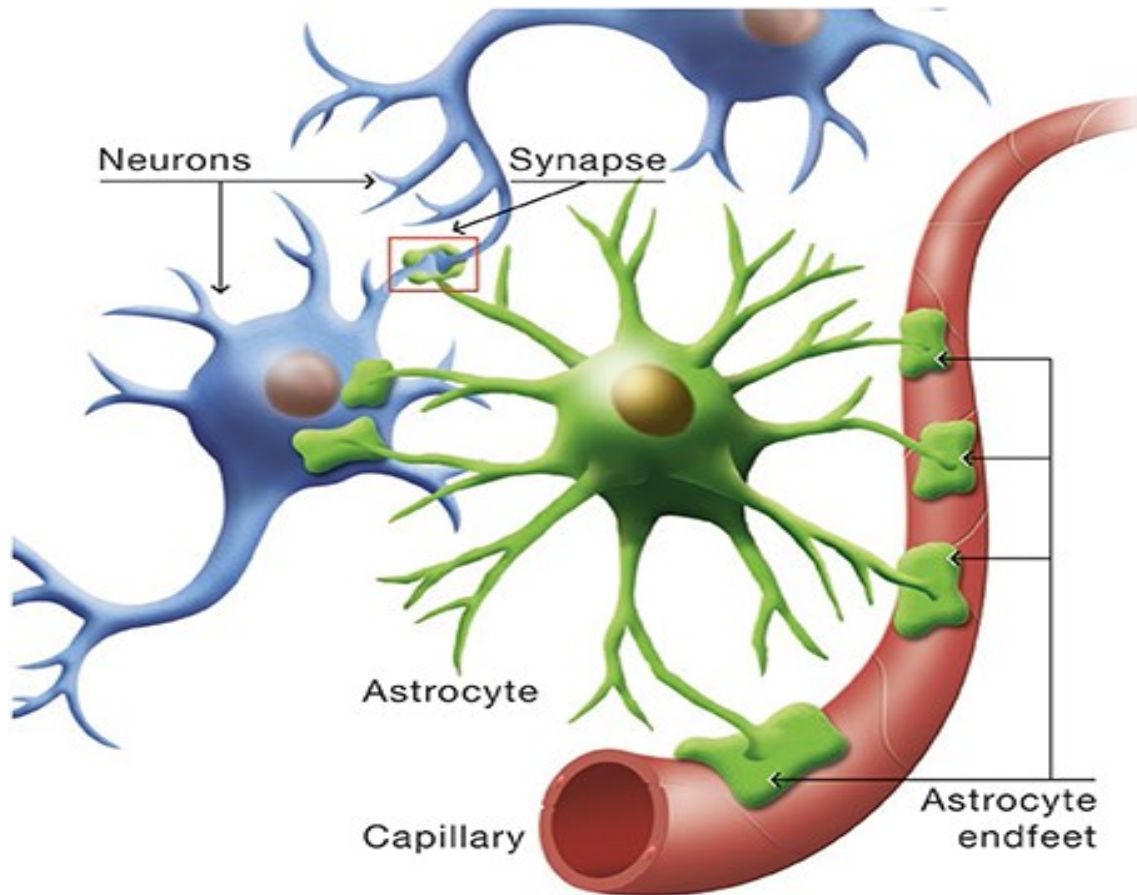
Figure 1.3   Schematic representation of the ability of an astrocyte to communicate via end-feet on blood capillaries and neurons. Astrocytes project characteristic processes called endfeet to contact blood vessels (capillaries), as well as sending projections to "talk" to neurons, or participate in the "tripartite synapse". Schematic taken from (Demetrius et al., 2015).

1.2.1. Astrocyte roles in synaptic function

In the central nervous system, astrocytes occupy non-overlapping territories, called astrocytic domains through characteristic processes (Halassa et al., 2007, Bushong et al., 2002) and molecular mechanisms of "contact inhibition" between neighbouring astrocytes (Distler et al., 1991). In the human brain it is estimated that up to 2×10^6 synapses can be contacted by a single astrocyte within grey matter, whereas this number is at least an order of magnitude lower in rodents (Verkhratsky et al., 2011, Oberheim et al., 2006). Occupying a unique position between arterioles and neurons, astrocytes have been considered to play a key role in modulating neuronal activity and synaptic transmission and plasticity via their structural character of the tripartite synapse (Araque et al., 1999), which has caused a paradigm shift in our thinking about brain function. Astrocytes actively participate in the formation of synapses through their close interaction with neuronal pre- and post-synaptic structures via peri-synaptic processes, which act as a means structurally to separate different synapses (Ventura and Harris, 1999). Based on these unique morphologic and functional characteristics, astrocytes are well-positioned to maintain synaptic transmission at a single synapse (Panatier et al., 2011) and neuronal network level (Araque et al., 2014a).

Accumulating evidence supports a crucial role for astrocytes to participate in information processing in the brain during the activation of neuronal network activity by either clearing metabolites, such as glutamate (Araque et al., 1999) from the extra-synaptic milieu, or releasing gliotransmitters in response to transmitter-mediated activation (Halassa and Haydon, 2010), and consequently to regulate synaptic transmission and neuronal excitability. In recent decades, more signalling molecules secreted by astrocytes have been identified and found to play crucial roles in regulating every stage of astrocytic formation, development and maturation (Gordon et al., 2009, Hughes et al., 2010), which has been increasingly implicated in neurodevelopmental, neuropsychiatric and neurodegenerative diseases. Due to the potential importance of astrocytic involvement in communication with neurons and synaptic plasticity, GPCRs expressed on astrocytes have been identified as playing an important role in neuronal-glial integration. Important glial GPCRs implicated in such communication include adrenoceptors and metabotropic glutamate receptors (Panatier and Robitaille, 2016).

1.2.2. Integration of bidirectional astrocyte-neuron regulation

Interest in neuron-astrocyte interactions has grown significantly over the past decades (Table 1). Astrocytes, far more than possessing merely a structurally-supportive function for neurons in central nervous system, are increasingly appreciated as multifunctional cells that play pivotal roles in a range of brain functions. In the brain, astrocytes occupy a substantial territory, accounting for nearly half of cerebral volume (Magistretti and Pellerin, 1999). In addition, the increasing recognition of characteristically non-overlapping territories of astrocytes (Bushong et al., 2002) and their important involvement in the modulation of synaptic transmission has given rise to the functional unit of the "tripartite synapse". Astrocytes are involved in the regulation of cerebral blood flow (CBF) via the pivotal role of being a 'bridge', connecting neurons and blood vessels. An example where astrocyte function is well studied is in functional hyperaemia: during a period of neuronal activation, neurons release neurotransmitters which trigger Ca^{2+}-dependent astrocytic mechanisms. As a consequence, vasoactive metabolites, such as arachidonic acid, are released from astrocytic endfeet on to blood vessels, leading to vessel dilation and functional hyperaemia (MacVicar and Newman, 2015). Therefore, astrocytes mediate neurovascular coupling, allowing the bioenergetic requirements of neurons to be met by adjustments in local blood flow.

Astrocyte syncytial functions are localized to fine distal processes where gap junctions form connexions between cells that allow free exchange of small (<1000 Da) molecules (Rose and Ransom, 1997). This astrocytic functional network enables participation in neural regulatory activities. An early recognized astrocytic function was in the regulation of water (Amiry-Moghaddam et al., 2003) and pH (Ghandour et al., 2000) homeostasis, and a capability to buffer extracellular K^+ concentration (Zhou and Kimelberg, 2000), through which increases in extracellular K^+ as a result of increased neuronal firing can be mitigated by astrocytes that redistribute the K^+ to maintain extracellular K^+ at optimal levels for continued neuronal function.

Astrocytes also play a critical role in the process of energy metabolism through the "glutamate-glutamine cycle"(Choi et al., 2012a) and the "astrocyte-neuron lactate shuttle" (Steinman et al., 2016) pathways. A number of recent studies have focused on the interactions between astrocytes and synaptic transmission, in which gliotransmission is

especially emphasized and considered to coordinate networks of neurons and synapses. It is now well-accepted that the release of gliotransmitters is a consequence of Ca^{2+} elevation in astrocytes. However, there remains controversy over the release mechanism(s), since Ca^{2+}-dependent and Ca^{2+}-independent mechanisms have both been identified and proposed (Bezzi et al., 2004, Woo et al., 2012).

Table 1   Integration of astrocyte-neuron interconnectivity in CNS

Purpose	Neuron	Astrocyte
Homeostatic		
H$_2$O and pH balance	Neuropeptides regulate water balance and osmolarity	Water channel AQP4 and ion transporters balance H$_2$O, H$^+$
K$^+$ sequestration or redistribution	K$^+$ release	K$^+$ uptake and redistribution
Neurotransmitter adjustment	Glutamate release	Glutamate uptake
Metabolic		
Glycogen and energy metabolism	Neuronal activity needs energy consumption	Glycogenolysis and energy supplier
Astrocyte–neuron lactate shuttle	Uptake and utilize lactate via MCT2	Produce and transport lactate via MCT1
Glutamate-glutamine cycle	Glutamate release and glutamine uptake	Glutamine synthesis and release
Ammonium fixation	Ammonium release	Ammonium fixation
Detoxification function	NH$_4^+$ and free radical release	NH$_4^+$ and free radical scavenging
Signalling		
Cell excitability	Voltage-dependent action potential	Electrically non-excitable
Transmitter release	Membrane potential-dependent neurotransmitter release	Gliotransmitter release via a Ca^{2+}-dependent mechanism
Propagation pathway	Depolarization potential travel along the axon	Signal molecules transmission via functional syncytium (gap junction)
Neuron-astrocyte interaction	Neurotransmitters release triggers astrocytic Ca^{2+} elevation	Gliotransmitters modulate neuronal excitability and synaptic transmission
Structural association		
Tripartite synapse	Pre- and postsynaptic elements	Processes ensheath synapses
Blood-brain barrier	Regulate local blood flow indirectly	Bridge role connecting neurons and arterioles

1.2.3. Intracellular Ca^{2+} signalling

Unlike neurons, astrocytes are not considered to be 'excitable' and do not generate action potentials, the electrochemical signals that are the basis of neural communication. Astrocytes may lack the necessary ion channels to generate voltage-dependent action potential-generating currents, however, this does not mean that astrocytes are physiologically 'silent'. The concept of "astroglial excitability" has been forwarded since the observation of "calcium waves" in cultured astrocytes derived from rodent brain (Cornell-Bell et al., 1990). This observation has led to a profound change in thinking regarding astrocytes as 'non-excitable' cells. Astrocytes express an array of GPCR subtypes linked to the mobilization of Ca^{2+} from internal (endoplasmic reticulum) stores through intracellular ion channels that respond to changes in inositol 1,4,5-trisphosphate (InsP$_3$) concentration (Verkhratsky et al., 2012a). Astrocytic $[Ca^{2+}]_i$ can also be regulated through stimulation of Ca^{2+}-permeant ionotropic receptors under circumstances of synaptic activity (Verkhratsky and Kirchhoff, 2007). Besides this, the influx of Ca^{2+} through transient receptor potential (TRP) channels has also been reported to play an important role in gliotransmission, including the release of D-serine (Shigetomi et al., 2013b).

Accumulating evidence has shown that several transmitters, including noradrenaline and glutamate, can trigger marked increases in astrocyte free cytosolic calcium concentration ($[Ca^{2+}]_i$), which can spread through characteristic astrocytic gap junction communication to propagate intercellular Ca^{2+} waves (Laskey et al., 1998). Work from a multiple of laboratories has shown that astrocytes can generate Ca^{2+} oscillations via metabotropic glutamate receptor (mGluR) group I (Bradley and Challiss, 2012, Pirttimaki et al., 2011) and A$_{2B}$ adenosine receptor (Kawamura and Kawamura, 2011) activation, which might play important roles in the physiological (and pathophysiological) regulation of astrocyte function (Volterra et al., 2014). It also has been recognised that regulated increases in $[Ca^{2+}]_i$ represent a form of astrocytic 'excitability', which can result in the release of gliotransmitters, that stimulate pre- and/or post-synaptically disposed receptors in neurons to modulate aspects of synaptic transmission (Perea et al., 2009), as well as providing signals to blood vessels to regulate local blood-flow (Pangrsic et al., 2006). Therefore, astrocytes have an intimate communication link with neurons allowing bidirectional signalling to maintain a wide range of functions under physiological and/or pathophysiological conditions (Fellin, 2009).

1.2.4. Adenosine cyclic-3',5'-monophosphate signalling

Cyclic nucleotides also play an important role in intracellular signal transduction. Adenosine cyclic-3', 5'-monophosphate (cAMP) is a ubiquitous second messenger molecule that regulates a very wide range of cellular functions. The production of cAMP results from the activation of $G\alpha_s$-coupled GPCRs to cause G protein-dependent activation of the effector protein, adenylyl cyclase. The cAMP generated can bind to the regulatory subunits of cAMP-dependent protein kinase (PKA), which is composed of two regulatory (R) and two catalytic (C) subunits (Sassone-Corsi, 2012). The binding of cAMP causes dissociation of the regulatory and catalytic subunits, thereby enabling the catalytic units to become active and to phosphorylate specific serine or threonine residues within substrate proteins (Taylor et al., 2008). PKA also can also enter the nucleus to phosphorylate substrates such as the important transcription factor, cAMP response element binding (CREB) protein, and thus regulate gene transcription (Figure 1.4).

Also integral to this signalling pathway, phosphodiesterases are key enzymes that hydrolyse cAMP to 5'-AMP, and thus can terminate signalling by this second messenger. In the CNS, it is clear that cAMP signalling occurs locally in glial cells, especially in astrocytes, to execute many functions under physiological or pathophysiological conditions (Huneycutt and Benveniste, 1995). However, much has still to be elucidated with respect to some aspects of this astrocytic signalling pathway, for instance, how cAMP and relevant regulated proteins appropriately modulate specific downstream responses, and how these alterations in signal transduction are altered in neurological disorders. Such knowledge is important, as pharmacological targeting of the cAMP transduction pathways may be a druggable route to augment or improve existing therapeutic strategies.
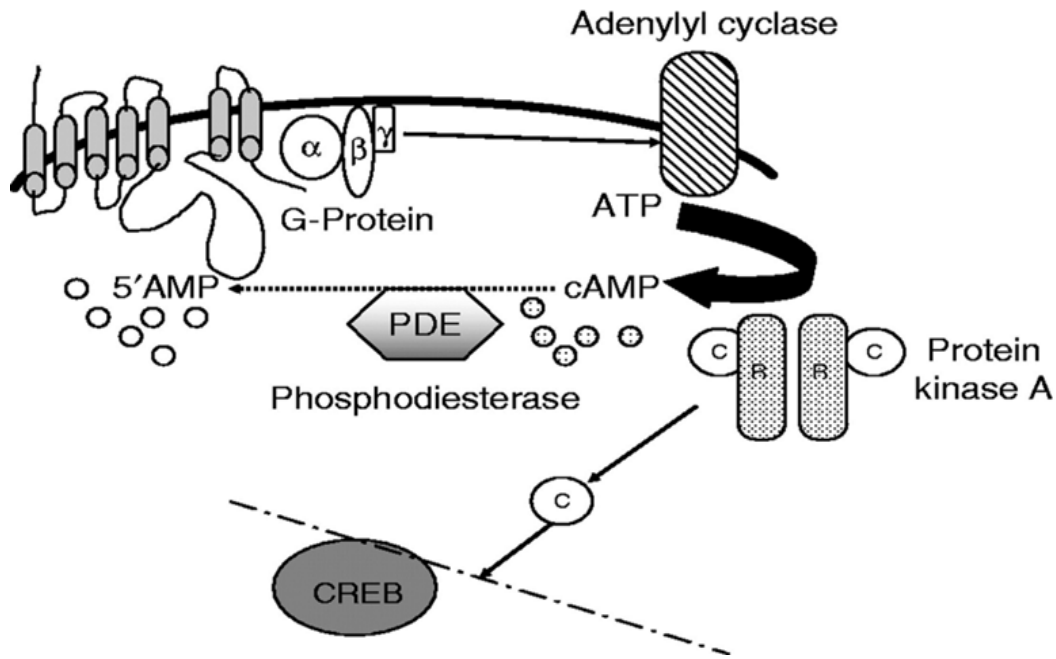
Figure 1.4. Schematic illustration of the cAMP pathway. G protein-coupled receptor activated by extracellular ligand leads to a conformational change. Gα-GTP subunit released from the heterotrimeric G protein complex binds to adenylyl cyclase, increasing its catalytic activity and the formation of cAMP from ATP. Subsequently cAMP activates PKA, which can regulate downstream effector proteins (e.g. to activate CREB). Phosphodiesterases (PDE) are enzymes responsible for the hydrolysis of cAMP to form inactive 5'-AMP and the termination of cAMP signalling. Diagram adapted from (Vezzosi and Bertherat, 2011).

1.2.5. The extracellular signal-regulated kinase (ERK) pathway

The ERK pathway, the prototypic signalling cascade of mitogen-activated protein kinase (MAPK) signalling pathways, plays multi-functional roles in regulating an array of different cellular processes, including gene transcription, metabolism, cell proliferation, synaptic plasticity and long-term memory. Like other MAPK cascades the ERK pathway involves the activation of three hierarchical kinases, Raf (MAPKKK), MEK (MAPKK) and ERK (MAPK). A variety of mammalian forms of each kinase exists, with the most studied being the *c*-Raf-MEK1/2-ERK1/2 cascade (Macdonald *et al.*, 1993). Many studies have emerged that seek to elucidate how the ERK pathway is involved in different aspects of cell physiology and development within CNS (Zsarnovszky and Belcher, 2004). ERK signalling has also been proposed to play significant roles in astrocytic function under both physiological and pathological conditions (Peng et al., 2010a, Cheng et al., 2013). Accumulating evidence has shown that ERK signalling in glial cells can be activated by different stimuli, such as growth factors, chemokines, oxidative metabolites and ischemic injury (Liu et al., 2005, Su et al., 2011, Lin et al., 2014). It has also been demonstrated that the ERK pathway can be activated by receptor tyrosine kinases (RTKs) and GPCRs (Figure 1.5).

1.2.5.1. Receptor regulation of ERK activation

Receptor tyrosine kinase (RTK) family proteins are activated by growth factors, such as epidermal growth factor (EGF) and platelet-derived growth factor (PDGF). Upon activation, receptor protomers dimerize and increase intrinsic tyrosine kinase activity to catalyse (auto)phosphorylation of specific tyrosine residues within the cytoplasmic domains of the receptor. These phosphorylated domains then act as docking sites to assemble a number of signalling scaffolds. Phospho-tyrosine residues act as binding recognition sites for protein-protein interactions with Src-homology-2 (SH2) domain-containing proteins, which may possess effector activity and/or the capacity to recruit other proteins (e.g. via Src-homology-3 (SH3) domains) to the signalling scaffold. For example, specific phosphotyrosines (e.g. Y in the PDGF receptor) recruit growth factor receptor-bound protein 2 (Grb2) and mammalian son-of-sevenless (mSoS) to the membrane and to then cause activation of the small GTP-binding protein Ras which in turn recruits the MAPKKK, c-Raf to the plasma membrane. c-Raf can then complete the MEK/ERK phosphorylation cascade by recruiting MEK1/2 and ERK1/2 (An et al., 2015).

GPCRs constitute the largest superfamily of cell-surface receptors and are involved in multiple signal transduction pathways, including ERK activation. It is now evident that the ERK pathway can be activated by an array of GPCRs that preferentially couple through a spectrum of G protein subtypes (Goldsmith and Dhanasekaran, 2007). For example, G_q-coupled GPCRs via phospholipase C can activate ERK by Ca^{2+}-dependent (e.g. Pyk2) or DAG-dependent (protein kinase C) mechanisms. A role for free Gβγ subunits in ERK activation has also been described (Saini et al., 2007, Crespo et al., 1994), with Gβγ subunits released by G_i-coupled GPCRs activating the non-receptor tyrosine kinase Src to execute a Ras-dependent Raf-MEK-ERK signalling cascade. GPCRs can also bring about G protein-*independent* ERK activation through their ability to become phosphorylated and to recruit arrestin proteins; the GPCR-arrestin complex can act as a scaffold to assemble components of the ERK pathway, such as Raf1 and ERK1/2 (Shenoy and Lefkowitz, 2003). It has been demonstrated that GPCR-bound β-arrestin may be responsible for slower, sustained ERK1/2 phosphorylation, characterized by the localization of ERK1/2 to the cytosol, rather than translocation to nucleus (Tohgo et al., 2002, Luttrell, 2003, Coffa et al., 2011).
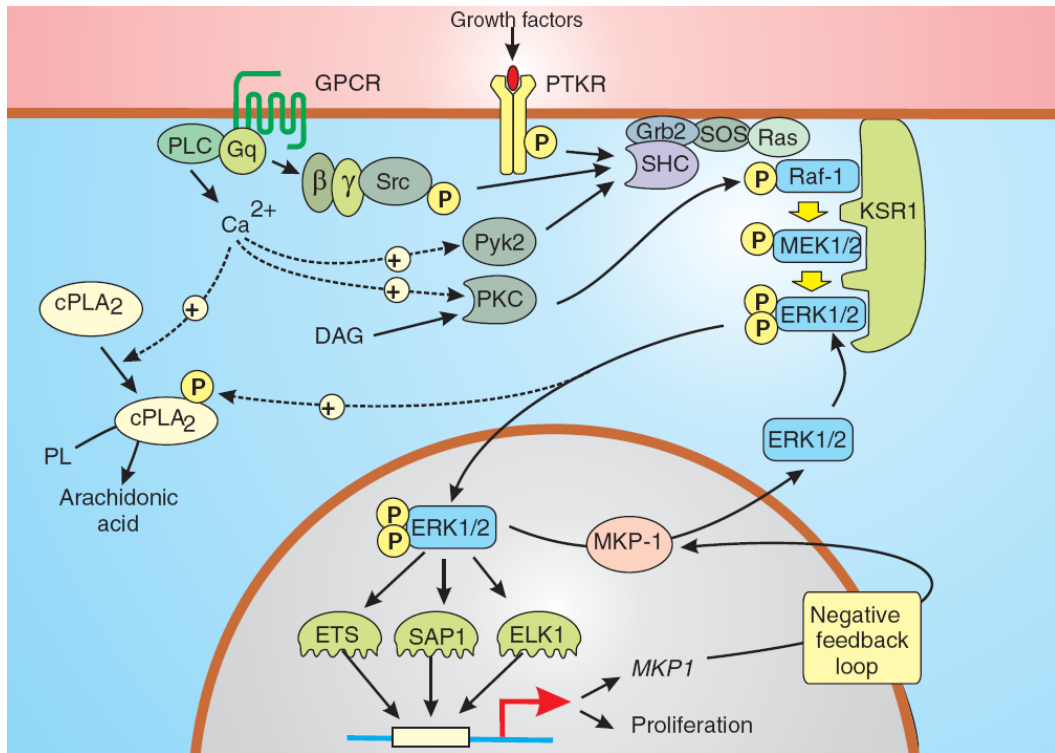
Figure 1.5 Schematic illustration of the extracellular signal-regulated kinase (ERK) pathway. The extracellular signal-regulated kinase (ERK) pathway comprises of two main signalling cascades, the prototypic RTK receptors are stimulated by growth factors and mediate signalling through recruitment of upstream scaffolds for Ras/Raf/MEK/ERK recruitment to the plasma membrane. Furthermore, ERK signal transduction pathways can also be activated in response to GPCR stimulation. Schematic taken from (Berridge, 2014).

1.3. G Protein-Coupled Receptors (GPCRs)

GPCRs are a superfamily of proteins that possess seven transmembrane domains and link to heterotrimeric G proteins to transduce cellular actions. In contrast to the large numbers of GPCRs that have been identified (>800), there are relatively few downstream effector pathways. Most cells possess a variety of GPCRs, which preferentially utilize different effectors.

Signal transduction by a GPCR begins with G protein coupling in the presence of an agonist to form the ternary (ligand-receptor-G protein) complex (De Lean et al., 1980) (Figure 1.6). In the simplest model of GPCR activation, the receptor is generally considered to exist in one of two states; the inactive "R" state and the active "R*" state. In its inactive form, the GPCR can be thought of as residing within a signalling microdomain possessing relevant heterotrimeric G proteins, each of which consists of a Gα-subunit, bound by guanosine 5'-diphosphate (GDP), and a Gβ and Gγ subunit; the latter are irreversibly associated to form a Gβγ-subunit. Upon agonist binding the now active (R*) GPCR facilitates the exchange of GDP for guanosine 5'-triphosphate (GTP), which results in Gα-GTP dissociating from the Gβγ-subunit (Ross, 2008). Following G protein activation, both Gα-GTP and/or Gβγ subunits can interact with downstream effector pathways, predominantly via increasing or decreasing second messenger concentration and/or modulating the activities of key ion channels. Such signal transduction pathways include cAMP and Ca^{2+} signalling. The duration of these signalling events is regulated by a number of factors, including (i) intrinsic Gα-GTPase activity, (ii) regulator of G protein signalling (RGS) proteins, (iii) the activity of mechanisms that oppose second messenger changes (e.g. phosphodiesterase activities; Ca^{2+} uptake/extrusion mechanisms), and (iv) Mechanisms that regulate the ability of the GPCR to be activated: this includes heterologous and homologous desensitization mechanisms that involve the phosphorylation of the GPCR leading to its uncoupling for G proteins and removal from the cell-surface.
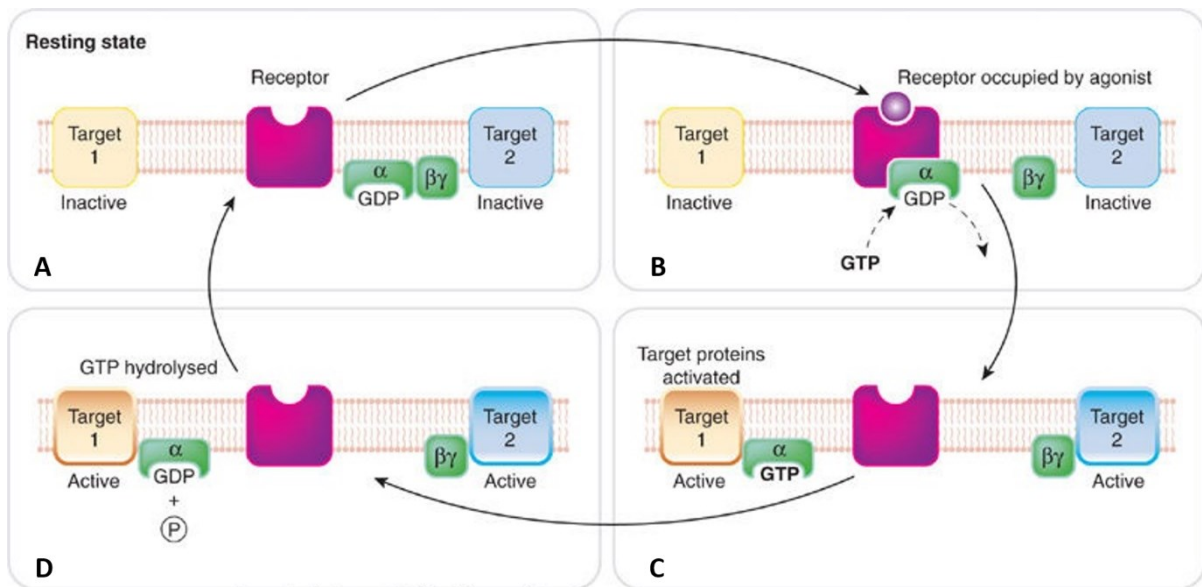
Figure 1.6 Schematic illustration of G protein-coupled receptor (GPCR)-G protein interactions. G proteins consist of Gα and Gβγ subunits, which upon activation dissociate and independently activate intracellular cascades by binding to relevant target proteins. (**A**) In the resting state, the GPCR is unliganded and the GDP-bound form of G protein is heterotrimeric and inactive. (**B**) The GPCR is activated by its cognate ligand and acts as a guanine nucleotide exchange factor (GEF) facilitating GDP-GTP exchange and dissociation if the GTP-bound Gα-subunit from the Gβγ-subunit. (**C**) Both Gα-GTP and free Gβγ-subunits can regulate effectors to initiate signal transduction through downstream effector proteins until the GTP bound to the Gα-subunit is hydrolysed (**D**). Schematic taken from (Rang, 2006).

1.4. Astroglial Adrenoceptors

Astrocytes express a variety of functionally important receptors, including GPCRs, those are activated by an array of neurotransmitters, neuromodulators, and growth factors. GPCRs can regulate cytosolic second messengers such as cAMP or Ca^{2+} to facilitate a number of astrocytic functions, including bidirectional communication with neurons and modulation of synaptic function. In recent decades, considerable attention has been paid to the expression and function of distinct adrenoceptor in astrocytes (Haydon and Carmignoto, 2006). The adrenoceptors (also known as adrenergic receptors) are a class of GPCR that are targets of the neurotransmitter/hormone molecules, noradrenaline and adrenaline. Originally adrenoceptors were pharmacologically sub-divided into two types, α and β; however, genetic approaches have revealed 9 genes encoding adrenoceptors, including 6 'α' (α_{1A}, α_{1B}, α_{1D}, α_{2A}, α_{2B}, α_{2C}) and 3 'β' (β_1, β_2, β_3) adrenoceptor subtypes (Bylund et al., 1994, Hertz et al., 2010). In the CNS, astrocytes are considered to play a critical role in regulating morphological plasticity, energy metabolism and inflammatory reactions through adrenoceptor stimulation (Heneka et al., 2002). Therefore, an understanding of the characteristics of astrocytic adrenoceptors in CNS function is an important research objective.

1.4.1. Locus coeruleus

The locus coeruleus (LC), located in the dorsal part of pons, is the predominant source of noradrenergic neurons and the principal site for the synthesis of noradrenaline in CNS. The projections of LC reach far and wide, sending ascending axonal fibres to the hypothalamus, thalamic relay nuclei, amygdala and cerebral cortex, while the LC also innervates the cerebellum, and descending axonal fibres can also project to the spinal cord (Bekar et al., 2008a).

1.4.2. β-Adrenoceptors

As stated above, β-adrenoceptors can be divided into three subtypes: β_1, β_2, and β_3. Similar to all other GPCRs, β-adrenoceptor subtypes possess seven membrane-spanning domains, three intra- and three extracellular loops, an extracellular *N*-terminal domain, and an intracellular *C*-terminal tail. β-Adrenoceptors all activate G_s family G proteins, leading to the exchange of bound GDP for GTP, to induce a dissociation of the Gα and Gβγ subunits leading

to activation of the enzyme adenylyl cyclase and increases in the concentration of the second messenger cAMP. Increases in cellular cAMP concentration lead to dissociation of catalytic from regulatory subunits of protein kinase A (PKA), with the released free catalytic subunits causing phosphorylation of key cellular substrates. Recent research using receptor subtype knockout mice, has demonstrated expression of all three types of β-adrenoceptor in astrocytes (Catus et al., 2011b).

In recent decades, more attention has been paid by β-adrenergic receptor kinase (βARK also referred to as or GRK), a serine/threonine protein kinase, which can phosphorylate β-adrenoceptors, resulting in desensitization of the receptors and/or ensuing uncoupling of the receptors from its associated G proteins (so called endocytosis) (Pitcher *et al.*, 1992), then the internalized β-adrenoceptors can be sequestered into specific organelles known as "endosomes" (Koenig and Edwardson, 1997). Depending on how receptors are trafficked through the endosomal pathway they can be recycled to the plasma membrane or degraded by lysosomes, resulting in a loss in total receptor number. Under normal circumstances it is likely that phosphorylated β-adrenoceptors are mainly dephosphorylated by protein phosphatases (e.g. protein phosphatase 2A) and recycled. In this way, many GPCRs, including adrenoceptors, will be expressed on the cell membrane in a relatively constant level under normal physiological conditions despite an ever-changing extracellular environment. Besides, G protein-coupled receptor kinase 2 (GRK2) also has been recognized as a target of Gβγ subunits by its carboxyl-terminal pleckstrin homology domain (βARK-ct) (Eichmann et al., 2003). Overexpression of βARK-ct can sequester Gβγ subunits and then inhibit the function of Gβγ by blocking its downstream signalling transduction (Koch et al., 1994b). Nevertheless, prolonged exposure to adrenoceptor agonists causes a down-regulation of receptor number and an attenuation of associated signalling events (Mills, 2002). It is well accepted that receptor down-regulation usually develops over longer time periods (hours to days) compared to agonist-induced receptor desensitization, which can occur within seconds of agonist exposure (Wallukat, 2002). Since Gβγ dimers are a ubiquitously expressed family of proteins involving almost every aspect of cellular functions, it will become more promising to develop new strategies focusing on Gβγ as a therapeutic target (Eichmann et al., 2003), especially in β-ARs related diseases to prevent and/or treat heart failure, hypertension and inflammatory disease (Han et al., 2016).

1.4.3. α-Adrenoceptors

The α-adrenoceptors consist of six distinct gene products: α_1-adrenoceptors (α_{1A}, α_{1B}, α_{1D}) and three α_2-subtypes (α_{2A}, α_{2B}, α_{2C}). Astroglia have been shown to express α_1-adrenoceptors, which belong to the G_q protein-coupled receptor superfamily, are very sensitive to noradrenaline (NA), and can mobilize intracellular Ca^{2+} (Paukert et al., 2014b) through the "G_q-PLC-PIP$_2$-IP$_3$-Ca^{2+}" pathway (Figure 1.7).
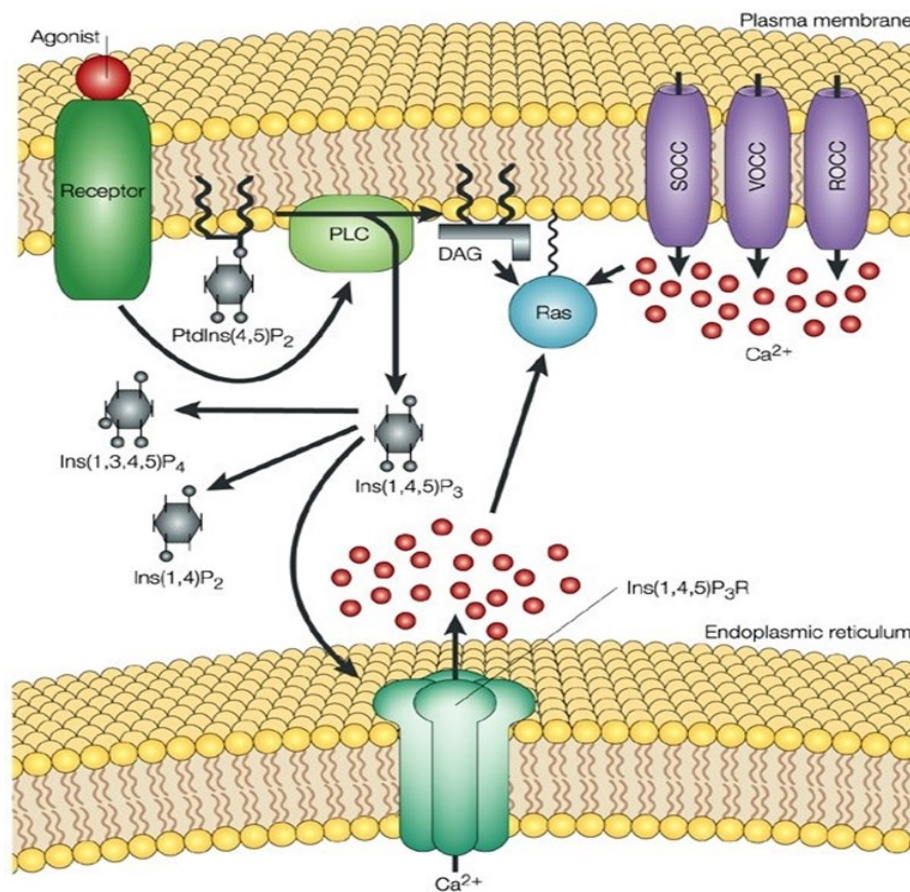
Figure 1.7 Schematic illustration of the noradrenaline-mediated intracellular Ca^{2+} signalling pathway through α_1-adrenoceptors. Once noradrenaline (NA) has bound to and activated the G_q-coupled α_1 adrenoceptor, the signal is transduced primarily by $G\alpha_q$-GTP to activate phospholipase C (PLC), which catalyses the hydrolysis of phosphatidylinositol 4,5-bisphosphate (PIP$_2$) to inositol 1,4,5-trisphosphate (IP$_3$) and diacylglycerol (DAG). The former second messenger (IP$_3$) stimulates receptor-ion channels located on endoplasmic reticulum (ER), resulting in an increase of intracellular Ca^{2+} concentration ($[Ca^{2+}]_i$), while DAG binds to and activates different isoenzymes of protein kinase C (PKC). Schematic taken from (Cullen and Lockyer, 2002).

Like β-adrenoceptors, there appear to be two different patterns relating to the desensitization in glial α_1-adrenoceptors (Akinaga et al., 2013), including fast receptor desensitization and internalization due to receptor phosphorylation by GRK2, and perhaps also PKC (Garcia-Sainz et al., 2000). Astrocytic α_1-adrenoceptors play critical roles and are important participants in Ca^{2+} signalling (Ding et al., 2013a, Araque et al., 2014a) (Pankratov and Lalo, 2015a).

The α_2-adrenoceptors preferentially couple to $G_{i/o}$ proteins. Upon G protein activation, each α_2-adrenoceptor subtype can be shown to inhibit adenylyl cyclase and to reduce the levels of cAMP. Formerly, α_2-adrenoceptors were considered primarily as neuronal presynaptic receptors that allow a negative feedback to occur regulating neurotransmitter release. Thus, α_2-adrenoceptor activation in the locus coeruleus opposes membrane depolarization and noradrenaline release. More recently studies have found that these receptors are also expressed by astrocytes (Milner et al., 1998). This is of potential medical significance as the application of α_2-adrenoceptor agonists is widely used in clinical settings, such as anaesthesiology and the control of blood pressure (Mavropoulos et al., 2014). Studies seeking to distinguish the roles of different α_2-adrenoceptor subtypes have shown that α_{2A} and α_{2C} subtypes are expressed in the CNS, while the α_{2B}-adrenoceptor subtype is expressed primarily by vascular smooth muscle (Giovannitti et al., 2015), which might allow pharmacological differentiation between central sedative and peripheral antihypertensive effects, respectively (Buerkle and Yaksh, 1998).

1.5. Energy metabolism

The brain has a great demand for energy provision, utilizing glucose almost exclusively as its basic fuel. The adult human brain makes up only around 2% of the body weight, however, it consumes approximately 25% of the total body glucose consumption under resting conditions (Mathur et al., 2014). CNS bioenergetics therefore depend on ready glucose availability from the blood circulation and via the GLUT1 glucose transporter. However, the role of astrocytic glycogen to serve as a glucose 'reservoir' is also well-recognized, with its function being long proposed to be to protect vulnerable neurons against hypoglycaemic injury and to support neuronal elements during increased firing activity, especially in some pathological conditions (Brown and Ransom, 2015b). Although the amount of glycogen

present in astrocytes is relatively limited (around 3-12 μmol glucosyl equivalents/g tissue) and will be quickly exhausted in times of energy stress (Obel et al., 2012), such as occurs in cerebrovascular ischaemia (Brown, 2004), epilepsy (Cloix et al., 2010) and migraine (Charles, 2013), it is generally accepted that astrocyte glycogen is an important emergency fuel. More recent studies have further addressed whether astrocytic glycogen has additional roles besides those of emergency energy storage, pointing towards additional physiological functions in synaptic activity and memory formation (Suzuki et al., 2011).

1.5.1. The blood-brain barrier

The blood-brain barrier (BBB), comprising of three main cellular elements; endothelial cells, capillary basement membrane embedded by pericytes, and astrocyte end-feet, plays an important role in maintaining a regulated microenvironment for functional neuronal signalling under physiological and pathological conditions in CNS (Ballabh et al., 2004). The BBB is characterised by endothelial cell tight junctions, which together with pericytes and astrocytic end-feet envelope the wall of capillary, producing a unique diffusion barrier to regulate selectively the influx (and efflux) of the majority of blood-borne substances into brain. While some molecules, such as O_2 and CO_2, can diffuse across this important interface, dependent on their relative concentration gradients, many more important metabolites, including glucose and amino acids, require specific transport mechanisms to cross the BBB. The function of astrocytes in forming and maintaining BBB is well-described (Abbott et al., 2006), in addition, astrocytic end-feet can regulate local blood vessel diameter and hence blood flow within CNS via releasing various molecular mediators, such as nitric oxide (NO) and arachidonic acid (AA) (Iadecola and Nedergaard, 2007). In the last decade, it has become well known that BBB dysfunction is closely related to a number of diseases including multiple sclerosis (Zlokovic, 2008), migraine and neuropathic pain (DosSantos et al., 2015).

1.5.2. Astrocytes and brain homeostasis

Astrocytes can release a variety of biomolecules in response to various stimuli. A number of release mechanisms have been proposed, including vesicular exocytosis, solute transporters, ion channels, and ligand-gated ion channels (Hamilton and Attwell, 2010, Pirttimaki and Parri, 2013). It is also widely accepted that astrocytes are responsible for providing substrates to neurons to facilitate the homeostasis of neuronal neurotransmitters

via direct provision of neurotransmitter precursors or metabolic substrates, for example, through the catabolism of glycogen to pyruvate/lactate and the glutamate-glutamine transport cycle (Belanger et al., 2011).

It has already been noted that astrocytes can store glucose in the form of glycogen, which is considered the largest energy reserve of the brain, and to play an important role in the processes such as learning and memory (Gibbs et al., 2006, Gold, 2016). A recent study (Muller et al., 2014) has provided evidence for a new pathway regulating astrocytic glycogenolysis that involves store-operated Ca^{2+} entry (SOCE) via a cAMP-dependent mechanism, suggesting a link between astrocytic Ca^{2+} homeostasis and glycogen metabolism to support neuronal activities, through the provision of metabolic energy substrates. In recent years, accumulating evidence has demonstrated that syncytial networks of astrocytes can transport glucose and its metabolites through gap junctions (Rouach et al., 2008), such a pathway is also regarded to be important to more efficiently provide glucose delivery and energetic metabolites from blood vessels to distal neurons. Astrocytic glycogen is catabolized to lactate, which is released and taken up by neurons where it is converted to pyruvate and mitochondrially metabolized as an oxidative substrate (Newman et al., 2011). Astrocytes also appear to possess more metabolic flexibility than do neurons as they can utilize glutamine as a metabolic substrate to maintain homeostasis (Hertz et al., 2013).

Another well-established function of astrocytes is the removal of neurotransmitters from the extracellular space, via a number of neurotransmitter transporters. Glutamate is the primary excitatory neurotransmitter in the CNS, and its activity is bi-directionally manipulated by interplay between neurons and astrocytes. Astrocytes can efficiently take-up synaptically-released glutamate through astrocytic transporters EAAT1 (GLAST) and EAAT2 (GLT1) (Chaudhry et al., 1995). Following glutamate uptake, glutamine synthetase (GS) converts glutamate into glutamine, which can be released and transported back to neurons via astrocytic release, or potentially through gap junctions (Maragakis and Rothstein, 2006). The astrocyte-derived glutamine is then converted to glutamate within neurons by glutaminase and repackaged into vesicles for release. Astrocytes are also implicated in the clearance of GABA and glycine from the synaptic cleft. Astrocytes express GABA (GAT-1 and GAT-3) and glycine transporters (Zafra et al., 1995, Wang and Bordey, 2008). Further research has also shown that extracellular GABA (in the synaptic cleft) can

be taken up by astrocytes, converted glutamine and recycled to GABAergic neurons for GABA re-synthesis (Schousboe, 2000, Bradley and Challiss, 2012).

1.5.3. Glycogen metabolism

Glycogen, existing in the form of a highly-branched glucose polymer, consists of thousands of glycosyl units connected by either α-1,4 or α-1,6 glycosidic bonds. Glucose is added to the glycogen polymer by a series of enzymes with glycogen synthase being the key regulator of glycogen synthesis. Brain glycogen is found at relatively low concentrations (3-12 μM) (Cruz and Dienel, 2002) compared to that found in skeletal muscle (300-350 μM) or liver (100-500 μM), respectively (Brown and Ransom, 2007).

It has been well known that the accumulation of glycogen is determined by the reciprocal regulation of two important processes: glycogen synthesis (glycogenesis) and glycogen breakdown (glycogenolysis). Glycogenolysis is controlled primarily by glycogen phosphorylase (GP), a key rate-limiting enzyme. GP catalyses the formation of glucose 1-phosphate which can be converted to the glycolytic intermediate glucose-6-phosphate (G6P) by phosphoglucomutase. G6P is metabolized to lactate via glycolysis and this metabolite can be transported out of astrocytes to fuel neuronal energy requirements (Brown and Ransom, 2015b). GP exists in two distinct forms: the active glycogen phosphorylase a (phosphorylated state) and inactive glycogen phosphorylase b (dephosphorylated state)(Brown, 2013). The activity of GP can be regulated allosterically by ATP (inhibitory), while high AMP concentrations activate GP. Besides these allosteric effects, GP activity is also regulated by phosphorylation. Thus, β-adrenoceptor activation by noradrenaline can trigger a G_s protein-mediated signalling cascade, causing activation of adenylyl cyclase, elevation of intracellular cAMP, and PKA activation. Activated PKA can phosphorylate and activate phosphorylase kinase, which in turn phosphorylates and activates GP (Figure 1.8).

Glycogen synthesis requires the entry, via GLUT1 transporters, of glucose which is immediately phosphorylated to G6P by hexokinase. G6P is converted to G1P by phosphoglucomutase, and then to UDP-glucose by UDP-glucose pyrophosphorylase. UDP-glucose is acted on by glycogen synthase (GS), which, like GP, exist in two forms: the active, dephosphorylated form (GS-a) and the inactive phosphorylated form (GS-b). The phosphorylation state of GS-a/GS-b is determined by PKA, protein phosphatase 1 (PP1) as

well as other regulatory enzymes (e.g. glycogen synthase kinase 3) (Obel et al., 2012). Thus, the cAMP cascade has reciprocally impact glycogen synthesis and glycogenolysis. Of important note is that the glycogenolytic process does not constitute a simple reversal of glycogen synthesis, but occurs via a distinct metabolic pathway. Besides, recent study has found that glycogenolysis and K$^+$ uptake are functionally linked (Mangia et al., 2013, DiNuzzo et al., 2013a), the precise mechanism of this latter regulation has still to be fully understood.
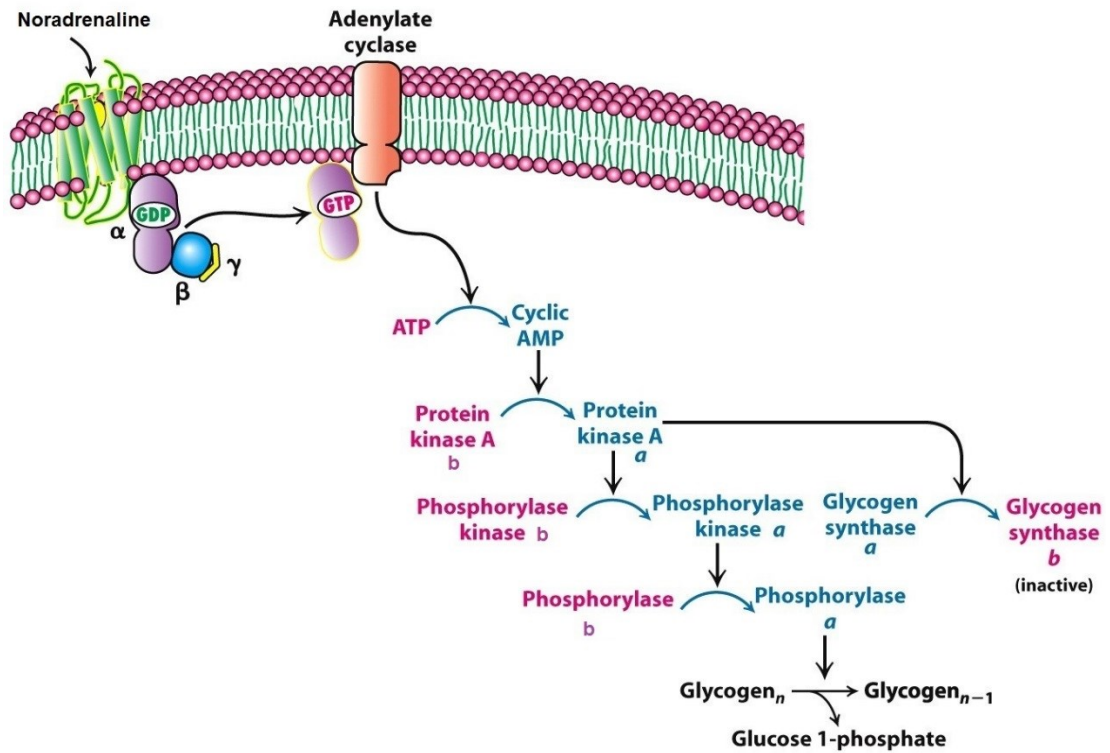
Figure 1.8 Schematic illustration of receptor-mediated glycogenolysis. Upon activation of a G_s-coupled GPCR by a ligand, such as noradrenaline, adenylyl cyclase is activated and converts ATP to cAMP. Increased cAMP concentration facilitates the activation of PKA, which acts to facilitate the transition of phosphorylase kinase-b to active phosphorylase kinase-a, which then converts glycogen phosphorylase-b to active glycogen phosphorylase-a. Active glycogen synthase-a can also be deactivated through phosphorylation by protein kinase A (as well as additional mechanisms) to inactive glycogen synthase-b. Diagram adapted from: (Berg et al., 2002)

1.5.4. Glucose metabolism

As described above, glucose is transported into brain by glucose transporters at the blood brain barrier (BBB). In the human genome, glucose transporters are encoded by 14 different GLUT genes (GLUT1-14), which are expressed in a tissue-specific manner. For example, liver and pancreatic β-cells have a distinct glucose transporter 2 (GLUT2), muscle and fat cells express insulin-regulated GLUT4, while in central nervous system (CNS), GLUT1 is expressed on astrocytes and endothelial cells, as well as oligodendrocytes, microglia express mainly GLUT5, while neurons predominantly express GLUT3 (Espinoza-Rojo et al., 2010). In the human brain, glucose is considered the most important energy substrate, although glutamine/glutamate, ketone bodies and lactate are viewed as alternative energy sources under some (patho)physiological conditions (van Hall et al., 2009). Glucose is transported into the CNS interstitium by a specific glucose transporter (GLUT1), and then gains entry into astrocytes by GLUT1 and/or neurons by GLUT3. Once transported into the cell glucose is instantly phosphorylated and, in neurons metabolized first to pyruvate and then fully oxidized within mitochondria; in contrast, in astrocytes the glucose might be stored as glycogen, metabolized to lactate or mitochondrially oxidized.

1.5.5. The astrocyte-neuron lactate shuttle

It has been two decades since the concept of the "astrocyte-neuron lactate shuttle (ANLS)" was first proposed (Pellerin and Magistretti, 1994), which fundamentally re-framed our understanding of brain energy metabolism. The ANLS model proposes that glutamatergic transmission is not only detected by neurons (through ionotropic and metabotropic glutamate receptors), but this information about local activity is also passed to astrocytes by activating astrocyte glutamate transporters, which results in the Na^+,K^+-ATPase activation, an energy-consuming process. In response to this driver, glucose is taken up by the astrocyte, and perhaps glycogenolysis too is activated leading to the production of lactate (van Hall et al., 2009), which can be transported out of astrocytes to fuel neuronal activity, in which process, monocarboxylate transporter (MCT) is essential for transmembrane movement of lactate. There exist two MCT subtypes, MCT1 expressed on astrocytes, which is associated with lactate efflux, and neuronally MCT2 that can transport this metabolite into the neuron (Tekkok et al., 2005). When lactate is taken up into neurons or axons via MCT2, it can further metabolized into pyruvate by lactate dehydrogenase (LDH)

and enters the mitochondria to be converted to acetyl CoA and then to enter the tricarboxylic acid (TCA) cycle to generate adenosine 5'-triphosphate (ATP), and thus match the increased neuronal energy demand (Figure 1.9).
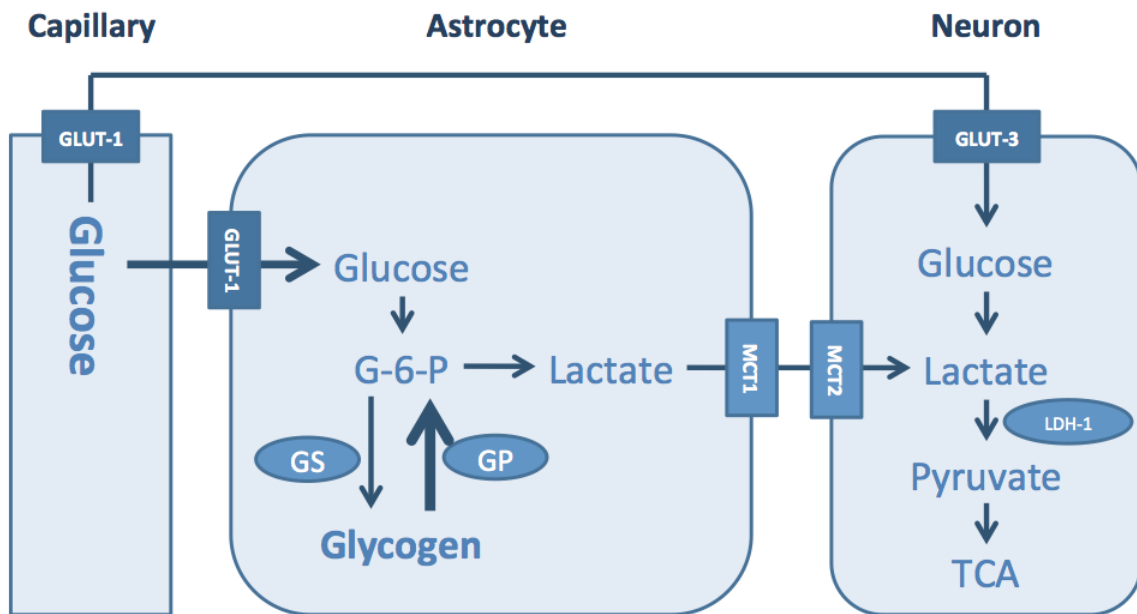
Figure 1.9 Schematic representation of astrocyte–neuron lactate shuttle pathway. Glucose enters either astrocyte or neuron through glucose transporters (GLUT1) or (GLUT3) respectively, then phosphorylated by HK to produce glucose 6-phosphate (G-6-P). G-6-P can be further metabolized into lactate through glycolysis. Lactate generated by astrocytes can be released into the extracellular space through monocarboxylate transporters (MCT1) and taken up via MCT2 expressed at the neuronal membrane. Schematic adopted from (Brown et al., 2004).

1.6. Morphological Plasticity

There are two main categories of astrocytes in the brain: protoplasmic and fibrous astrocytes (Allen and Barres, 2009a). The former exists predominantly within grey matter and play an important and active role in maintaining efficient synaptic transmission via tripartite synapses (Dityatev and Rusakov, 2011, Heller and Rusakov, 2015). However, astrocytic morphology is not always constant, when astrocytes are isolated from the brain and maintained in culture, they exhibit a polygonal shape, they possess a remarkable morphological plasticity. Cultured primary astrocytes usually exhibit polygonal morphology, while co-culture with neurons or under some specific circumstances, such as pathological stress like brain injury and up-regulated during gliosis (Eddleston and Mucke, 1993), or given some pharmacologic treatment such as noradrenaline, cultured primary cortical astrocytes will experience profound morphologic change, so called "stellation" (Rodnight and Gottfried, 2013), which is a rapid, probably reversible and concentration-dependent process (Favero and Mandell, 2007). Furthermore, changes in astrocyte morphology also occur in pathological conditions termed reactive gliosis, astrocytes become reactive in response to brain tissue damages caused by hypoxia, ischemia or seizures (Abe and Misawa, 2003). Such activity-dependent astrocytic structure changes, mainly featured as cytoplasmic retraction and cell body rounding with process formation (Tas et al., 2007), are considered to be responsible for dynamic synaptic remodeling, and subsequently leading to intimate connection with neurons. This functional role of astrocytes contributed to synaptic plasticity has been considered as a basis for learning and long-term memory formation in the brain (Kwon and Sabatini, 2011, Ota et al., 2013). It was proposed that the characteristic stellated astrocytes make abundant processes interact with neurons, potentiating synapse plasticity, to facilitate learning and memory (Zorec et al., 2015).

However, the mechanisms of astrocytic morphology plasticity are still far from understood, although in recent years, great strides have been made achieved in this field. Evidence accumulated in the past decades demonstrates that cyclic AMP (cAMP)-raising agents can induce astrocytes growing *in vitro* to adopt a morphologic change (Dong et al., 1998, Won and Oh, 2000). Recent work also shows some growth factors, such as fibroblast growth factor (FGF), can increase the number and branching of processes in developing and cultured astrocytes, facilitating the formation of stellation morphology, which resembles the maturate astrocytes *in vivo* (Kang et al., 2014, Roybon et al., 2013). Besides, the shape

change of cultured astrocytes can be modulated either in the presence or in the absence of serum in the cultured medium (Safavi-Abbasi et al., 2001). A great deal of progress has been achieved recently in identifying the mechanisms involved in the morphological plasticity in primary astrocytes. The small GTPases, RhoA and Rac1, have been most studied and shown to play pivotal roles in maintaining and regulating astrocyte phenotype (Burridge and Doughman, 2006, Oishi et al., 2012). However, the intracellular machinery of astrocytic morphological plasticity, as well as the corresponding functional consequences, still remain to be further explored. It is worth noting that astrocytes participate in the morphological remodelling contributing to synaptic plasticity and memory formation are energy-demanding process that is supposed to require mobilization of glycogen from astrocytes (Harris et al., 2012).

1.6.1. Reactive gliosis

Under a variety of conditions astrocytes can become activated ('reactive'). These conditions include a number of pathologies, such as stroke, trauma and neurodegenerative disease (Pekny and Nilsson, 2005, Pekny and Pekna, 2014). Reactive gliosis involves the proliferation and hypertrophy of a number of different glial cell-types (Burda and Sofroniew, 2014). The activation of astrocytes ('reactive astrogliosis') results in an array of proteins being up-regulated, including the intermediate filament protein, GFAP (Bushong et al., 2002), and characteristic changes in cell morphology (Sun and Jakobs, 2012).

Reactive astrogliosis is considered to be a defensive mechanism that counters an acute or chronic pathological stressor to limit any structural damage and restore CNS homeostasis (Pekny and Pekna, 2014). Gliosis involves a de-differentiation of the mature phenotype, at least in a sub-population of astrocytes, and the signalling mechanisms involved in this pleiotropic response are beginning to be elucidated (Robel et al., 2011). It is likely that different types of reactive astrogliosis can occur, with transcriptional activation patterns being tailored to the provoking stressor (Zamanian et al., 2012).

1.7. Thesis Aims and Objectives

As discussed, the traditional view that astrocytes play only a passive, supporting role in the CNS has changed following the profound evidence supporting the existence of a bi-directional communication between astrocytes and neurons and tripartite synapses in which astrocytes play a pivotal role to maintain and regulate the synaptic plasticity, as well as

effectively support brain energy metabolism by motivating. However, energy metabolism in the brain is a relatively complex process that is still incompletely understood. Although glucose is regarded as the main energy support in central nervous system and provides the fuel for physiological brain function through the generation of ATP. Therefore, glucose metabolism in the brain has provided comprehensively pathophysiological basis for many brain disorders such as Alzheimer's disease (AD).

It has been well accepted that astrocytes are the principal storage sites of glycogen in the CNS, and adrenergic receptors are found to be highly expressed in astrocytes, which can trigger the most important second messages including cyclic AMP and Ca^{2+} in astrocytes. Therefore, it has attracted a great interest in recent decades focusing on the relation between the activation of adrenoceptor and astrocytic energy and metabolism. My initial aim of this thesis was focused on a characterization of adrenoceptors expression and their signalling of different subtypes in rat cerebrocortical astrocytes.

Since astrocytes have been proved to play important roles in maintaining extracellular homeostasis via the uptake of extracellular K^+ and glutamate following neuronal firing via the consumption of energy storage – glycogen, which possesses versatile functions participating in synaptic and morphologic plasticity besides serving an emergency fuel to neurons under conditions of glucose deprivation or intense neural activity. In addition, due to distinct signalling change (mainly for cAMP and Ca^{2+}) initiated by specific adrenoceptor subtype, this thesis makes it possible to clarify the mechanism of glycogen metabolism in rat astrocytes which are all considered to actively participate in the process of learning and memory consolidation.

In addition, I have attempted to elucidate the precise mechanisms underlying adrenoceptor-mediated ERK phosphorylation in astrocytes. The aim of these experiments was to pinpoint the specific pathway of ERK activation, which is thought to be involved in multi-functional cellular processes, such as gene transcription, metabolism, cell proliferation, synaptic plasticity and long-term memory.

CHAPTER 2
Materials and Methods

2.1. Materials

2.1.1. General chemicals, reagents and consumables

Laboratory electrophoresis and blotting equipment, including SDS running buffer, nitrocellulose transfer membrane, 30% acrylamide/Bis solution, and Bradford protein assay reagent were purchased from Bio-Rad (Hertfordshire, UK). Gel blotting paper was from SLS (Scientific Laboratory Supplies). Enhanced chemiluminescence (ECL) reagent was purchased from Schliecher & Schuell (London, UK). Poly-D-lysine, cover-slips, tissue culture plasticware, such as 6-well plates, 24-well plates and 175 cm^2 tissue culture flasks were purchased from BD Biosciences Europe (Oxford, UK). TC Microwell Plate Nunclon (96 well) was supplied by Fisher Scientific UK Ltd. Pre-stained protein molecular size markers were from New England Biolabs (Hitchin, U.K.). All mammalian cell culture reagents including, minimum essential medium (MEM), fetal bovine serum (FBS), heat-inactivated fetal bovine serum (HI-FBS), Dulbecco's phosphate-buffered saline (D-PBS) without calcium and magnesium, gentamycin, fungizone, penicillin, streptomycin, trypsin, Earle's balanced salt solution (EBSS) were supplied by Invitrogen (Paisley, UK). Triton X-100, dithiothreitol (DTT), Folin-Ciocalteu's reagent, isopropyl alcohol, D-glucose, bovine serum albumin (BSA), ionomycin and other chemicals, including isoprenaline, noradrenaline, phenylephrine hydrochloride, A61603 hydrobromide, dexmedetomidine hydrochloride, (*S*)-timolol maleate, CGP20712A, ICI118,551, phentolamine, uridine 5'-triphosphate (UTP), adenosine 5'-triphosphate (ATP), (*S*)-3,5-dihydroxyphenylglycine (DHPG), phorbol-12,13-dibutyrate (PDBu) and 3-isobutyl-1-methylxanthine (IBMX) were obtained from Sigma-Aldrich Chemical Co. (Poole, UK). L-quisqualic acid, L-glutamic acid, Gö6976 and GF109203X were purchased from Tocris-Cookson Ltd. (Bristol, UK).

2.1.2. Peptides, antibodies, enzymes, primers, siRNA and cDNA

The DNA polymerases, Taq and Phusion, restriction endonucleases (RE), T4 DNA ligase, SuperScript III reverse transcriptase, all the primers, the relevant working buffers and supplements were supplied by Invitrogen (Paisley, U.K.). Fluo-4-AM (Fluo-4-acetoxymethylester), G5 supplement, Alexa Fluor® 488 goat anti-mouse IgG (H+L), Alexa

Fluor® 594 goat anti-rabbit IgG (H+L), rhodamine phalloidin and Hoechst 33342 were also from Invitrogen (Paisley, U.K.). Trypsin from bovine pancreas, trypsin inhibitor from soybean, DNase I (type IV), protease inhibitor cocktail, glycogen from bovine liver, glucose oxidase, horse-radish peroxidase, Amplex-red reagent and amyloglucosidase were from Sigma-Aldrich Chemical Co. (Poole, UK). Anti-rabbit HRP-conjugated secondary antibody, p44/p42 MAPK (ERK1/2) mouse mAb, phospho-p42/p44 MAPK (T^{185}/Y^{187}; T^{202}/Y^{204}) rabbit mAb, anti-rabbit IgG (H+L) 680, anti-mouse IgG (H+L) 800 conjugate and the antibody raised against glial fibrillary acidic protein (GFAP mouse mAb) were purchased from Cell Signaling. The mGlu5 receptor antibody, CREB mAb and phospho-CREB (SER 133) were from Millipore (Hertfordshire, UK). Anti-GRK2 antibody - *C*-terminal ab137666 was from Abcam Ltd.

2.1.3. Specific reagents and kits

Rat astrocyte nucleofector® kit was from Lonza (Wokingham, UK). Nucleic acid extraction and purification kits HiSpeed Plasmid Maxi Kit were obtained from QIAGEN (Crawley, U.K.). SafeFluor scintillation cocktails were purchased from PerkinElmer (Cambridgeshire, UK). [2,8-^{3}H]-adenosine 3', 5'-cyclic monophosphate, ammonium salt ([^{3}H]cAMP; 40 Ci/mmol) was from Amersham Biosciences (GE Healthcare U.K. Ltd, Bucks., U.K.). MAX Efficiency® DH5α™ competent cells (*E. coli* strain) was from Invitrogen (Paisley, U.K.). pcDNA3 plasmid cDNA for GRK2 was kindly provided from Dr Jonathon Willets (Dept. of Molecular & Cell Biology, University of Leicester).

Table 2.1. Usage of regular chemicals, inhibitors and antibodies

Name of item	Concentration	Supplier
noradrenaline	0.1-100 µM	Sigma
isoprenaline	0.1-10 µM	Sigma
A61603 hydrobromide	1 nM-10 µM	Sigma
dexmedetomidine hydrochloride	1 nM-10 µM	Sigma
(*S*)-timolol maleate	10 µM	Sigma
GF109203X	1 µM	Tocris
CGP 20712A	1 nM-10 µM	Sigma
ionomycin	2 µM	Sigma
ICI 118,551	1 nM-10 µM	Sigma
phentolamine	10 µM	Sigma
uridine 5'-triphosphate (UTP)	1 nM-100 µM	Sigma
adenosine 5'-triphosphate (ATP)	1 nM-100 µM	Sigma
IBMX	300 µM	Sigma
DHPG	0.3 µM-10 µM	Sigma
AG1478	1 µM	Sigma
EGTA	3 mM	Sigma
BAPTA-AM	100 µM	Sigma
GM 6001	10 µM	Tocris
pertussis toxin	100 ng	Tocris
Gö 6976	1 µM	Tocris
UBO-QIB	100 nM	Gift
BAPTA-AM	100 µM	Sigma
Fluo-4-AM	4.5 µM	Invitrogen

Table 2.2. Concentrations of reagents, inhibitors and enzymes for glycogen assay.

Name of item	Concentration	Supplier
glycogen from bovine liver	1µg/mL-16 µg/mL	Sigma
D-glucose	5 µM -80 µM	Sigma
glucose oxidase	20 units/mL	Sigma
horse-radish peroxidase	100 units/mL	Sigma
Amplex-red reagent	2.5 mg/mL	Sigma
amyloglucosidase	1% (v/v)	Sigma
Triton X-100	0.1% (v/v)	Sigma
sodium acetate	0.1 M, pH 4.7	Sigma
sodium phosphate	50 mM	Sigma

Table 2.3. Antibodies used for western blotting analysis and immunocytochemistry

Antibody	Primary antibody	Secondary antibody
phospho-p44/p42 MAPK(rabbit)	1:3000 in 5% BSA in PBS	anti-rabbit IgG (H+L) 680 (1:15,000) in PBS
p44/42 MAPK (mouse)	1:1000 in 5% BSA in PBS	anti-mouse IgG (H+L) 800 conjugate (1:15,000) in PBS
GRK2 *C*-terminal	1:1000 in 5% milk in PBS	anti-mouse IgG (H+L) 800 conjugate (1:15,000) in milk
CREB (rabbit)	1:1000 in 5% BSA in PBS	anti-rabbit IgG (H+L) 680 (1:15,000) in PBS
phospho-CREB (Ser^{133}) (mouse)	1:1000 in 5% BSA in PBS	anti-mouse IgG (H+L) 800 conjugate (1:15,000) in PBS
GFAP	1:400 in PBS; O/N @ 4°C	1:400 Alexa Fluor® 488 goat anti-mouse in PBS; 1 h @ RT
rhodamine phalloidin	1:400 in PBS; 1 h @ RT	----
Hoechst staining	1:250,000 in PBS; 10 min @ RT	----

2.2. Primary rat cerebrocortical astrocytes

The biochemical and physiological properties of astrocytes are difficult to study in the intact brain and spinal cord due to the complexity and the cellular heterogeneity of these organs. Besides, the progress in understanding astrocyte biology also has been impeded for long time since the inability to purify and culture astrocytes to study the functions of these cells *in vitro*. To address this problem, an astrocyte culture approach (McCarthy and de Vellis, 1980) has been developed from rodent neonatal brains to generate a relatively well-defined cell population such as neurons, astroglial and oligodendroglia in order to study their physiological and functional characteristics at a single-cell or molecular level. This pioneering research has provided us with a reliable method to isolate and maintain purified populations of cells from neonatal rat tissue, which, since then, has been great used for studying astrocytic functions and understanding the integrity of central nervous system. Furthermore, a modified method for the preparation of cortical astrocytes from postnatal P1 to P2 mouse brain has also been described (Zhang et al., 2005). Much has been learned about astrocyte biology using this method. This method, presented here in a slightly modified form, has been adapted for P1/P2 rat neonates and is well established in our laboratory highly reproducibly yielding comparably pure primary astrocytes.

2.3. Preparation of cell cultures

2.3.1. Primary culture of rat cortical astrocytes

All animal procedures were performed in accordance with and approved by the Animal Welfare and Ethical Review Body (AWERB) committee. Animals basically euthanized by quick decapitation. Rat cortical astrocytes were prepared according to a modified protocol described by (Zhang et al., 2005). Compositions of solutions used for the rat cortical astrocyte preparation are summarized in Table 2.3. Wistar rats (postnatal day 1-2) were killed according to a mandated Schedule 1 method (United Kingdom Animals (Scientific Procedures) Act 1986).

2.3.2. Isolation and Plating of Mixed Cortical Cells

During the dissection, heads were kept on ice after the decapitation, brain tissue was scooped out using curved forceps and put into ice-cold EBSS solution (EBSS, 3.17 mM MgSO$_4$, 0.3% (w/v) bovine serum albumin (BSA), 16.65 mM D-glucose). Repeat this step for

the number of heads required for the dissection, then use the mini-scissors to cut out the cortex layer from the both hemispheres, or the cerebellum if needed. In order to avoid contamination of the final astrocyte culture by meningeal cells and fibroblasts, the meninges was carefully peeled away by pulling with the fine forceps and tissue was cut up into small pieces and then incubated at 37°C for 15 min in 10 mL sterile EBSS solution containing 0.025% (w/v) trypsin (bovine pancreas) (Solution 1). The suspension was agitated gently 3 times during this period. After 15 min, 10 mL EBSS solution containing 50.72 μM MgSO$_4$, 6.4 μg/m$_l$ DNase-I, and 0.019% (w/v) trypsin inhibitor (Solution 2) was added, and the suspension was left to settle for 5 min. The supernatant was subsequently decanted off, and 2.5 mL EBSS solution containing 317 μM MgSO$_4$, 40 μg/mL DNase-I and 0.12% (w/v) trypsin inhibitor (Solution 3) was added. Tissue was slowly triturated using a glass, fire-polished Pasteur pipette, and then transferred to a fresh Sterilin tube. Trituration was repeated again and then 2.5 mL EBSS solution containing 0.4% (w/v) BSA and 254 μM MgSO$_4$ (Solution 4) was added.

The cell suspension was centrifuged (1000 r.p.m.; 8 min), and the pellet re-suspended in culture medium, Dulbecco's minimum essential medium (DMEM), which contains GlutaMAX-1, sodium pyruvate and 4500 mg/L glucose, to which were added 15% heat-inactivated fetal calf serum (HI-FBS), 250 μg/mL fungizone and 0.1 μg/mL gentamycin. Cells were seeded into poly-D-lysine-coated cell culture flasks and incubated at 37°C in a humidified air: 5% CO$_2$ atmosphere for 7 days, with medium being replaced after 3 or 4 days.

2.3.3. Obtaining an Astrocyte-Enriched Culture

Medium was replaced 2 days after plating of the mixed cortical cells and all 3 days thereafter. At 7-8 days *in vitro* (DIV), when astrocytes are confluent and overlaying microglia sit exposed on the astrocyte layer, astrocyte culture medium was replaced by 'shaking medium', which was same as culture medium, except for a lower concentration of 10% HI-FBS, and transferred to a shaking incubator overnight (37°C; 320 r.p.m.). On the following day (DIV 8-9), astrocytes should be separated from microglia and oligodendrocyte precursor cells (OPCs) by shaking, then the remaining confluent astrocytes were washed twice with PBS (without Ca^{2+}/Mg^{2+}) and harvested with 0.25% (w/v) trypsin, 0.02% (w/v) EDTA. Then cells were centrifuged (1500 r.p.m.; 4 min) and re-suspended into fresh medium. Cells were subsequently seeded onto pre-coated poly-D-lysine tissue culture plates for experiments (DIV 11-13).

Table 2.4.   Composition of solutions for rat cortical astrocyte preparation

EBSS solution	100 mL EBSS (Ca^{2+}/Mg^{2+}-free), 0.3 g BSA, 1 mL MgSO$_4$ (stock 3.82 g/100 mL), 0.25 g D-(+)-glucose
Solution 1	2.5 mg trypsin (Bovine pancreas), 10 mL EBSS solution
Solution 2	1.6 mL solution 3, 8.4 mL EBSS solution
Solution 3	100 µL DNase I (stock 4 mg/ml), 12 mg trypsin inhibitor, 100 µL MgSO$_4$, 10 mL EBSS solution
Solution 4	0.4 g BSA, 80 µL MgSO$_4$, 10 mL EBSS solution

2.3.4. Purity of primary astrocyte culture

The modified method of the isolation and culture of cortical astrocytes from postnatal P1 to P2 rat neonate brain described in this protocol provides high efficient and reproducible yields of pure primary astrocytes, and it has become a powerful tool to investigate astrocyte biology. The astrocyte culture purity can be characterized by light microscopy morphological studies, usually at day 7, astrocytes are confluent and microglia or some oligodendrocyte progenitor cells (OPCs) sit exposed on the astrocyte layer (Figure 2.1A), nearly pure astrocytes will be separated by shaking for overnight (Figure 2.1B). The obtained primary astrocyte culture purity can be reflected by immunolabelling of rat primary astrocyte cultures with the astrocyte-specific marker GFAP (Figure 2.1C). Our isolation and culture method of cortical astrocytes resulted in an astrocyte purity of greater than 98%.
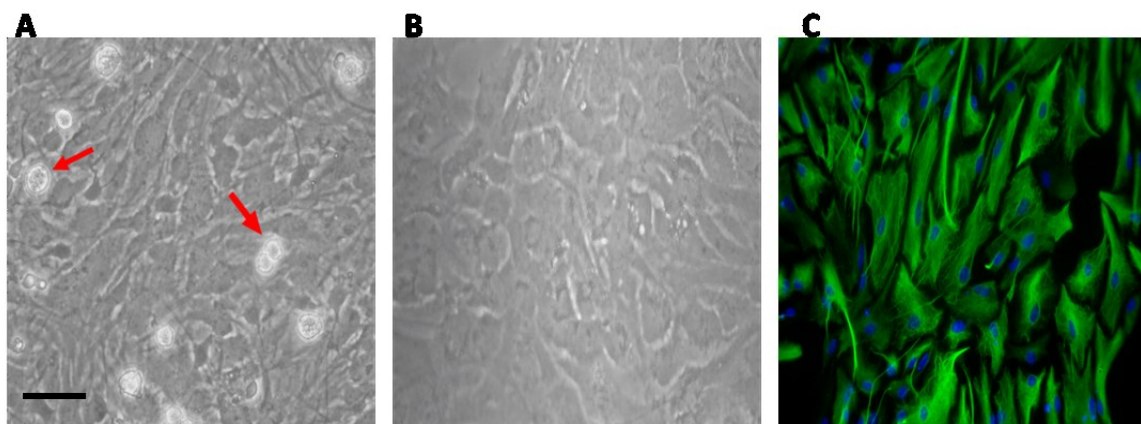
Figure 2.1. Overview of isolated mixed cortical cells and pure astrocyte culture at different time-points after isolation. (**A**) 7 days after plating of mixed cortical cells in astrocytes. Microglia and OPCs on top of astrocyte layer (red arrows). (**B**) After removing microglia and oligodendrocyte progenitor cells (OPCs) by vigorous shaking for overnight, attached cells show pure astrocyte morphology. (**C**) The astrocyte culture purity was examined by immunocytochemical examination using an antibody against the GFAP protein, nuclei are stained with Hoechst (blue). Scale bar = 100 µm.

2.3.5. Vector and plasmid preparation

Plasmids, small circular and double-stranded DNA molecules, usually exist in bacteria and considered as replicons capable of replicate independently within a suitable host (Lipps, 2008). Plasmids can carry diverse genes including antibiotic resistance genes which might be beneficial for their hosts to survive under certain situations or particular conditions, which has been considered to be of significant medical importance. DNA constructs usually contain the gene sequence encoding a protein of interest, which can be inserted into a vector. Therefore, this kind of artificial plasmid can subsequently be transformed into a target tissue or host cell. _E. coli_, most widely used prokaryotic model organism, has been studied for more than half century and served as the host cell for the majority of work such as recombinant DNA (Bower and Prather, 2009).

2.3.5.1. DH5α

DH5α (Invitrogen, Paisley,U.K.) competent cells are well-known, versatile _E. coli_ strain in many everyday cloning applications, which possess very high and stable capability to efficiently insert and transform the plasmid DNA. Like most _E. coli_ strains, DH5α is sensitive to common antibiotics, such as ampicillin, since it does not contain any antibiotic resistant gene, therefore, plasmids used for the cloning of DNA and transformation have to carry antibiotic-resistant gene.

2.3.5.2. Plasmid transformation using DH5α

E. coli cells (DH5α) were defrosted on ice and target plasmid DNA (5-10 ng) was then added to 100 μL of cells and mixed gently for 30 min. The competent cells will take up DNA after a heat shock step for 2 min at 42°C water bath followed by 2 min cool down on ice. Cells were then incubated in shaking incubator (225 r.p.m.; 37°C) for 45 min by adding 900 μL SOC medium (0.5% w:v yeast extract, 2% w:v tryptone, 10 mM NaCl, 10 mM $MgSO_4$, 20 mM D-glucose). Transformed cells (50 μL-100 μL) were spread onto LB agar plate prepared beforehand which should containing appropriate concentration of ampicillin (100 μg/mL) and then incubated at 37°C overnight. The plates should be placed upside-down in the incubator.

HiSpeed Procedure

Pelleted bacteria

↓

Alkaline lysate

↓

Clear lysate
by filtration using
QIAfilter Cartridge

↓

Bind DNA,
wash, elute on
HiSpeed Tip

Add isopropanol

↓

Collect DNA using
QIAprecipitator

Elute

↓

Ultrapure plasmid DNA
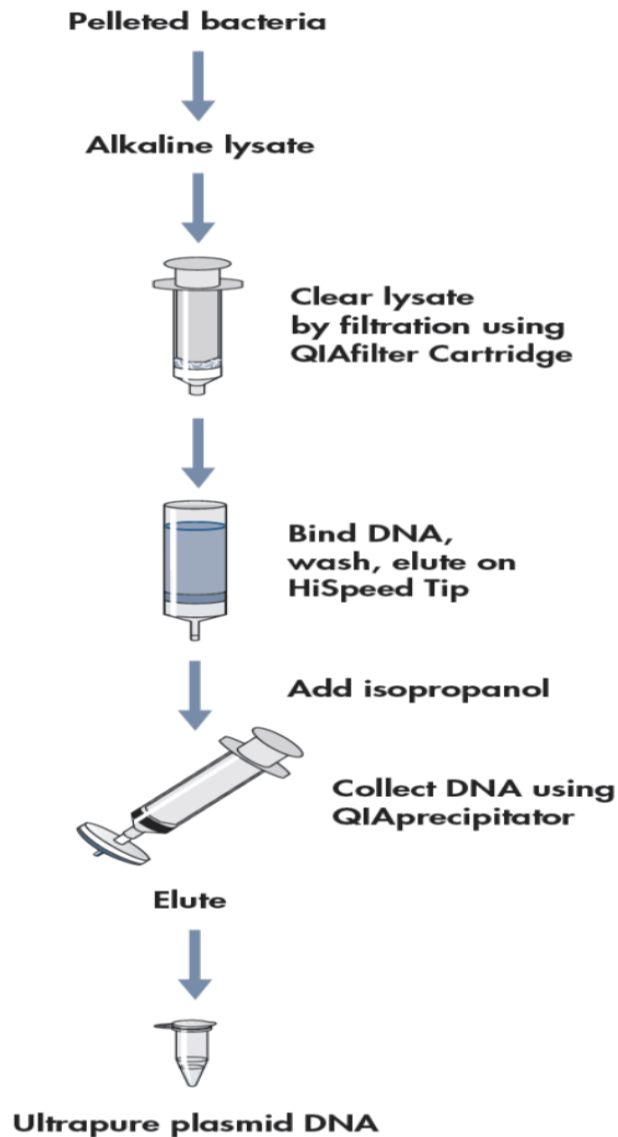
Figure2.2.   QIAGEN's HiSpeed plasmid purification procedure. QIAGEN plasmid purification protocols are based on a modified alkaline lysis procedure, followed by binding of plasmid DNA to QIAGEN resin under appropriate low-salt and pH conditions. RNA, proteins, dyes, and low-molecular–weight impurities are removed by a medium-salt wash. Plasmid DNA is eluted in a high-salt buffer and then concentrated and desalted by isopropanol precipitation. Plasmid DNA from the filtered lysate is then efficiently purified using a HiSpeed Tip. Diagram adopted from (QIAGEN, 2012).

2.3.5.3. Preparation of plasmid DNA

Since transformation is subject to antibiotic selection, and transformed bacteria incorporated with antibiotic resistance genes can keep growing by picking a colony from agar plate and inoculating into approximate media (LB broth) containing correct antibiotic (ampicillin). Plasmid DNA can be isolated and purified follow QIAGEN's HiSpeed plasmid purification handbook/protocol (Figure 2).

2.3.5.4. Transfection of rat cortical astrocytes

Procedures for transferring genes of interest into cells to assay their functions have been the subject of intensive research. Nucleofection, invented by the biotechnology company Amaxa and been considered as most basic method, is an electroporation-based transfection method which enables transfer of nucleic acids into cells by applying a specific voltage and reagents.

According to manufacturer's instructions, astrocytes were transfected using a rat astrocyte nucleofector® kit. In brief, astrocytes, prepared as discussed above, grew in culture medium for approximately 7-8 DIV. After overnight shaking, cells were harvested using 0.25% (w/v) trypsin, 0.02% (w/v) EDTA. The cells were centrifuged (1000 r.p.m.; 4 min) and medium was carefully aspirated. After counting cell number using a haemocytometer, so that each sample contained approximately 2×10^6 cells, the pellet was re-suspended into 10 mL of fresh medium and centrifuged again. 100 µL/transfection of rat astrocyte nucleofection reagent then add into cell pellet after removing as much medium as we can to avoid media inhibiting nucleofection reagent. According to the experimental plan, either 2 µg pmaxGFP or 3.5 µg plasmid DNA was added to each Eppendorf tube containing 100 µL cell suspension, then transferred all these solution into Amaxa-certified cuvettes using filtered pipette tips. Transfection was performed using an Amaxa/Lonza nucleofector device, set to program T-20. 500 µL pre-warmed culture medium (DMEM containing GlutaMAX-1 with sodium pyruvate and 4500 mg/L D-glucose, 15% HI FBS, 2.5 µg/mL fungizone and 0.1 µg/mL gentamycin) was added to each cuvette, and the cells were transferred into Eppendorf tubes using plastic Pasteur pipettes provided. Cells were put into 37°C incubator for maximum 30 min prior to seeding onto poly-D-lysine-coated plates or coverslips. 24 h following nucleofection, medium was replaced with fresh DMEM containing GlutaMAX-1. Cells were used for experiments 48 h later. Transfection efficiency was monitored by analyzing the expression of pmaxGFP using confocal microscopy (Figure 2.3).
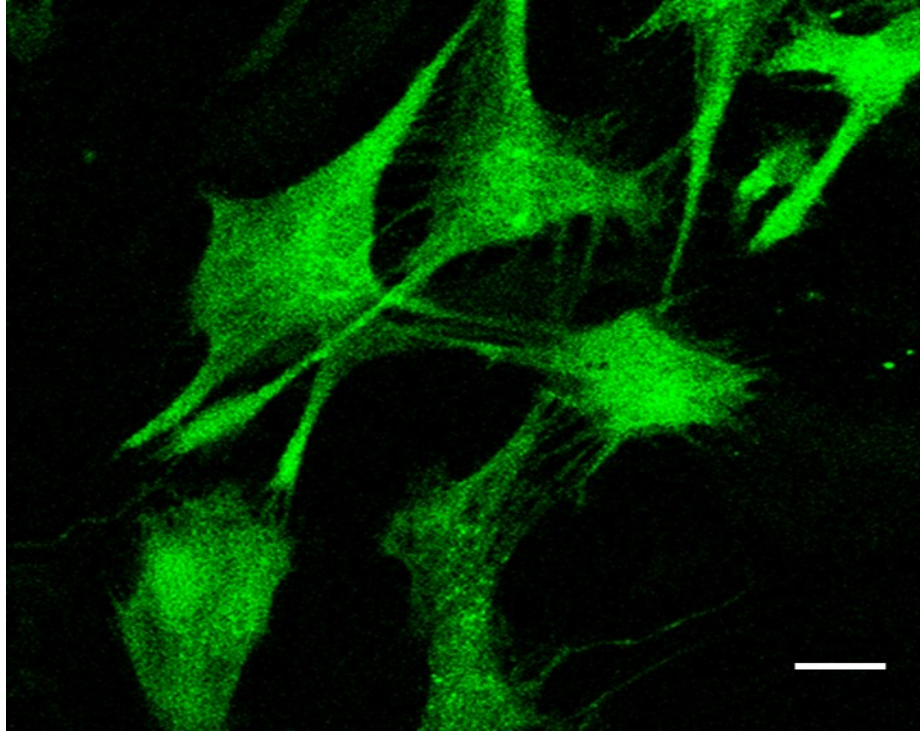
Figure 2.3.   Nucleofection of primary rat astrocytes. 2×10^6 rat astrocytes were transfected with 2 µg of pmaxGFP™ vector using program T-20. Image shows fluorescent cells recorded using confocal microscopy connected with OLYMPUS FLUOVIEW software 48 h post-nucleofection. Scale bar = 50 µm.

2.4. Polymerase Chain Reaction (PCR)

PCR is a common and often indispensable technique in clinical and research laboratories to clone a particular DNA sequence (Bartlett and Stirling, 2003), which utilises a heat-stable DNA polymerase (Taq polymerase) to form a new DNA strand from nucleotides by using a single-stranded DNA (cDNA) as a template and proper DNA primers (oligonucleotides) as initiating elements for DNA synthesis.

2.4.1. RNA isolation

RNA was extracted according to the manufacturer's instructions. At least 10^6 primary astrocytes growing in tissue cultured dish (p100) were harvested by centrifugation at 12,000 r.p.m. for 5 min at 4°C. The pellet was re-suspended in lysis buffer (Ambion, RNA Mini kit) with 2-mercaptoethanol. Physical homogenization was proceeded by passing the lysate 5-10 times through an 18-21 gauge syringe needle to shear genomic DNA. Then the PureLink™ RNA mini kit was used for the RNA purification by using spin-column technology and selective binding properties of silica membranes. In brief, 70% ethanol was added to the cell homogenate with a thorough mix to disperse any visible precipitate, which followed by wash using Wash Buffer I (Ambion, RNA Mini kit) to further remove some of the salts present in the leftover supernatant. After twice wash using Wash Buffer II, only pure RNA adsorbs to the silica membrane while all other contaminants are unable to bind to the silica column and therefore pass through the column. The loaded column is finally washed and then any bound RNA is eluted in 30 μL RNase-free water. Extracted RNAs were stored at −80°C until subsequent use or for RNA quantification and PCR amplification.

2.4.2. RNA quantification by spectroscopy

The concentration of RNA was estimated by spectroscopy (Nanodrop – Thermo Scientific). A 1 μL sample of each RNA extract was placed on the Nanodrop and the absorbance at 260 nm was measured. RNase-free water was used as a blank. The 260/280 ratio should be greater than 1.8. If less than 1.5-1.6 or so, the RNA is likely to be at least partially degraded or contaminated by DNA. The concentration of RNA was automatically calculated by the software and would be the equivalent of the OD at 260 nm (in μg/μL).

2.4.3. First-Strand cDNA synthesis

cDNA was prepared from 1 μg total RNA by reverse transcription using the Superscript III reverse transcriptase system (Invitrogen) according to the manufacturer's instructions. After DNase-I treatment (1 μg RNA sample, 1 μL 10X DNase-I reaction buffer, 1 μL DNase I, DEPC-treated water to 10 μL) for 15 min at room temperature and following 1 μL EDTA (25 mM) addition for 10 min at 65°C, the RNA sample is ready to use in reverse transcription. In the above mixture, 1 μL oligo(dT)$_{20}$ (50 μM) and 1 μL dNTP Mix (10 mM) are added and incubated 5 min at 65 °C, then placed on ice for 2 min. 7 μL cDNA Synthesis Mix (4 μL 5X First-Strand buffer, 1 μL 0.1 M DTT, 1 μL RNase Out (40 U/μL) and 1 μL Superscript^{TM} III RT) was added to make total solution volume of 20 μL, mixed gently and then incubated 50 min at 50°C, then 70°C for another 15 min to stop the reaction. cDNA is obtained and stored at -20°C for use.

2.4.4. Design of primers

All primers used were designed based on construct boundaries to be approximately 20 nucleotides in length complimentary to the DNA template sequence. In my project, in order to explore the expression of different beta adrenoceptor subtypes in rat neonatal astrocytes, the appropriate primers for rat β_1 (ADRB1), β_2 (ADRB2) and β_3 (ADRB3) adrenoceptors have been designed and purchased from Invitrogen. Details of primers used are set out in Table 2.5.

Table2.5. Primers for generating gene constructs of β-adrenoceptors subtypes.

Primer	Oligonucleotides sequence	Expected product size
GAPDH	Forward 5'-GGCATTGCTCTCAATGACAA-3' Reverse 5'-TGTGAGGGAGATGCTCAGTG-3'	92 bp
β_1-adrenoceptor	Forward 5'-GCATCATCATGGGTGTGTTC-3' Reverse 5'-CCAGTTGAAGACGAAGAGG-3'	370 bp
β_2-adrenoceptor	Forward 5'-ATTTCTGGTGCGAGTTCTGG-3' Reverse 5'-AAGGGCGATGTGATAGCAAC-3'	330 bp
β_3-adrenoceptor	Forward 5'-TAGCAAGGAGCCTGACTTCTG-3' Reverse 5'-GGTTCTGGAGAGTTGCGGTT-3'	517 bp

2.4.5. Performing PCRs on a thermocycler

The PCR mixture was set up in a PCR reaction tubes with a total volume of 25 µL in each tube, which contains 5 µL of 10X ThermoPol reaction buffer, 0.75 µL of 50 mM $MgCl_2$, 0.5 µL of 10 mM dNTPs, a thermostable DNA polymerase (Taq polymerase, 0.25 µL), appropriate volume of primers (0.5 µg/ µL), 1 µg cDNA and finally added DNase-free water to make total volume of 25 µL.

The PCR was carried out in a thermal cycler consists of 30 cycles of temperature changing steps including denaturation, annealing and elongation. The thermal cycler heats and cools the reaction tubes to achieve the temperatures required at each step of the reaction. In the first step, DNA polymerases was activated by temperature reaching around 94–96°C for 1 min, followed by annealing step (65°C, 1 min) and subsequent extension step (72°C, 3 min). When the last cycle was finished, the temperature decreased to 4°C to keep PCR tubes for following use, or storing these tubes in -20°C if not immediately needs.

2.4.6. Agarose gel electrophoresis of DNA

DNA was separated by agarose gel electrophoresis to allow visualisation and confirmation of band size in accordance with the method described by (Sambrook and Russell, 2001). According to the size of the target DNA (β-adrenoceptors), the concentrations of 1% (w/v) agarose was dissolved in TAE buffer (40 mM Tris-acetate, 1 mM EDTA, pH 8.0) and ethidium bromide (0.1 µL/mL) was added to allow visualization of added DNA. The gel was then poured into a casting tray with a comb to make loading wells. Once solidified, the gel was inserted into the electrophoresis chamber to be just immersed by TAE buffer, then the PCR products (16 µL for each) were mixed with 5X DNA loading buffer (4 µL), then loaded into each well in the gel. 5 µL of DNA ladder (100 kb) was loaded to quantitate the size of target DNA fragments. Electrophoresis was carried out at 85 V for 50 min. After that, gel was removed and placed on the UV trans-illuminator and the photograph was achieved using a digital camera connected with computer.

2.5. Determination of cyclic AMP

2.5.1. Preparation of samples

Cells were seeded into 24-well culture plates and incubated at 37°C in a 5% CO_2, humidified air atmosphere. When cells were confluent, monolayers were washed twice 2x and

incubated for 30 min at 37°C in freshly oxygenated Krebs-Henseleit/HEPES (KHB) buffer (118 mM NaCl, 4.69 mM KCl, 4.2 mM $NaHCO_3$, 1.3 mM $CaCl_2$, 1.18 mM $MgSO_4$, 1.18 mM KH_2PO_4, 11.7 mM D-glucose, 10 mM HEPES, pH 7.4), then experiments were performed by stimulating with appropriate agonists at a required concentrations and/or indicated time points either in the absence or presence of the PDE inhibitor, 3-isobutyl-1-methylxathine (IBMX; 300 µM) and in a total volume of 500 µL. Incubations were terminated by rapid aspiration of buffer and addition of 0.5 M ice-cold trichloroacetic acid (TCA). Plates were kept on ice for at least 20 min before the aqueous phase was recovered, 50 µL of 10 mM EDTA (pH 7.0) added before neutralization by addition of 500 µL of a freshly prepared oil mixture (tri-*n*-octylamine and 1,1,2-trichlorotrifluoroethane; 1:1 v/v) at room temperature (RT) for approximately 15 min. After three times vortex-mixing, samples were centrifuged (14,000 r.p.m., 2 min at RT) and 200 µL of the neutral supernatant was collected and transferred to an Eppendorf tube containing 50 µL of 60 mM $NaHCO_3$. Samples were either assayed immediately or stored at 4°C for up to 3 days.

2.5.2. Cyclic AMP assay

The concentration of cAMP in each cell-extract was assayed using a competitive binding with [³H]-cAMP to a specific cAMP-binding protein purified from bovine adrenal glands (Brown *et al.*, 1971). Either 50 µL of known cAMP standard ranging from 0-10 µM (to construct a standard curve) (Figure 2.3) or sample was added to 100 µL [³H]-cAMP (40 Ci/mmol) in 50 mM Tris/HCl, 4 mM EDTA, pH 7.5, followed by addition of 150 µL of the cAMP binding protein preparation. After vortex-mixing and incubation on ice for at least 90 min, 250 µL of an activated charcoal solution (0.5% w/v charcoal, 0.2% w/v BSA, 50 mM Tris/HCl, 4 mM EDTA, pH 7.5) was added to each Eppendorf tube for 10 min in order to absorb cAMP/[³H]-cAMP not bound to the cAMP binding protein. Samples were again vortex-mixed and centrifuged (14,000 r.p.m., 4 min, 4°C). 400 µL of supernatant was transferred to scintillation vial and 3 mL scintillation cocktail added and radioactivity quantified by liquid-scintillation spectrometry. The concentration of cAMP in each sample was determined by interpolation of the standard curve (Figure 2.4) and expressed per unit of cell protein determined by Lowry assay.

cAMP Standard Curve

Log [cAMP]	DPM	
	Y1	Y2
-2.000	35017	35535
-0.903	32535	33159
-0.602	30081	30599
-0.301	26507	26416
0.000	20920	20770
0.301	15474	15376
0.602	11067	10823
0.778	9231	8855
0.903	7776	7801
1.000	7029	7119
2.398	1048	1031
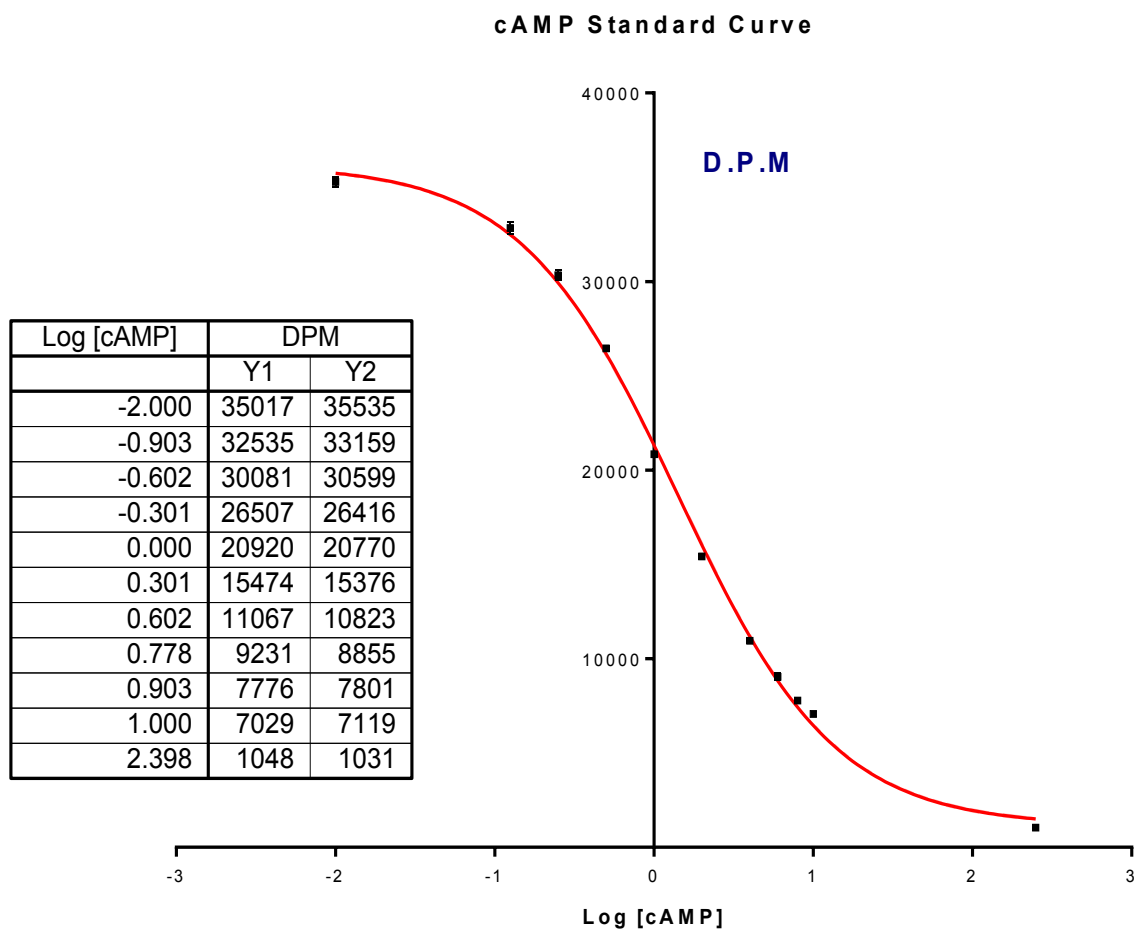
Figure 2.4. A cAMP standard curve determined for a radioactive [3H]-cAMP-based competition assay for cAMP accumulation in the cell lysates. cAMP standards and samples were counted overnight in a scintillation counter. The cAMP standards were used to generate a standard curve (as seen above) and the concentration of cAMP in the samples was determined by interpolating from this standard curve. In this assay, each log value was converted from cAMP concentration unit (pmol/50 µL sample).

2.5.3. Lowry protein assay

A standard curve was prepared using bovine serum albumin (BSA; 0 to 250 μg) diluted in appropriate vehicle. Tubes containing either 200 μL of sample or standard BSA were added 1 ml of freshly mixed complex-forming reagent (2% Na_2CO_3/0.4% NaOH, 1% $CuSO_4$, 2% K/Na tartrate in a ratio of 100:1:1). The solution was incubated at room temperature for 10 min. After this, 100 μL of diluted Folin reagent was added followed by vortex-mixing and incubation at room temperature for 30 min. The absorbance value at 750 nm was measured using a spectrophotometer. Finally, a standard curve of absorbance as a function of protein concentration was plotted and used to interpolate unknown protein concentrations.

2.6. Western Blotting Analysis

2.6.1. Treatment of cells and sample preparation

Cells were seeded 6-well or 24-well plates and cultured in DMEM until they were more than 80% confluent, then cells were starved for 24 h in serum-free medium. After washing twice with warm (37°C) KHB buffer (composition:120 mM NaCl, 4.8 mM KCl, 25 mM $NaHCO_3$, 1.3 mM $CaCl_2$,1. 2 mM $MgSO_4$, 1.2 mM KH_2PO_4, 10 mM D-glucose, 5 mM HEPES, pH 7.45), cells were incubated in water bath at 37°C with or without agonists and/or other agents for times indicated in individual experiments. For the western blot analysis of phosphorylated ERK1/2, serum-starved confluent astrocytes seeded in 6-well plates were rinsed twice with DPBS (Dulbecco's phosphate Buffered Saline) and incubated in 2 mL of fresh serum-free medium for 30 min. Cells were then exposed to the agents at a required concentrations and/or indicated time-points.

Reactions were terminated by transferring the plates on ice and aspirating the solution immediately. Cells were solubilized by adding 300 μL per well (6 well plates) or 150 μL per well (24 well plate) of lysis buffer (20 mM Tris-base, pH 7.4, 1% (v/v) Triton X-100, 10% (v/v) glycerol, 137 mM NaCl, 2 mM EDTA and a 1:100 dilution of a protease inhibitor cocktail and phosphatase inhibitors including sodium orthovanadate and β-glycerophosphate), and then samples were collected into 1.5 mL Eppendorf tubes by scraping on ice and centrifuged at 13,000 r.p.m. for 10 min at 4°C. Aliquots of the supernatant were extracted and cell lysates were stored at -20°C until use.

2.6.2. Bradford protein assay

The Bradford assay was used to determine the concentration of protein in cell lysates. BSA standards or protein samples (10 µL) were mixed with a 1/5 dilution of Bradford reagent (1 mL) with distilled water (each test performed in duplicate), and incubated at room temperature for at least 5 min. Absorbance at 595 nm was measured using a WPA spectrophotometer. The BSA standard curve (range 0 to 20 µg) was used as a reference for determining the protein concentration of each sample. Protein concentrations were normalized to that of the sample with the lowest protein amount by addition of lysis buffer.

2.6.3. SDS-polyacrylamide gel and electrophoresis

After adjustment of protein concentrations (see above), 4 volumes of lysate were added to 1 volume of 5X sample buffer (312.5 mM Tris-base, pH 6.8, 10% w/v SDS, 50% v/v glycerol, 250 mM DTT and 0.01% bromophenol blue). Then samples were heated for 5 min at 95°C and centrifuged at 13,000 xg for 2 min.

A 20 mL aliquot of 10% separating gel (composition: 6.75 mL 30% acrylamide; 5 mL Tris-HCl, 1.5 M, pH 8.8, 200 µL 10% sodium dodecyl sulphate (SDS); 80 µL 10% ammonium persulfate (APS); 30 µL N,N,N',N',-tetramethylethylenediamine (TEMED) and water to 20 mL) was made by gently pouring this mixture into the gel cassettes comprising pairs of clean glass plates with 1.5 mm spacer. The top-layer of the gel was covered with 0.5 mL isopropanol to provide a flat interface. After around 30 min, the gel was solidified and the top layer of isopropanol was removed carefully followed by briefly rinsing by distilled water. Subsequently, 5% stacking gel (composition: 2.125 mL 30% acrylamide; 3.125 mL Tris-HCl, 0.5 M, pH 6.8, 125 µL 10% SDS; 125 µL 10% APS; 12.5 µL TEMED and water to 12.5 mL) was prepared and poured onto the top of the separating gel followed by immediately inserting a comb to form loading lanes. The gel will be ready at RT for around 30 min.

Combs were then gently removed and briefly rinsed by distilled water and then mounted into a Mini-BioRad gel electrophoresis tank filled with running buffer (25 mM Tris-HCl, pH 8.3; 192 mM glycine, and SDS 0.1% w/v). Up to 30 µL of samples were loaded into each lane together with 3 µL of pre-stained protein marker loaded on one side of the gel. The electrophoresis was carried out at 200 V the dye front reached the bottom of the gel (about 60 min), then empty the running buffer and gently wash the gels for a few minutes.

2.6.4. Electrophoretic transfer technique of proteins

Separated proteins were transferred onto nitrocellulose membranes using tank transfer systems or the BioRad semi-dry blotting apparatus according to manufacturer's instructions. Nitrocellulose membrane and blotting papers were cut to the size of the each gel and then immersed in transfer buffer (40 mM glycine; 48 mM Tris; 0.0375% w/v SDS and 20% v/v methanol) for 5 min for the reason of equilibration. After electrophoresis, the gel was carefully removed from gel cassette and the stacking gel was cut away. In tank blotting systems, a non-conducting cassette holds the membrane in close contact with the gel constituting typical "blotting sandwich", which is entirely submerged under transfer buffer within a buffer tank. In a semi-dry transfer, the gel and membrane are sandwiched between two stacks of blotting paper that are in direct contact with plate electrodes. The latter method has been widely used in recent electrophoretic transfer since it requires considerably less buffer and much easier to set up than the tank blotting system. Using POWER PAC 200 apparatus (Bio-Rad, Hemel Hempstead, UK), it usually takeS 40 min at 25 V to complete transferring process.

2.6.5. Immunoblotting and Protein Detection and Analysis

Once the transfer was finished, the effect of transferred proteins can be visualized using Ponceau-S solution (0.25% in 1% acetic acid). After twice washing with distilled water, a blocking step was performed with 5% non-fat milk powder or 5% BSA/TBST buffer (50 mM Tris/HCl, pH 7.4, 150 mM NaCl, 0.1% Tween-20) for 60 min on a rocker at room temperature. The blots were then incubated in primary antibody diluted in 5% BSA/TBST buffer overnight at 4^oC overnight followed by 3 x 10 min washes with TBST on the next morning, blots were incubated with secondary antibody (Table 2.3) for 1 h at room temperature followed by another 3 x 10 min washes with TBS-T. Finally, the result of blots using chemiluminescence detection was developed using ECL and exposure to film. The fluorescent immunoblotting technology using Odyssey Fc Imaging System to scan and analyse the protein has provided much simplified method and more reproducible results.

2.7. Immunocytochemistry

Cells were seeded onto poly-D-lysine-coated 13mm cover-slips in 24-well plates and grown to sub-confluency (approximately 60-80% confluent), incubated at 37°C in a humidified air: 5% CO_2 atmosphere. After cells treatment at a required concentration and applied time

period if needed, plates were removed from the incubator, and medium was aspirated followed by two washes with PBS. Cells were fixed with 4% paraformaldehyde or methanol for 10 min at room temperature. After further washes with PBS, cells were permeabilized and simultaneously non-specific binding was blocked by incubation in PBS containing 0.1% Triton X-100/1% BSA for 30 min at room temperature. Following this, cells were washed with PBS for 3 x 5 min and then incubated with primary antibody (diluted in 1% BSA in PBS) at the relevant dilution overnight at 4°C. After decanting the solution on the next morning, cells were washed with PBS 3 x 5 min, and then incubated with fluorescence-conjugated secondary antibody (1:400 in 1% BSA in PBS) for 1 h at room temperature in the dark. Coverslips were washed with PBS 3 x 5 min followed by incubating with Hoechst (0.1 µg/mL) for 5 min. After two rinses with PBS, coverslips were mounted onto microscope slides with a drop of mounting medium (Fluoroshield^{TM}) and then stored in the dark at 4°C or wrapped by foil to be ready for investigating by fluorescence microscopy.

2.8. Ca^{2+} imaging

For fluorescent measurements of cytosolic free Ca^{2+} concentration in intact cells, an Olympus FV500 confocal microscope was used to record fluorescence intensity of Fluo-4-loaded cells grown on 28 mm coverslips pre-coated with poly-D-lysine to observe the changes of intracellular calcium concentration [Ca^{2+}]$_i$. Cells at approximately 60-80% confluency were washed with KHB solution (KHB: 120 mM NaCl, 4.8 mM KCl, 25 mM NaHCO$_3$, 1.3 mM CaCl$_2$,1. 2 mM MgSO$_4$, 1.2 mM KH$_2$PO$_4$, 10 mM D-glucose, 5 mM HEPES, pH 7.45), and then loaded with 4.5 µM Fluo-4 AM for about 40 min at room temperature in the dark to allow the Ca^{2+} dye ester to permeate the cells and be hydrolysed by endogenous esterases to the Ca^{2+}-sensitive free-acid form of Fluo-4. Subsequently, the coverslip was placed into the perfusion chamber, 1 mL of KHB buffer added and mounted onto the stage of the microscope, where the temperature was maintained at 37°C by a temperature controller (Harvard Applications Inc., Kent, UK). Live cells were routinely viewed using a 40x oil emersion lens. After the imaging system and parameters were appropriately set, reagent solutions were either perfused or bath applied to the cells at specified concentrations and for the time-periods indicated in the Results. Images were taken using a laser excitation wavelength of 488 nm and emitted light collected at wavelength >510 nm. The changes in fluorescence was recorded using OLYMPUS FLUOVIEW software and analysed as an index of

$[Ca^{2+}]_i$ relative to the basal levels using Graphpad Prism. In experiments where repetitive agonist addition was applied, washes between additions were performed by perfusion of the cells with KHB.

2.9. Glycogen assay

Glycogen is usually determined by hydrolysis to glucose which is then estimated chemically with the method of enzymatic analysis. A relatively simple assay has been described for the determination of glycogen content, this method was adapted from the previous work (Sorg and Magistretti, 1991b), glucose was released from glycogen via the action of amyloglucosidase. The released glucose was determined with glucose oxidase and peroxidase utilizing Amplex red as a chromogenic substrate. This method was found to be highly sensitive and was well established to study the effects of some neurotransmitter, especially adrenoceptor stimulation on the glycogen content in the primary astrocytes. The value was normalized to protein content assayed with the method of Bradford and finally presented as cellular glycogen content per unit protein.

2.9.1. Cell treatment and harvesting

Astrocytes were incubated in 24 well culture plate in normal cell culture medium described in detail previously, mainly containing 4.5 g/L glucose and 15% heat-inactivated fetal calf serum. Once cells were grown to confluence, the culture medium was replaced the day before experiments by 1 mL/well of serum free DMEM medium containing 5 mM glucose, cells were kept maintaining in a 95% air/5% CO_2 humidified incubator at 37°C. Experiments were performed by adding relevant agents in desired time period. Antagonists and inhibitors were pre-incubated 30 min before the addition of agonists. Incubations were terminated by immediately transferring plates on ice, followed by quickly aspirating medium, washing cells twice with ice-cold phosphate buffered saline (PBS) and lysing cells in 100 μL of 30 mM HCl/0.1% Triton X-100. Cell lysates, with volume of 100 μL per well, were transferred into Eppendorf tube and followed by centrifuging at speed (12,600 r.p.m.) for 10 min. After this step, samples can be either assayed immediately or stored at 4°C for up to 3 days.

2.9.2. Glycogen determination

Since glycogen is a polymer of D-α-glucose of indeterminate molecular-mass, which result in the difficulty in measuring the direct quantification of molar units. However, an enzymatic

fluorimetric method (including glucose oxidase, horseradish peroxidase and Amplex- red) to assay glycogen content has been well established and proved simple and sensitive. In this assay, glucose oxidase reacts with D-glucose to form D-gluconolactone and hydrogen peroxide, then in the presence of horseradish peroxidase (HRP), the production of hydrogen peroxide can react with the Amplex-red reagent in a 1:1 stoichiometric ratio to generate the red-fluorescent product resorufin. The concentration of glycogen in each sample was calculated from the appropriate standard curve (glycogen and glucose).

Firstly, to set up glycogen standard, using 16 µg/mL glycogen stock solutions diluted in 30 mM HCl/0.1% Triton-X100 to make a dilution series of glycogen standards in the range of 0 - 16 µg/mL. For the preparation of glucose standard, making 500 µM D-glucose solution in 30 mM HCl/0.1% Triton-X100, pH 4.7 sodium acetate buffer (1:1) for stock, from which a series of dilution solutions were made to give concentrations as follows: 80, 60, 40, 20, 15, 10, 5 and 0 µM in (1:1) solutions.

Secondly, 2x25 µL aliquots of each lysate supernatant and the same amount of each glycogen dilution were transferred to adjacent wells of a 96 WP. To this duplicate 25 µL aliquots of lysates or glycogen standards, add 25 µL of either 0.1 M sodium acetate (NaOAc) buffer with pH 4.7 or 1% (M:V) amyloglucosidase in diluted in the same pH 4.7 NaOAc buffer, then microplate was left on a rocking platform at room temperature for incubation at least 30 min. At the end of amyglucosidase digest, setting up glucose standard through pipetting duplicate 50 µL aliquots of each glucose dilution into available wells of the microplate, followed by adding 50ul of the assay mixture containing Tris-phosphate buffer (9 mL 50mM sodium phosphate, pH 7.4 + 1 ml 1.5 M Tris-HCl, pH 8.8), 100 µL glucose oxidase (10 units/mL), 100 µL horse-radish peroxidase (100 units/mL) and 80 µL Amplex-Red reagent (2.5 mg/mL in DMSO) to each well. The plate was wrapped in foil and left overnight at room temperature. On the following morning, the absorbance values were measured in TECAN microplate fluorometer set at 560 nm (the maximal number of absorption of Amplex-red is approximately 563 nm), from which, the first aliquot (without amyloglucosidase) gives the sum of glucose and glucose-6-phosphate,whereas the second aliquot (with amyloglucosidase) gives the sum of glycogen, glucose, and glucose-6-phosphate; the amount of glycogen is then determined by the difference between the two aliquots, finally glycogen concentration in each cell lysate was interpolated from the standard curve and expressed per unit of protein content determined by the assay method of Bradford.

2.9.3. Microplate Bradford assay

Unlike the Bradford protein assay for the purpose of western blot described previously, using the microplate assay is more convenient when determining the protein concentration of a number of unknown sample, for example during glycogen assay experiment, the stock BSA concentration is 1 mg/mL dissolved in 30 mM HCl/0.1% Triton-X100, from which different concentrations of BSA ranging from 0, 50, 100, 150, 200, 300, 400, 500 µg/mL were made for protein standard. After that 5 µl of either BSA standard or each lysate was added into available microplate (96 well plate), immediately followed by adding 200 µL of Bradford reagent (diluted 1:4 in distilled H_2O). After about 5 min of incubation on room temperature, protein values were determined at 595 nm absorbance using TECAN microplate reader.

2.10. Data analysis

Specific binding of the ligands (^{125}I-cyanopinolol, [3H]CGP-12177 or [3H]cAMP) was calculated as the difference between total binding and NSB. For intact cell binding assays, the bound radioactivity was related to the content of cellular protein value.

All data obtained were analyzed using Prism 7.0 (GraphPad Software Inc.). Each dataset shown are expressed as the mean ± s.e.m. of at least three experiments (unless otherwise stated). For immunocytochemistry data and Ca^{2+} imaging result, representative data from at least 3 experiments are presented. Concentration-response curves were analyzed using non-linear regression analysis. The statistical analysis was performed by unpaired Student's t-test (two-tailed) for comparisons of two datasets and one-way analysis of variance (ANOVA) for more than two datasets using Prism 7.0. Statistical significance was accepted at $p < 0.05$. Where statistical comparisons are shown for normalized data, the statistical analyses were performed on the 'raw' data, but shown as normalized data for clarity.

Chapter 3

Characterization of Adrenoceptor Expression and Signal Transduction in Rat Cerebrocortical Astrocytes

3.1. Introduction

Astrocytes were once regarded only as structurally supportive cells, but in recent decades it has become clear that this cell-type fulfils numerous functions in CNS (MacVicar and Newman, 2015, Hol, 2015, Gonzalez-Perez et al., 2015, Sofroniew and Vinters, 2010a). Key roles include astrocytic involvement in energy metabolism and synaptic plasticity through regulation of the abilities of different neurotransmitters to exert actions on neurons. In the CNS the different roles of the catecholamines, adrenaline and noradrenaline, are some of the most studied. Previous *in vivo* research has demonstrated that astrocytes located as a target of locus coeruleus (LC) activation, which is deemed to be the preeminent source of noradrenergic neurons innervating the cerebral cortex, are capable of responding to LC-network neuromodulatory functions (Bekar et al., 2008a, Wang et al., 2006). For example, neuropsychological-related stressful events stimulate the adrenal gland/adrenaline/LC pathway, leading to noradrenaline release and subsequent adrenoceptor activation in the brain involving both neurons and astrocytes. In addition, there is a large body of evidence indicating that noradrenaline can regulate many aspects of brain energy metabolism through widespread adrenoceptor subtype expression in CNS, especially on astroglia, to participate in various aspects of neuron-astrocyte interactions (Cohen et al., 1997b, Obel et al., 2012). Thus, adrenoceptors, their signal transduction mechanisms, and their pathophysiological significance, particularly in astrocytes, has attracted considerable attention. Recent data have shown the expression of a broad spectrum of adrenoceptor subtypes in primary cultured astrocytes and their potential to modulate an array of astroglial cell functions (Hertz et al., 2004, Hertz et al., 2010).

The adrenoceptors are a major sub-class of G protein-coupled receptor, which respond to adrenaline or noradrenaline and can be subdivided into three broad sub-groups, the α_1-, α_2- and β-adrenoceptors. Each adrenoceptor sub-group contains three distinct gene-products (α_{1A}, α_{1B}, α_{1D}; α_{2A}, α_{2B}, α_{2C}; β_1, β_2, β_3). Thus, the biological actions of adrenaline and noradrenaline are mediated via these nine adrenoceptor subtypes (Hertz et al., 2010), which can be shown to be primarily located at the plasma membrane of neurons and glia. The

neurotransmitter noradrenaline is considered to be primarily responsible for activating astrocytic adrenergic signalling and thus participating in neuron-astrocyte communication by means of important intracellular second messengers, such as cyclic AMP and Ca^{2+}.

It is well known that Ca^{2+} elevation in astrocytes following stimulation of neuronal afferents can be attributed to activation of astrocytic G_q-coupled GPCRs (Agulhon et al., 2008), which in turn can result in the release of gliotransmitters, including glutamate, ATP, and perhaps D-serine (Wolosker et al., 2016), to interact with pre- and/or postsynaptic neuronal receptors, thus leading to the activation of neuron-to-astrocyte communication and synaptic plasticity (Verkhratsky et al., 2012a). However, *in situ* or *in vivo*, it becomes more difficult to precisely and selectively pinpoint the astrocyte-derived Ca^{2+} response, because of the widespread expression of adrenoceptors in the CNS. This gives rise to another advantage of *in vitro* experiments to more easily identify G_q protein-triggered Ca^{2+} responses using pharmacological or genetic manipulation in purified primary cultures of astrocytes. It is well accepted that the α_1-adrenoceptor couples to G_q to produce an increase in intracellular Ca^{2+} via activation of phospholipase C and consequent generation of inositol 1,4,5-trisphosphate (IP_3) and diacylglycerol. In this Chapter, different adrenoceptor agonists and antagonists have been used to investigate the expression of the G_q-coupled α_1-adrenoceptor subtype in rat primary astrocytes, and how this regulates Ca^{2+} mobilization.

Cyclic adenosine 3',5'-monophosphate (cAMP) is also regarded as an influential astrocytic second messenger. cAMP is generated following activation of adenylyl cyclase by G_s-coupled GPCRs stimulation, while its formation is negatively regulated by $G_{i/o}$-coupled GPCRs. β-adrenoceptors are reported to be expressed throughout the CNS (Nicholas et al., 1993), however, the adrenoceptor subtype distribution and their relative roles are still unclear and controversial (Junker et al., 2002b, Mori et al., 2002, Sapena et al., 1996). The activation of $G_{i/o}$-protein-coupled α_2-adrenoceptors can exert a direct inhibitory effect on the adenylyl cyclase, which opposes the effect of β-adrenoceptor stimulation. In addition, α_2-adrenoceptor agonists, such as dexmedetomidine, have been shown robustly to inhibit forskolin-stimulated cAMP accumulation (Chen et al., 2000). Further complexity also appears possible: for example, although β-adrenoceptors are considered primarily to couple to G_s proteins, there have also been reports of β_2 and/or β_3 adrenoceptors coupling to $G_{i/o}$ proteins (Woo et al., 2009, Hutchinson et al., 2007). Since β-adrenoceptors are considered to play crucial roles in synaptic plasticity and, even more importantly to this project, to

regulate glycogen turnover, one of my initial aims was to use membrane preparations and the PCR technique to determine β_1-, β_2-and β_3-adrenoceptor expression in rat primary astrocytes. Subsequent studies were aimed at identifying the roles of different adrenoceptor subtypes in regulating Ca^{2+} and cAMP signalling in primary rat cerebrocortical astrocytes.

3.2. Results

3.2.1. Analysis of β-adrenoceptor subtype transcripts in the rat cerebrocortical astrocytes

To determine the expression of mRNA for each of the β-adrenoceptor subtypes in rat cerebrocortical astrocytes, total RNA was extracted as described in section 2.3.7.1 of the *Methods*. First-strand cDNA was synthesized from mRNA and used in the subsequent PCR as described in sections 2.3.7.3 and 2.3.7.5, respectively. The level of message for a housekeeping gene, glyceraldehyde 3-phosphate dehydrogenase (GAPDH), was used as a positive PCR control. Cultured rat cerebrocortical astrocytes were found to express mRNAs encoding β_1, β_2 and, to a much lesser extent, β_3 adrenoceptors (Figure 3.1). The GAPDH band was detected at 92 bp, while β_1-, β_2- and β_3-adrenoceptor bands were detected at 370, 330 and 517 bp, respectively. mRNAs for β_1- and β_2-adrenoceptors appear to be present at comparable levels, while message for the β_3 subtype was much less. A previous study (Oberheim et al., 2012) demonstrated that primary astrocytes derived from different regions of rat brain display physiological heterogeneity, including distinct receptor expression and different densities of specific receptor subtypes. Here, I have compared regional heterogeneity of β-adrenoceptor subtype expression using astrocytes derived from cerebellum. Compared to the data in rat cerebral astrocytes, there were no marked differences in β-adrenoceptor subtype expression in cells derived from this brain region (Figure 3.2).

To assess whether sex differences in β-adrenoceptor subtype expression occur in rat cerebrocortical astrocytes, primary cultures were prepared from male or female neonatal rats. Expression of β_1- and β_2-adrenoceptor subtypes appeared quite consistent between astrocyte extracts derived from male and female rats (Figure 3.3), however, some evidence for differences in β_3-adrenoceptor expression was obtained. In male astrocytes β_3-adrenoceptor expression was hardly detectable, while in female rat-derived astrocytes, the expression of β_3-adrenoceptor was more robust, approaching the level observed for β_1-adrenoceptor expression (Figure 3.3).
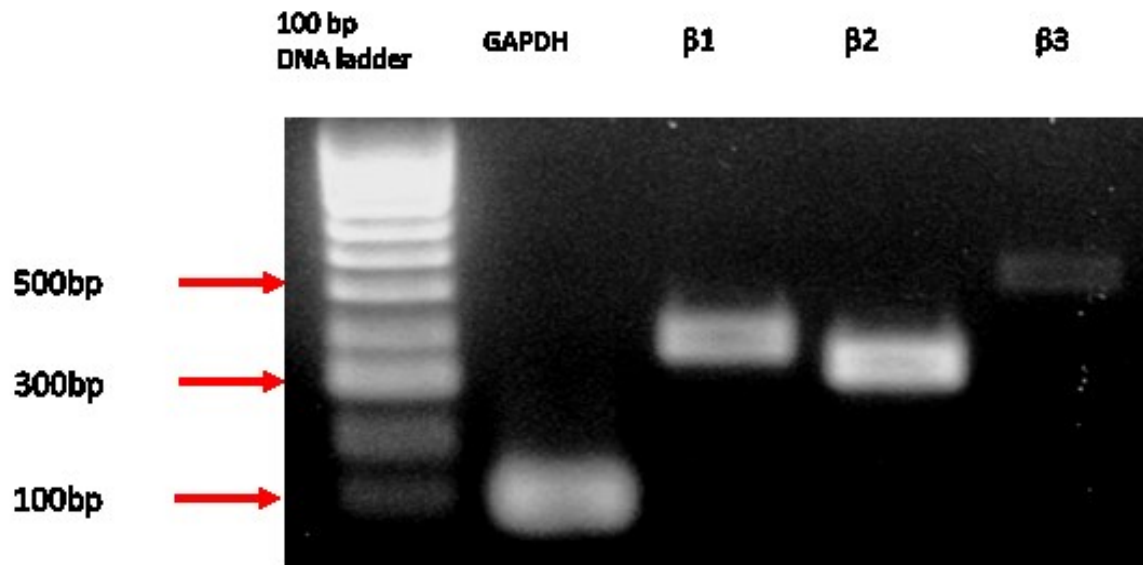
Figure 3.1. PCR products indicative of GAPDH, β_1-, β_2- or β_3-adrenoceptor mRNAs were assessed in rat astrocytes prepared from <u>cerebrocortices</u> obtained from mixed male and female neonates. A 1% agarose gel electrophoresis showed the correct size band of GADPH (92 bp), β_1-adrenoceptor (370 bp), β_2-adrenoceptor (330 bp) and β_3-adrenoceptor (517 bp). Gels were run at 85V in TAE buffer. The figure shows a representative experiment of 2 similar experiments with consistent results.
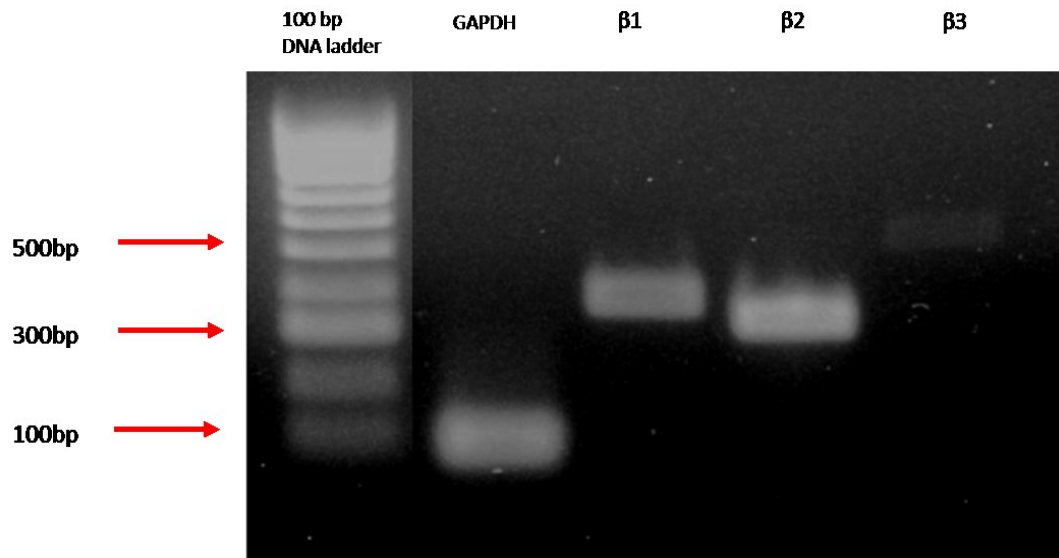
Figure 3.2. PCR products indicative of GAPDH, β_1-, β_2- or β_3-adrenoceptor mRNAs were assessed in rat astrocytes prepared from cerebella obtained from mixed male and female neonates. A 1% agarose gel electrophoresis showed the correct size band of GADPH (92 bp), β_1-adrenoceptor (370 bp), β_2-adrenoceptor (330 bp) and β_3-adrenoceptor (517 bp). Gels were run at 85V in TAE buffer. The figure shows a representative experiment of 2 similar experiments with consistent results.
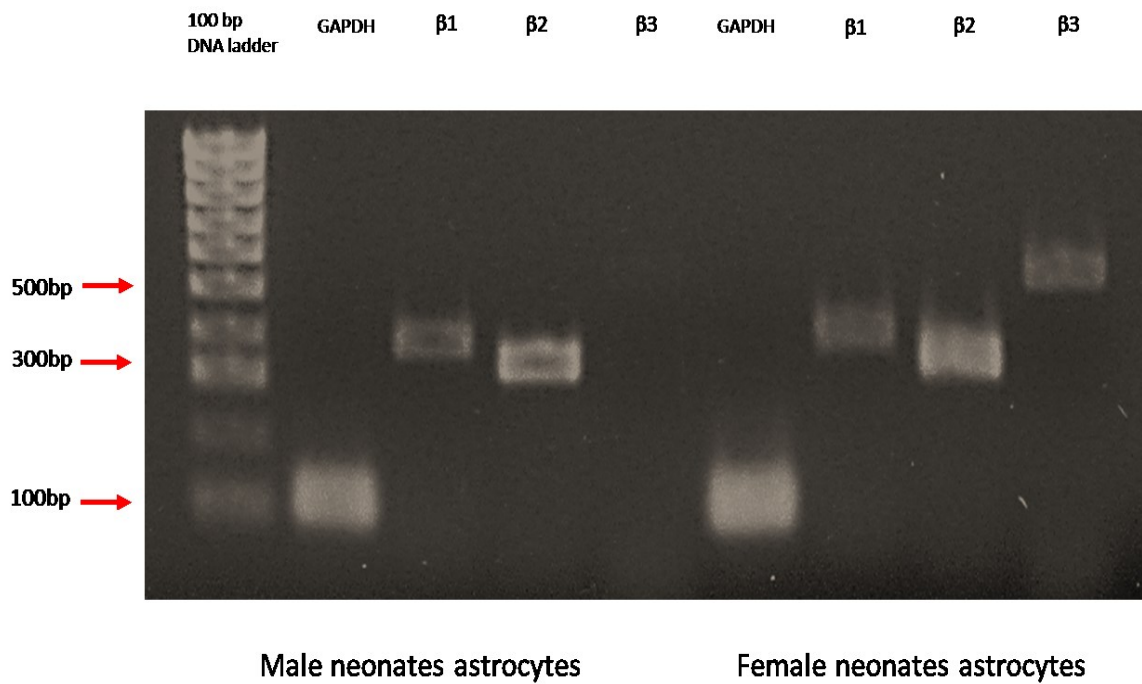
Figure 3.3. Comparison of β_1-, β_2- and β_3-adrenoceptor mRNA expression in rat astrocytes prepared from cerebrocortices of either male or female neonates. GAPDH as a positive control. A 1% agarose gel electrophoresis showed the correct size band of GADPH (92 bp), β_1 (370 bp), β_2 (330 bp) or β_3 adrenoceptor (517 bp). The gel was run at 85V in TAE buffer. The figure shows a representative experiment of 2 similar experiments with consistent results.

3.2.2. β-adrenoceptor quantification and subtyping

Having demonstrated the presence of mRNA for β-adrenoceptors in rat cerebrocortical astrocytes, radioligand binding assays were used to quantify the expression of β-adrenoceptors. As this work was carried out by another member of the laboratory only key findings are reported here. Initial attempts to quantify β-adrenoceptor density in monolayers of cerebrocortex astrocytes using the radioligands [^{3}H]CGP12177 and [^{125}I]cyanopindolol were unsuccessful. However, using highly-washed membranes prepared from cultured astrocytes, a high concentration of [^{125}I]cyanopindolol (200-250 pM) (to occupy all high-affinity binding sites) and timolol (5 µM) to determine non-β-adrenoceptor binding, it was possible to determine a β-adrenoceptor population of 101 ± 22 fmol/mg protein (mean ± s.e.m. for membranes prepared from 3 different batches of astrocytes). Competition binding curves were also constructed using the β-adrenoceptor antagonist CGP20712A. Used at concentrations of 10^{-10}-10^{-5} M, this highly β$_1$-selective agent maximally displaced 81 ± 8% of the timolol-displaceable binding, indicating that the majority of the β-adrenoceptors are of the β$_1$-subtype, with the remainder likely to be β$_2$-adrenoceptors.

3.2.3. Pharmacological analysis of adrenoceptor-stimulated cAMP accumulation in rat astrocytes

Functional evidence for β-adrenoceptor expression in rat astrocytes was obtained by analysis of cAMP responses following application of subtype-selective adrenoceptor agonists and antagonists. Experiments were initially performed to determine the time-dependency of cAMP accumulation in cultured rat primary astrocytes and whether the addition of phosphodiesterase inhibitors was required to maximize the dynamic range of the assay. Time-course experiments (Figure 3.4) showed that stimulation of astrocytes with either the β-adrenoceptor agonist, isoprenaline (1 µM; Figure 3.4A) or the direct adenylyl cyclase activator, forskolin (10 µM; Figure 3.4B) caused substantial, time-dependent increases in cAMP accumulation, which reached plateau levels after 15-30 min and then slowly declined. Perhaps surprisingly, pre-addition of the PDE inhibitor IBMX (300 µM) had no detectable effect on the initial cAMP accumulation time-course to either stimulatory agent, although in the presence of the inhibitor peak cAMP responses were sustained for longer (Figure 3.4A, B). In subsequent experiments a time-point of 10 min was selected as a convenient observation point and a PDE inhibitor was not used.
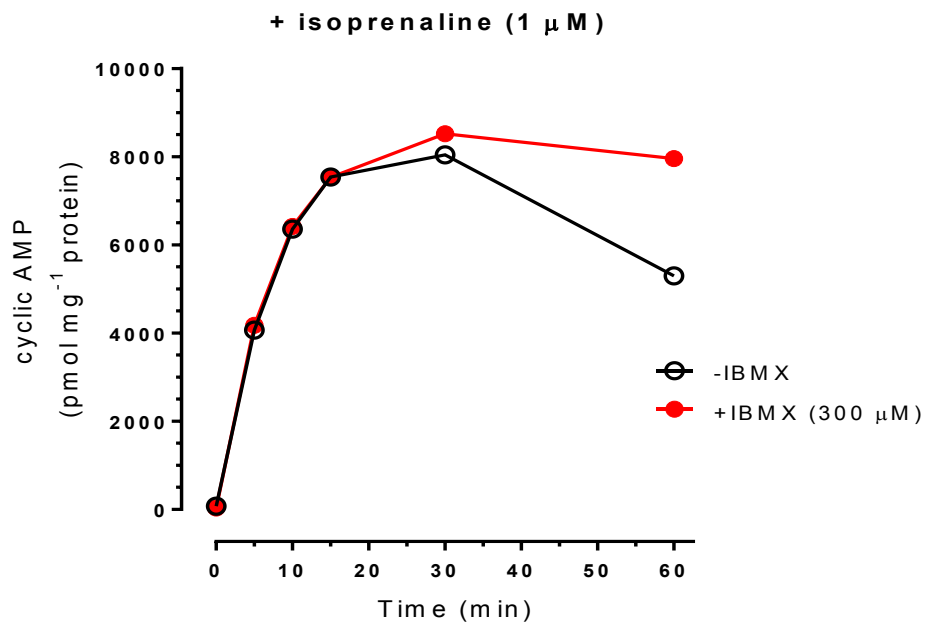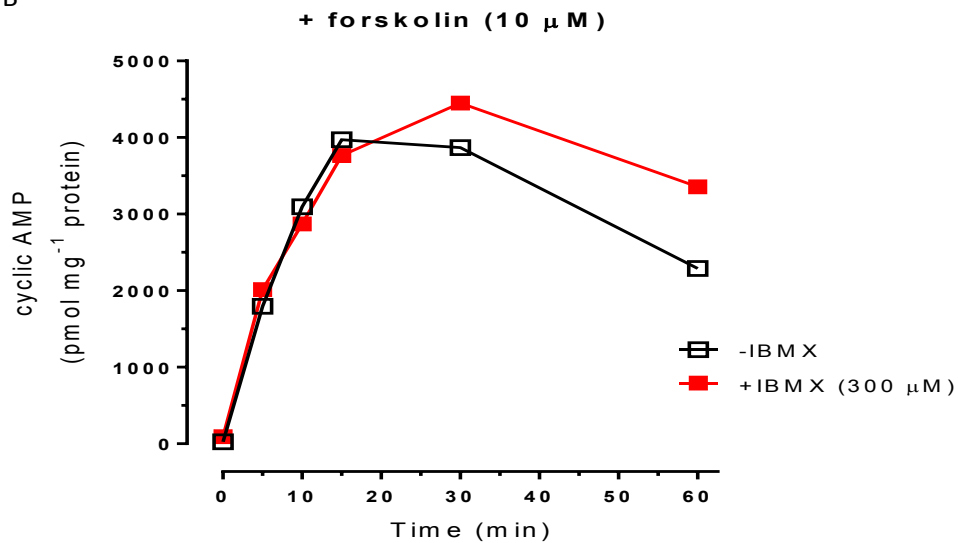
Figure 3.4. Representative time-course experiments showing cAMP accumulations stimulated by isoprenaline or forskolin in the absence and presence of IBMX. Near confluent monolayers of cerebrocortical astrocytes were incubated for different periods of time with isoprenaline (1 μM; panel A) or forskolin (10 μM; panel B) and cAMP determined as stated in *Methods*. Similar results were obtained in at least three independent experiments performed on different batches of primary astrocytes.

3.2.3.1. β-adrenoceptor subtype-mediated cAMP accumulation

The above findings, along with the previous evidence of mRNA expression β-adrenoceptor subtypes, which demonstrated a predominant expression of β_1 and β_2 adrenoceptors in astrocytes, were strongly suggestive of an involvement of β-adrenoceptor activation in the process of cAMP generation. To explore the role of β_1- and β_2-adrenoceptors in cAMP accumulation, isoprenaline was used to stimulate cAMP accumulation in the presence of different concentrations of different β-adrenoceptor antagonists (non-selective antagonist, timolol; selective β_1 adrenoceptor antagonist, CGP 20712A; selective β_2 adrenoceptor antagonist ICI 118,551). None of these antagonists alone affected cAMP accumulation in rat astrocytes. Pre-treatment (for 30 min) with either timolol or CGP 20712A concentration-dependently inhibited the cAMP accumulation to subsequent addition of isoprenaline (0.1 µM; 10 min): timolol: pIC_{50} (-log M) 8.823 ± 0.15; n=3; K_i = 3.02 x 10^{-10} M and CGP 20712A: pIC_{50} (-log M) 8.57 ± 0.14; n=4; K_i = 5.42 x 10^{-10} M (Figure 3.5A, B). In contrast, pre-treatment with different concentrations of ICI 118,551 only had a modest inhibitory effect on isoprenaline-stimulated cAMP accumulation (<20% inhibition at 1 µM ICI118,551; Figure 3.5C). These data indicate that β_1-, not β_2-adrenoceptors are functionally predominant in isoprenaline-stimulated cAMP accumulation in rat astrocytes.

3.2.3.2. Adrenoceptor involvement in cAMP responses to noradrenaline

The ability of the β-adrenoceptor agonist, isoprenaline to stimulate cAMP accumulation was compared to the neurotransmitter, noradrenaline. Addition of a maximally effective concentration of isoprenaline caused the basal cAMP level (27.9 ± 2.1 pmol/mg protein) to increase to 6598 ± 136 pmol/mg protein after a 10 min agonist exposure. This >200-fold increase occurred concentration-dependently (pEC_{50} (-log M) 7.60 ± 0.07; n=4). In contrast, noradrenaline evoked a much more variable increase in cAMP accumulation, which maximally was less 100-fold increase-over-basal (+noradrenaline (3 µM; 10 min), 2503 ± 451 pmol/mg protein). Pre-incubation with the broad spectrum α-adrenoceptor antagonist, phentolamine (10 µM; 30 min) markedly affected the concentration-dependent cAMP response to noradrenaline, with the peak cAMP accumulation (+noradrenaline (3 µM; 10 min), 6482 ± 232 pmol/mg protein) now approaching that seen for isoprenaline (Figure 3.6A). These data suggest that noradrenaline is stimulating opposing stimulatory (β) and inhibitory (α) adrenoceptor populations in cerebrocortical astrocytes to give the net cAMP accumulation responses to noradrenaline observed.

Similar experiments were performed in rat cerebellar astrocytes (Figure 3.6C). Although the cAMP response to isoprenaline was somewhat lower ($\geq$100-fold increase) there was again a large difference observed between the cAMP responses observed to isoprenaline versus noradrenaline. Again, pre-treatment with the α-adrenoceptor blocker, phentolamine markedly increased the response to noradrenaline to a level approaching, though in this case, not quite reaching that observed in response to isoprenaline addition (Figure 3.6C). Pertussis toxin (PTx) can be used to uncouple $G_{i/o}$-proteins from G protein-coupled receptor guanine nucleotide exchange factor activity (Moss and Vaughan, 1988). Pre-treatment of cerebrocortical astrocytes with PTx (100 ng/mL; 18 h) markedly increased cAMP responses to noradrenaline (Figure 3.6D), having a quantitatively similar effect to α-adrenoceptor blockade by phentolamine.

Since the importance of the sex of animals used in research studies has often been overlooked, a brief study was performed to determine whether any differences are observed with respect to the α- versus β-adrenoceptor involvement in mediating noradrenaline effects on cAMP accumulation in cerebrocortical astrocytes (Figure 3.7). Similar effects of phentolamine on noradrenaline-stimulated cAMP accumulation was observed in batches of primary astrocytes derived from male or female neonatal rats. In the presence of α-adrenoceptor blockade EC_{50} values for noradrenaline-stimulated cAMP responses were also similar (pEC_{50} (-log M) male, 6.80 $\pm$ 0.07; female 6.71 $\pm$ 0.09; n=3). These data indicate that there are no significant sex differences concerning the functional (cAMP) response to adrenoceptor subtype activation by the neurotransmitter, noradrenaline.
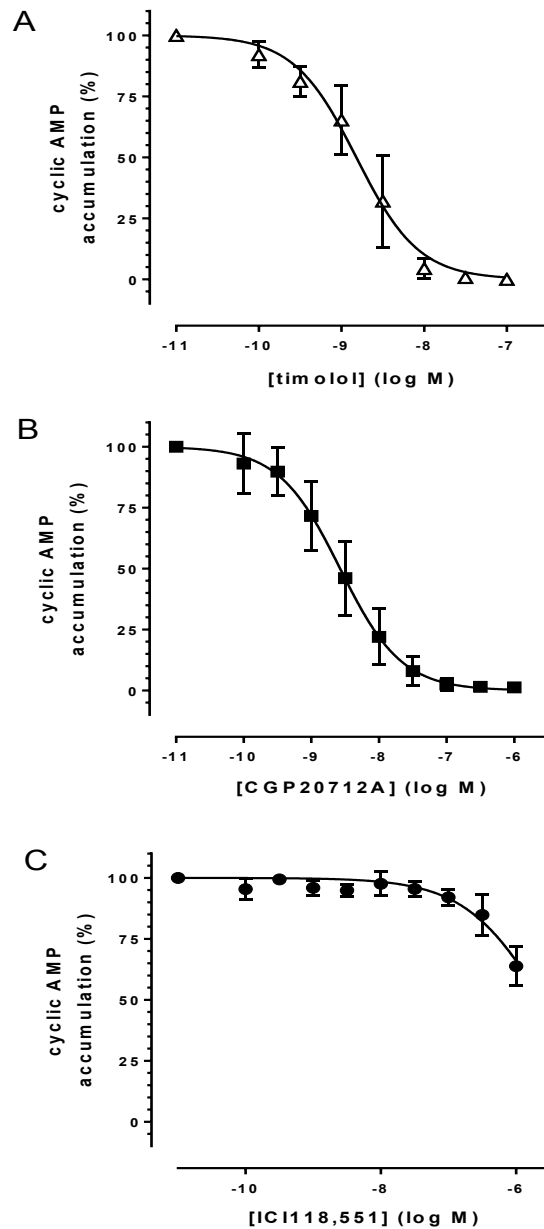
Figure 3.5. Inhibitory effects of the β-adrenoceptor antagonists on cAMP accumulation stimulated by isoprenaline (0.1 μM). Near confluent monolayers of cerebrocortical astrocytes were pre-incubated with different antagonists (non-selective antagonist, timolol; panel A), (selective β1 adrenoceptor antagonist, CGP 20712A; panel B) and (selective β2 adrenoceptor antagonist ICI 118,551; panel C) for 30 min prior to isoprenaline (0.1 μM, 10 min) and cAMP determined as stated in *Methods*. Data are shown as means ± S.E.M, for n=3 separate batches of cells.
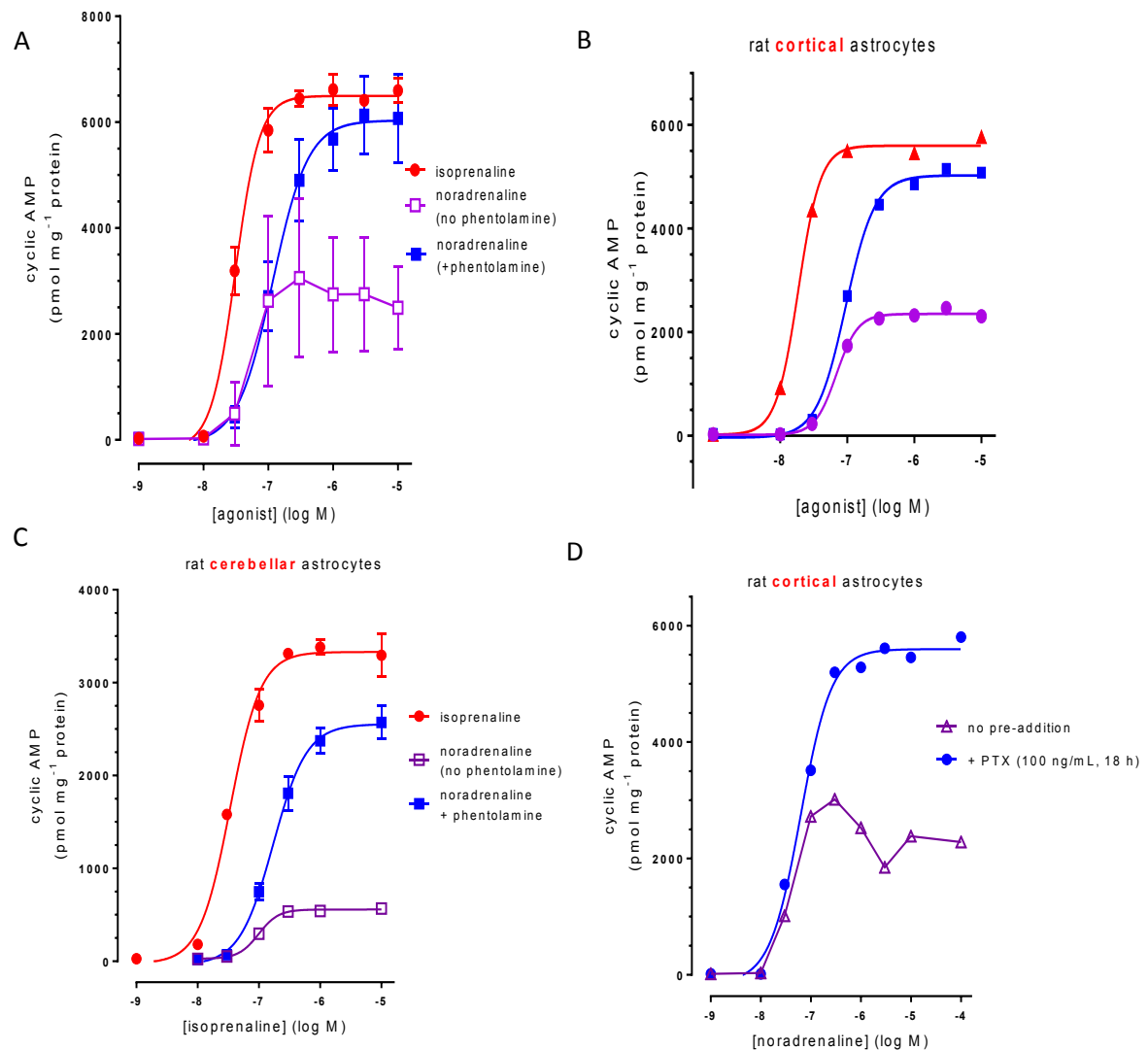
Figure 3.6. The cAMP response to noradrenaline in rat astrocytes involves co-activation of different adrenoceptor populations. Concentration-dependent cAMP accumulations stimulated by addition for 10 min of isoprenaline, noradrenaline or noradrenaline in the presence of the α-adrenoceptor antagonist phentolamine (10 μM; 30 min pre-treatment) in rat cerebrocortical astrocytes are shown for cumulative (n= 4) data (A) and a representative dataset (B). A similar response profile was found what this experiment was repeated in rat astrocytes obtained from cerebellum (C). Representative data (or 3 independent replicates) are also shown for the effect of overnight pertussis toxin treatment (PTX; 100 ng/mL, 18 h) on noradrenaline-stimulated cAMP accumulation in rat cortical astrocytes (D). Cyclic AMP levels were determined as described in *Methods*.

A

M ale neonate-derived astrocytes

cyclic AMP (pmol mg^{-1} protein) vs [noradrenaline] (log M)

□ no pre-addition
■ +phentolamine (10 μM)

B

Fem ale neonate-derived astrocytes

cyclic AMP (pmol mg^{-1} protein) vs [noradrenaline] (log M)

▽ no pre-addition
▼ +phentolamine (10 μM)
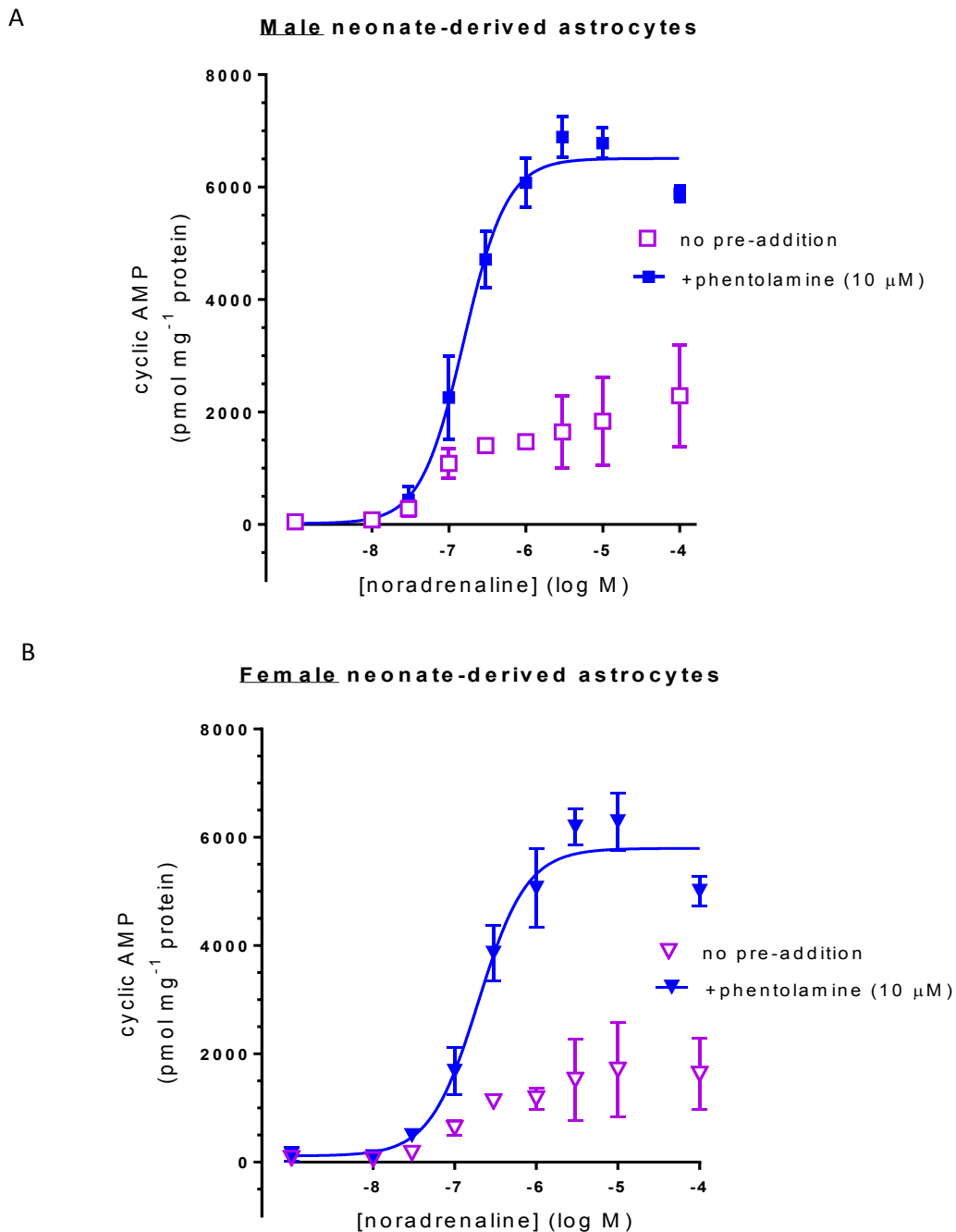
Figure 3.7. The interplay between α- and β-adrenoceptor activation to regulate cAMP accumulation is similarly observed in cerebrocortical astrocytes derived from male or female rats. The concentration-dependent action of noradrenaline on cAMP accumulation was determined the presence or absence of phentolamine (10 μM; 30 min pre-treatment) in near confluent astrocyte monolayers derived from cerebral cortex obtained from male (A) or female (B) neonatal rats. Cyclic AMP levels were determined as described in *Methods*. Data are shown as means ± S.E.M, for n=3 separate batches of cells.

3.2.3.3. Characterization of the inhibitory effects on astrocyte cAMP responses mediated by α₂-adrenoceptors

Preceding data suggest that astrocytes express mixed populations of adrenoceptor subtypes and as well as expressing an adenylyl cyclase stimulatory population of β-adrenoceptors (from a functional standpoint, primarily β₁), this cell-type co-expresses α-adrenoceptors that couple via Gα$_{i/o}$ proteins to inhibit adenylyl cyclase activity. Thus, in response to the natural ligand, noradrenaline, the observed response is a synthesis of both stimulatory and inhibitory inputs. The PTx-sensitivity of the inhibitory α-adrenoceptor likely indicates the involvement of an α₂-adrenoceptor subtype. To consolidate and extend these observations either isoprenaline or forskolin was used to stimulate cAMP accumulation and the effects of the α₂-adrenoceptor-selective agonist, dexmedetomidine investigated (Figure 3.8).

Dexmedetomidine (DEX) potently and concentration-dependently inhibited isoprenaline (ISO; 0.1 μM) -stimulated cAMP accumulation (pIC$_{50}$ (-log M), 8.71 ± 0.12; n=4; Figure 3.8A) in rat cerebrocortical astrocytes. The maximal inhibitory DEX effect was 50.5 ± 8.2% (+ISO, 6202 ± 142; +ISO/DEX, 3606 ± 390 pmol/mg protein; n=4), with quite a marked batch-to-batch astrocyte variation being observed (range of inhibitory DEX effects: 33.8-72.9%; n=4). DEX also potently and concentration-dependently inhibited cAMP accumulation stimulated by forskolin (10 μM)(pIC$_{50}$ (-log M), 8.85 ± 0.08; n=4; Figure 3.8B, C). In this case the maximal inhibitory DEX effect was greater (82.5 ± 3.9%; n=4) and the magnitude of the inhibitory effect more consistent from batch-to-batch of astrocytes (see Figure 3.8C). Finally, pre-treatment of cerebrocortical astrocytes with PTx completely ablated the DEX inhibitory effect on ISO-stimulated cAMP accumulation (Figure 3.8D).
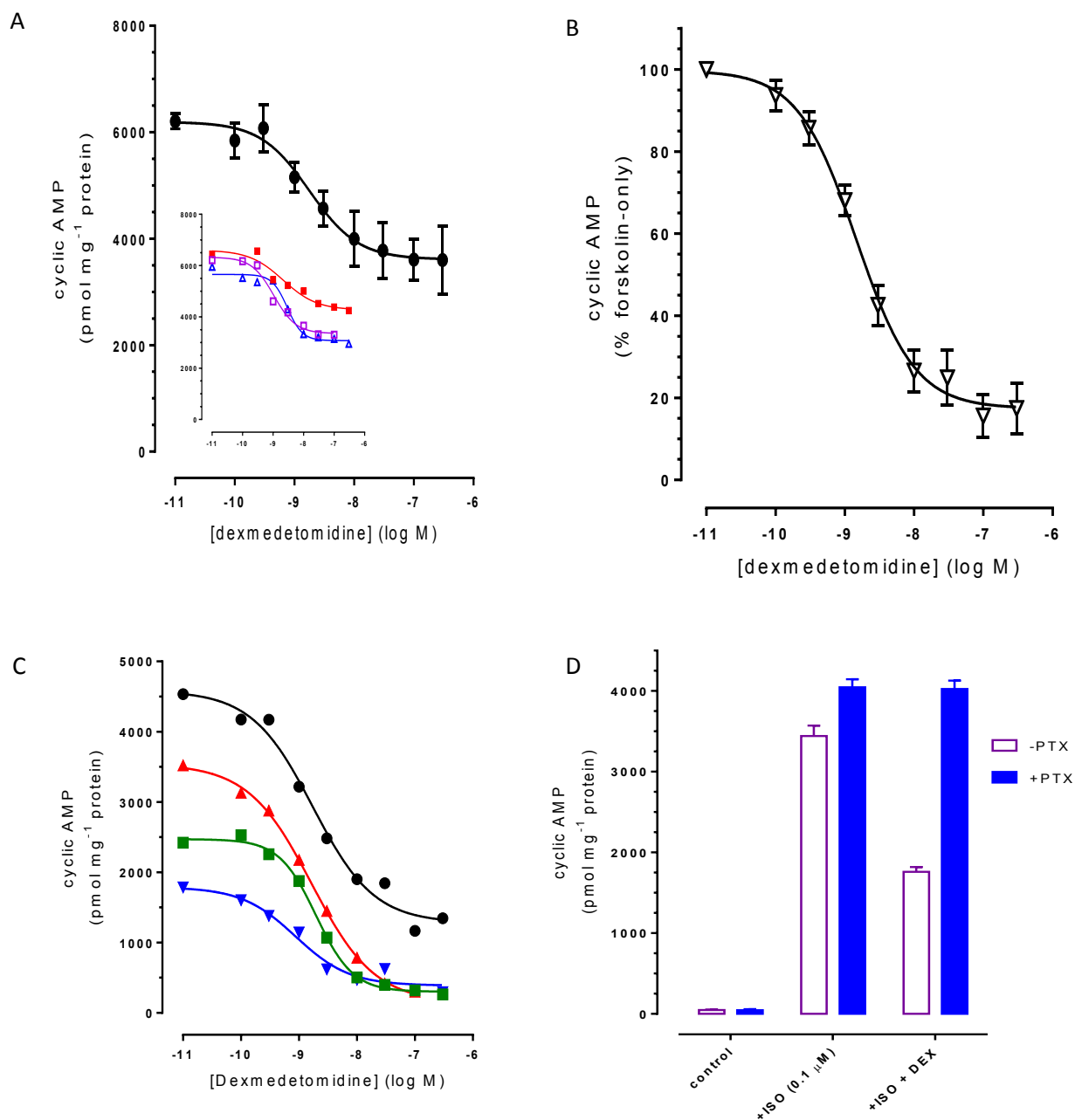
Figure 3.8. Inhibitory effects of the α_2-adrenoceptor agonist, dexmedetomidine on cAMP accumulation stimulated by either isoprenaline or forskolin. Panel (A) shows for a cumulative dataset (n=3) and individual experiments (inset) that pre-addition (for 10 min) of dexmedetomidine can concentration-dependently inhibit cAMP accumulation stimulated by isoprenaline (0.1 µM; 10 min) in rat cerebrocortical astrocytes. A more marked inhibitory effect of dexmedetomidine was observed with respect to cAMP responses stimulated by forskolin (10 µM; panel B; n=4; individual experiments on different batches of astrocytes are shown in panel C). The inhibitory effects of dexmedetomidine are ablated by pertussis toxin pre-treatment (D). Data are presented as means ± S.E.M.

3.2.4. Adrenoceptor-stimulated Ca²⁺ responses in rat cerebrocortical astrocytes

There is a wealth of evidence suggesting that astrocytes can communicate with neurons by means of Ca^{2+}-dependent gliotransmitter release. Diverse ranges and patterns of intracellular calcium concentration ($[Ca^{2+}]_i$) changes are triggered by exposure to various neurotransmitters in astrocytes (Rasooli-Nejad et al., 2014, Paukert et al., 2014a, Mothet et al., 2005), with noradrenaline and glutamate being considered particularly important neurotransmitters to stimulate astrocytes and trigger their downstream signalling transduction, through dynamic changes in $[Ca^{2+}]_i$. The Challiss lab has previously described the characterization of Ca^{2+} responses stimulated by the type 5 metabotropic glutamate (mGlu5) receptor in rat cerebrocortical astrocytes. Here I have performed a characterization of the adrenoceptor subtypes that contribute to astrocyte intracellular Ca^{2+} signalling.

Preliminary experiments focused on investigating the signalling changes and distribution in adrenoceptor-stimulated intracellular Ca^{2+} responses. Under basal conditions, fluo4-AM-loaded rat cerebrocortical astrocytes were treated with a maximal concentration of noradrenaline (100 µM), all cells exhibited immediate fluorescence changes reflecting increases in cytosolic free Ca^{2+} (Figure 3.9A, B). Astrocytes cultured in normal FCS medium display a flat and polygonal morphology, such that I could only observe fluorescence changes in the cell body. To further explore the involvement of astrocytic processes in the propagation of intercellular Ca^{2+} waves, we cultured astrocytes in serum-free medium containing G5 supplement for 3 days. After this time cells exhibited as a stellate phenotype astrocytes, and characteristic cell processes could be observed using microscopy. On noradrenaline addition the majority of cells analysed produced robust peak-plateau Ca^{2+} responses in both the soma and processes (Figure 3.9C, D), indicating that astrocytic processes may provide a means for communication with neighbouring astrocytes and neurons.
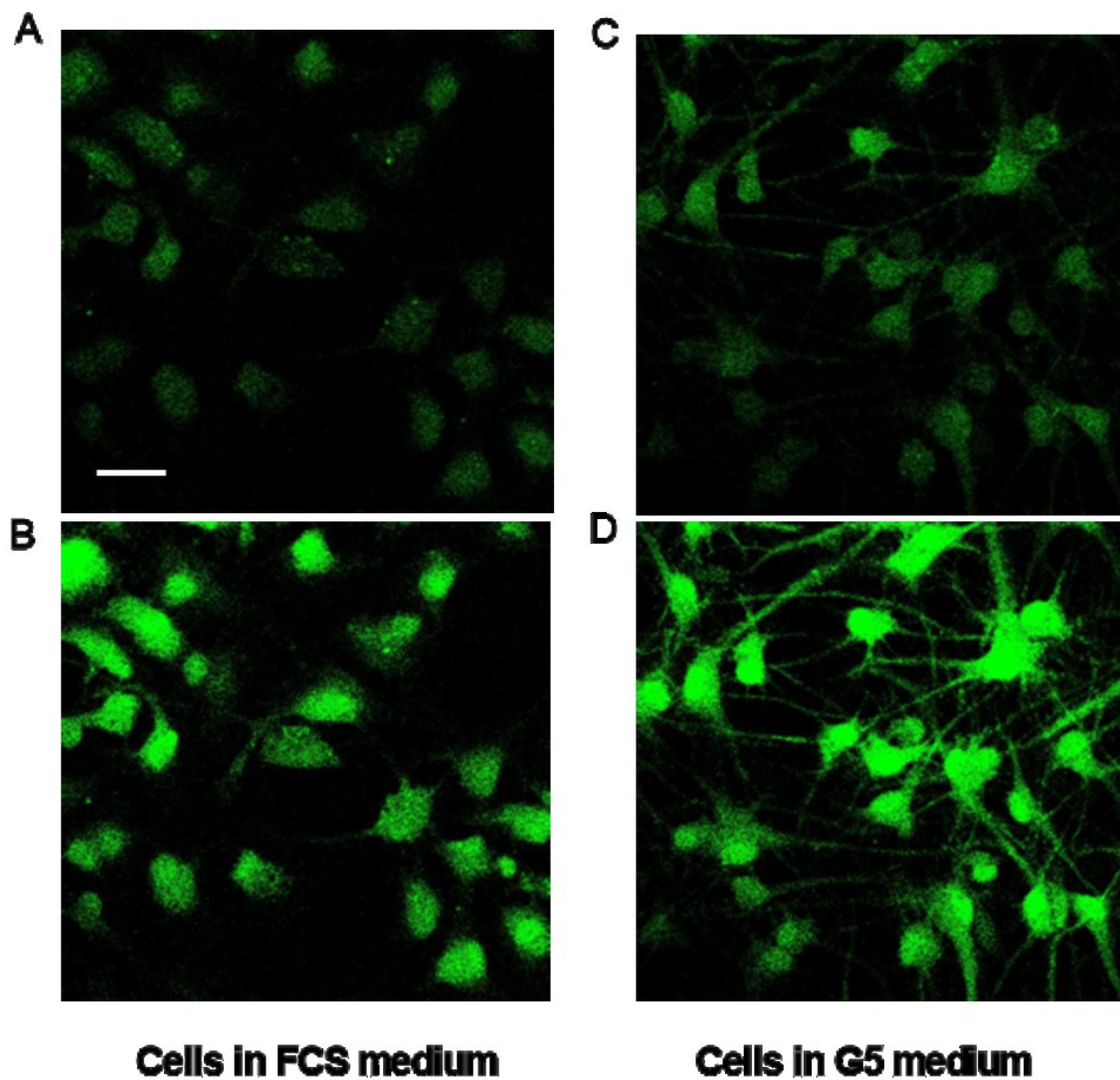
Figure 3.9. Noradrenaline (100 µM) increases [Ca^{2+}]$_i$ in rat cerebrocortical astrocytes. Cells were grown on coverslips in either FCS or G5-containing medium until sub-confluent; cells were loaded with fluo-4 AM for 30 min prior to agonist treatment. Digitized images of resting fluorescence from fields of astrocytes grown either in normal FCS medium (A, B) or in G5-supplemented medium (C, D) are shown. Application of noradrenaline (100 µM) triggered a rapid increase in fluorescence emission, indicative of a robust increase in [Ca^{2+}]$_i$ in all cells. Scale bar = 100 µm.

3.2.4.1. Noradrenaline-stimulated Ca^{2+} responses are β-adrenoceptor-independent

Since noradrenaline can bind to all adrenoceptor subtypes, including $α_1$-, $α_2$- and β-adrenoceptors, in order to identify which subtype(s) might be responsible for the Ca^{2+} response, single-cell Ca^{2+} responses elicited by agonist challenge were investigated in rat cortical astrocytes. Initially, cells were treated with the non-selective β-adrenoceptor agonist, isoprenaline (10 µM) for 2 min. No obvious Ca^{2+} response was observed (Figure 3.10A). In contrast, after a 5 min wash, an addition of noradrenaline (100 µM) produced a robust peak-plateau type Ca^{2+} response (Figure 3.10A). Addition of different concentrations of noradrenaline (ranging from 100 nM-10 µM), produced concentration-dependent increases in $[Ca^{2+}]_i$ (Figure 3.10D-F).

To confirm the lack of β-adrenoceptor involvement in the Ca^{2+} response to noradrenaline the β-adrenoceptor-selective antagonist timolol was used. Pre-incubation with timolol (10 µM), did not affect the Ca^{2+} response to noradrenaline (1 µM) addition to astrocytes (Figure 3.11A), with respective 4.3- and 4.2-fold Ca^{2+} responses relative to the basal level being observed (Figure 3.11C). In contrast, pre-incubation with the α-adrenoceptor-selective antagonist phentolamine (10 µM) completely blocked noradrenaline-stimulated Ca^{2+} responses (Figure 3.11D-F). These data suggest that α-, not β-adrenoceptors are responsible for astrocytic Ca^{2+} responses.
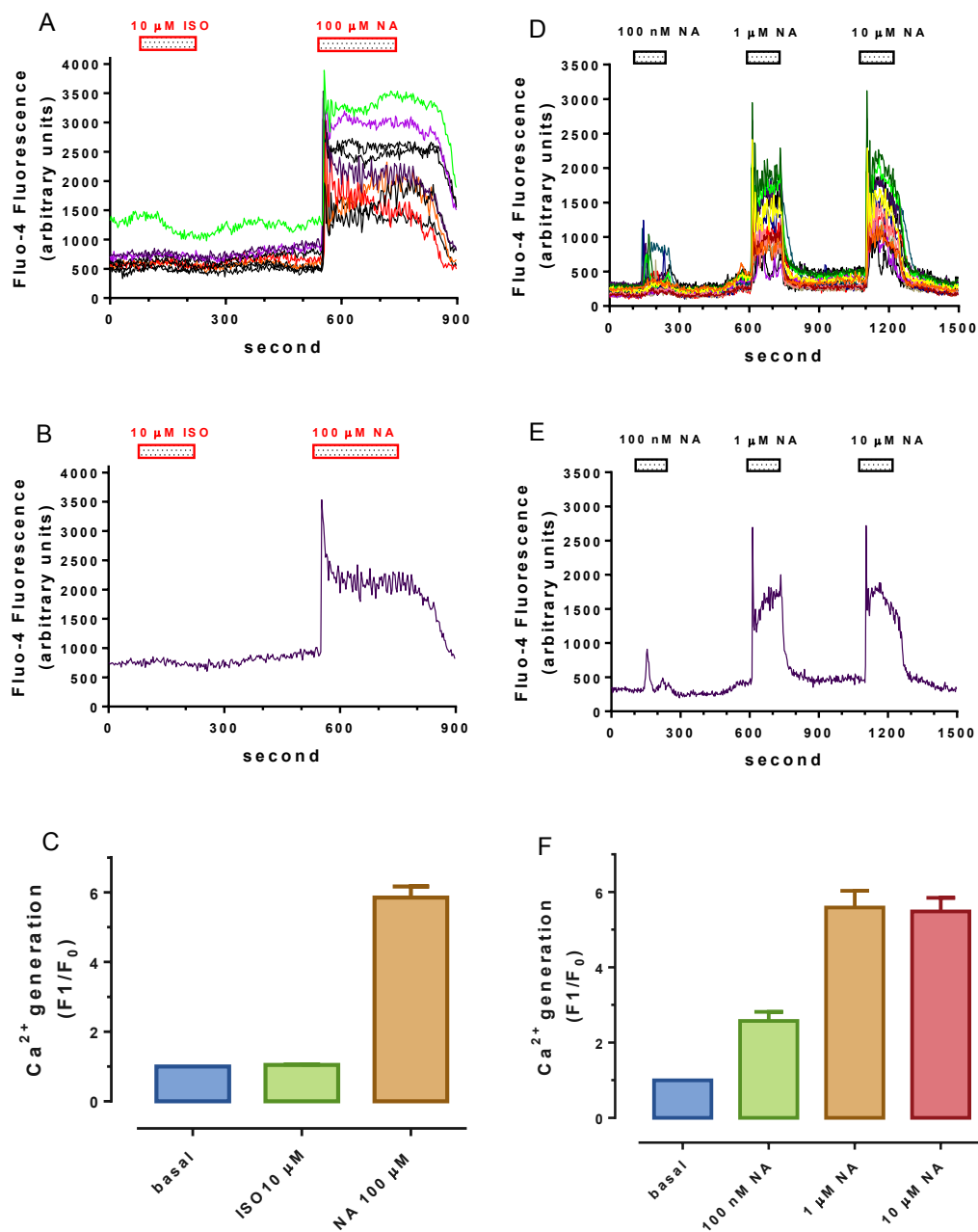
Figure 3.10. **Effects of noradrenaline and isoprenaline on intracellular Ca^{2+} responses in rat cerebrocortical astrocytes.** Cells were grown on coverslips in FCS medium until sub-confluent; cells were loaded with fluo-4 AM 30 min prior to agonist treatment. Panel (A) shows Ca^{2+} responses to sequential additions of isoprenaline or noradrenaline (NA). Panel (D) shows the effect of different NA concentrations on single cell Ca^{2+} responses in rat cortical astrocytes. Single representative traces are shown in panels (B) and (E). Agonist-elicited changes in [Ca^{2+}]$_i$ are quantified in panels (C) and (F), which are presented as means ± S.E.M. for at least 30 individual cells recorded in 3 separate experiments.
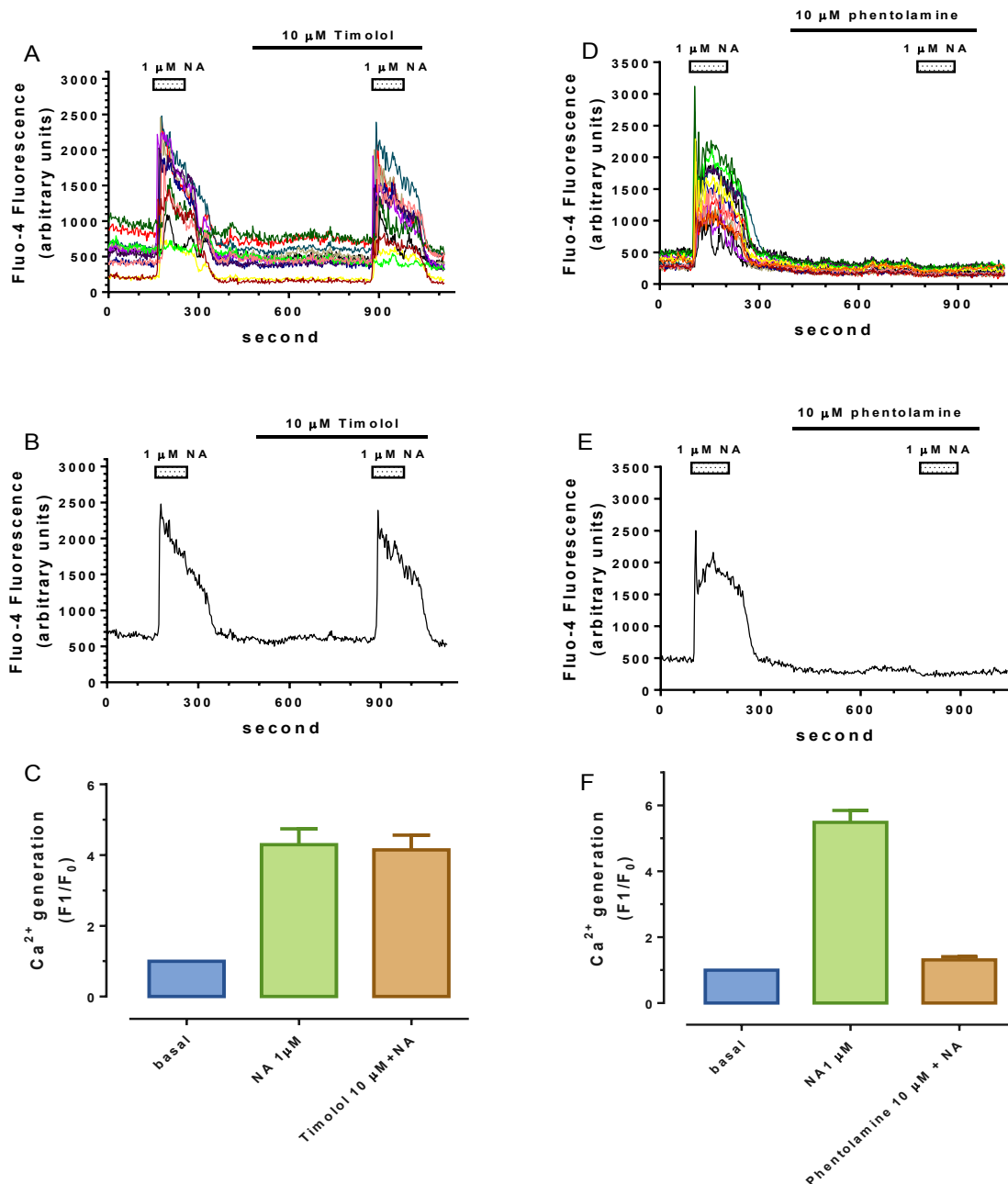
Figure 3.11. **Effects of non-selective α- and β-adrenoceptor antagonists on NA stimulated Ca^{2+} responses in rat cortical astrocytes.** Cells were grown on coverslip in FCS medium until sub-confluent, cells were loaded with fluo-4 AM 30 min prior to experiments and perfused with agonists and antagonists as indicated. Panel (A) shows NA elicited Ca^{2+} response was not blocked by pre-incubation with timolol. Panel (D) shows Ca^{2+} response stimulated by NA was completely inhibited by phentolamine pre-treatment. Representative traces showing the response of a single cell are shown in panels (B) and (E) respectively, agonists elicited Ca^{2+} increasing folds are shown in panels (C) and (F), which presented as means ± S.E.M. From at least 30 individual cells were recorded in 3 separate experiments.

3.2.4.2. α_1-Adrenoceptor subtype contributes to Ca^{2+} signalling in rat astrocytes

To determine the role of α-adrenoceptor subtypes in astrocytic [Ca^{2+}]$_i$ signalling activation, subtype-selective agonists and antagonists were used. Initially, we analysed whether activation of α_1- and α_2-adrenoceptor expressed in rat cortical astrocytic cells could lead to [Ca^{2+}]$_i$ increases. Dexmedetomidine (Dex, 100 nM) was first used at a concentration that should selectively activate α_2-adrenoceptors; at this concentration Dex did not trigger Ca^{2+} responses in the majority of cells analysed (Figure 3.12A-C). On the other hand, application of the α_1-adrenoceptor-selective agonist A61603 (100 nM) stimulated a robust Ca^{2+} response (Figure 3.12A-C). The contribution of α_1-adrenoceptors to Ca^{2+} homeostasis in astrocytes was confirmed using the α_1-adrenoceptor-selective antagonist prazosin. As seen in Figure 3.12D, prazosin (1 μM) addition completely blocked the Ca^{2+} response generated by addition of noradrenaline (100 μM).

However, a role of α_2-adrenoceptor in Ca^{2+} mobilization should not be completely discounted, since many studies carried out in different laboratories (Hertz et al. 2010; Hertz et al. 2004; Bekar et al. 2008; Chen et al. 2000) have shown that α_2-adrenoceptors can trigger Ca^{2+} responses in astrocytes. Addition of a higher concentration of dexmedetomidine (10 μM) caused a moderate increase in Ca^{2+} response that was either a single spike or baseline oscillatory (Figure 3.13A, B, E). To explore further if α_2-adrenoceptor stimulation contributes to astrocytic [Ca^{2+}]$_i$ increases, the α_2 adrenoceptor-selective antagonist yohimbine was used. Pre-addition of yohimbine (1 μM) failed to block Ca^{2+} responses stimulated by Dex (10 μM) (Figure 3.13A, B); in contrast, the α_1-adrenoceptor-selective antagonist prazosin (1 μM) did block Dex-induced [Ca^{2+}]$_i$ increases (Figure 3.13D, E). These data strongly suggest that the α_1-adrenoceptor subtype is responsible for noradrenaline-stimulated Ca^{2+} mobilization in rat cerebrocortical astrocytes and that at high (>μM) concentrations of dexmedetomidine (Dex) also stimulates this receptor subtype.
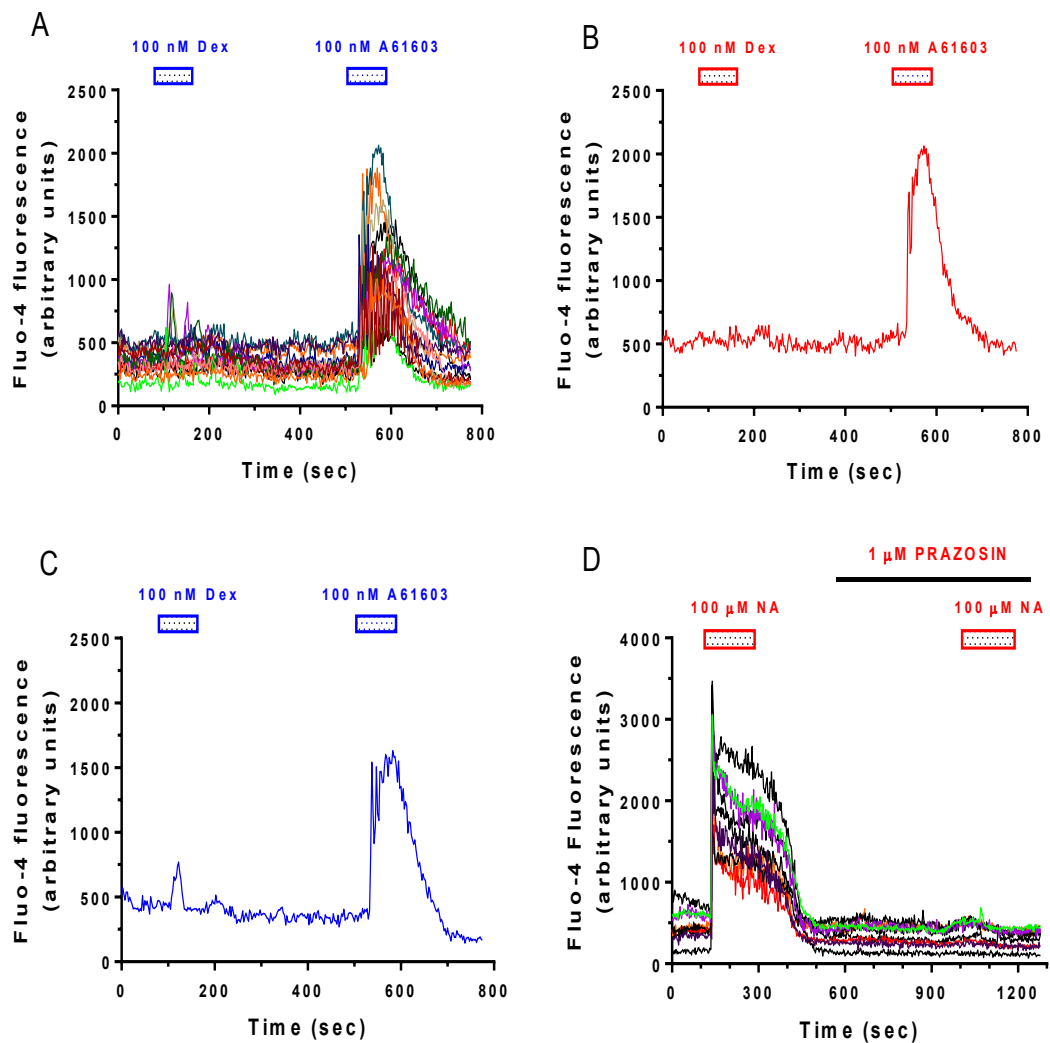
Figure 3.12. Ca^{2+} responses stimulated by selective α_1- and α_2-adrenoceptor agonists, and the effect of an α_1 adrenoceptor antagonist on noradrenaline-stimulated Ca^{2+} responses in rat astrocytes. Cells were grown on coverslip in FCS medium until sub-confluent, cells were loaded with fluo-4 AM 30 min prior to selective concentration of α_2-agonist dexmedetomidine (Dex, 100 nM) and α_1 agonist A61603 (100 nM). Data represent a number of superimposed single cell Ca^{2+} responses from one of three different astrocyte preparations (A), and two representative single-cell traces (B) and (C). Panel D shows that the effect of a maximally effective concentration of noradrenaline can be ablated by pre-treatment with the α_1-adrenoceptor antagonist prazosin (1 μM).
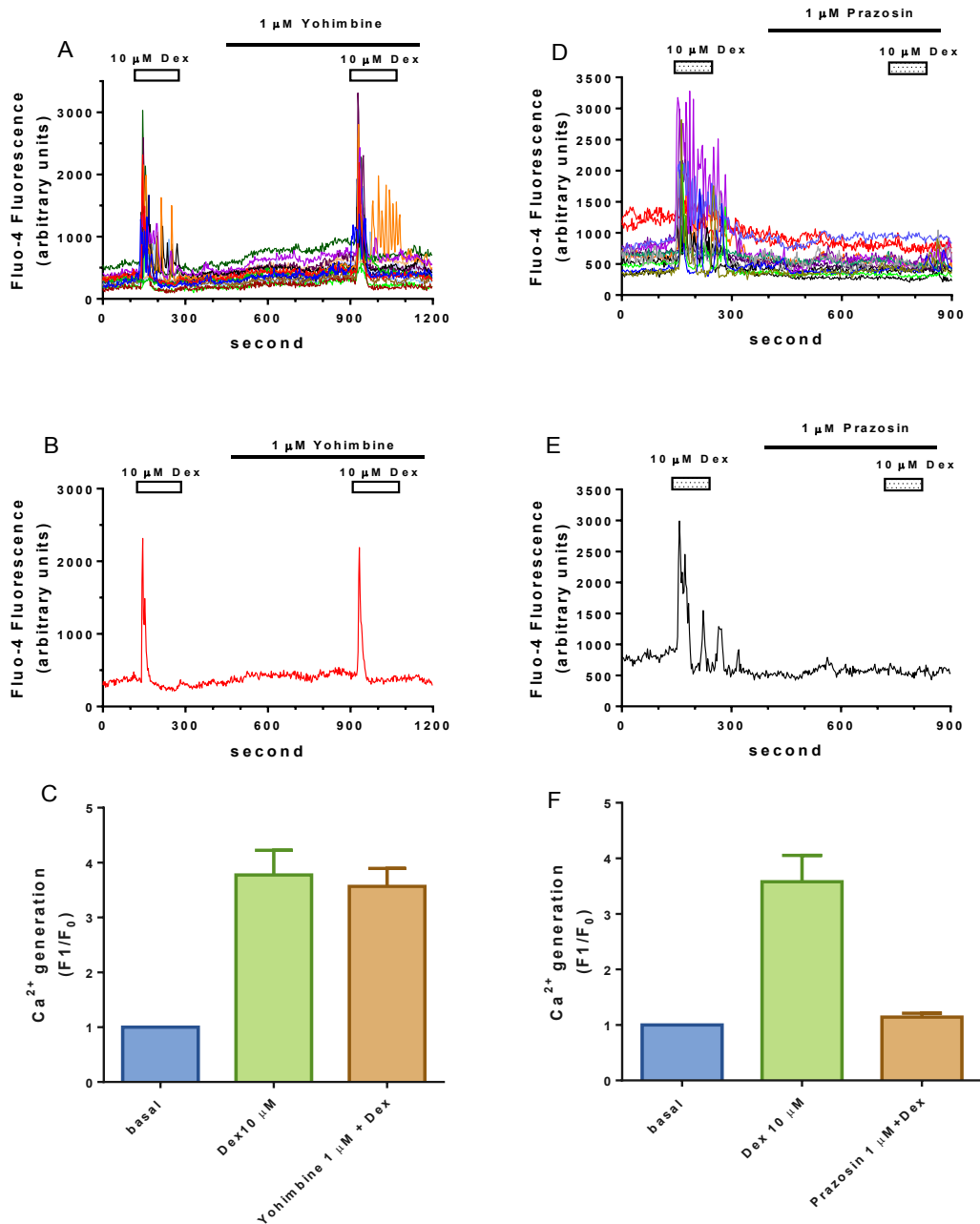
Figure 3.13. Ca²⁺ responses stimulated by a high concentration of the α₂-adrenoceptor agonist dexmedetomidine (Dex) are not blocked by α₂ adrenoceptor antagonist, yohimbine, but are inhibited by prazosin. Cells were grown on coverslip in FCS medium until sub-confluent, cells were loaded with fluo-4 AM 30 min prior to experiments and perfused with agonists (Dex) and/or antagonists as indicated. Data represent a number of superimposed single cell Ca²⁺ responses from one of three different astrocyte preparations (yohimbine, A; prazosin, D). Representative traces showing the response of single cells is shown in panels (B) and (E), respectively. Cumulative data are shown in panels (C) and (F), as means ± S.E.M. for at least 30 individual cells in 3 separate experiments.

3.2.4.3. Assessing the astrocytic α_1-adrenoceptor-mediated Ca^{2+} response

G protein-coupled receptors are subject to a number of regulatory mechanisms, including receptor desensitization, which usually occurs within minutes or even seconds of exposure to agonist (Freedman and Lefkowitz, 1996). The desensitization of astroglial α_1-adrenoceptors has been studied recently (Pankratov and Lalo, 2015a). To investigate further α_1-adrenoceptor desensitization, fluo-4-loaded astrocytes were stimulated by short (2 min) additions of a concentration of the α_1-adrenoceptor agonist A61603 (10 nM) that caused a sub-maximal increase in $[Ca^{2+}]_i$ (Figure 3.14). Using this protocol, no evidence for an attenuated Ca^{2+} response was observed with a second and third agonist application.

An alternative experimental protocol was next adopted. Two applications of A61603 (10 nM, 2 min) were again made, but in this case a high concentration of A61603 (1 µM, 3 min; termed R_{max}) was introduced between the two stimuli (termed R_1 and R_2). As shown in Figure 3.15A, when 5 min wash periods were used between R_1/R_{max} and R_{max}/R_2 only small differences were seen between R_1 and R_2 responses. However, when the second wash period between R_{max}/R_2 was shortened to 3 min an attenuation of the R_2 response relative to R_1 could be observed (Figure 3.15D, F; $p<0.01$) suggesting that desensitization does occur, but that α_1-adrenoceptor-mediated Ca^{2+} responses recover quickly following agonist washout.

Taken together, I conclude that α_1-adrenoceptor stimulation can result in receptor desensitization that can be observed as a diminished Ca^{2+} response, and which presents a time- and concentration-dependent phenomenon. Full recovery (re-sensitization) was achieved after only a short washout period ($\leq$5 min).
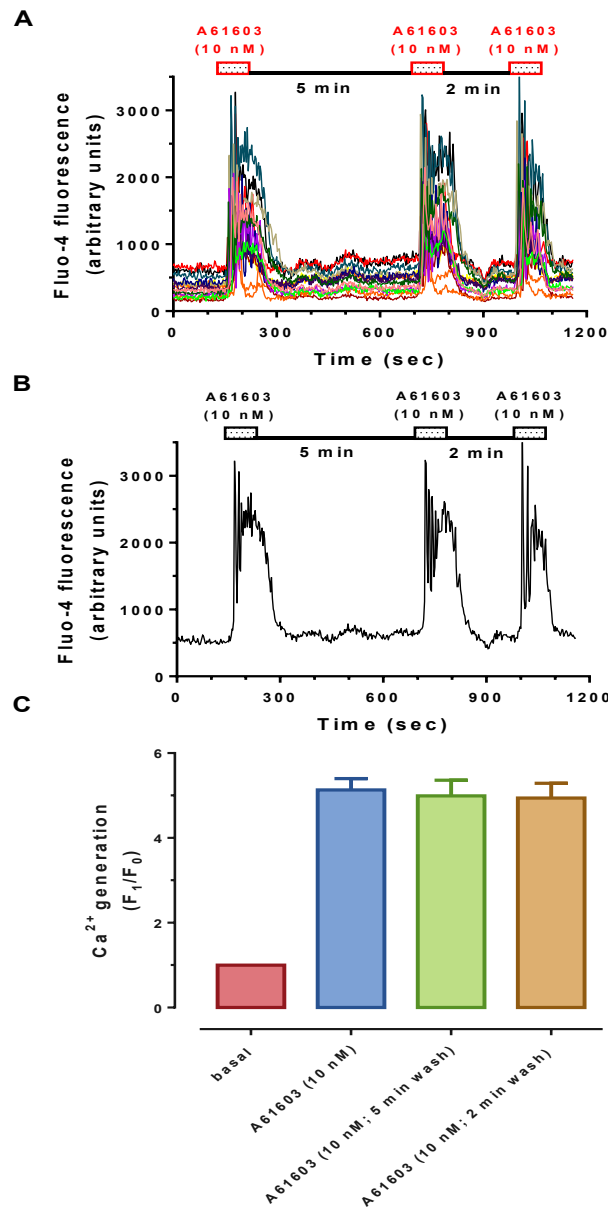
Figure 3.14. **Repeated addition of sub-maximal concentrations of A61603 does not cause attenuation of α₁-adrenoceptor-mediated Ca²⁺ responses.** Cells were grown on coverslip in FCS medium until sub-confluent, cells were loaded with fluo-4 AM 30 min prior to experiments and perfused with repetitive agonist treatment as indicated. Representative traces showing the response of a single cell are shown in panels (B). Agonist elicited Ca²⁺ increasing folds are shown in panels (C), which presented as means ± S.E.M. From at least 30 individual cells were recorded in 3 separate experiments.
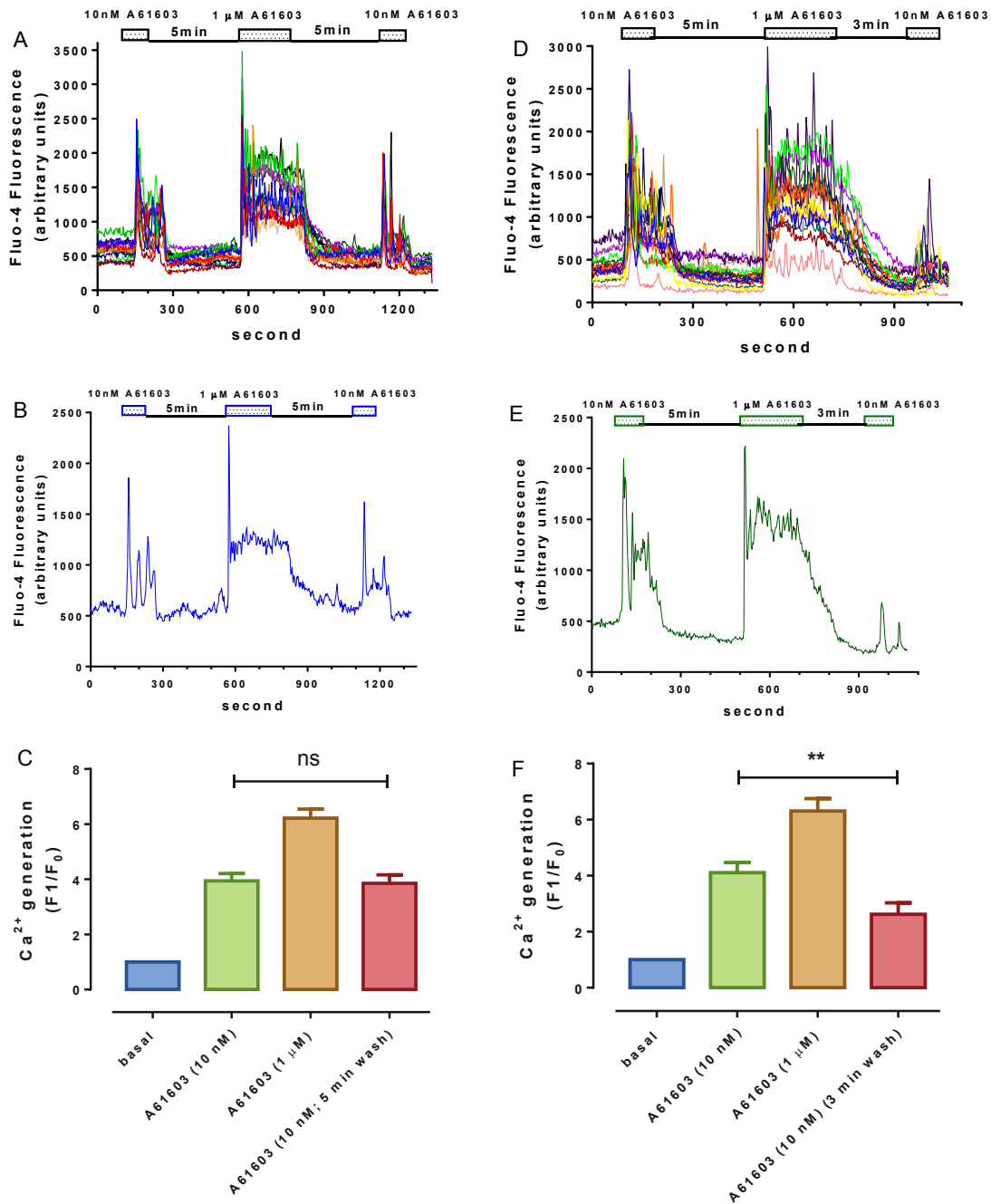
Figure 3.15. Time- and concentration-dependent desensitization of α_1-adrenoceptor-Ca^{2+} response in rat cortical astrocytes. Astrocytes were cultured on coverslip in 6-well plates until sub-confluent, then cells were loaded with fluo-4-AM for 30 min prior to experiments and perfused with agonists as indicated. Representative traces showing the response of a single cell are shown in panels (B) and (E) respectively. Agonists elicited Ca^{2+} increasing folds are shown in panels (C) and (F), which presented as means ± S.E.M. From at least 30 individual cells were recorded in 3 separate experiments.

3.2.4.4. Concentration-dependency of α_1-adrenoceptor-mediated Ca^{2+} responses in rat cortical astrocytes

I next examined the effects of different α_1-adrenoceptor agonists to increase $[Ca^{2+}]_i$ in rat cortical astrocytes. The α_1 adrenoceptor-selective agonists, A61603 (Figure 3.16A-C) and phenylephrine (Figure 3.16D-F) caused a concentration-dependent increases of Ca^{2+} response, analysis of the concentration-response curves revealed EC_{50} values of 6.3 nM (pEC_{50} (-log M), 8.20 ± 0.10) and 0.55 µM (pEC_{50} (-log M), 6.56 ± 0.20), respectively.

Our lab has previously reported that rat cortical astrocytes grown in serum-free medium supplemented with G5 growth factors have increased expression of the mGlu5 receptor (Bradley and Challiss, 2012). In order to assess whether growth in G5-containing medium also alters α_1-adrenoceptor responses, we assessed Ca^{2+} responses to phenylephrine in cells grown for >48 h in G5 supplemented medium. Under these growth conditions the concentration-response curve to phenylephrine was ≥10-fold left-shifted (pEC_{50} (-log M): 7.34 ± 0.11; Figure 3.16G-I). A more simple explanation for this change in responsiveness is an up-regulation in α_1-adrenoceptor expression, although proving this using western blotting and a subtype-specific antibody proved problematic (Jensen et al. 2009)
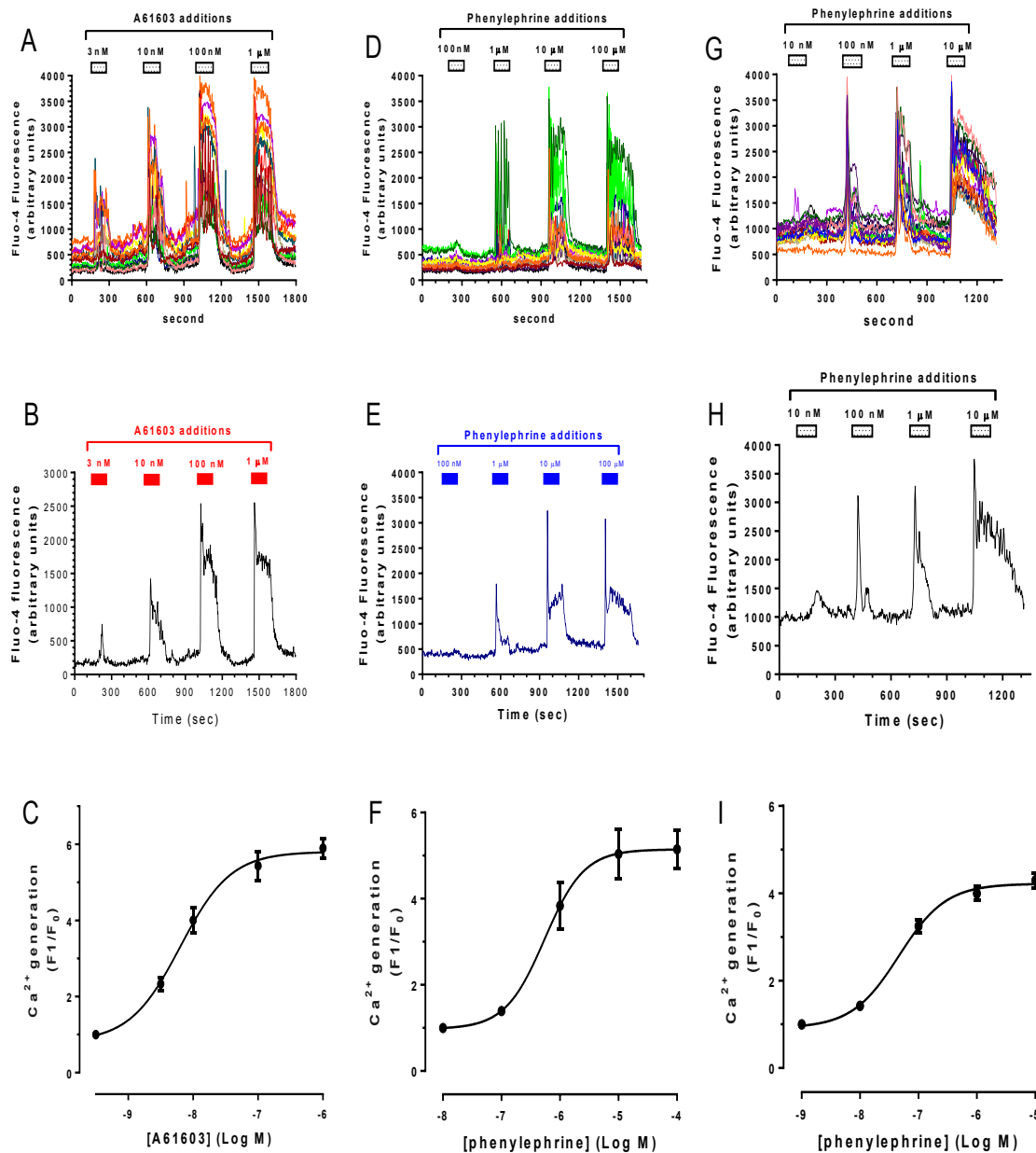
Figure 3.16. Concentration-dependent Ca^{2+} responses mediated by α$_1$-adrenoceptor activation in rat cortical astrocytes. Astrocytes were cultured on coverslip in FCS medium (A and D) or in G5-supplemented medium (G) until sub-confluent, then cells were loaded with fluo-4-AM for 30 min prior to experiments and perfused with α$_1$ agonists A61603 (A) or phenylephrine (D and G). The washout intervals between each addition was 5 min. Representative traces showing the response of a single cell are shown in panels (B), (E) and (H), respectively. Concentration-response curves for the Ca^{2+} response are shown in panels (C), (F) and (I), where data-points present means ± S.E.M. from at least 30 individual cells recorded in 3 separate experiments.

3.2.4.5. Cross-talk between adrenoceptor subtypes: effects of co-activation on intracellular Ca^{2+} responses

It has been well documented that Ca^{2+} signalling by one type of GPCR can be influenced by stimulation of a different type of GPCR, since there exists a possibility that interactions between different GPCRs coupling preferentially to different signalling pathways might result in potentiation or attenuation of Ca^{2+} signalling (Werry et al., 2003). Such interactions have important implications, allowing cells precisely to regulate $[Ca^{2+}]_i$ in a diversity of cellular processes and physiological functions.

Previous work reported earlier has demonstrated that β-adrenoceptors do not stimulate Ca^{2+} responses *per se* (see Figure 3.10). Here, a further experiment has been performed to assess the possibility that cross-talk between G_s-coupled β-adrenoceptors and G_q-linked α_1-adrenoceptors might modify Ca^{2+} responses in astrocytes. Therefore, phenylephrine (PE, 1 μM) was applied in the absence or presence of isoprenaline (1 μM); as shown in Figure 3.17A-C, co-addition of isoprenaline did not significantly alter phenylephrine-stimulated Ca^{2+} responses.

Cross-talk interactions between G_i- and G_q-coupled receptors have also been identified as modifiers of Ca^{2+} responses in a number of different systems (Selbie and Hill, 1998). Experiments presented here provided no evidence for α_2-adrenoceptor-mediated Ca^{2+} signalling in astrocytes *per se* (see Figures 3.12 and 3.13). In order to identify whether the co-activation of a G_i-coupled receptor could enhance Ca^{2+} signalling in the presence of G_q protein-coupled receptor stimulation, α_1- (phenylephrine, 0.1 μM) and α_2-(dexmedetomidine, 0.1 μM) agonists were used. At this concentration, each agonist induced a small Ca^{2+} response (1.4 and 1.5-fold, respectively; Figure 3.17F), however, co-stimulation with both agonists simultaneously produced a more robust Ca^{2+}-response (2.7-fold; Figure 3.17F). If the dexmedetomidine concentration was increased further (to 1 μM) a further significant augmentation (3.4-fold, Figure 3.17F) could be observed. These data suggest that synergistic effects can be observed when a sub-maximal stimulus at the α_1-adrenoceptor is accompanied by co-activation of α_2-, but not β-adrenoceptors.
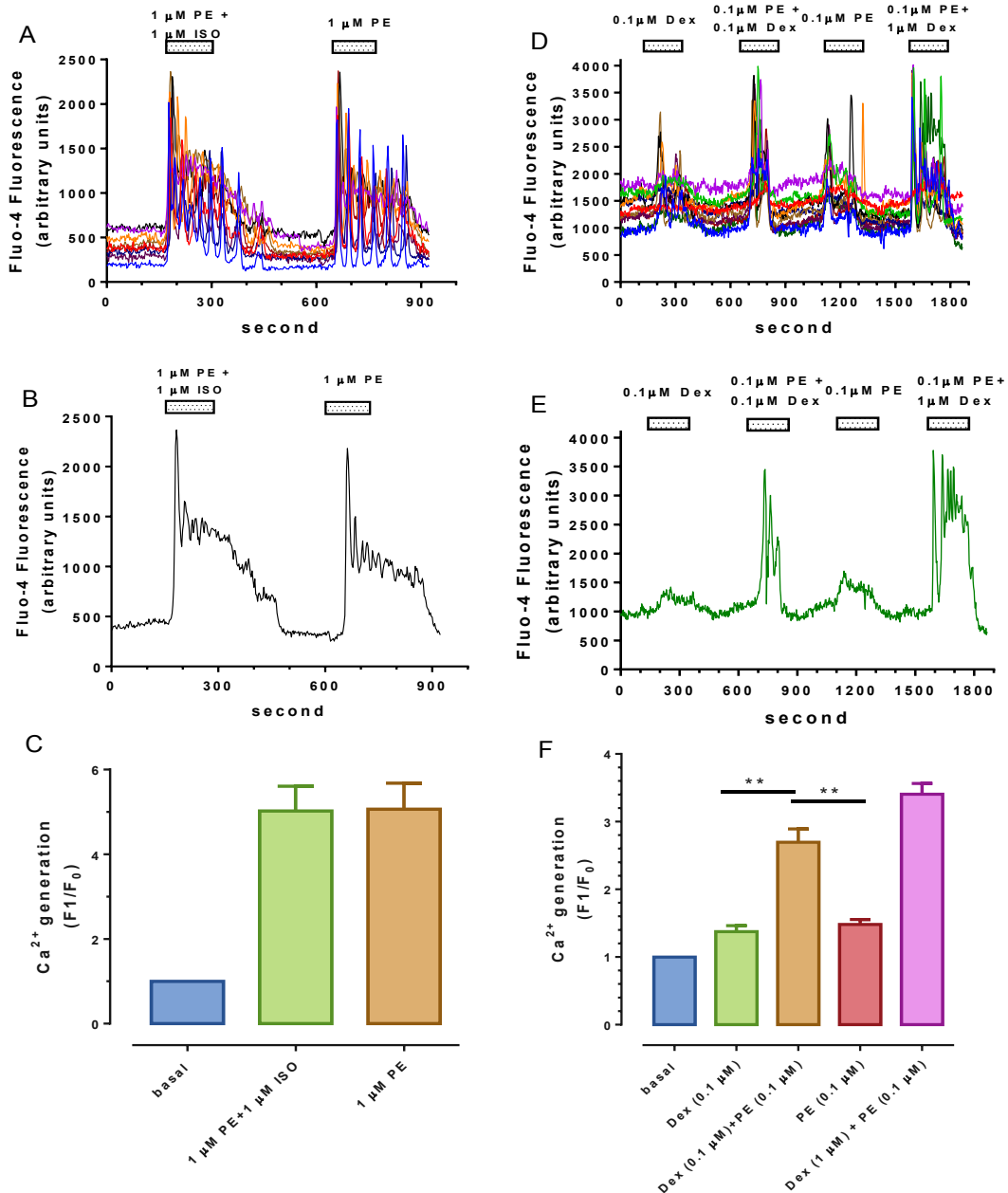
Figure 3.17. **The effects of adrenoceptor subtype interactions on intracellular Ca^{2+} responses in rat cortical astrocytes.** Astrocytes were cultured on coverslips in 6-well plates until sub-confluent, then cells were loaded with fluo-4-AM for 30 min prior to experiments. (A-C) shows phenylephrine-stimulated Ca^{2+} responses in the absence or presence of isoprenaline. (D-F) shows the cross-talk relationship between phenylephrine and dexmedetomidine. Representative traces showing the response of a single cell are shown in panels (B) and (E) respectively. Cumulative data for agonist-stimulated Ca^{2+} responses are shown in panels (C) and (F), presented as means ± S.E.M. from at least 30 individual cells were recorded in 3 separate experiments. [**]$p<0.01$ (one-way ANOVA, Dunnett's *post hoc* test).

3.2.4.6. The roles of intracellular and extracellular Ca^{2+} in α_1-adrenoceptor stimulated Ca^{2+} responses

The concentration-dependent effects of α_1-adrenoceptor agonist on intracellular Ca^{2+} signalling were described previously (Figure 3.16). From those experiments, different patterns of change in intracellular Ca^{2+} concentration could be observed following agonist addition, including single-peak, oscillatory and peak-plateau responses. Representative traces showing single-cell Ca^{2+} responses to different concentrations of A61603 are shown in Figure 3.18A-C. Although some Ca^{2+} response variation was attributable to astrocyte-to-astrocyte heterogeneity, and donor animal preparations, a striking correlation between the concentration of agonist applied and the signature Ca^{2+} response could often be observed. As can be seen in Figure 3.18, low concentrations of A61603 (3 nM) trigger small, single-peak responses (28 out of 50 cells; others no response); increasing the agonist concentration (to 10 nM), increased response amplitude in each cell, and caused a significant proportion of cells (40%, 20 out of 50 cells) to exhibit an oscillatory Ca^{2+} response. Increasing A61603 concentration to 100 nM, caused some cells to continue to show oscillatory responses (often on an elevated baseline; 24%, 12 out of 50 cells), however, other cells transitioned into peak-plateau Ca^{2+} responses; indeed at a A61603 concentration of 1 μM, almost all cells exhibited as peak-plateau responses (49 out of 50 cells).

Next, I investigated the effects of altering the availability of different sources of Ca^{2+} for the $[Ca^{2+}]_i$ response to G_q-coupled α_1-adrenoceptor activation. Loading astrocytes with BAPTA-AM (100 μM; 20 min) could completely abolish any changes in $[Ca^{2+}]_i$ caused by A61603 addition (Figure 3.19C). Astrocytes were next challenged with concentrations of A61603, which cause primarily a peak-plateau (1 μM; Figure 3.19A) or an oscillatory (100 nM; Figure 3.19B) Ca^{2+} response; agonist was washed out after 2 min agonist exposure and cells perfused with medium containing a high concentration of EGTA (3 mM) to chelate $[Ca^{2+}]_o$ (Figure 3.19A). Under these conditions, re-addition of the same concentration of A61603 resulted in a single-peak increase in Ca^{2+} indicative of the discharge of intracellular (endoplasmic reticular) stores. To confirm this, cells were challenged with A61603 in the absence of extracellular Ca^{2+}, either before or after the discharge of intracellular ER Ca^{2+} stores by addition of the SERCA inhibitor thapsigargin (2 μM; Figure 3.19D). It is noteworthy that following initial discharge of the ER Ca^{2+} store by A61603 addition, a sustained increase in $[Ca^{2+}]_i$ was observed upon re-addition of $[Ca^{2+}]_o$ (Figure 3.19D); this reflects store-operated Ca^{2+} entry (SOCE). These results indicate that α_1-adrenoceptor-stimulated Ca^{2+}

responses are initiated by mobilization of Ca^{2+} from intracellular stores, while extracellular Ca^{2+} is essential to sustain the (oscillatory or peak-plateau) response.
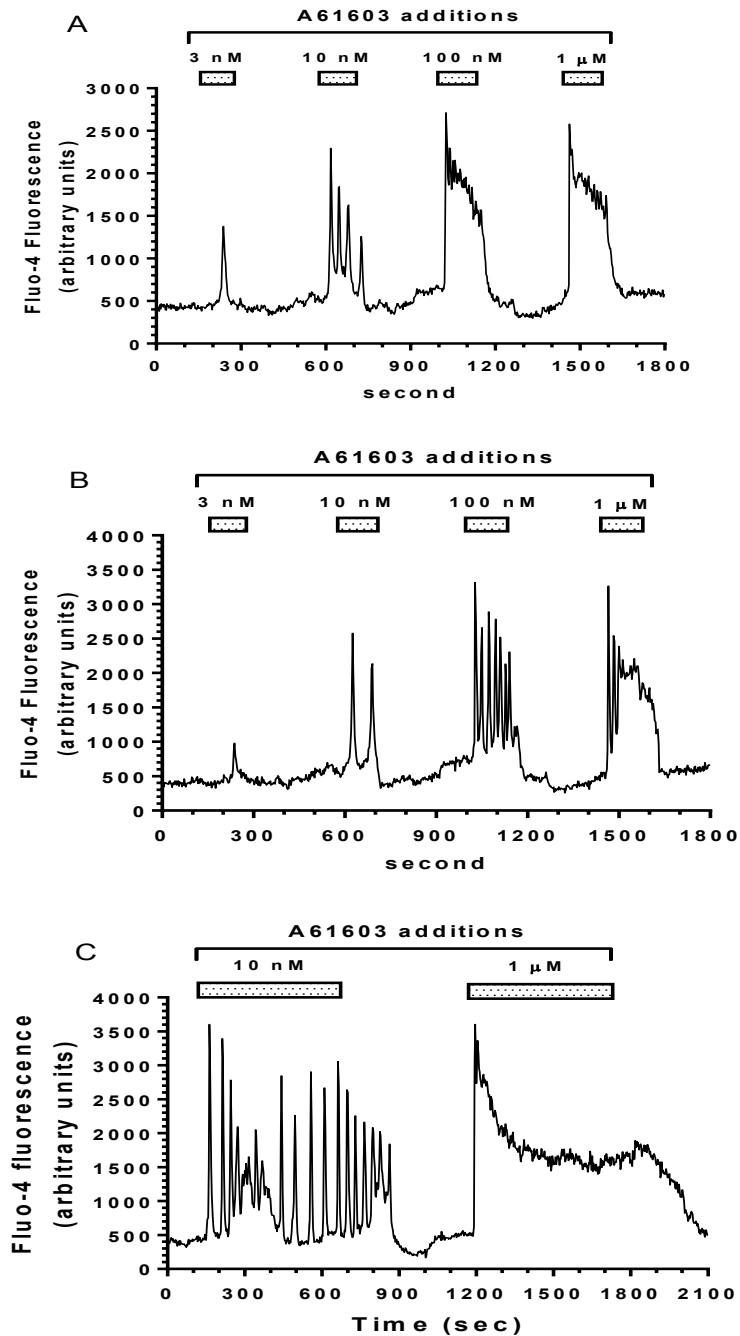
Figure 3.18. Representative examples of the different types of single-cell Ca^{2+} responses initiated in rat cortical astrocytes by addition of different concentrations of A61603. Cells were loaded with fluo-4-AM for 30 min prior to experiments and perfused with the indicated concentrations of α_1-adrenoceptor agonist A61603. (A) and (B) show two representative concentration-responses to A61603 (0.003 - 1 µM) stimulation from 50 cells were recorded in 4 experiments. Panel C shows different response patterns at low (10 nM) and high (1 µM) concentrations of A61603, representative of at least 30 cells recorded in 3 experiments.
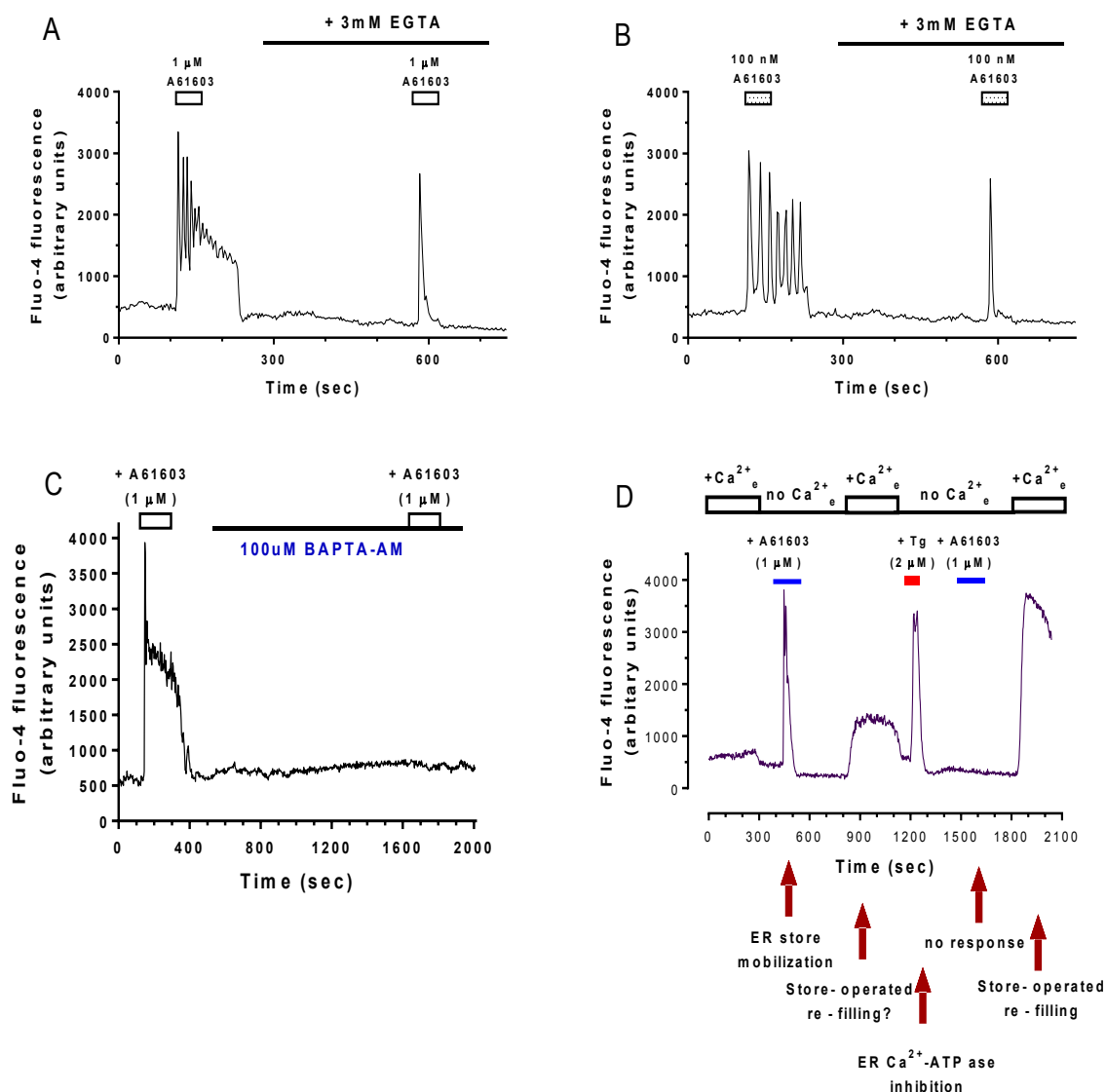
Figure 3.19. **The roles of intracellular and extracellular Ca²⁺ in rat cerebrocortical astrocytes stimulated by α₁-adrenoceptor agonist.** Representative traces show the effect of extracellular Ca^{2+} chelation by adding 3 mM EGTA on A61603 (1 μM) -stimulated Ca^{2+} responses (peak-plateau, A; oscillation, B). Panel C shows the effect of BAPTA-AM (100 μM, 20 min) pre-treatment on A61603 (1 μM) -stimulated Ca^{2+} responses. Panel D illustrates the roles of ER store Ca^{2+} and store-operated Ca^{2+} entry (SOCE) in the response to A61603. In all cases traces are representative of >25 cells recorded in at least three different batches of rat cortical astrocytes.

3.2.4.7. The effect of metabotropic glutamate (mGlu) receptor 5 activation on intracellular Ca^{2+} regulation in rat astrocytes

Another G_q-coupled GPCR, the type 5 metabotropic glutamate (mGlu5) receptor, has been previously characterized by our lab in rat cortical astrocytes grown in G5-supplemented serum-free medium (Bradley and Challiss, 2012). Here, single-cell confocal microscopy has been used to monitor Ca^{2+} responses to mGlu5 receptor activation in astrocytes grown in either FCS-containing or G5-supplemented medium. Addition of the mGlu1/5 receptor agonist, (S)-3,5-Dihydroxyphenylglycine (DHPG), caused concentration-dependent increases in Ca^{2+} response (Figure 3.20). At 0.3 µM DHPG only small, single-spike Ca^{2+} responses were observed (in 28 out of 50 cells, Figure 3.20A) in astrocytes grown in FCS-containing medium. Increasing the DHPG concentration to 1 µM resulted in bigger Ca^{2+} responses with only a minority of cells showing oscillatory as opposed to peak-plateau responses. At 10 µM, DHPG stimulated robust peak-plateau responses in the vast majority of cells (Figure 3.20A-C). The pattern of Ca^{2+} responses to DHPG in astrocytes grown in G5-supplemented medium was different. At a concentration of agonist (0.3 µM) that has only a modest effect in cells grown in serum, all cells exhibited an oscillatory Ca^{2+} response of low frequency (average 5 oscillations per 2 min). Increasing DHPG concentration (to 1 µM) did not alter the amplitude of the response, but increased the oscillation frequency (Figure 3.20E, F); another step increase in DHPG concentration (to 10 µM) caused a transition to a peak-plateau response in a minority of astrocytes.

In another set of experiments, astrocytes were grown in G5 supplemented medium for 5 days; this generated a population of cells that exhibited almost wholly Ca^{2+} oscillatory responses across the full range of DHPG concentrations (Figure 3.21). It was found that increasing the concentration of agonist did not affect the amplitude of the Ca^{2+} oscillation, but did alter oscillation frequency. Increasing the concentration of DHPG from 1 µM to 10 µM resulted in an approximate 50% increase in Ca^{2+} oscillation frequency (from 5 min^{-1} to 7.5 min^{-1}; Figure 3.21C, D). These data contrast somewhat with previous findings where it was reported that Ca^{2+} oscillation frequency is largely agonist-independent (Nash et al., 2002).
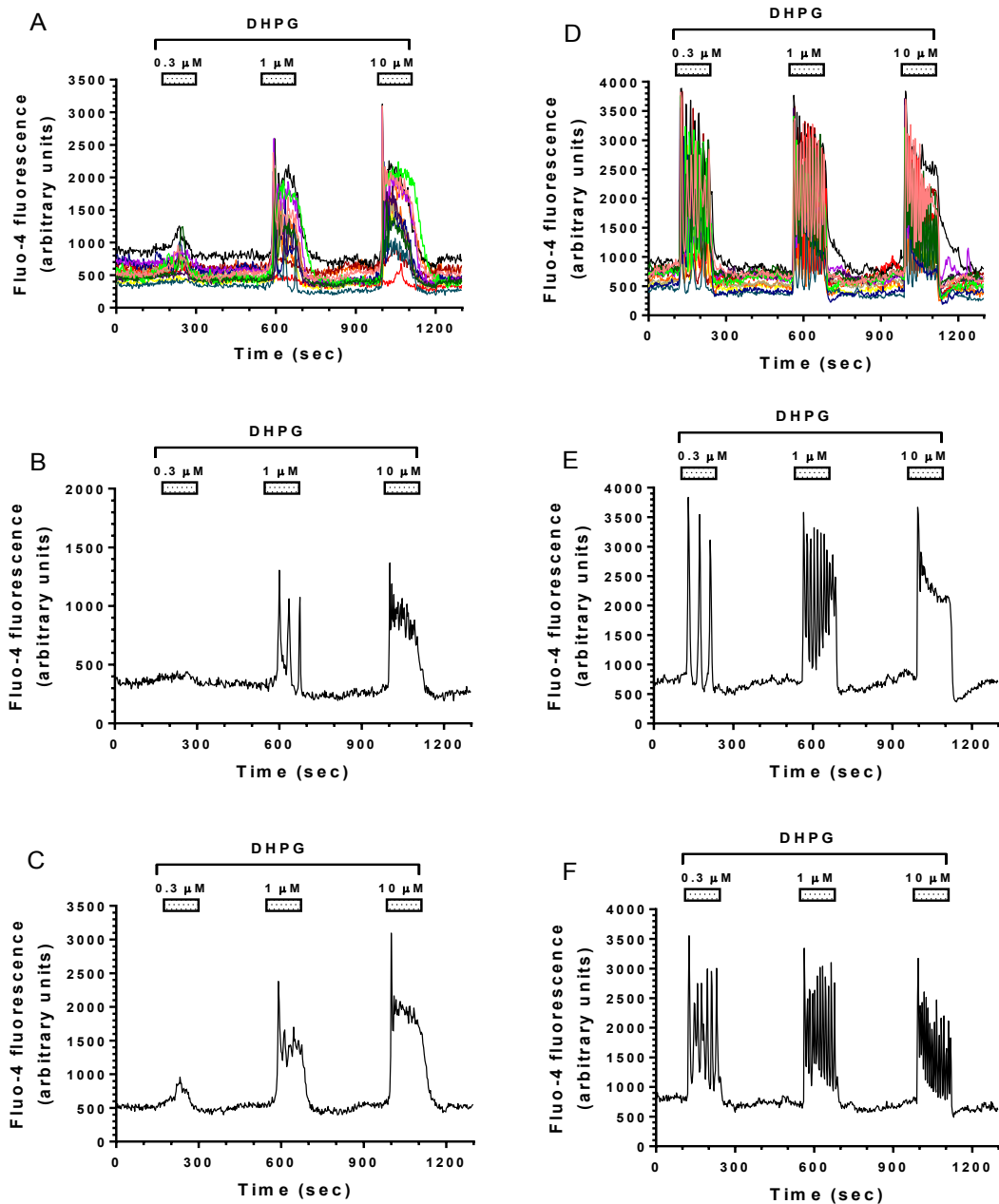
Figure 3.20. **Concentration-dependent Ca^{2+} response to (*S*)-3,5-dihydroxyphenylglycine (DHPG) in rat cortical astrocytes growing in either FCS-containing or G5-supplemented medium.** Astrocytes were cultured on coverslips in FCS-containing medium (A-C) or in G5-supplemented medium (D-F) until sub-confluent. Cells were preloaded with fluo4-AM and perfused with the indicated concentrations of DHPG (0.3 - 10 µM). Representative traces show the responses of a single cell in FCS medium (B, C) or in G5 medium (E, F). At least 30 cells were recorded in 3 separate experiments.
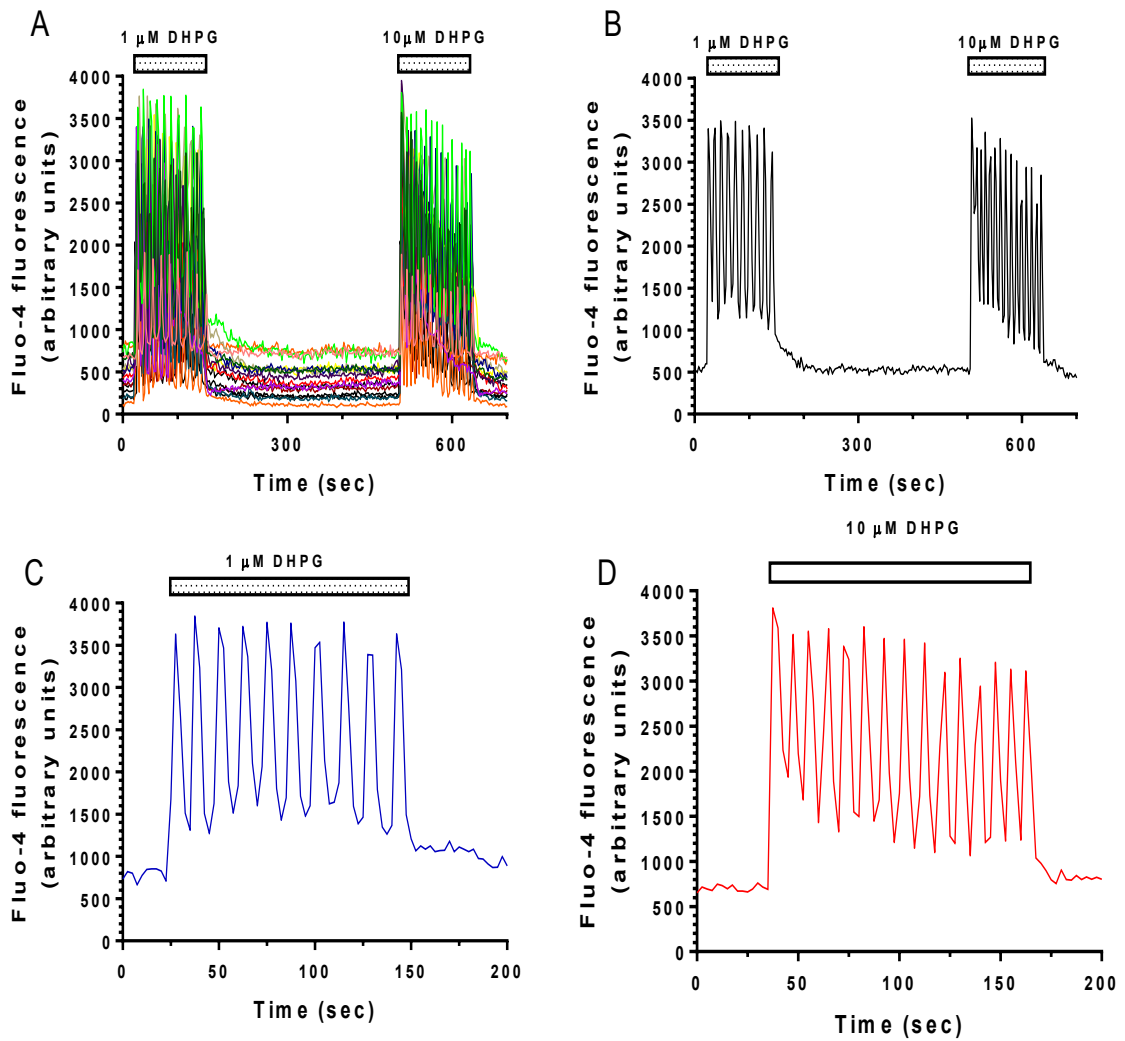
Figure 3.21.   The frequency of DHPG-stimulated Ca^{2+} oscillations in rat cortical astrocytes grown in G5 medium is concentration-dependent. Cells growing in G5 medium for 5 days were perfused with 1 μM DHPG for 2 min, with re-addition of 10 μM DHPG following a 5 min washout period (A). Representative traces showing the changes in Ca^{2+} oscillation frequency elicited by two different concentrations of DHPG are shown (B-D). At least 30 cells were recorded in 3 separate experiments.

3.3 Discussion

Considerable attention has recently been paid to how astrocytes functionally communicate with neurons through sending and receiving neurotransmitter signals. Recent studies *in vivo* have considered astrocytes as a major target for receiving noradrenergic signals generated via the locus coeruleus projection (Bekar et al., 2008b), with astrocytic adrenoceptor activation being linked to a variety of downstream effects that regulate the supportive functioning of astrocytes (Hertz et al., 2010). Such studies indicate a need for additional information about the expression and distribution of adrenoceptor subtypes in the CNS, in particular in astrocytes. The primary aims of this Chapter were to characterise the expression of adrenoceptor subtypes on rat cortical astrocytes, and to begin to characterise how these receptors link to functional activity, focusing on the two most commonly studied second messengers, cyclic AMP and $[Ca^{2+}]_i$.

Adrenoceptor expression

The first aspect studied was to identify and quantify β-adrenoceptor expression in neonatal rat cerebrocortical astrocytes. A number of previous studies have reported β-adrenoceptor expression by mammalian astrocytes (Ghosh and Das, 2007, Jozwiak-Bebenista et al., 2016, Junker et al., 2002a). Using polymerase chain reaction (PCR) experiments, the mRNAs of all β-adrenoceptor subtypes, β_1-, β_2- and β_3-, could be detected with the β_1- and β_2- subtypes more prevalent and the β_3- subtype often barely detectable. Work by another member of the lab used membranes prepared from astrocyte cultures I had generated to perform saturation binding experiments with the radioligand $[^{125}I]$-cyanopindolol. These experiments quantified the expression of β-adrenoceptors and indicated, using highly subtype-selective β_1/β_2-adrenoceptor antagonists that the majority of the receptors (≥ 80%) were the β_1-subtype.

These data are consistent with previous literature reporting the dominant expression of the β_1-adrenoceptor subtype (Maderspach and Fajszi, 1982). However, it would be inappropriate to conclude that other β-adrenoceptor subtypes physiologically unimportant. A number of studies have pointed to roles for non-β_1-adrenoceptors in regulating key activities of astrocytes (Catus et al., 2011a, Day et al., 2014).

Recent decades have seen a surge in our understanding of the multifunctional roles of β-adrenoceptors in astrocytes (Braun et al., 2014). Some neurological diseases, such as migraine, Parkinson disease and depressive disorders, have showed, at least to some extent, gender differences, which has sparked the idea that there might exist different levels/compositions of β-adrenoceptor expression among the different sexes. Here, I have reported that mRNA for the β_3-adrenoceptor subtype was more consistently detected in astrocytes prepared from female versus male neonates. There is some evidence suggesting differential anatomical and cellular distributions of β-adrenoceptor subtypes in different structures of brain (Catus et al., 2011b, Paschalis et al., 2009, Joyce et al., 1992, Rainbow et al., 1984).

Astrocytic functional responses: cyclic AMP

Activation of β-adrenoceptors, via stimulatory (G_s) G proteins, activate adenylyl cyclase (AC) to generate the pathway second messenger, cyclic AMP. The aim of the next part of my work was to study the ability of β-adrenoceptor agonists to increase cyclic AMP accumulation in astrocytes. An initial objective here was to assess whether the pharmacological profile of the functional response agreed with the PCR/radioligand binding data finding that astrocytes express mainly β_1-adrenoceptors. Using the subtype-selective antagonists CGP20712A (β_1-selective) and ICI118,551 (β_2-selective), as well as the non-selective antagonist timolol, I was able to demonstrate that functionally the β_1-adrenoceptor is essentially the only subtype contributing to cyclic AMP accumulation. Indeed, it was surprising that essentially no functional evidence of β_2-adrenoceptor coupling to cyclic AMP accumulation was obtained. One possibility is that the different β-adrenoceptors expressed in astrocytes exhibit different coupling efficiencies (efficacies) with respect to cyclic AMP generation. Such differences have been highlighted by others (Wenzel-Seifert et al., 2002), however, when studies in a different cell background it was reported that the efficacy of β_2- is greater than that of β_1-adrenoceptors with respect to cyclic AMP generation (Levy et al., 1993). There is a wealth of evidence suggesting that both β_1-and β_2-subtypes can produce highly distinct signalling signatures (Communal et al., 1999, Nikolaev et al., 2006). Thus, there is a consensus that cyclic AMP signals evoked by β_2-adrenoceptors are often small and locally restricted, compared to those generated by β_1-adrenoceptors (Nikolaev et al., 2006). Studies have also indicated differential compartmentation of β_1- and β_2-adrenoceptor-mediated cyclic AMP signalling (Xiao, 2001), and different localized efficiency with respect to

cyclic AMP degradation by phosphodiesterases (PDEs) (Nikolaev et al., 2006). In addition, the switching of β_2- (Gong et al., 2002, Xiao et al., 1999) and also β_3-, but not β_1-adrenoceptors, from G_s to G_i proteins has been described (Hutchinson et al., 2007, Sato et al., 2007). Further work will be needed to distinguish which of these mechanisms is responsible for the apparent 'silencing' of functional β_2-adrenoceptor-cyclic AMP signalling in rat cortical astrocytes.

Another striking finding was the contrasting effects of noradrenaline and isoprenaline on cyclic AMP accumulation in rat cortical astrocytes. The non-selective α-adrenoceptor antagonist phentolamine was able to increase noradrenaline-stimulated cyclic AMP responses to approach those seen when the β-adrenoceptor-selective full agonist isoprenaline was used. Further experiments demonstrated that the net observed response to noradrenaline was caused by co-activation of β_1- and α_2-adrenoceptor populations with the net change in cyclic AMP reflecting the co-activation of G_s and G_i proteins. The α_2-adrenoceptor agonist dexmedetomidine was able to potently (IC_{50} ~2 nM) and concentration-dependently inhibit cyclic AMP accumulation stimulated by isoprenaline via a pertussis toxin-sensitive mechanism. While it is known that astrocytes express α_2-adrenoceptors (most likely of the α_{2A}-subtype) (Reutter et al., 1998), my study provides additional pharmacological information regarding the robustness of the β_1- versus α_2-adrenoceptor-mediated actions to regulate cyclic AMP accumulation.

Astrocytic functional responses: $[Ca^{2+}]_i$

The mechanisms underlying noradrenaline-mediated Ca^{2+} responses in astrocytes have been extensively characterized (Duffy and Macvicar, 1995, Hertz et al., 2010, Bekar et al., 2008a, Pankratov and Lalo, 2015a), as have its potential role in Ca^{2+}-dependent release of various gliotransmitters (Lalo et al., 2014, Gordon et al., 2005) that participate in the intimate communication across the glia-neuronal network (Araque et al., 2014b, Halassa et al., 2007). As for the unique feature of non-electrical excitability (Dallérac et al., 2014), astrocytic function is primarily regulated by intracellular Ca^{2+} signalling forming the characteristic "glial-Ca^{2+} excitability" (Nedergaard et al., 2010) and "tripartite synapses", which incorporate astrocytic processes. In addition, astrocytic Ca^{2+} signalling is also important in modulating the function of cerebral blood vessels, since more than 99% of the cerebrovascular surface is

ensheathed by astrocyte processes (MacVicar and Newman, 2015, Takano et al., 2006, Simard et al., 2003).

My preliminary experiments used confocal fluorescence Ca^{2+}-imaging in rat cortical astrocytes to observe Ca^{2+} responses to noradrenaline stimulation which could be seen in both astrocytic soma and processes. Challenge with either α_1- or α_2-adrenoceptor-selective agonists (A61603 and dexmedetomidine, respectively) produced more robust Ca^{2+} responses upon α_1-agonist addition. In addition, the Ca^{2+} responses observed to dexmedetomidine were not blocked by an α_2-selective antagonist (yohimbine), but were blocked by an α_1-selective antagonist (prazosin) indicating that at $\geq\mu M$ concentrations dexmedetomidine can also activate α_1-adrenoceptors expressed in astrocytes. The robust and concentration-dependent effects of A61603 and phenylephrine on astrocytic $[Ca^{2+}]$ indicate the principal involvement of an α_1-adrenoceptor consistent with a number of previous reports (Pankratov and Lalo, 2015a, Paukert et al., 2014a, Ding et al., 2013a).

Interactions between cyclic AMP and Ca^{2+} signalling are widely recognised (Rasmussen and Barrett, 1984, Fabbri et al., 1995), for example, through cyclic AMP-dependent protein kinase-mediated phosphorylation of IP_3 receptors to potentiate ER Ca^{2+} release (Bird et al., 1993). In astrocytes I could find no evidence for such pathway cross-talk. Thus, β-adrenoceptor activation *per se*, or co-activation with a α_1-adrenoceptor agonist did not cause or facilitate the Ca^{2+} response.

Signalling cross-talk between GPCRs is not restricted to cyclic AMP and Ca^{2+} signalling, with many examples of GPCR pairs that can generate different types of cross-talk (Hur and Kim, 2002). Cross-talk constitutes a fine-tuning mechanism integrating information across multiple receptor-signalling pathways, to control cellular, physiological, and biological phenomena (Werry et al., 2003, Selbie and Hill, 1998). Although my experimental data discussed above appear to rule-out direct α_2-adrenoceptor-mediated Ca^{2+} signalling, this does not rule out the possibility of modulatory role for the α_2-receptor, since this adrenoceptor subtype links to the activation of G_i pathways and a series of studies have demonstrated that G_i-and G_q-mediated signalling pathways can crosstalk to regulate important physiological process in diverse cells (Philip et al., 2010, Rozengurt, 2007, Abrams, 2005, Werry et al., 2003, Shah et al., 1999). My results, indicate that when α_1-and α_2-subtype-selective agonists are used as subtype-specific concentrations (phenylephrine, 100

nM; dexmedetomidine, 100 nM), co-addition significantly enhanced the Ca^{2+} response compared to phenylephrine addition alone, strongly suggesting that co-activation of G_i and G_q proteins can exert a synergistic effect on astrocytic Ca^{2+} signalling. Further work will be necessary to pinpoint the mechanism of this cross-talk.

As my studies of Ca^{2+} signalling in astrocytes progressed it became clear that α_1-adrenoceptor agonist addition can generate complex Ca^{2+} signatures that are dependent on the concentration of agonist applied. At low agonist concentrations single-spike Ca^{2+} responses were seen that transitioned into complex oscillatory patterns at sub-maximal concentrations, and then at higher agonist concentrations into peak-plateau responses. Additional experiments using extracellular Ca^{2+} chelation (with EGTA) or the SERCA inhibitor thapsigargin demonstrated the reliance of these responses on both ER store mobilization and Ca^{2+} entry across the plasma membrane consistent with previous reports (Duffy and Macvicar, 1995, Kirischuk et al., 1996, Hamilton et al., 2008). The importance of intracellular Ca^{2+} as a primary trigger source in astrocytic Ca^{2+} signalling likely underlies the mechanism that brings about the different Ca^{2+} signatures across a range of α_1 agonist concentrations. The results obtained here appear mechanistically consistent with those reported previously (Young et al., 2003) and involve complex regulatory effects of IP_3 and Ca^{2+} on the opening of the IP_3 receptor, although other contributory mechanisms cannot be excluded (Thore et al., 2004).

It has previously been shown that astrocytic mGlu5 receptor activation can also stimulate Ca^{2+} oscillations via a distinct mechanism involving receptor phosphorylation by protein kinase C (Bradley and Challiss, 2011, Nash et al., 2002) with studies by independent researchers also showing that IP_3 levels oscillate synchronously with the cytoplasmic Ca^{2+} concentration (Politi et al., 2006). Despite this, the nature of mechanism(s) regulating the Ca^{2+} fluxes responsible for mGlu5 receptor-mediated Ca^{2+} oscillations have been controversial (Dupont et al., 2011, Bird and Putney, 2005, Shuttleworth, 1999). Finally, in this Chapter, I have compared Ca^{2+} signalling initiated by the mGlu5 receptor and α_1-adrenoceptor and found similarities and differences. My data largely recapitulate those reported previously by my lab with respect to Ca^{2+} signalling by mGlu5 receptor, however, my data differ from previous reports in that I do find orthosteric agonist concentration-dependent effects on Ca^{2+} oscillation frequency that have not been highlighted before (Bradley et al., 2009, Bradley and Challiss, 2011).

The data presented in this Chapter have characterized adrenoceptor expression and how the different adrenoceptor subtypes couple to different signalling pathways in rat cortical astrocytes. The Chapters that follow will investigate the characteristics of ERK signalling downstream of adrenoceptor activation and the regulation of glycogen metabolism by adrenoceptors and the roles of cyclic AMP and Ca^{2+} in controlling this important metabolic process.

Chapter 4

Investigating Adrenoceptor Regulation of Extracellular Signal-Regulated Kinase Activity in Rat Cerebrocortical Astrocytes

4.1 Introduction

The G protein-coupled receptors (GPCRs) constitute a large family of plasma membrane proteins, which can regulate multiple cellular functions by involving diverse signal transduction pathways (Marinissen and Gutkind, 2001), such as the second messengers (cAMP and Ca^{2+}) discussed in Chapter 3. Another potential GPCR target is a family of closely related proline-targeted serine/threonine kinases, collectively known as extracellular signal-regulated kinases (ERKs), which can also be activated by receptor tyrosine kinases. These kinases play critical roles in many physiological and pathological events, including cell growth, gene transcription, cell proliferation and synaptic plasticity (Cheng et al., 2013, Peng et al., 2010a, Lin et al., 2014). Accumulating evidence has shown that ERK signalling in glial cells can be activated by different stimuli, including growth factors, chemokines, ischemic injury and a number of neurotransmitters (Liu et al., 2005, Su et al., 2011, Lin et al., 2014). As I described in the previous Chapter, all of the major adrenoceptor subclasses (α_1, α_2 and β) have been shown to be functionally present in rat cortical astrocytes. It is now known that many GPCRs regulate mitogen-activated protein kinase (MAPK) cascades, via different G protein (G_s, G_i, G_q) -dependent signalling pathways (Goldsmith and Dhanasekaran, 2007), however, the signalling pathway(s) contributing to ERK activation by noradrenaline's actions at the different adrenoceptor subtypes in astrocytes have not been definitively determined.

α_1-Adrenoceptors couple to the $G_{q/11}$ proteins to activate phospholipase C (PLC) (Minneman and Esbenshade, 1994) to generate diacylglycerol (DAG) and IP_3, respectively leading to the activation of PKC and release of $[Ca^{2+}]_i$ (Litosch, 2002). Both DAG/PKC and IP_3/Ca^{2+} pathways have been shown to be able to activate ERK phosphorylation in at least some cell backgrounds (Dessy et al., 1998, Hu et al., 1996). Whether α_1-adrenoceptor-dependent ERK activation is always $G\alpha_q$-mediated, or might also involve $G\beta\gamma$ continues to be a matter of contention (Goldsmith and Dhanasekaran, 2007, Katz et al., 1992).

β-Adrenoceptor activation can lead to either activation or inhibition ERK signalling via the G_s/AC pathway depending on cell background. In many cell types, PKA inhibits ERK signalling via phosphorylation of the MAPKKK, c-Raf-1 (Dhillon et al., 2002). cAMP is also regarded as an important effector to stimulate cell growth and differentiation through activation of the ERK cascade; this is believed to involve Rap1-dependent signalling, which can activate a different MAPKKK, B-Raf (Houslay, 2006, Takahashi et al., 2016). Alternately, a recent study has provided evidence that β-adrenoceptors can activate ERK by covalent modification switching their coupling preference to G_i proteins (Du et al., 2010a, Martin et al., 2004).

α_2-Adrenoceptor coupling via PTx-sensitive G_i proteins can also active MAPK cascades in several cell types (Edamatsu et al., 1998, Pace et al., 1995, Peng et al., 2010b). $G\alpha_i$-mediated decreases in cAMP and PKA activity may disinhibit c-Raf-1 activity (Radhika and Dhanasekaran, 2001); however, it is more likely that α_2-adrenoceptor activation increased the cellular levels of free $G\beta\gamma$ subunits (Goldsmith and Dhanasekaran, 2007), which have been implicated in ERK activation via a number of mechanisms, including matrix metalloprotease activation to cleave HB-EGF resulting in EGF receptor 'transactivation' (Prenzel et al., 1999). The latter signalling mechanism requires further explanation; in particular, to clarify the relationship between GPCRs and protein tyrosine kinase activities (Gavi et al., 2006). Cross-talk between receptor tyrosine kinases and GPCRs to regulate ERK activity has been widely reported (Gavi et al., 2006). A wealth of evidence indicates that 'transactivation' of growth factor receptors (e.g. EGF, PDGF receptors) may be common mechanism by which GPCRs can activate ERK pathways (Pierce et al., 2001, Luttrell et al., 1999).

The primary aims of this Chapter are to address the following research questions: (i) Which adrenoceptor subtypes are responsible for noradrenaline altering ERK signalling? (ii) Do adrenoceptors 'cross-talk' with tyrosine kinase activities to regulate ERK? (iii) Do signalling pathways activated by multiple adrenoceptor subtypes interact to 'synthesize' an astrocyte ERK response?

4.2. Results

4.2.1. Time-course and concentration-dependency of noradrenaline-stimulated ERK phosphorylation in rat cortex astrocytes

It has been known for >20 years that GPCRs can activate mitogen-activated protein kinase (MAPK) pathways, which is sufficient and necessary for the control of proliferation in different cellular systems (Kranenburg and Moolenaar, 2001). I have assessed the activation of a subfamily of MAPKs, ERK1/2, by different GPCRs in astrocytes. My initial experiments to investigate astrocytic adrenoceptor involvement focused on evaluating noradrenaline-stimulated changes in ERK1/2 phosphorylation. ERK activity was assessed by western blotting using a phospho-specific antibody that detects the pT/pY dual-phosphorylated (active) forms of the ERK1/2. Because changes in ERK1 and ERK2 phosphorylation are generally considered to be similar and synchronous, both bands were combined in the analysis. The time-course of ERK activation by noradrenaline (100 µM) in rat cortical astrocytes is shown in Figure 4.1A with a representative blot showing phospho-ERK and total ERK immunoreactivities also shown (right panel). Peak ERK1/2 activation occurred at 10 min and this maximal plateau of activation was maintained at the 30 min time-point, with some evidence of decline after that. Based on the time course data, a concentration dependency was determined using a 10 min exposure to noradrenaline (0.01 - 100 µM; Figure 4.1B). This analysis revealed that noradrenaline stimulated ERK1/2 activation with an EC_{50} value of 0.3 µM (pEC_{50} (-log M), 6.56 ± 0.05; n=3). To assess the dependency of this variable on the time of observation, two individual concentration-dependency experiments were repeated at 10 min or 30 min (Figure 4.1C); the responses to noradrenaline were essentially identical at the two time-points.

4.2.2. The role of different adrenoceptor subtypes in ERK activation

Since multiple adrenoceptor subtypes have been demonstrated in previous binding and/or functional studies to be expressed in rat cortical astrocytes, it was important to define the subtype(s) responsibility for the observed noradrenaline-stimulated ERK1/2 activation. As a first step I initially pre-incubated astrocytes with either a non-selective α- (phentolamine; 10 µM) or β- (timolol; 10 µM) adrenoceptor antagonist. Following antagonist pre-treatment for 30 min noradrenaline was added (10 µM; 10 min). As illustrated in Figure 4.2A the presence of phentolamine completely blocked the noradrenaline-stimulated increase in ERK1/2

phosphorylation, whereas β-adrenoceptor blockade was without effect, indicating that this response is predominantly driven by α-adrenoceptor activation.

To further investigate this adrenoceptor regulation a number of subtype-selective adrenoceptor agonists were used. Addition of an α_1- (A61603; 1 µM) or α_2- (dexmedetomidine; 10 µM) adrenoceptor agonist, each caused increases in ERK1/2 phosphorylation similar to noradrenaline (Figure 4.2B), whereas β-adrenoceptor agonist (isoprenaline, 1 µM) addition appeared to cause a small decrease in basal pERK1/2 immunoreactivity. Direct protein kinase C activation using the phorbol ester, phorbol 12,13-dibutyrate (PDBu, 1 µM) also evoked an increase in pERK immunoreactivity that approached than caused by noradrenaline (Figure 4.2B). Essentially identical data were obtained irrespective of whether cerebrocortical astrocytes were derived from male or female batches of donor neonates (Figure 4.2C). These data provide strong evidence for ERK1/2 phosphorylation being mediated by α_1-adrenoceptor activation, with some evidence that α_2- adrenoceptor activation can also activate this pathway. To confirm the latter proposal further, more substantive evidence will be required.
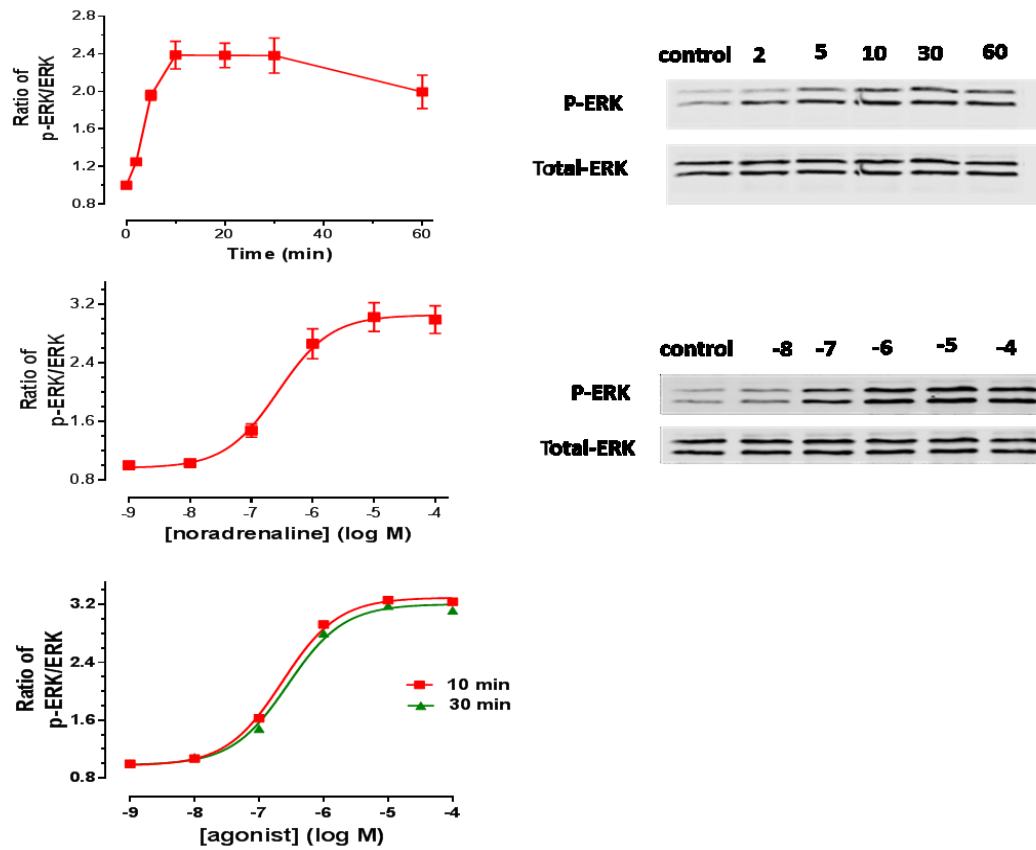
Figure 4.1. **Time-course and concentration dependency of noradrenaline-stimulated phospho-ERK1/2 immunoreactivity in rat cortex astrocytes.** Overnight serum-starved astrocytes were stimulated with noradrenaline (100 µM; panel A) for the times indicated, or incubated with different concentrations of noradrenaline for 10 min (panel B) and then assayed for pERK1/2 immunoreactivity as described in *Methods*. Data are shown as means ± SEM for three experiments using different batches of astrocytes, all data are normalized to control level. The right panels show representative ERK1/2 immunoblots for pERK and total ERK expression. In panel C, an individual experiment showing the concentration-dependency of noradrenaline-stimulated phospho-ERK immunoreactivity at either 10 min or 30 min in rat cortical astrocytes is shown.
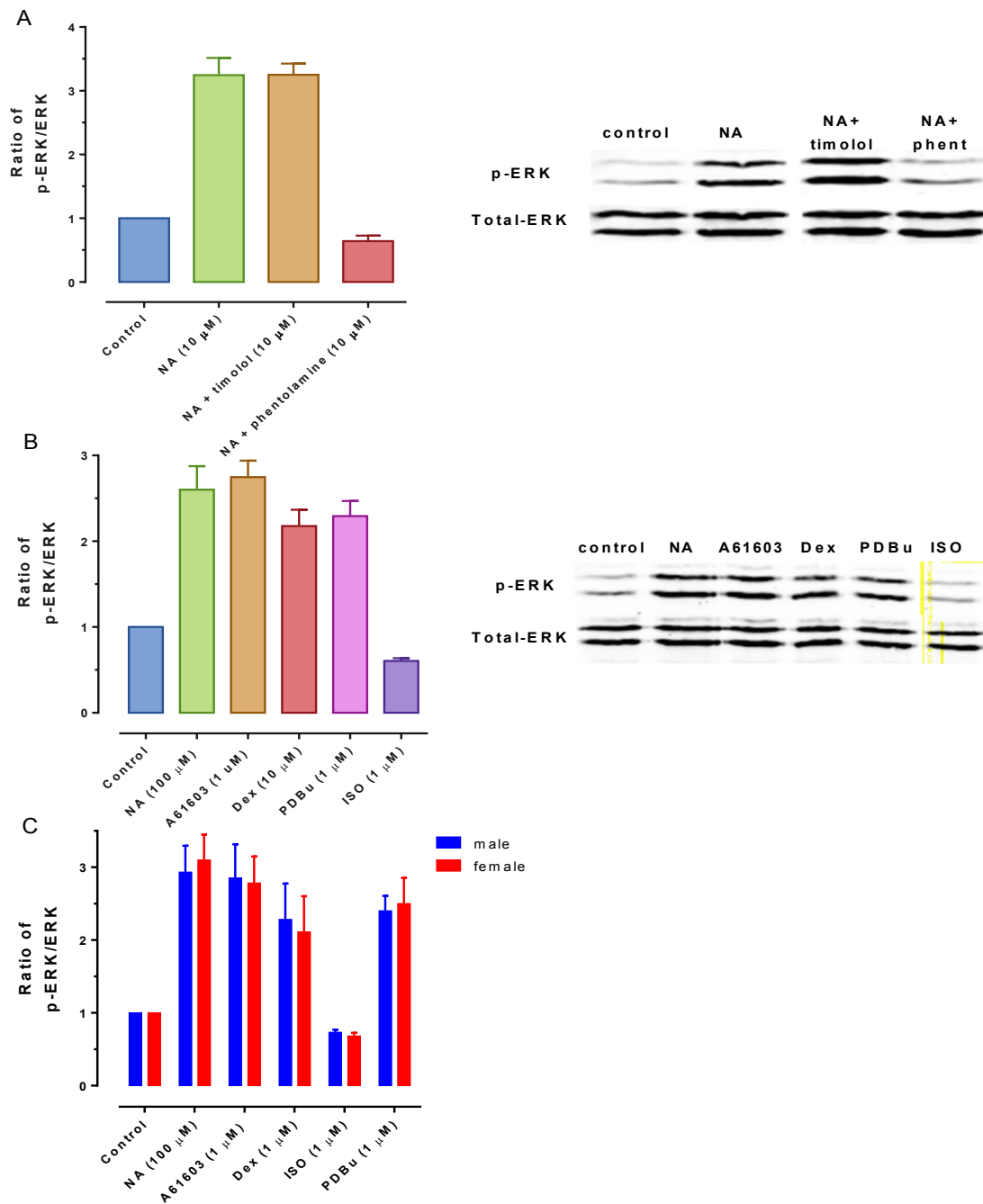
Figure 4.2. Noradrenaline-induced ERK1/2 phosphorylation is mediated by α-adrenoceptors.
Overnight serum-starved astrocytes were pre-incubated with either phentolamine (10 µM), or timolol (10 µM) for 30 min before stimulation with noradrenaline (10 µM, 10 min)(panel A). Different adrenoceptor agonists, including A61603, dexmedetomidine (Dex), isoprenaline (ISO), or the PKC activator, PDBu were added to cortical astrocytes for 10 min (panel B), whereas panel C shows a comparison between astrocytes derived solely from male or female neonates. Lysates were prepared and pERK and total-ERK immunoreactivities were determined as described in the *Methods*. Data are shown as means ± S.E.M. from at least 3 independent experiments.

4.2.3. Characterization of α-adrenoceptor subtype involvement in ERK1/2 phosphorylation in rat cortex astrocytes

To further characterize the contributions of α_1- and α_2-adrenoceptors to ERK1/2 activation, I next stimulated serum-starved monolayers of rat cortex astrocytes with noradrenaline (10 µM), A61603 (1 µM) or dexmedetomidine (1 µM) for up to 4 h (Figure 4.3). The profiles for agonist-stimulated changes in pERK1/2 immunoreactivity were remarkably similar (Figure 4.3A). Each agonist caused a maximal increase at 30 min with near maximal increases being already seen at a 5 min time-point; responses were maintained to the 60 min time-point with a subsequent decrease in pERK1/2 at 120 min and a complete return to basal levels at 240 min (Figure 4.3B). Next, the concentration-dependency of ERK1/2 phosphorylation was determined for noradrenaline, A61603 and dexmedetomidine at a 10 min exposure time-point. Each agonist caused concentration-dependent increases in pERK1/2 (Figure 4.4A-C): Noradrenaline stimulated an increase in ERK phosphorylation (EC_{50}, 280 nM) highly reproducibly with previous experiments (see Figure 4.1B); A61603 evoked ERK activation with an EC_{50} value of 28 nM (pEC_{50} (-log M) 7.55 ± 0.10), while dexmedetomidine was slightly more potent (pEC_{50} (-log M), 7.82 ± 0.15). Consistent with previous experiments, A61603 evoked a maximal increase in pERK1/2 immunoreactivity that was similar to noradrenaline, while dexmedetomidine evoked a lesser maximal response that nevertheless was ≥80% of that evoked by noradrenaline (Figure 4.4C). The concentration-dependencies of the three adrenergic agonists were also assessed in rat astrocytes derived from cerebellum (Figure 4.4D): the experimental data were remarkably similar to those already reported here in cortex-derived astrocyte cultures, suggesting that α_1- and α_2-adrenoceptor-stimulated ERK1/2 regulation is a common feature of astroglia.
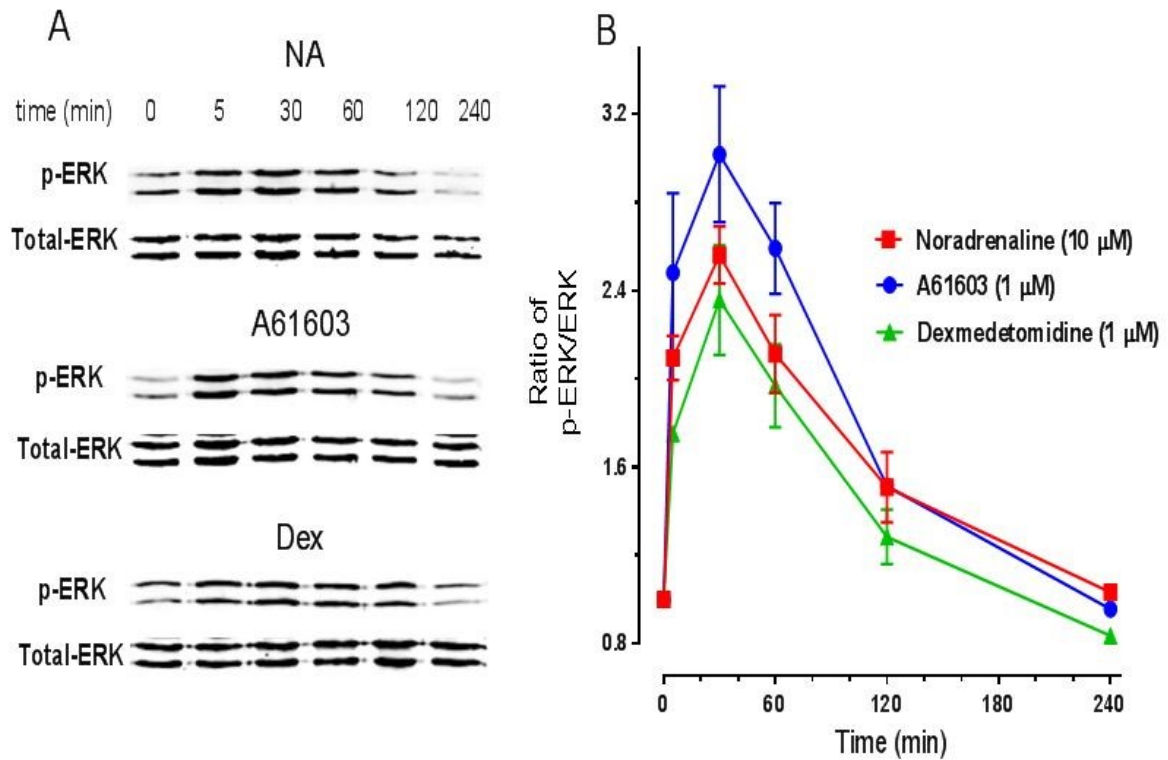
Figure 4.3. Time-courses of phospho-ERK responses to different adrenoceptor agonists in rat cortex astrocytes. Serum-starved cells were incubated in the absence of any drug (control) or in the presence of different adrenoceptor agonists, noradrenaline (NA; 10 µM), A61603 (α_1-selective; 1 µM) or demedetomidine (α_2-selective; Dex, 1 µM) for 5, 30, 60, 120 or 240 min. Lysates were prepared and processed as described in the *Methods*. Antibodies recognising either pERK1/2 (p-ERK), or total-ERK were used for visualization/quantification. (A) Immunoblots from a representative experiments. (B) Cumulative data from three independent experiments and presented as means ± s.e.m.
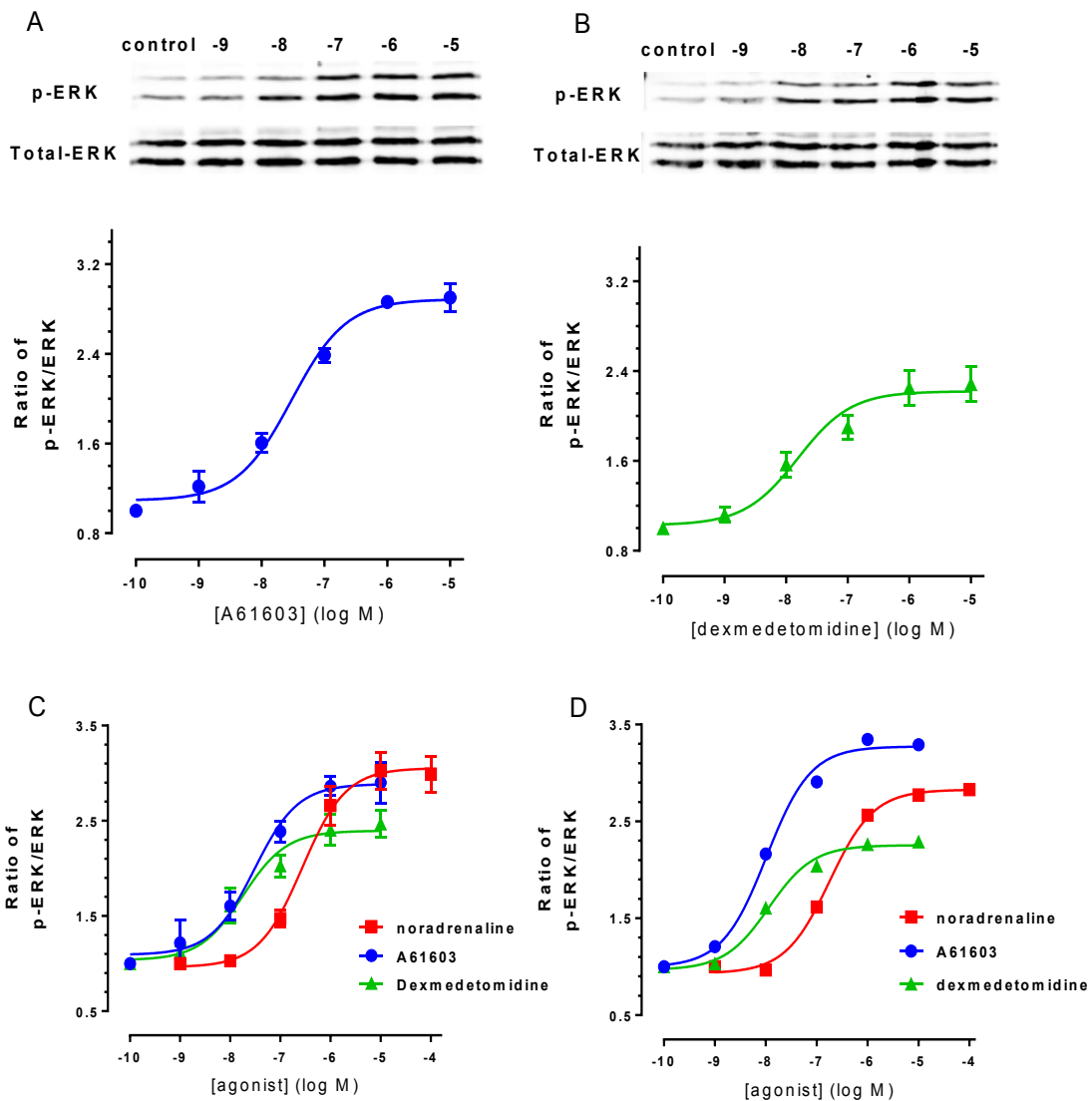
Figure 4.4. Concentration-dependent effects on phospho-ERK responses to different adrenoceptor agonists in rat cortex astrocytes. Serum-starved cells were incubated in the absence of any drug (control) or in the presence of different concentrations of three adrenoceptor agonists (noradrenaline, A61603, demedetomidine) for 10 min. Lysates were prepared and processed as described in the *Methods*. (A) Immunoblot from a representative experiments and cumulative data for A61603 response; (B) Immunoblot from a representative experiments and cumulative data for dexmedetomidine response; (C) Combined data for noradrenaline, A61603 and dexmedetomidine; (D) A representative experiment performed in cerebellar astrocytes. For panels (A-C) data are shown for three independent experiments and are presented as means ± s.e.m.

4.2.4. The G_q protein-dependency of ERK1/2 phosphorylation stimulated by α_1 adrenoceptor activation

A highly-selective $G\alpha_q$ inhibitor (UBO-QIC) was made available to me (kindly provided by Professor Andrew Tobin, MRC Toxicology Unit, Leicester) (Schrage et al., 2015). In preliminary experiments I was able to show that addition of UBO-QIC (1 µM; 20 min) is able to completely prevent the increase in $[Ca^{2+}]_i$ caused by addition of the mGlu receptor agonist (S)-3,5-dihyroxyphenylglycine (DHPG; 100 µM) or the α_1-adrenoceptor agonist A61603 (1 µM) in fluo-4-loaded rat cortex astrocytes (Figure 4.5A, B).

The presence of UBO-QIC (1 µM; 20 min) also markedly inhibited the ability of either DHPG or A61603 to stimulate the phosphorylation and activation of ERK1/2 (Figure 4.5C). These data suggest that UBO-QIC is an effective inhibitor of receptor-dependent G_q protein activation in this primary cell-type and provides evidence for a G_q-dependent pathway linking α_1-adrenoceptor activation and ERK1/2 phosphorylation.

4.2.5. Pertussis toxin-sensitivity of adrenoceptor-mediated ERK1/2 phosphorylation in rat cortex astrocytes

To investigate the $G_{i/o}$ protein-dependency of ERK signalling by adrenoceptor subtypes, cortex astrocytes were pre-treated with pertussis toxin (PTx, 100 ng/mL for 18 h). Toxin pre-treatment partially attenuated pERK1/2 signalling by noradrenaline and A61603 (Figure 4.6A, C), but completely ablated this response when dexmedetomidine was the stimulus (Figure 4.6B, D). The different consequences of PTx pre-treatment are nicely illustrated by the experiments where the concentrations of A61603 and dexmedetomidine were varied (Figure 4.6C, D). These data indicate that the pERK1/2 response to dexmedetomidine is wholly dependent on (α_2-) adrenoceptor-$G_{i/o}$ protein coupling, however, the (α_1-) response to A61603 was also partially inhibited (by ~50%) PTx.

Because the partial PTx sensitivity of the α_1-adrenoceptor-mediated pERK1/2 response was unexpected, the possibility that PTx is having a more general (negative) effect on astrocytes was explored. Pre-treatment with PTx (100 ng/ml; 18 h), did not alter the ability of the phorbol ester, PDBu (1 µM; 10 min) to stimulate ERK1/2 phosphorylation (Figure 4.7) indicating that the actions of PTx are likely to be selectively mediated by it causing receptor-$G_{i/o}$ uncoupling.
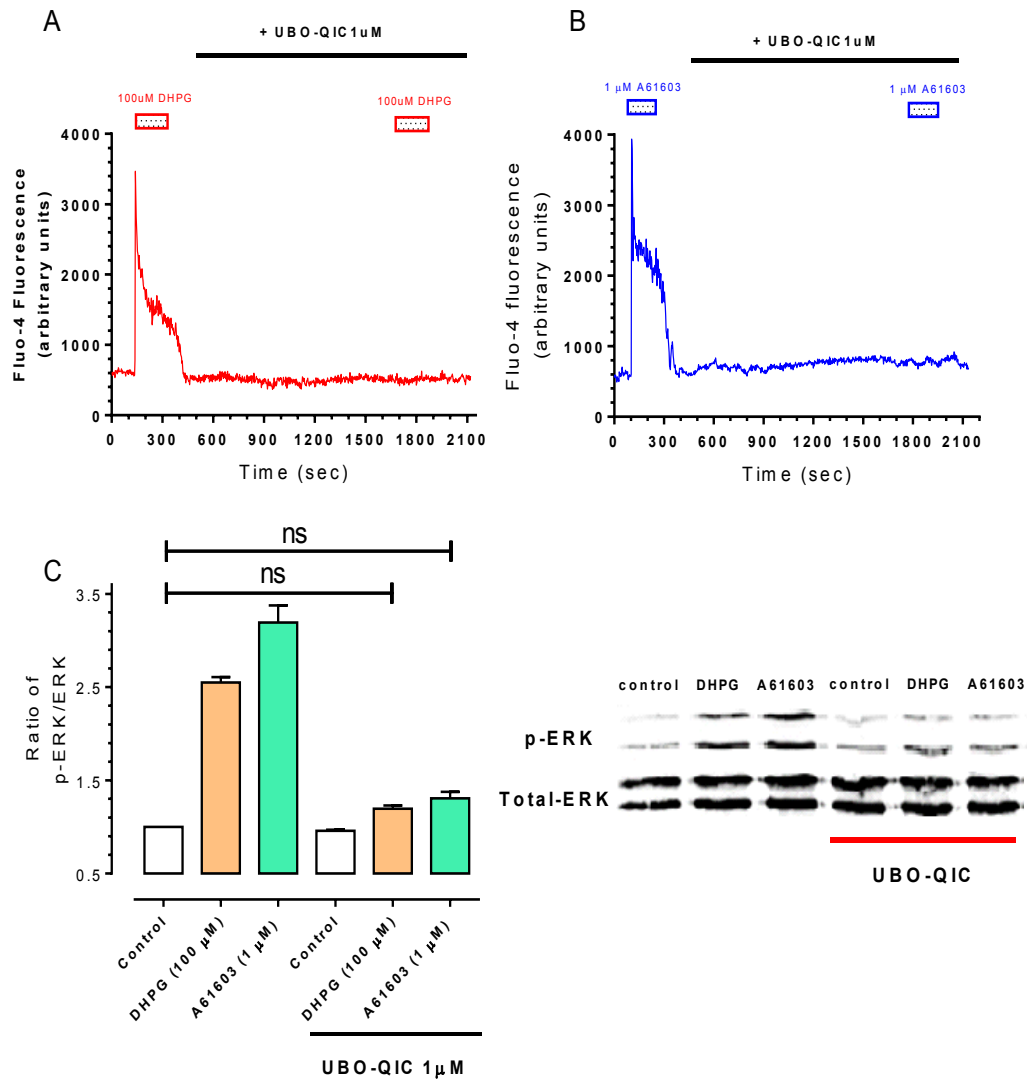
Figure 4.5. Effects of the G_q-inhibitor UBO-QIC on Ca^{2+} and ERK phosphorylation responses in primary rat astrocytes. Cells were grown on coverslip in FCS medium until sub-confluent, cells were loaded with fluo-4 AM 30 min prior to agonist treatment. Representative traces from three individual experiments showing the response of single cells to perfusion with DHPG (100 μM) (A) and A61603 (1 μM) (B) followed by 20 min incubation with UBO-QIC (1 μM) prior to another agonist addition are shown. (C) serum starved astrocytes were incubated in the absence or presence of UBO-QIC (1 μM) for 30 min, the cells were then stimulated with either DHPG (100 μM) or A61603 (1 μM) for 10 min. Date are shown as means ± SEM for three separate experiments. ERK1/2 phosphorylation in rat cortical astrocytes were quantitated as ratios between p-ERK1/2 and ERK1/2. Statistical analysis was performed by one-way ANOVA followed by Bonferroni's multiple comparison test.
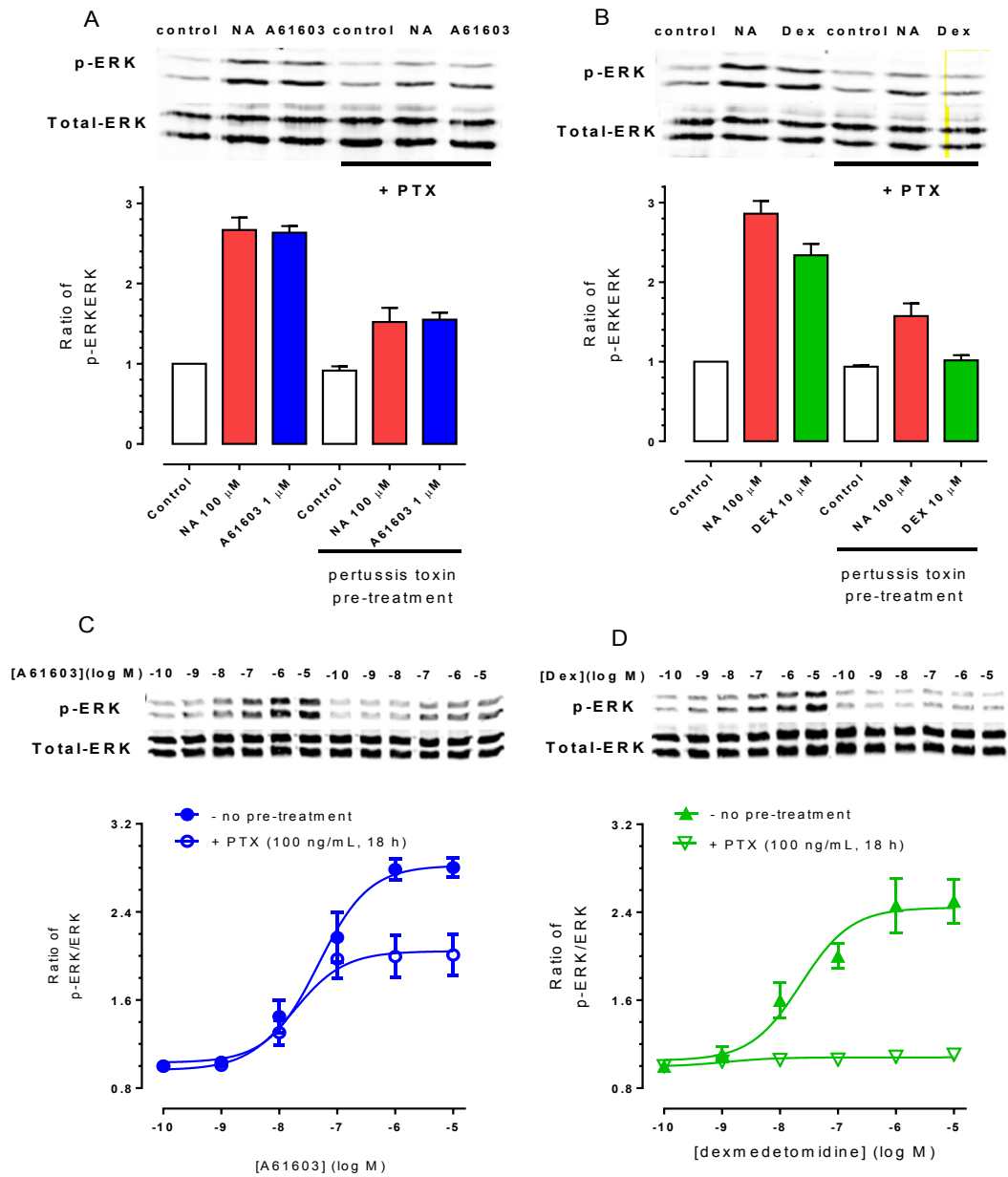
Figure 4.6. Adrenoceptor-mediated ERK activation in rat astrocytes is pertussis toxin-sensitive.
Serum-starved cells were incubated in the absence or in the presence of 100 ng/ml PTx for 18 h. The cells were then challenged with KHB as a control, maximal concentration of NA (100 µM) and A61603 (1 µM) (A), or KHB, NA (100 µM) and Dex ((10 µM) (B) for 10 min. The top panel show representative ERK immunoblot for phospho-ERK and total ERK expression. Under the same condition of PTx pre-incubation, astrocytes were challenged with increasing concentrations of A 61603 (C) and dexmedetomidine (D) for 10 min. Lysates were analysed with antibody that recognizes the phosphorylated form of ERK1/2(pERK), or total-ERK antibody (anti-ERK). Date are shown as means ± SEM for three separate experiments. ERK1/2 phosphorylation in rat cortical astrocytes were quantitated as ratios between p-ERK1/2 and ERK1/2.
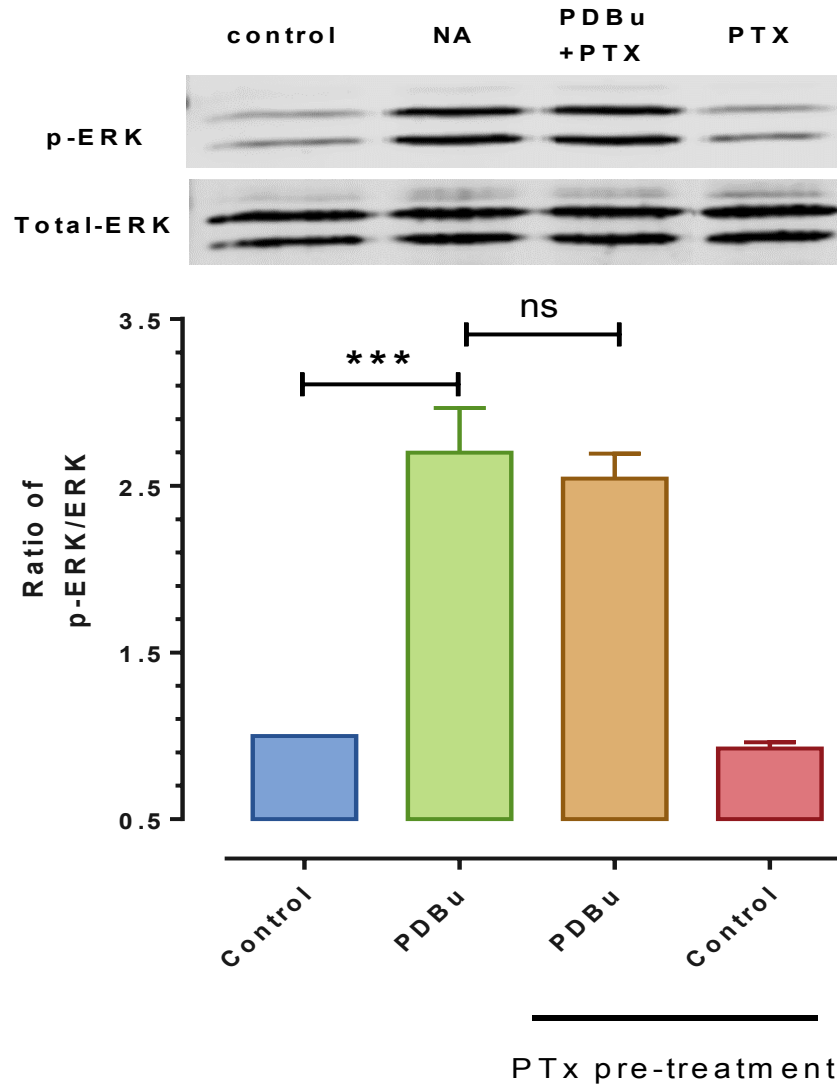
Figure 4.7. **PTx pre-treatment does not affect the PKC-dependent increase in ERK1/2 phosphorylation in rat cortex astrocytes.** Serum-starved cells were incubated in the absence or in the presence of PTx (100 ng/mL; 18 h). The cells were then challenged with PDBu (1 μM) or vehicle for 10 min. The top panel shows representative immunoblot for phospho-ERK (p-ERK) and total ERK expression. Data are shown as means ± SEM for three separate experiments. ERK1/2 phosphorylation in rat cortical astrocytes were quantitated as ratios between p-ERK1/2 and ERK1/2 with the control value being designated as 1. Statistically significant differences (***$p<0.001$) were determined using one-way ANOVA followed by Bonferroni's multiple comparison test.

4.2.6. Gβγ subunit-dependency of adrenoceptor-mediated ERK1/2 phosphorylation in rat cortex astrocytes

A number of previous studies have highlighted a key role for Gβγ-subunits as key transducers between GPCRs and ERK1/2 regulation (Ito et al., 1995, Goldsmith and Dhanasekaran, 2007). Therefore, the role of Gβγ in adrenoceptor-induced ERK activation has been examined in rat cortex astrocytes by introducing a minigene construct encoding a *C*-terminal polypeptide (495–689) of β-adrenergic receptor kinase 1 (βARK1), termed βARKct, which leads to over-expression of this Gβγ subunit binding domain, to 'chelate' free Gβγ subunits and thus to inhibit interaction with normal cellular effector targets (Koch et al., 1994b).

In my experiments, either pRK-βARK1 (495-689), or an 'empty' pRK5 vector plasmid were nucleofected into astrocytes (see *Methods*). 3 days after nucleofection, expression of the ~24-kDa minigene βARKct product could be demonstrated by immunoblotting of astrocyte lysates using an anti-GRK2 antibody, while no expression was detected in cells nucleofected with pRK5 vector (Figure 4.8A).

To investigate whether free Gβγ-subunits are involved in ERK activation by adrenoceptor subtypes in astrocytes, cells nucleofected and expressing βARKct were stimulated with either noradrenaline (100 µM) or A61603 (1 µM). No significant effects of βARKct expression on ERK1/2 phosphorylation were seen (Figure 4.8B). Similarly, the ERK1/2 phosphorylation response to addition of the α_2-selective adrenoceptor agonist dexmedetomidine (at 100 nM or 1 µM) was unaltered in the absence or presence of βARKct (Figure 4.8C). In a further set of experiments, the effects of βARKct and PTx on dexmedetomidine responses were further verified (Figure 4.9). These data appear to indicate that free Gβγ released by activation of either α_1-adrenoceptor-G_q or α_2-adrenoceptor-G_i pathways are not essential for transduction in the pathway(s) leading to ERK1/2 phosphorylation.
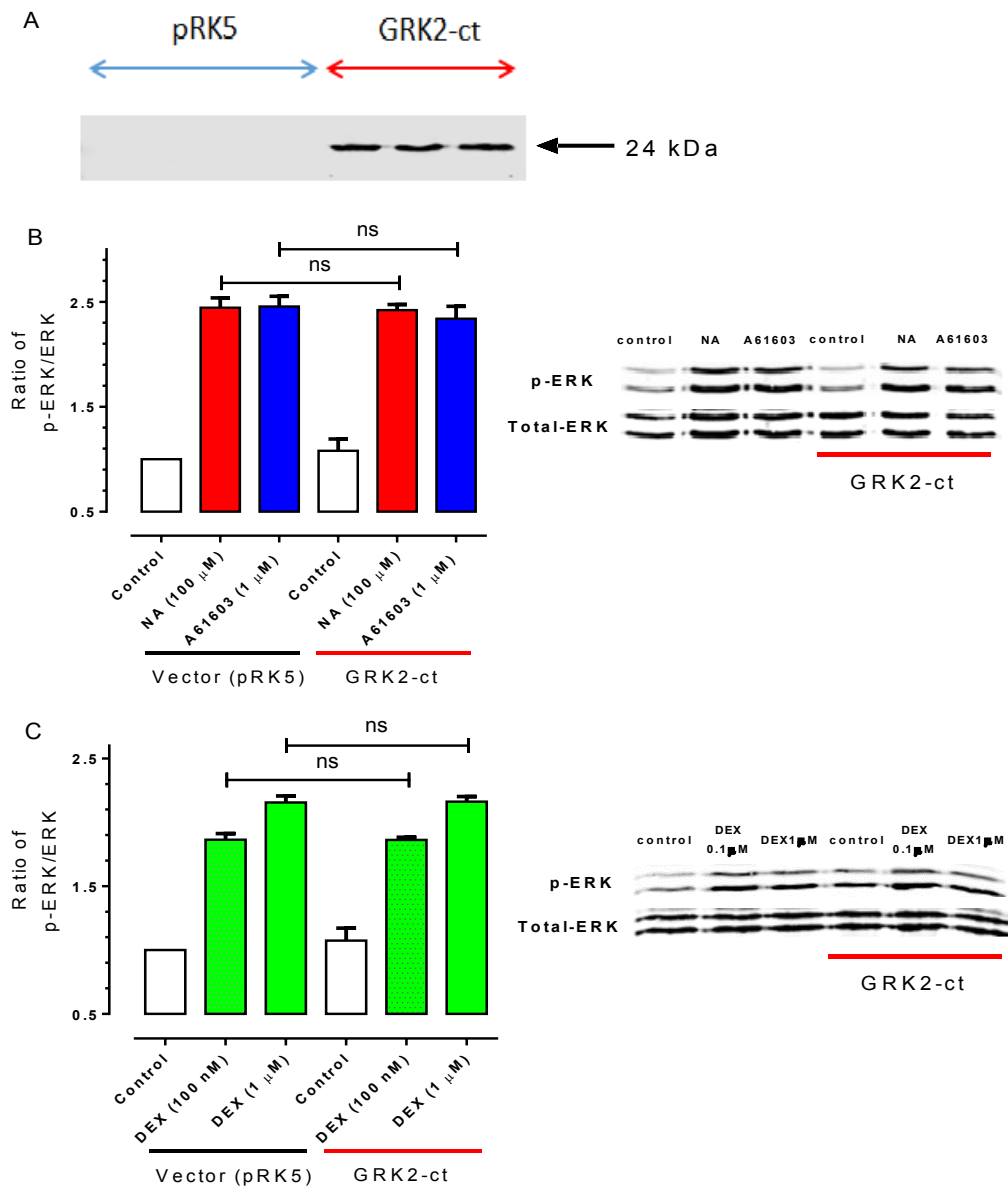
Figure 4.8. Effect of βARKct expression on adrenoceptor-stimulated ERK1/2 phosphorylation in rat cortex astrocytes. (A) Immunoblot demonstrating the expression of the βARKct minigene. Lysates of astrocytes nucleofected with either empty pRK5 vector or pRK-βARK1(495-689) cDNA were analysed for minigene expression. Serum-starved cells were incubated with noradrenaline (NA; 100 μM) or A61603 (1 μM) (B), or challenged with demedetomidine (DEX; 100 nM or 1 μM) (C) for 10 min. Data are shown as means ± SEM for three separate experiments. ERK1/2 phosphorylation was quantified as the ratio between p-ERK1/2 and ERK1/2 with the control value being assigned a value of 1. Data were statistically evaluated by one-way ANOVA followed by Bonferroni's multiple comparison test.
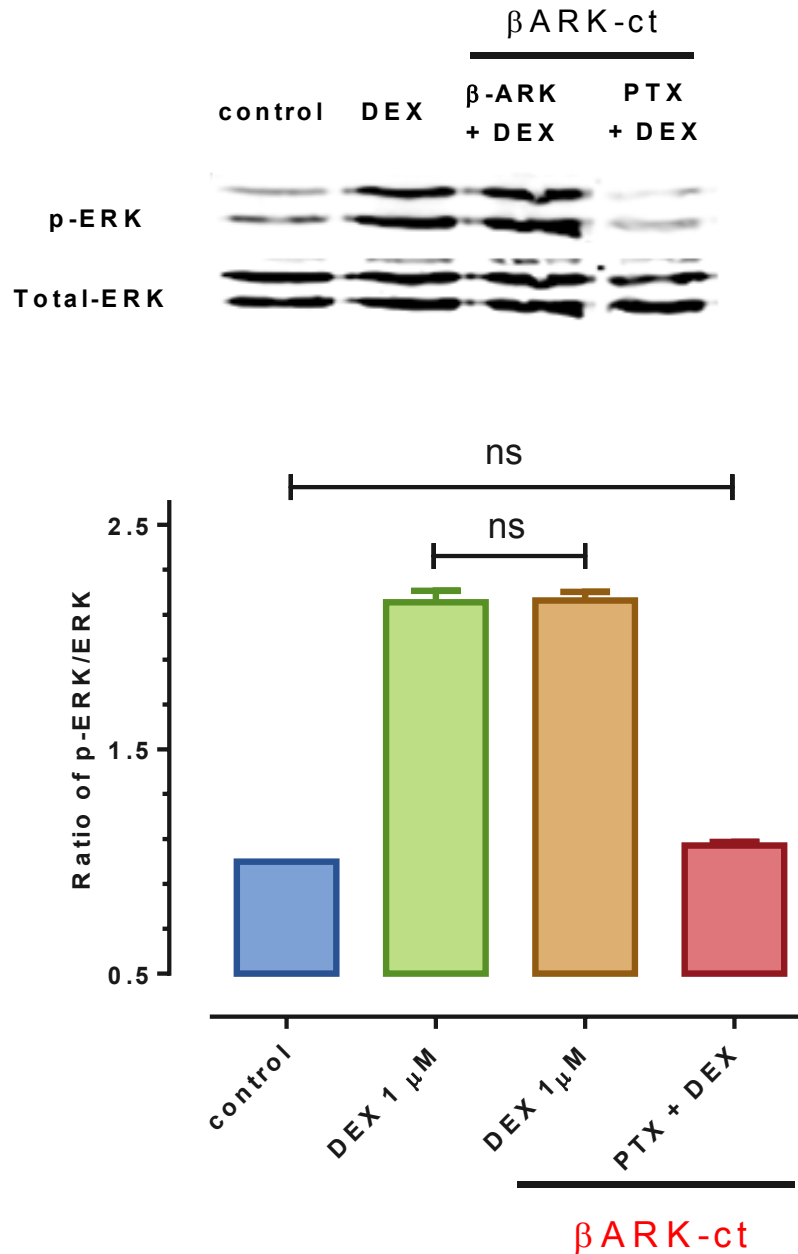
Figure 4.9.   Activation of ERK1/2 phosphorylation by dexmedetomidine is PTx-sensitive but unaffected by βARKct over-expression. Serum-starved astrocytes were nucleofected with pRK-βARK1(495-689) cDNA and/or pre-treated with PTx (100 ng/mL; 18 h) before challenge with dexmedetomidine (1 μM) for 10 min. Data are shown as means ± SEM for three separate experiments and statistically evaluated by one-way ANOVA followed by Bonferroni's multiple comparison test.

4.2.7. Unmasking an inhibitory component of adrenoceptor regulation of ERK1/2 phosphorylation

Receptors that cause an increase in cAMP concentration can exert either positive or negative effects on ERK1/2 activation pathway depending on cell background (Dugan et al., 1999, Cook and McCormick, 1993). In my preliminary experiments (see Figure 4.2B), the β-adrenoceptor agonist isoprenaline appeared to cause a decrease in basal pERK1/2 in rat cortex astrocytes, which is inconsistent with some prior findings (Kaya et al., 2012, Du et al., 2010b). The previous experiments were repeated and whether β-adrenoceptor activation might inhibit mechanisms known to stimulate ERK activity was also assessed. Therefore, different adrenoceptor subtypes present in astrocytes were selectively activated. In the absence or presence of β-adrenoceptor activation (isoprenaline, 1 μM), ERK1/2 phosphorylation stimulated by α_1-adrenoceptor activation (A61603; 1 μM) was not significantly altered (Figure 4.10A), whereas the ERK response to α_2-adrenoceptor activation (dexmedetomidine; 1 μM) was significantly attenuated (64 ± 1% inhibition; $p<0.01$).

Similar effects were seen when a receptor-independent approach was adopted to elevate astrocyte cAMP concentrations. Thus, in the presence of forskolin basal and dexmedetomidine-stimulated levels of pERK1/2 phosphorylation were partially and significantly reduced, whereas the response to A61603 was not significantly altered (Figure 4.10B). The inhibitory effect of β-adrenoceptor stimulation was concentration-dependent: increasing concentrations of isoprenaline caused a maximal 60% inhibition with an IC_{50} value of approx. 5 nM (Figure 4.10C).
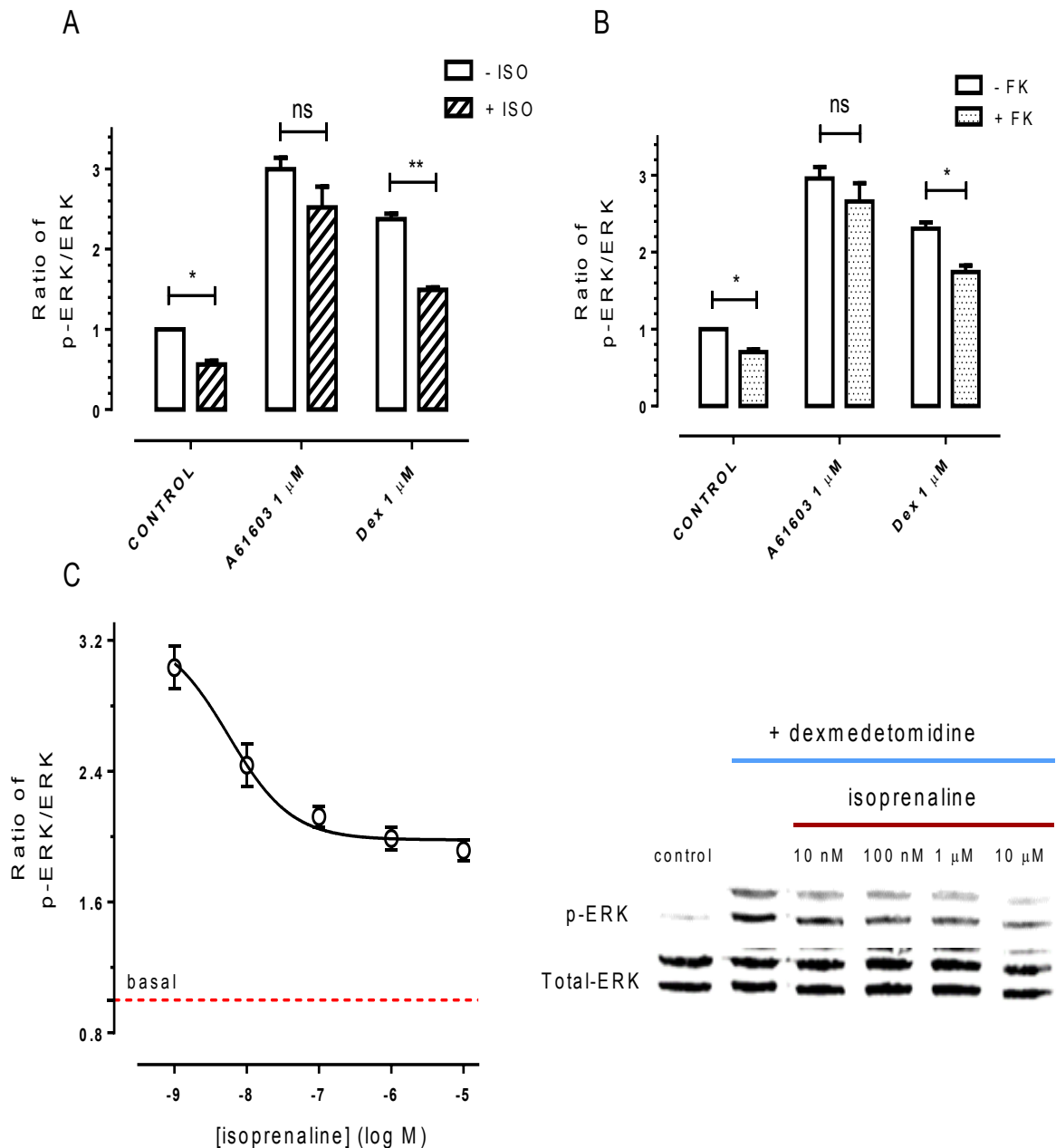
Figure 4.10. Inhibitory effects of cAMP on ERK1/2 phosphorylation stimulated by α_2-adrenoceptor activation in rat cortex astrocytes. Serum-starved astrocytes were incubated in the absence or in the presence of either isoprenaline (ISO, 1 μM; A) or forskolin (FK, 10 μM; B) for 15 min. Cells were then challenged with vehicle, A61603 (1 μM) or dexmedetomidine (Dex, 1 μM) for 10 min. Astrocytes were also pre-treated with increasing concentrations of isoprenaline for 15 min before addition of dexmedetomidine (1μM; 10 min; C). Data are shown as means ± SEM for at least three separate experiments. Statistically significant differences (*$p<0.05$; ** $p<0.01$) were determined by one-way ANOVA followed by Bonferroni's multiple comparisons test.

4.2.8. Defining the signal transduction pathways linking G_q-coupled receptors to ERK1/2 phosphorylation

Previous studies indicated that α_1-adrenoceptors and mGlu5 receptors can activate ERK1/2 signalling via $G\alpha_q$-dependent signalling in astrocytes. To further investigate the important mechanisms involved, PKC activity and $[Ca^{2+}]_i$ have been experimentally manipulated. The selective PKC inhibitor, GF109203X (10 µM, 30 min pre-addition) was able to completely inhibit the ability of PDBu (at 0.1 µM or 1 µM) to stimulate pERK1/2 phosphorylation (Figure 4.11A). When ERK1/2 phosphorylation was stimulated by either A61603 (1 µM) or DHPG (100 µM), GF109203X (10 µM, 30 min) pre-addition caused only a partial attenuation of the agonist-stimulated responses (Figure 4.11B).

Similar data were obtained utilizing a different strategy to 'inhibit' PKC activity. Chronic treatment of cells with the PKC activator, PDBu (1 µM for 18 h), causes a marked down-regulation of both conventional and atypical PKC isoenzymes (Pearce and Murphy, 1993). This manipulation also caused only partial attenuations of ERK1/2 phosphorylation responses to either A61603 (1 µM) or DHPG (100 µM) (Figure 4.11C) yielding a dataset similar to that seen using the PKC inhibitor, GF109203X. These data suggest that pathways other than PKC are involved in α_1-adrenoceptor- and mGlu5 receptor-mediated activation of ERK1/2 signalling.

PKC activation is only one arm of the proximal pathways utilized by $G\alpha_q$-GPCRs, such as α_1-adrenoceptors and mGlu5 receptors, which can also stimulate IP_3-dependent $[Ca^{2+}]_i$ mobilization. I have therefore investigated the Ca^{2+} requirement for ERK activation via α_1-adrenoceptors and mGlu5 receptors in rat cortical astrocytes. Experiments were carried out using the intracellular calcium chelator, BAPTA-AM, and extracellular calcium chelator EGTA. Through the use of these Ca^{2+}-chelating agents it is possible to alter the availability of extracellular and intracellular Ca^{2+}. Reducing extracellular Ca^{2+} from 1.3 mM to ≤100 nM , did not prevent A61603-stimulated Ca^{2+} mobilization (Figure 4.12A), whereas loading the cell-permeant Ca^{2+} chelator BAPTA-AM (100 µM, 20 min), caused a complete attenuation of the A61603-Ca^{2+} response (Figure 4.12C). The former manipulation (effective removal of extracellular Ca^{2+}) caused marked decreases in the ERK1/2 phosphorylation responses to A61603 or DHPG (Figure 4.12B), whereas BAPTA-AM loading to prevent any changes in $[Ca^{2+}]_i$ was essentially without effect (Figure 4.12D). Interestingly, if cells are pre-treated

with phorbol ester to down-regulate cellular PKC activity there is a small inhibition (for A61603 addition; $p<0.05$), whereas PKC down-regulation and Ca^{2+} exclusion from the extracellular medium (by omission and EGTA addition) caused an almost complete inhibition of either A61603 or DHPG-stimulated ERK1/2 phosphorylation (Figure 4.12E), suggesting that G_q-coupled GPCR activation of ERK in astrocytes requires both extracellular Ca^{2+} and PKC activation to generate a normal pattern of signal transduction to this MAPK readout.
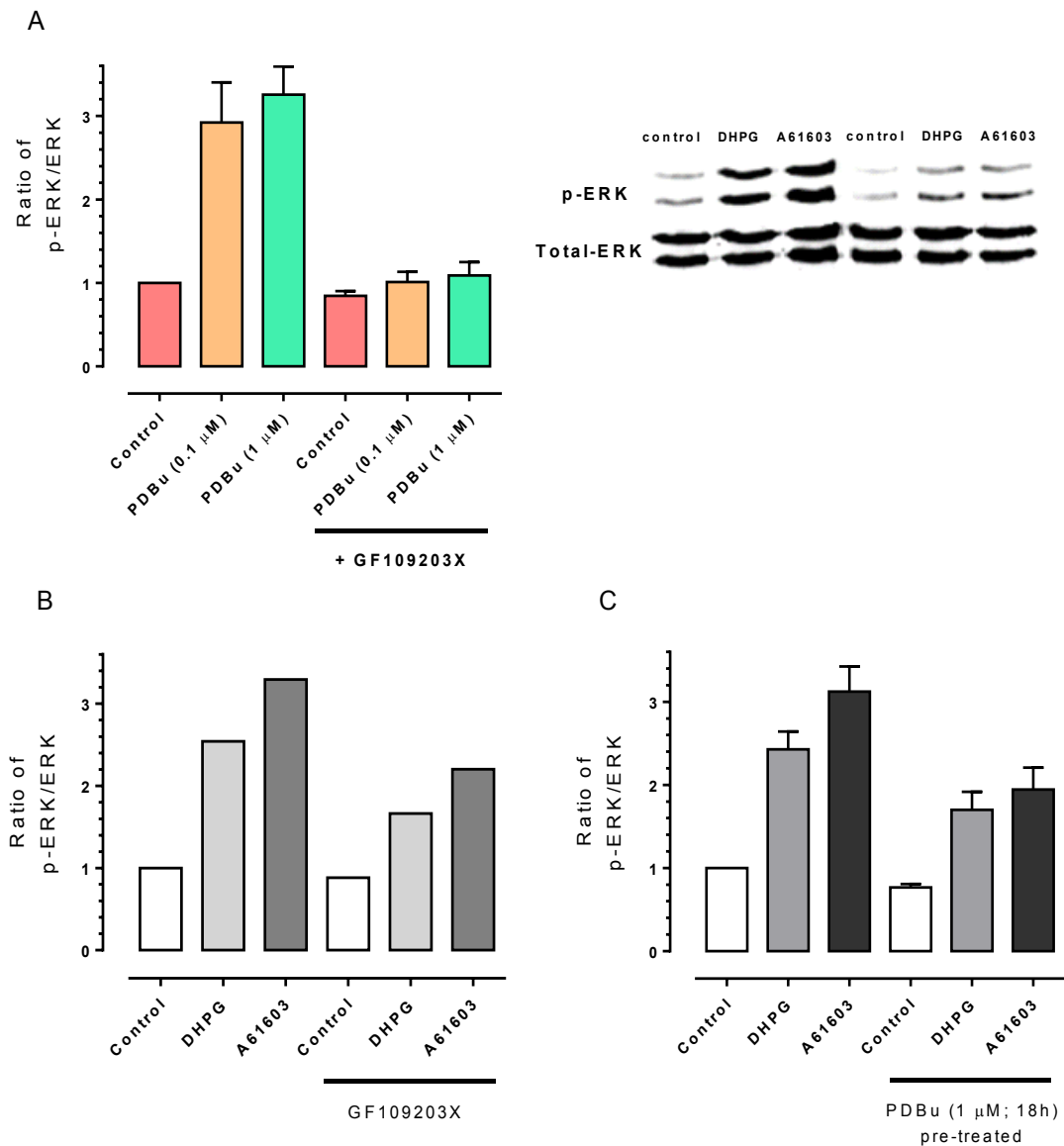
Figure 4.11. Effects of protein kinase C inhibition or down-regulation on agonist-stimulated ERK1/2 phosphorylation in rat cortex astrocytes. (A) Serum-starved astrocytes were incubated with or without the PKC inhibitor, GF109203X (10 μM, 30 min), before challenge with different concentrations (0.1 μM or 1 μM) of PDBu for 10 min. The effect of the PKC inhibitor (GF109203; 10 μM, 30 min, panel B) or chronic pre-treatment with phorbol ester (PDBu 1 μM; 18 h) was assessed on the ERK response to α_1-adrenoceptor agonist, A61603 (1 μM) or mGlu5 receptor agonist, DHPG (100 μM) for 10 min. Data are shown as means ± s.e.m. for 3 (A) or 4 (C) separate experiments. Note that panel B shows a single experimental dataset.
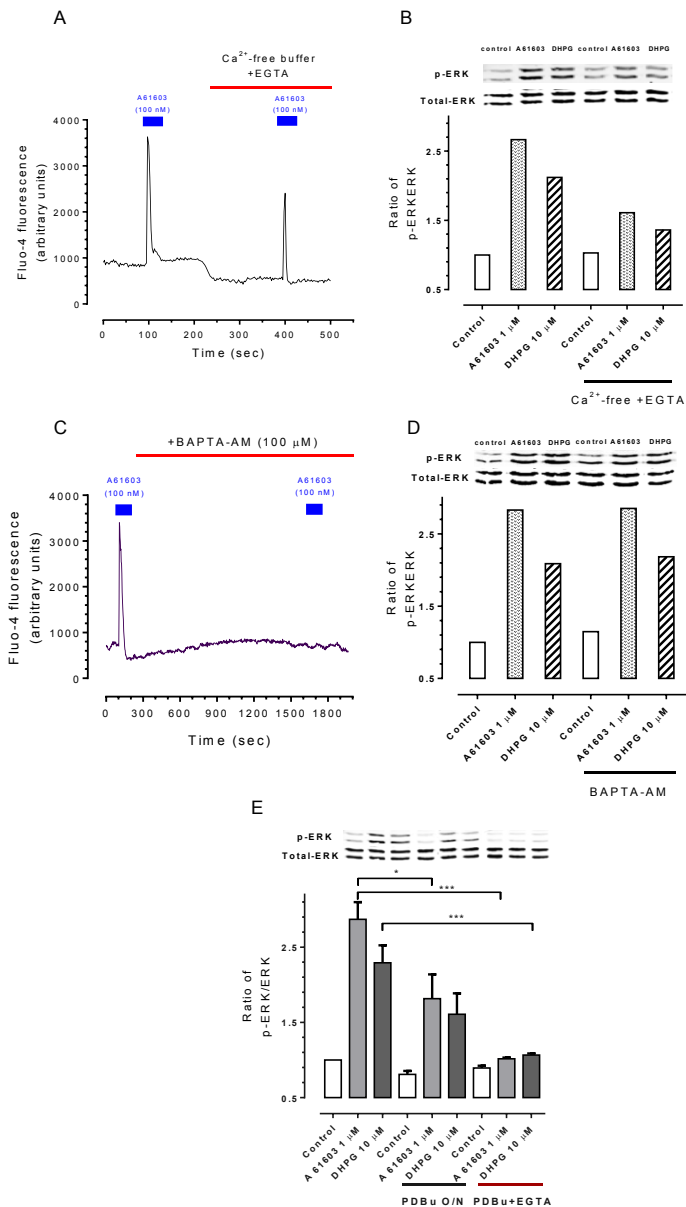
Figure 4.12. **Ca^{2+}-dependency of G$_q$-coupled receptor-activated ERK1/2 phosphorylation.** To manipulate Ca^{2+} concentrations astrocytes were exposed to either normal KHB (1.3 mM) or Ca^{2+}-free KHB + EGTA (A, B) or cells were loaded with BAPTA-AM (C, D) before challenge with either A61603 or DHPG. Left-hand panels (A, C) show Ca^{2+} traces that were performed to validate the manipulations used to alter Ca^{2+} availability. Additions of A61603 (1 μM) or DHPG (100 μM) were for 10 min. Panel E shows agonist-stimulated ERK1/2 phosphorylation in control cells and cells pre-treated with PDBu (1 μM; 18 h) to assess the combined effects of inhibiting PKC activity in combination with extracellular Ca^{2+} removal. For [Ca^{2+}]$_i$ experiments representative traces are shown. Panels B and D show single experimental datasets, whereas panel E shows data that are means ± s.e.m. for three separate experiments. Statistically significant treatment effects are indicated as *p<0.05; ***p<0.001 determined by two-way ANOVA and post hoc Bonferroni testing.

4.2.9. MEK1/2 activity is essential for ERK1/2 phosphorylation stimulated by either α_1- or α_2-adrenoceptor activation in rat cortex astrocytes

Although ERK1/2 activation is normally associated with phosphorylation by the upstream MAPKK, MEK1/2 (Alessandrini et al., 1992, Crews et al., 1992), MEK-independent activation of ERK has been reported in a number of cell-types (Tapinos and Rambukkana, 2005, Bapat et al., 2001). To determine the MEK1/2-dependency of ERK1/2 phosphorylation in astrocytes, the MEK1/2 inhibitor, PD98059 (Dudley et al., 1995) has been used. The inhibitor binds directly to the inactive (non-phosphorylated) form of MEK1/2 to prevent its activation by upstream MAPKKKs (Favata et al., 1998). Pre-incubation with PD98059 (1 µM; 30 min) was sufficient to completely block ERK1/2 phosphorylation following addition of either A61603 (1 µM) or dexmedetomidine (1 µM) for 10 min (Figure 4.13), indicating that both signal transduction pathways utilize the conventional MEK/ERK phosphorylation cascade in rat astrocytes.

4.2.10. Pharmacological assessment of the roles of EGF-receptor, metalloproteinase and Src in G_q-coupled receptor stimulation of ERK1/2 phosphorylation

GPCRs in a variety of cell backgrounds can activate the MEK/ERK cascade via various signal transduction systems, with one well-recognised mechanism involving 'transactivation' by recruitment of receptor tyrosine kinases (RTKs)(Wetzker and Bohmer, 2003). ERK transactivation by adrenoceptors in astrocytes has been partially explored (Peng et al., 2010b, Du et al., 2010a). To further evaluate the involvement of ERK transactivation in rat cortex astrocytes, a selective inhibitor of EGF-receptor kinase activity, AG 1478 (1 µM) was pre-incubated for 30 min before addition of G_q-coupled GPCR agonists, A61603 (1 µM) or DHPG (100 µM) for 10 min. The presence of AG1478 significantly attenuated ERK1/2 phosphorylation induced by either agonist (Figure 4.14A).

RTK transactivation by GPCRs can utilize "triple membrane-passing signalling", whereby GPCR activation leads to growth factor 'shedding' at the plasma membrane to induce RTK activation (Wetzker and Bohmer, 2003). The 'shedding' event can involve cleavage of a tethered growth factor at the cell-surface by matrix metalloproteinase (MMP) activity (Blobel, 2005). Astrocytes were pre-treated with the MMP inhibitor, GM 6001 (10 µM, 30

min), and stimulated with A61603 or DHPG for 10 min. As shown in Figure 4.14B, GM 6001 did not affect the ERK1/2 phosphorylation response to either α_1-adrenoceptor or mGlu5 receptor agonist challenge. Finally, the role of Src family non-receptor tyrosine kinases in GPCR-mediated ERK activation was assessed in astrocytes. PP2 has been reported to show selectivity for inhibition of a subgroup of Src family kinases (Hanke et al., 1996). Pre-addition of PP2 (10 µM; 30 min) caused a partial inhibition of ERK1/2 phosphorylation stimulated by either A61603 or DHPG (Figure 4.14C), suggesting that Src family kinases might also be involved in transduction of the signal from G_q-coupled GPCRs to ERK activation in rat astrocytes.
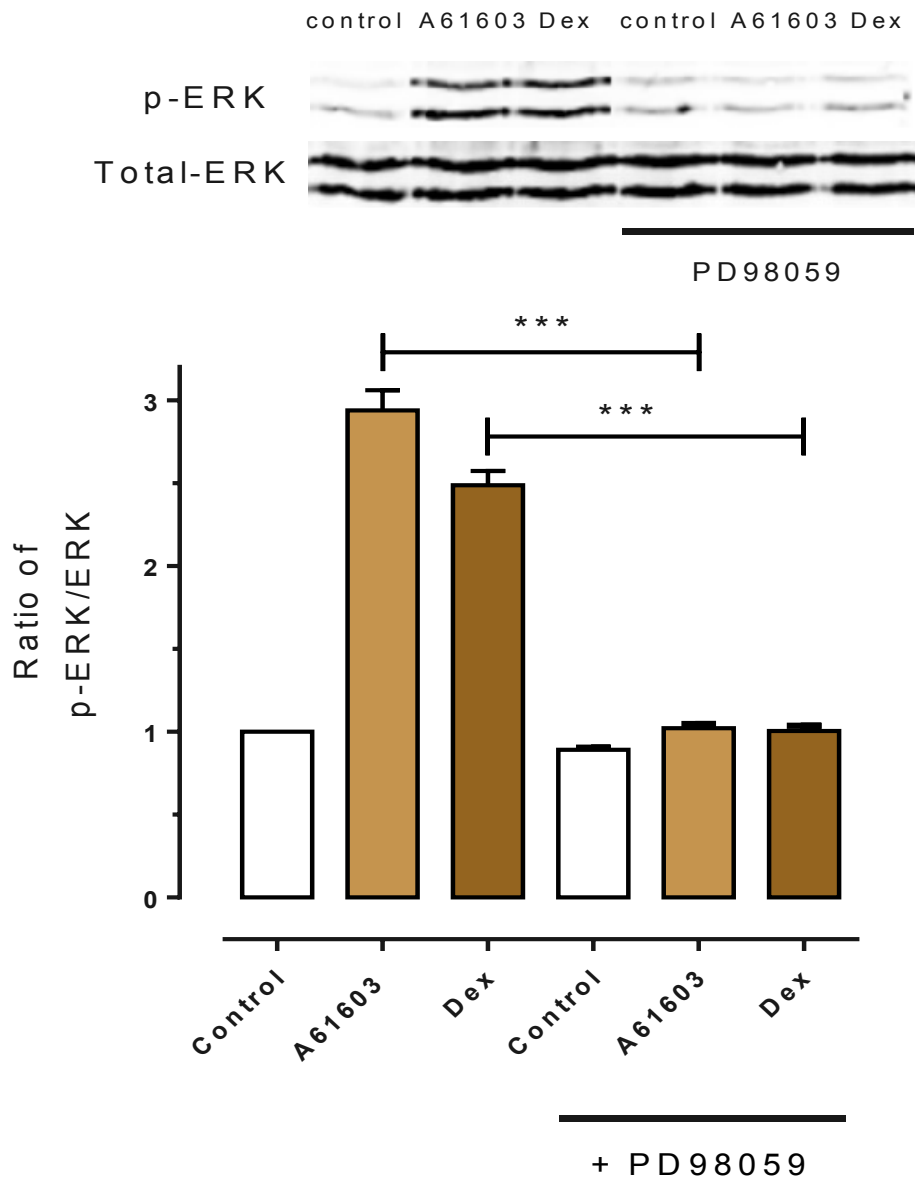
Figure 4.13. **MEK1/2 activity is essential for α_1- and α_2-adrenoceptor-activated ERK1/2 phosphorylation in rat cortical astrocytes.** Serum starved cells were incubated with or without the MEK1/2 inhibitor (PD98059, 1 µM) for 30 min, before challenge with vehicle, A61603 (1 µM) or dexmedetomidine (Dex, 1 µM) for 10 min. Upper panel shows representative ERK immunoblots for phospho-ERK and total ERK expression. Data are shown as means ± SEM for three separate experiments. Statistically significant differences between specific agonist responses in the absence versus presence of PD98059 were determined by Student's *t* test (***$p<0.001$).
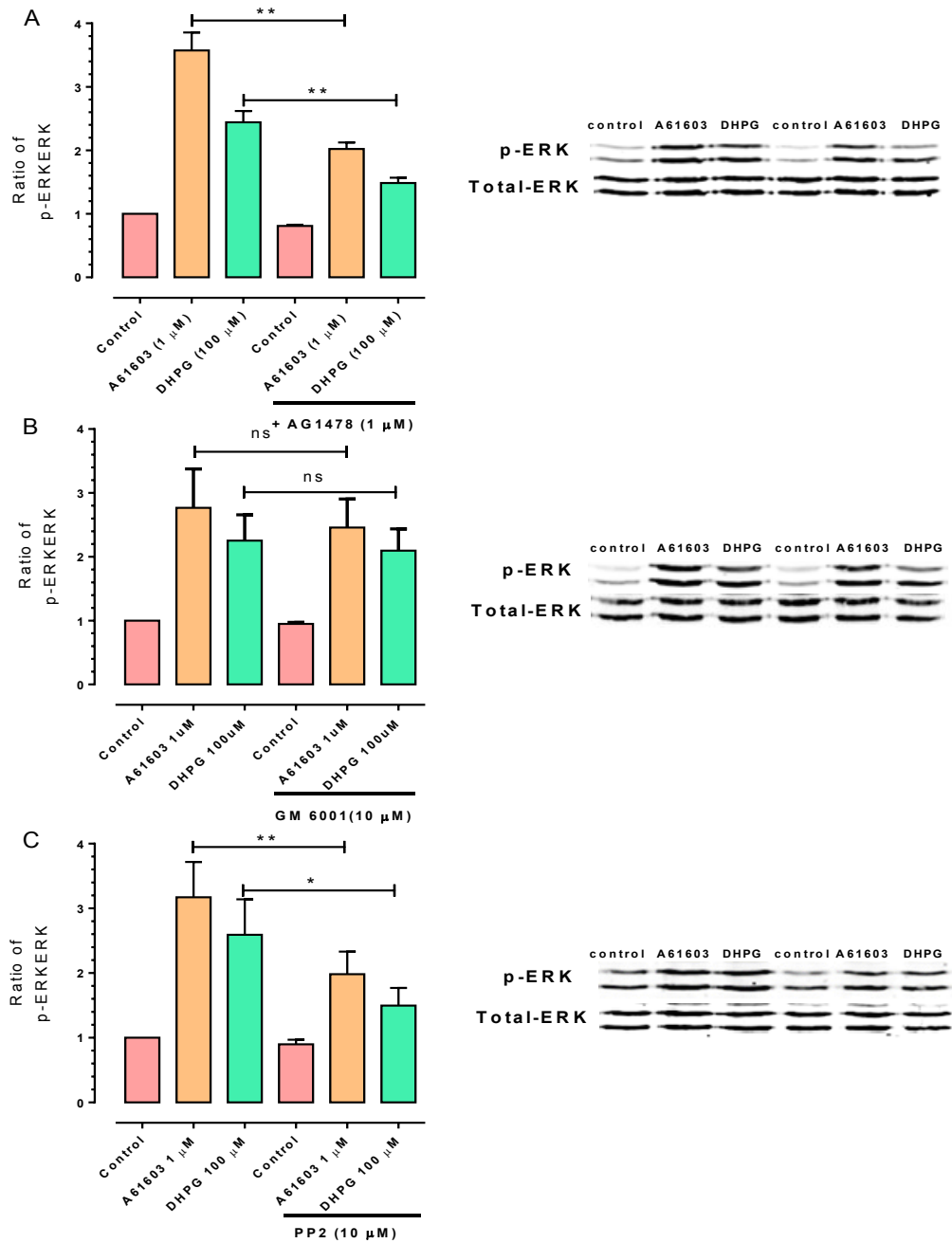
Figure 4.14. The effects of inhibitors of Src and 'transactivation' signal transduction pathways on G_q-coupled receptor-stimulated ERK1/2 phosphorylation. Serum-starved astrocytes were pre-incubated with vehicle or AG1478 (1 µM ; panel A), GM 6001 (10 µM; panel B) or PP2 (10 µM; panel C) for 30 min, before addition of A61603 (1 µM) or DHPG (10 µM) for 10 min. Right panels in each graph show representative ERK immunoblots. Data are shown as means ± s.e.m. for three separate experiments. Statistical analysis was performed two-way ANOVA followed by Bonferroni's multiple comparison test; *p<0.05; **p<0.01.

4.3. Discussion

Cell proliferation and differentiation can be regulated by MAPK/ERK signalling cascades in response to growth factors (Hynes et al., 2013), and it has been known for some time that a myriad of neurotransmitters, acting via GPCRs, can also utilize this pathway to regulate diverse physiological and pathological activities in CNS (Fukunaga and Miyamoto, 1998). Since β_1-, α_1- and α_2-adrenoceptors have been shown here, and by other groups to be expressed in astrocytes, it was decided to attempt to establish how ERK1/2 activity in primary rat cortex astrocytes is shaped by these receptors in response to the neurotransmitter, noradrenaline. My preliminary experiments in this Chapter provided time-course and concentration-dependency data for noradrenaline-stimulated ERK1/2 phosphorylation. Because the antibody utilized here selectively recognises the dually phosphorylated pT/pY ERK motif it is reasonable to assume that the observed increases in phospho-ERK accurately reflect increases in the enzymatic activity of this kinase.

To investigate the adrenoceptor subtype contributions to regulating ERK signalling in astrocytes, I first examined the role of the $G_{q/11}$-coupled α_1-adrenoceptor on activation by the subtype-selective agonist A61603. Similar to the effects of noradrenaline, A61603 induced a potent and rapid activation of the ERK pathway in astrocytes. α_1-Adrenoceptor-mediated increases in pERK1/2 was prevented by the selective G_q inhibitor, UBO-QIC, which functions by directly inhibiting guanine nucleotide exchange and thus preventing the activation of the $G\alpha_q$ protein (Carr et al., 2016, Inamdar et al., 2015). These data clearly indicate that α_1-adrenoceptor agonist-stimulated ERK phosphorylation is G_q-protein dependent, excluding the possibility that ERK activation might occur G protein-independently (Cervantes et al., 2010, Coffa et al., 2011).

It has been reported that $G_{q/11}$-coupled receptors primarily use $G\alpha$ subunits to mediate DAG/PKC- and/or IP_3/Ca^{2+} signalling pathway, rather than $G\beta\gamma$ subunits, to activate the ERK pathway (Blaukat et al., 2000, Hsieh et al., 2009). The phorbol ester, PDBu is a potent activator of protein kinase C, and this agent triggered robust ERK activation in astrocytes, indicating that PKC activation can positively regulate the astrocytic ERK response. I next evaluated the role of PKC as a signalling intermediate between α_1-adrenoceptor activation and ERK1/2 phosphorylation utilizing two distinct methods to manipulate PKC activity. Brief pre-treatment with the PKC selective inhibitor GF109203X (at a concentration that

completely blocked ERK activation by PDBu), or down-regulation of multiple PKC isoenzymes by chronic (18 h) treatment with PDBu, each significantly attenuated the ERK1/2 phosphorylation response stimulated by the α_1-adrenoceptor agonist, A61603. These data indicated that this receptor subtype activates ERK signalling in astrocytes at least in part via a PKC-dependent pathway. Similar data were obtained with respect to the pathway(s) linking another $G_{q/11}$-coupled GPCR, mGlu5 receptor to ERK activation, in agreement with previous reports on this receptor subtype expressed in other cell backgrounds (Thandi et al., 2002, Schonwasser et al., 1998).

Since $G_{q/11}$ protein activation results in the generation of both DAG and IP$_3$, a role for the IP3-induced Ca^{2+} response in ERK activation in astrocytes should also be considered. Ca^{2+} is a powerful regulator in astrocytic pathophysiological processes the ability of α_1-adrenoceptor activation to elevate $[Ca^{2+}]_i$ has been described in Chapter 3. Some previous studies have highlighted the Ca^{2+}-dependency of ERK signalling through activation of Ca^{2+}-dependent kinases, such as conventional PKC isoenzymes, Ca^{2+}/calmodulin protein kinase II (CaMKII) and the proline-rich tyrosine kinase 2 (Pyk2) (DellaRocca et al., 1997, Agell et al., 2002, Yan et al., 2016, Montiel et al., 2007). In the present study, neither A61603- nor DHPG-stimulated ERK responses were found to be altered when changes in intracellular Ca^{2+} were abolished by BAPTA-AM loading of the cells. These data are supported by early studies (Thandi et al., 2002, Peavy et al., 2001) that demonstrated that group I mGlu receptor-activated ERK responses in essentially Ca^{2+}-independent.

Interestingly, removal of extracellular Ca^{2+} and addition of EGTA, to remove completely the trans-plasmalemmal Ca^{2+} gradient, caused a partial attenuation of ERK1/2 activation by both agonists. Furthermore, in astrocytes where PKC isoenzymes had been down-regulated by phorbol ester pre-treatment (and in a single preliminary experiment using pharmacological PKC inhibitor, GF109203X), additional removal of the trans-plasmalemmal Ca^{2+} gradient appeared to lead to a further ablation of the ERK response to either A61603 or DHPG (see Figure 4.12E). These data suggest that the presence of extracellular Ca^{2+} and the trans-plasmalemmal Ca^{2+} gradient may play a 'permissive' role in allowing efficient coupling between at least two $G_{q/11}$-coupled GPCR subtypes and ERK activation in rat cortex astrocytes. These data confirm and extend a previous study, albeit in a different cell background (May et al., 2014), which also found extracellular Ca^{2+}, but not ER store-released Ca^{2+}, as an important regulator of the ERK signalling pathway.

Some of the experimental data here are not entirely consistent with the α_1-adrenoceptor-$G_{q/11}$-dependent mechanisms discussed so far. A seemingly anomalous finding was the partial inhibition of α_1-adrenoceptor-ERK signalling caused by PTx (Figure 4.6). A trivial explanation for this finding might be that at 1 μM, A61603 is activating both α_1 and α_2-adrenoceptors, although previous work suggests that this agonist is highly subtype-selective. In hindsight further experiments should have been carried out to confirm that the partial PTx-sensitivity is absolutely attributable to the α_1-adrenoceptor subtype. This caveat notwithstanding, it has been widely reported that many GPCRs can be shown to stimulate multiple G proteins eliciting complex signals downstream of each G protein (Offermanns et al., 1994, Laugwitz et al., 1996). In this case, α_1-adrenoceptors in the astrocyte background might couple to G_q and G_i family proteins with the latter coupling contributing to ERK signalling. It is interesting to note in this context that β_2-adrenoceptors have been reported to switch there G protein coupling preference from G_s to G_i proteins and this "G_s/G_i switching" is important for ERK signalling (Du et al., 2010a). Whether other adrenoceptors, such as the subtype can also either simultaneously or switch coupling between G protein subtypes in astrocytes is worthy of further investigation in the future.

It has been established, here and by others that G_i-coupled α_2-adrenoceptors can inhibit adenylyl cyclase activity, to oppose increases in astrocyte cAMP concentration caused by G_s-coupled GPCRs, or by receptor-independent mechanisms. In this Chapter I set out to determine whether activation of α_2 adrenoceptors also regulate ERK1/2 signalling in rat cortex astrocytes. Using an α_2-adrenoceptor-selective agonist, dexmedetomidine it has been shown that activation of this adrenoceptor-subtype can cause time- and concentration-dependent increases in ERK1/2 phosphorylation, via a mechanism that is completely pertussis toxin-sensitive. These results indicate that this G_i protein-coupled GPCR can also link to ERK in rat cortical astrocytes.

The interrelationship between cAMP and ERK signalling pathways is complex. cAMP/PKA signalling can inhibit ERK activity either by direct inhibition of Raf1 activity, or via an EPAC-mediated mechanism to cause Rap1 activation (Mochizuki et al., 1999). The actions of Rap1 seem to vary between cell backgrounds, but in cells were Raf1 (rather than B-Raf) is the dominant MAPKKK it can bind to and inhibit this upstream kinase to inhibit ERK activation (Stork and Schmitt, 2002, Wang et al., 2001, Schmitt and Stork, 2001). As α_2-adrenoceptor activation can reduce cAMP/PKA signalling, it is possible that this negative effect disinhibits

ERK leading to the increase in pERK1/2 seem on addition of dexmedetomidine. However, this seems unlikely. Let me consider the data shown in Figure 4.10. β-Adrenoceptor activation causes a very large increase in cAMP concentration (see Figure 3.4) and a small, but significant suppression of basal pERK1/2. Prior activation of β-adrenoceptors in astrocytes causes an incomplete suppression of the increase in pERK1/2 stimulated by α_2-adrenoceptor activation. Again, under these conditions the cAMP concentration would still be very high as dexmedetomidine will only have a small inhibitory effect on the β-adrenoceptor-mediated cAMP signal (see Figure 3.8). Therefore, it is much more likely that α_2-adrenoceptor-stimulated ERK activity involves mechanisms independent of any action on adenylyl cyclase activity in astrocytes.

Signal transduction via GPCRs causes the activation of heterotrimeric G proteins (αβγ), leading to Gα and Gβγ subunits each being able to transduce downstream signalling events. Gβγ subunits have been shown to stimulate the ERK signalling pathway. For example, GPCRs that preferentially couple to G_i have been reported to activate ERK via Gβγ-dependent mechanisms (Koch et al., 1994a, Crespo et al., 1994, LopezIlasaca et al., 1997). Transfection studies in model cells (Lev et al., 1995, Dikic et al., 1996) have illustrated that activation of α_2-adrenoceptors can release Gβγ subunits and activate ERK signalling pathway through a Gβγ/PLCβ/IP_3/Ca^{2+}/Pyk2 kinase-dependent cascade (DellaRocca et al., 1997). In addition, Gβγ released following G_q-coupled GPCR activation has also been reported to activate ERK signalling through pathways involving the 'transactivation' of receptor tyrosine kinases (Zhong et al., 2003). In my work, the role of Gβγ subunits in the activation of the ERK pathway was assessed by transfection of rat cortex astrocytes with the Gβγ 'scavenger' βARK-ct. Over-expression of βARK-ct has been shown to bind tightly to free Gβγ subunits, preventing their interaction with downstream effectors. The results presented in this thesis (Figure 4.8) did not demonstrate any inhibitory effect of βARK-ct over-expression.

It is widely accepted that GPCRs can induce transactivation of EGFR involving matrix metalloproteinase (MMP)-dependent shedding of growth factor, such as heparin-binding EGF-like growth factor (HB-EGF), giving rise to a mechanism termed triple-membrane-pass-signalling (TMPS) (Wetzker and Bohmer, 2003, Du et al., 2010a, Prenzel et al., 1999). Previous research has proposed that transactivation of the EGFR occurs following α_1-adrenoceptor stimulation via an MMP-independent pathway (Ulu et al., 2010). In my studies, α_1-adrenoceptor-mediated ERK1/2 phosphorylation was significantly attenuated by

the Src-family kinase inhibitor (PP2) and an EGFR kinase inhibitor, but not by inhibition of MMP, raising the possibility that non-receptor tyrosine kinase activity might be involved in α_1-adrenoceptor-mediated activation of ERK, possibly via pathway involving PKC, Src and EGFR cascades, a pathway reported previously by others (Shah et al., 2006, Biscardi et al., 1999). It should be emphasized that the use only of pharmacological inhibitors in a study rarely provides definitive evidence to define signalling mechanisms. Clearly, further work will be needed to establish the relative roles of conventional and transactivation signalling pathways in linking adrenoceptor subtypes to ERK signalling.

Although the canonical GPCR-initiated intracellular signalling is regarded to be mediated by G proteins *per se*, it is also worth noting that G protein-independent signalling by GPCRs might be directly involved with signalling proteins, such as β-arrestins, which, in some studies (Coffa et al., 2011, DeWire et al., 2007), have been found to trigger ERK phosphorylation, in a number of cell backgrounds including astrocytes. However, in my present results, α_1- and α_2- adrenoceptor agonist-stimulated ERK signalling were completely blocked by their respective G_q- and G_i protein inhibitors (UBO-QIC and PTx). This finding does not exclude the possibility that G protein-independent mechanisms assume a greater importance in other circumstances (e.g. after longer times of exposure to agonist).

In summary, in this Chapter I have explored how different adrenoceptor subtypes contribute to the regulation of ERK activity in rat cortex astrocytes. Selective activation of different adrenoceptor subtypes has demonstrated that ERK activity can be increased by both α_1- and α_2-adrenoceptors, whereas β-adrenoceptor activation has an inhibitory effect. I have been able to present new data that increase our knowledge of how ERK activity might be regulated by noradrenaline in astrocytes and have gained some new insights into the signal transduction mechanisms that link each adrenoceptor subtype to this important cellular kinase.

Chapter 5

Adrenoceptor Subtype-Dependent Regulation of Glycogen Metabolism in Rat Cerebrocortical Astrocytes

5.1 Introduction

Glycogen is considered to be exclusively localized to astrocytes in the brain, with its presence and role in brain energy metabolism being appreciated for many years (Cummins et al., 1983). However, more recently its function has expanded from being considered simply as an 'emergency' energy reserve, to a more current appreciation as a dynamic brain energy source under a variety of physiological, as well as pathological circumstances (Dienel and Cruz, 2014).

Glycogen is broken down via the action of glycogen phosphorylase which generates glucose 1-phosphate (G1P). Glycogen synthesis involves the conversion of G1P to UDP-glucose and addition of the glucosyl residue to glycogen by glycogen synthase (Brown and Ransom, 2015a). To prevent 'futile' cycling between G1P and glycogen, the synthase and phosphorylase enzymes are tightly regulated in opposing ways (Obel et al., 2012). Numerous neurotransmitters have been reported to stimulate either glycogen synthesis or degradation in the brain (Hertz et al., 2015b, Gibbs and Hutchinson, 2012, Hutchinson et al., 2011), with a good deal of effort devoted to studying noradrenaline-mediated glycogen turnover in astrocytes (Lee et al., 2001, Subbarao and Hertz, 1990a, Magistretti, 1987, Gibbs, 2015).

Glycogen phosphorylase, as the key rate-determining enzyme in the process of glycogenolysis, is regulated by phosphorylation in a cAMP and Ca^{2+}-dependent manner, and can be activated allosterically by 5'-AMP (Muller, 2014). Adrenergic signalling, by acting via different adrenoceptor subtypes, can either stimulate or inhibit cAMP accumulation, or increase intracellular Ca^{2+} concentration, thus exerting potentially quite complex impacts on astrocytic glycogen metabolism. Although a glycogenolytic effect of noradrenaline on astrocytes has been widely reported, the definite signalling mechanism and which adrenoceptor subtypes are responsible for glycogen metabolism still requires further clarification.

β-Adrenoceptors are G_s-coupled GPCRs, which are unequivocally expressed by astrocytes (Hertz *et al.*, 2010) and as confirmed in Chapter 3. This adrenoceptor subtype activates

adenylyl cyclase/cAMP/PKA signalling, resulting in phosphorylation of glycogen phosphorylase and increased glycogen breakdown (Brown et al., 2005, Dienel et al., 2007). Brain slice experiments in the mouse cortex have found β_1-adrenoceptors to be involved in glycogenolytic effects (Quach *et al.*, 1988), while another study demonstrated that β_2-adrenoceptors mainly mediate astrocytic glycogenolysis in the 1 day-old chicks (Gibbs et al., 2008, Dong et al., 2012).

In contrast, α_2 adrenoceptor activation decreases intracellular cAMP levels by coupling to $G\alpha_i$ proteins and the inhibition of adenylyl cyclase (Mori *et al.*, 2002). Although its effect on cAMP effect opposes that of β-adrenoceptors, the functional significance of α_2-adrenoceptors in astrocytic glycogen regulation remains elusive.

Astrocytic α_1-adrenoceptors utilize the G_q/phospholipase C/inositol 1,4,5-trisphosphate (IP$_3$) pathway to mobilize Ca^{2+} from intracellular endoplasmic reticulum (ER) stores. This might provide a link between noradrenaline and Ca^{2+}-dependent gliotransmission (Navarrete et al., 2012, Pankratov and Lalo, 2015b). Increases in intracellular Ca^{2+} concentration have also been reported to activate phosphorylase kinase (PK) by binding to its associated calmodulin subunit. In muscle, Ca^{2+} released from the internal (sarcoplasmic reticulum) store has been shown to 'couple' contraction and glycogenolysis (Chin, 2010). However, the physiological role of astrocytic Ca^{2+} signalling to regulate glycogen metabolism still remains controversial. In this Chapter I have investigated the relative roles of different adrenoceptor subtypes in the process of glycogen metabolism in rat cortical astrocytes, and extend my work further to examine how cAMP and Ca^{2+}, as well as increases in extracellular K^+, regulate astrocytic glycogenolysis.

The integrity of physiological brain function relies on neurotransmitter and ion homeostasis to control efficient neuro-glial communication. As we know, a prominent feature of neuronal excitation is the net release of K^+ into the extracellular space. In order to maintain synaptic plasticity and stability, any increase in extracellular K^+ must be cleared and this is achieved by astrocyte uptake and eventual return to neurons (Walz, 2000).

Recent advances have demonstrated the close functional relationship between astrocytic glycogen metabolism and extracellular K^+ clearance in central nervous system (CNS) (Hertz et al., 2015a, Xu et al., 2013, DiNuzzo et al., 2013b). Astrocytic K^+ uptake is mainly mediated by the Na^+/K^+-ATPase and $Na^+/K^+/Cl^-$ co-transporter-1 (Hertz et al., 2015a, Larsen et al., 2014).

Moreover, previous studies have found that the increase of $[K^+]_o$ leads to glycogenolysis in astrocytes and is Ca^{2+}-dependent (Wang *et al.*, 2012), although precise mechanistic detail is still missing. L-type voltage-gated Ca^{2+} channels and Na^+/Ca^{2+}-exchangers have been proposed as mechanisms that allow Ca^{2+} influx, to stimulate glycogen phosphorylase kinase activity (DiNuzzo et al., 2013b).

Although severe hypoglycaemia is uncommon, since whole-body regulatory mechanisms exist to maintain control blood glucose levels, this life-threatening condition can occur for example, if an excess amount of insulin is given to a diabetic patient, or following cerebral infarction (Frier, 2014). In these situations, endogenous substrates in brain, especially astrocytic glycogen can be hydrolysed to generate energy substrates like lactate by the concerted action of glycogenolysis and glycolysis (Schousboe *et al.*, 2010) although the limited glycogen store is depleted within short time period of ischaemia (Swanson *etal.*,1989). Hence, more recent thinking considers glycogen in the brain more as a dynamic glucose store, which may serve as an energy supply under physiological conditions.

Besides promoting glycogenolysis in astrocytes, β-adrenoceptor-stimulated cAMP mobilization has also been found to induce astrocyte stellation (Vardjan *et al.*, 2014). Cultured primary astrocytes usually exhibit a flat and polygonal morphology; following treatment with a cAMP-elevating agent, such as a β-adrenoceptor agonist, the neurotrophic peptide PACAP (pituitary adenylate cyclase-activating polypeptide) or the direct adenylyl cyclase activator, forskolin, astrocytes adopt a dramatic change to star-shaped (stellate), process-bearing appearance (Ramakers and Moolenaar, 1998, Perez et al., 2005, Rodnight and Gottfried, 2013). This morphological remodelling of astrocytes is thought to play an important role in synaptic plasticity and to facilitate memory formation (Zorec *et al.*, 2015). These processes are considered to be energy-demanding (Harris *et al.*, 2012), requiring glycogen utilization. My studies will also explore the link between cAMP, glycogenolysis and morphological adaptation in astrocytes.

5.2. Results

5.2.1. Glucose withdrawal-induced glycogenolysis in astrocytes

It has been estimated that the glycogen store normally available in the brain would be able to support function activity acting as an energy buffer for significant periods of time ranging from minutes to 2 hours (Brown and Ransom, 2015b, Tekkok et al., 2003, Brown, 2013). My initial investigation was to observe the role of astrocytic glycogen by focusing on the rate of glycogen turnover under glucose-free medium conditions to create a severely hypoglycaemic environment. From Figure 5.1 it can be seen that under normal conditions *in vitro* (i.e. in the presence of 5 mM glucose), astrocyte glycogen content is 12.59 ± 0.08 µg/mg protein. Transfer of cells to a zero glucose medium caused a prompt breakdown of glycogen, with about 50% of glycogen hydrolysed by the 5 min time-point (6.05 ± 0.38 µg/mg protein), and decreasing further to 1.90 ± 0.31 µg/mg protein at the 180 min time-point. The glycogenolytic response to glucose deprivation following pre-treatment with the glycogen phosphorylase inhibitor, 1,4-dideoxy-1,4-imino-D-arabinitol hydrochloride (DAB; 300 µM, 60 min) was almost completely prevented (Figure 5.1 inset). DAB pre-treatment under control conditions (5 mM glucose) did not alter the basal glycogen level (12.75 ± 0.34 µg/mg protein). These data imply that, during glucose deprivation, astrocytic glycogen can be metabolized into lactate and this can be pharmacologically prevented.

5.2.2. Glucose re-addition allows re-synthesis of glycogen in astrocytes

To observe glycogen synthesis in astrocytes, cells were glucose-deprived for short time (2 min), and normal medium (containing 5 mM glucose) quickly re-added, and glycogen levels determined over a 4 h time-course (Figure 5.2). In the 2 min period of glucopenia, glycogen content decreased by about 45% (to 6.63 ± 0.27 from a level of 11.87 ± 0.45 µg/mg protein; Figure 5.2). Upon restoration of medium glucose, astrocyte glycogen content recovered steadily and relatively slowly, taking approx. 4 h (11.64 ± 0.40 µg/mg protein) to approach pre-glucopenia levels; this equates to a glycogen re-synthesis rate of approx. 20 ng glucosyl equiv./mg/min.
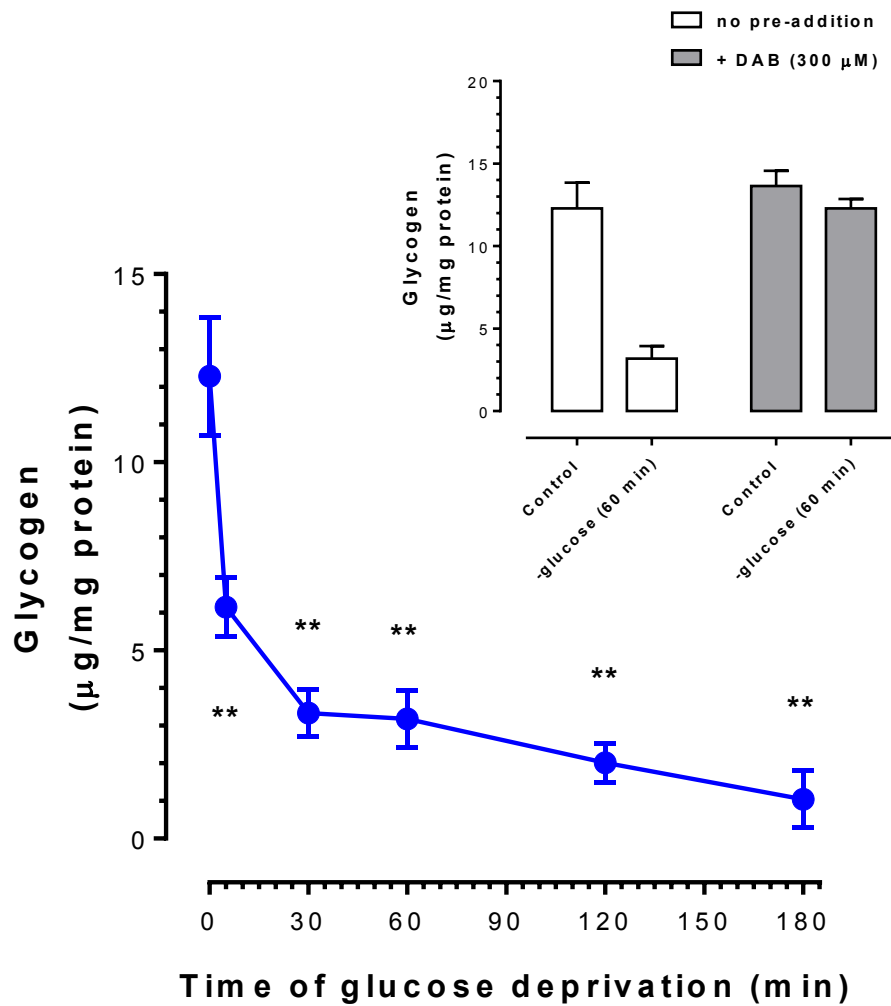
Figure 5.1. Effect of switching from 5 mM to zero D-glucose culture medium on glycogen levels in rat cerebral cortex astrocytes. Confluent monolayers of cells were serum-starved for 24 h in medium with 5 mM D-glucose prior to experiment, then medium was removed by zero D-glucose medium according to the indicating time (ranging from 0, 5, 30, 60, 120, 180 min, respectively). Glycogen content was then measured for each time condition (see method and material). Results are shown as means ± s.e.m. for three independent experiments performed in triplicate. Data were analysed by Bonferroni's multiple comparison test following one-way ANOVA; **$p<0.01$.
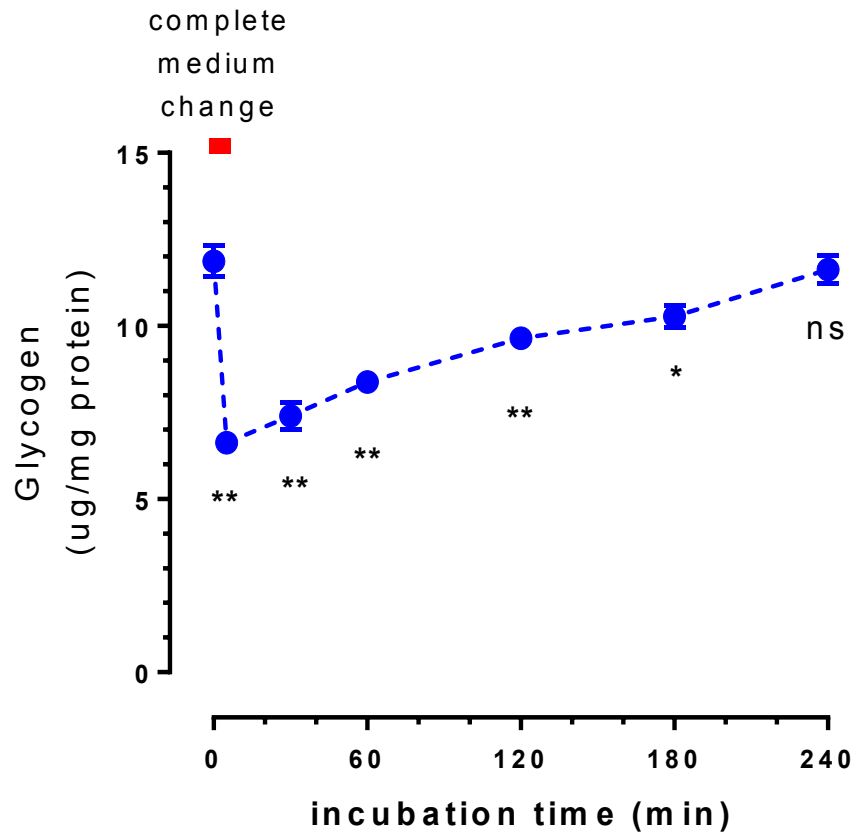
Figure 5.2. Glycogen re-synthesis following glucose containing medium re-addition in rat cortical astrocytes. Confluent monolayers of cells were serum-starved for overnight, then medium was aspirated (glucose withdraw) for about 2 min followed by re-incubation with 5 mM glucose medium. Glycogen content was determined according to indicated time-point (5-240 min, respectively). Results are shown as means ± s.e.m. for three independent experiments performed in triplicate. Data were analysed by Bonferroni's multiple comparison test following one-way ANOVA; *$p<0.05$, **$p<0.01$.

5.2.3. Initial characterization of adrenoceptor-mediated glycogenolysis in rat cortical astrocytes

Preliminary experiments were conducted in cultured rat cerebrocortical astrocytes and to ascertain optimum assay conditions for measurement of adrenoceptor-mediated glycogenolysis. Cells were serum-starved overnight before stimulation with either noradrenaline (NA; 1 µM) or isoprenaline (ISO; 1 µM) for a period of up to 4 h. Each agonist triggered a substantial reduction of glycogen content, and the maximal glycogenolytic effects with a maximum decrease in glycogen content observed at 60 min (basal, 11.57 ± 0.40; +NA (60 min), 5.09 ± 0.33 µg/mg protein; n=7; basal, 12.02 ± 0.60; +ISO (60 min), 5.05 ± 0.25 µg/mg protein; n=4; see Figure 5.3A). Over the subsequent time-course no further decrease in glycogen content was caused in the presence of ISO, while for NA stimulation, a gradual recovery in glycogen levels was observed (Figure 5.3A). These differences might reflect differences in the pharmacodynamics of the actions of these agents, or perhaps more likely a difference in their chemical stabilities. Next, concentration-dependencies of the glycogenolytic responses were assessed at a 60 min time-point for NA and ISO (Figure 5.3B). Each agonist caused concentration-dependent decreases in astrocyte glycogen content (pEC$_{50}$ (-log M) values: +NA: 7.77 ± 0.06; n=6; +ISO: 8.14 ± 0.08; n=4), with ISO being only about 2-fold more potent that NA (Figure 5.3B).

To identify whether there exists differences in the regulation of astrocyte glycogen metabolism between the sexes, experiments were conducted in astrocyte cultures prepared exclusively from either male or female neonates. Concentration-response curves for noradrenaline-stimulated glycogenolytic responses were similar, both in terms of the maximal responses observed and in terms of potency of noradrenaline (pEC$_{50}$ (-log M) values: male, 7.44 ± 0.17; female 7.56 ± 0.19; n=3; Figure 5.4A). These results are consistent with previous cAMP accumulation data, which also demonstrated no difference in adrenoceptor-mediated cAMP accumulation responses between the sexes (see in Chapter 3).

Earlier work found β-adrenoceptor activation can generate a robust cAMP response in cerebellar astrocytes. Isoprenaline also stimulated a concentration-dependent glycogenolytic effect (pEC$_{50}$ (-log M): 8.31 ± 0.12; Figure 5.4B) in astrocytes prepared from cerebellum.
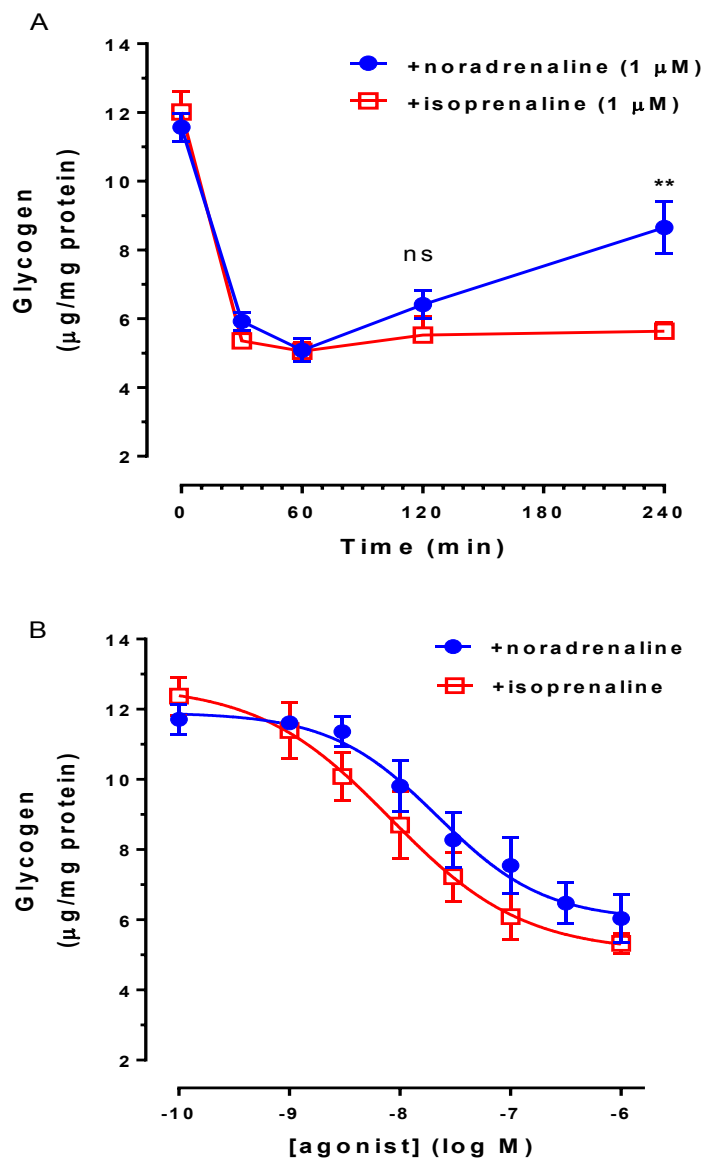
Figure 5.3. **Time-course and concentration-dependency of glycogenolysis stimulated by either noradrenaline or isoprenaline in rat cortical astrocytes.** Confluent monolayers of cerebrocortical astrocytes were serum-starved for overnight prior to experiments. (A) Shows time-course of increase in glycogenolytic effect stimulated by 1 μM NA or 1 μM ISO. (B) Astrocytes were incubated with the indicated concentrations of noradrenaline or isoprenaline for 60 min and then the amount of glycogen content was determined as described in *Methods*. Results are shown as means ± S.E.M. Statistical analysis was performed by Bonferroni's multiple comparison test following two-way ANOVA; **$p<0.01$.
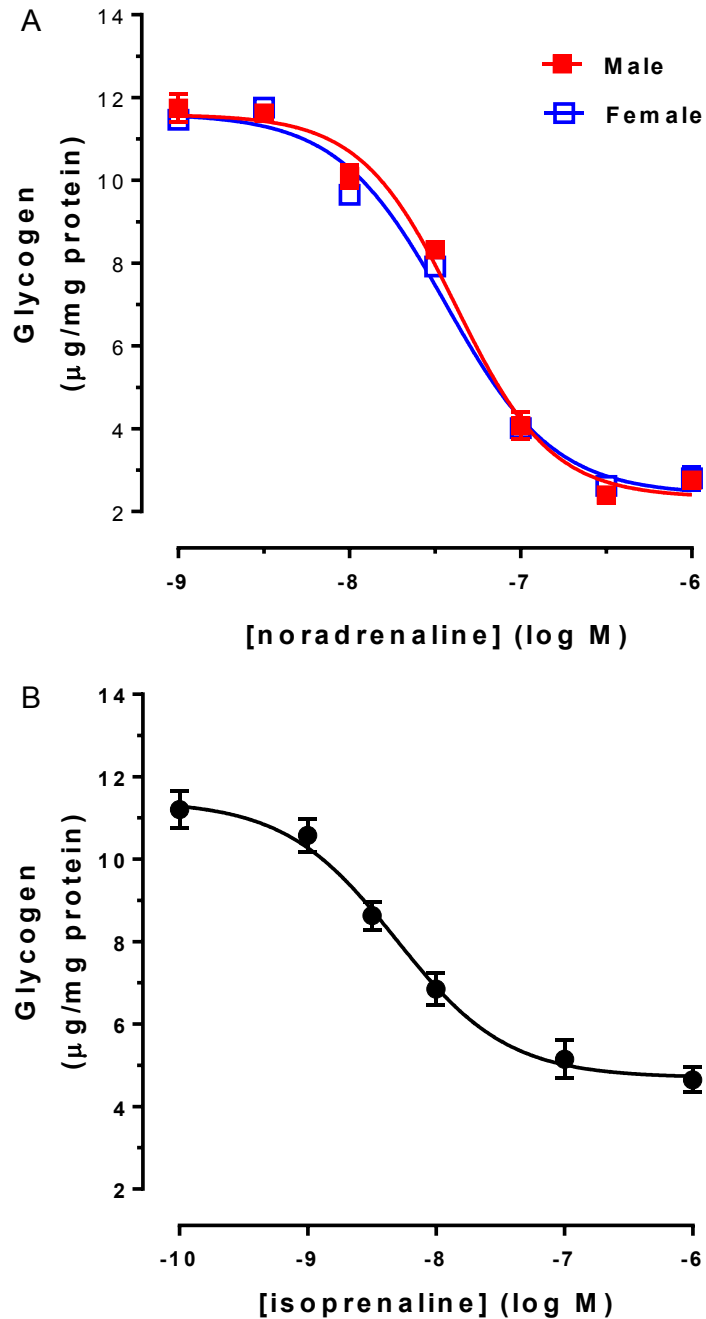
Figure 5.4. Concentration-response curves of adrenoceptor-activated glycogenolysis in astrocytes. Panel (A) shows concentration-dependent action of noradrenaline (ranging from 1 nM to 1 μM, 60 min) stimulated glycogenolysis in near confluent astrocyte monolayers derived from cerebral cortex obtained from male and female neonatal rats, respectively. Panel (B) shows dose response curve of β-AR agonist isoprenaline-stimulated glycogenolysis in rat astrocytes obtained from cerebellum. Glycogen contents were determined as described in *Methods*. Data are shown as means ± S.E.M, for n=3 separate batches of cells.

5.2.4. β₁-Adrenoceptors are the principal subtype mediating glycogenolysis in rat cerebrocortical astrocytes

To determine the roles of the different β-adrenoceptor subtypes that might regulate noradrenaline-stimulated glycogenolysis, astrocytes were pre-incubated with different concentrations of the β₁-adrenoceptor-selective antagonist CGP20712A (1 nM – 1 μM) for 30 min before addition of noradrenaline (1 μM, 60 min). The glycogenolytic effect of noradrenaline was antagonized by CGP20712A (pEC_{50} (-log M) 7.59 ± 0.13; K_i = 4.3 x 10^{-10} M n=4; Figure 5.5A), while pre-incubation with the β₂-adrenoceptor antagonist ICI118,551 had little inhibitory effect on noradrenaline-stimulated glycogenolysis, even at high ≥ micromolar concentrations (Figure 5.5B). These results strongly suggest the pre-eminence of the β₁-subtype in mediating astrocytic glycogenolysis, in agreement with my previous findings with respect to the adrenoceptor subtype mediating the adenylyl cyclase-stimulatory effect of this agonist (Chapter 3).

5.2.5. Investigation of the relationship between cAMP accumulation and mobilization of astrocyte glycogen

To further validate the link between adrenoceptor-induced glycogenolysis and the G_s/adenylyl cyclase (AC)/cAMP accumulation pathway, astrocyte cultures were pre-incubated in the absence or presence of the AC inhibitor 2',5'-dideoxyadenosine (DDA; 300 μM, 30 min) followed by addition of isoprenaline (at concentrations 1 nM - 1 μM for 60 min). In the presence of DDA, the glycogenolytic response to isoprenaline was significantly attenuated (Figure 5.6). At a maximally effective concentration of isoprenaline (1 μM) the presence of DDA caused a 56% reduction in glycogen breakdown.

The effect of phosphodiesterase (PDE) inhibition in astrocyte glycogen was also assessed by pre-incubating cells in the absence and presence of IBMX (300 μM, 15 min). Interestingly, considerable variability was observed between different batches of astrocytes. In some batches of astrocytes addition of IBMX alone did not alter basal glycogen levels, but did cause a 2-3-fold left-shift in the concentration-dependency of noradrenaline to cause glycogenolysis (Figure 5.7A). In contrast, in other astrocyte cultures pre-incubation with IBMX *per se* was sufficient to cause marked glycogen breakdown, with subsequent addition of noradrenaline having little or no further effect (Figure 5.7B). These results indicate that the modest effect IBMX addition has on cAMP accumulation in astrocytes is sufficient in

some cases to cause increased glycogenolysis, whereas in others an additional cAMP stimulus (noradrenaline) is required.

To more directly assess the relationship between cAMP accumulation and glycogen breakdown, we next compared cAMP and glycogenolytic responses to isoprenaline in the same batches of astrocytes. The relationship between cAMP accumulation and glycogen breakdown is illustrated in Figure 5.8. The concentration-response curve for isoprenaline-stimulated glycogenolysis (pEC_{50} (-log M), 7.86 ± 0.04, n=3) is approx. 10-fold left-shifted relative to that for cAMP accumulation (pEC_{50} (-log M), 6.92 ± 0.02, n=3). Thus, isoprenaline elicits a glycogenolytic response with one order of magnitude higher potency (EC_{50} 13.7 nM) compared to the cAMP response (EC_{50} 121 nM) in astrocytes indicating that signal amplification occurs between the two β_1-adrenoceptor-mediated events.
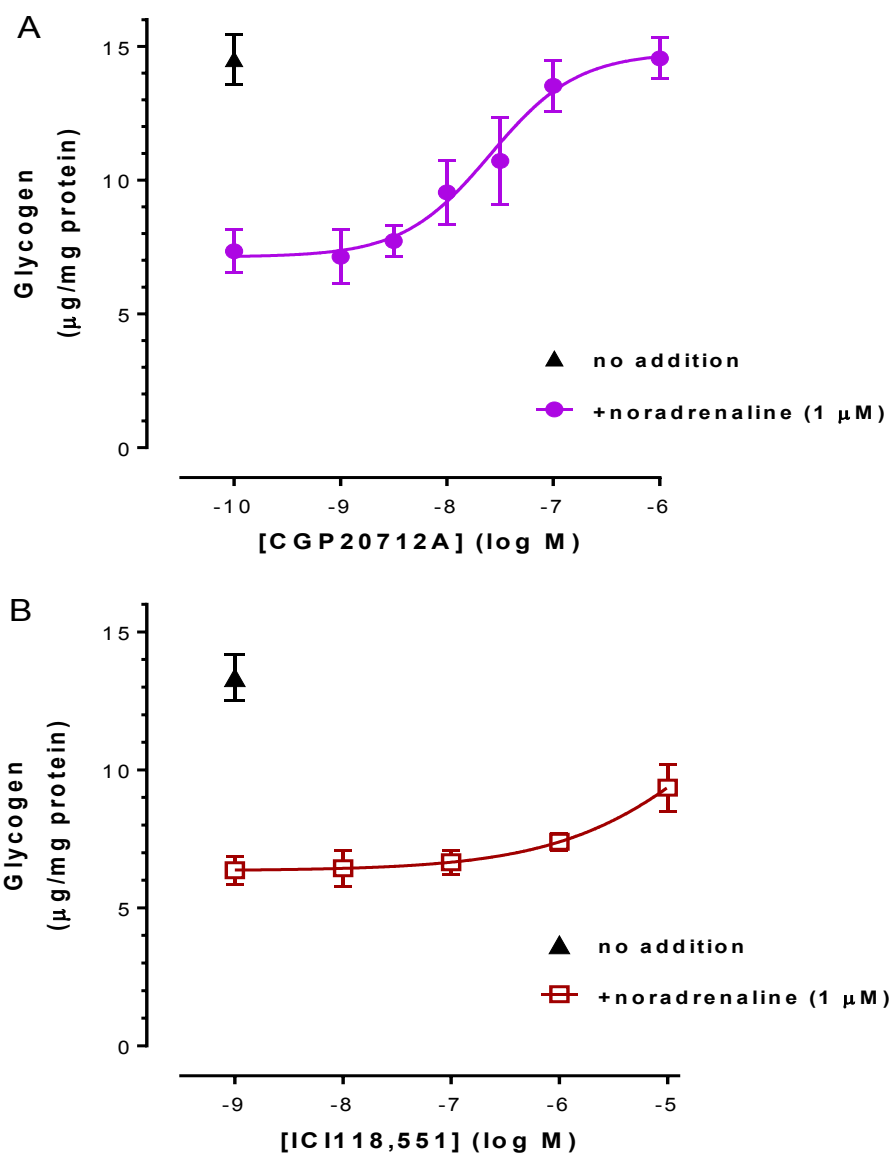
Figure 5.5. **Inhibition of β₁-, and β₂- adrenoceptor (ARs) antagonists to noradrenaline stimulated glycogenolysis in rat cortical astrocytes.** Confluent monolayers of cerebrocortical astrocytes were serum-starved for overnight prior to experiments. Panel (A) shows pre-addition (for 30 min) of β₁-AR antagonist CGP20712A concentration-dependently inhibit astrocytic glycogenolysis stimulated by noradrenaline (1 μM; 60 min). Panel (B) shows β₂-AR antagonist ICI118,551 hardly inhibit noradrenaline-stimulated glycogenolysis. Results are shown as mean ± S.E.M., n=3.
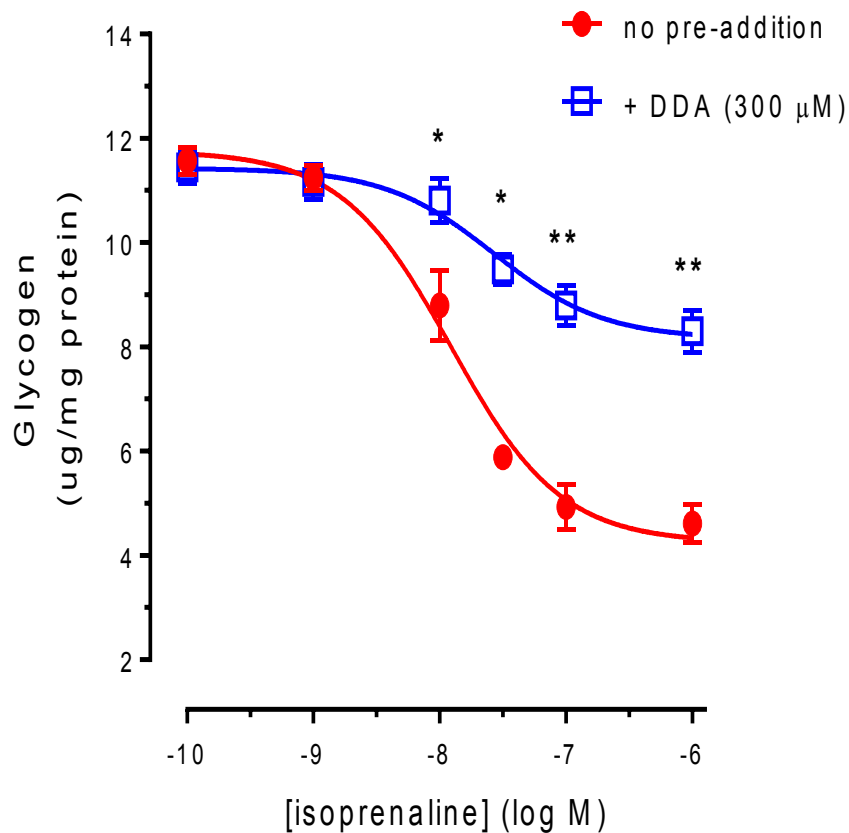
Figure 5.6. Inhibitory effects of adenylyl cyclase inhibitor (DDA) on isoprenaline stimulated glycogenolysis in rat cortical astrocytes. Confluent monolayers of cerebrocortical astrocytes were serum-starved for overnight prior to experiments. Cells were pre-incubated in the presence or absence of DAB (300 µM) for 30 min. Concentration-dependency of ISO-stimulated glycogenolysis was determined as described in *Methods*. Data are means ± S.E.M., n=3. Statistical analysis was performed using Bonferroni's multiple comparison following one-way ANOVA. *$p<0.05$, **$p<0.01$.
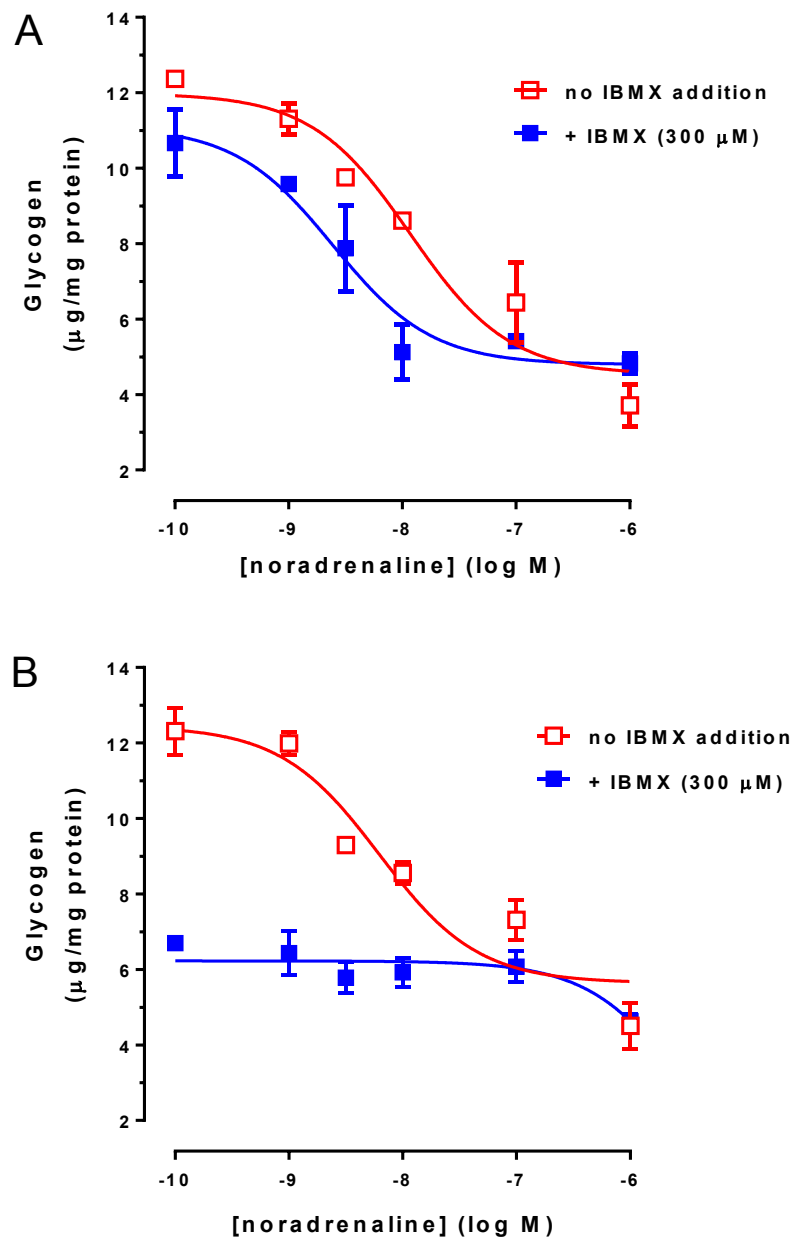
Figure 5.7. Glycogenolytic effects of noradrenaline in rat cortical astrocytes in the presence and absence of IBMX. Confluent monolayers of cerebrocortical astrocytes were serum-starved for overnight prior to experiments. Individual experiment in panel A and B respectively shows the different effects of pretreatment with IBMX (300 μM) on concentration increasingly stimulated glycogenolysis in astrocytes derived from different batch of rat neonates. Data are shown for a single representative experiment (of three) performed in duplicate.
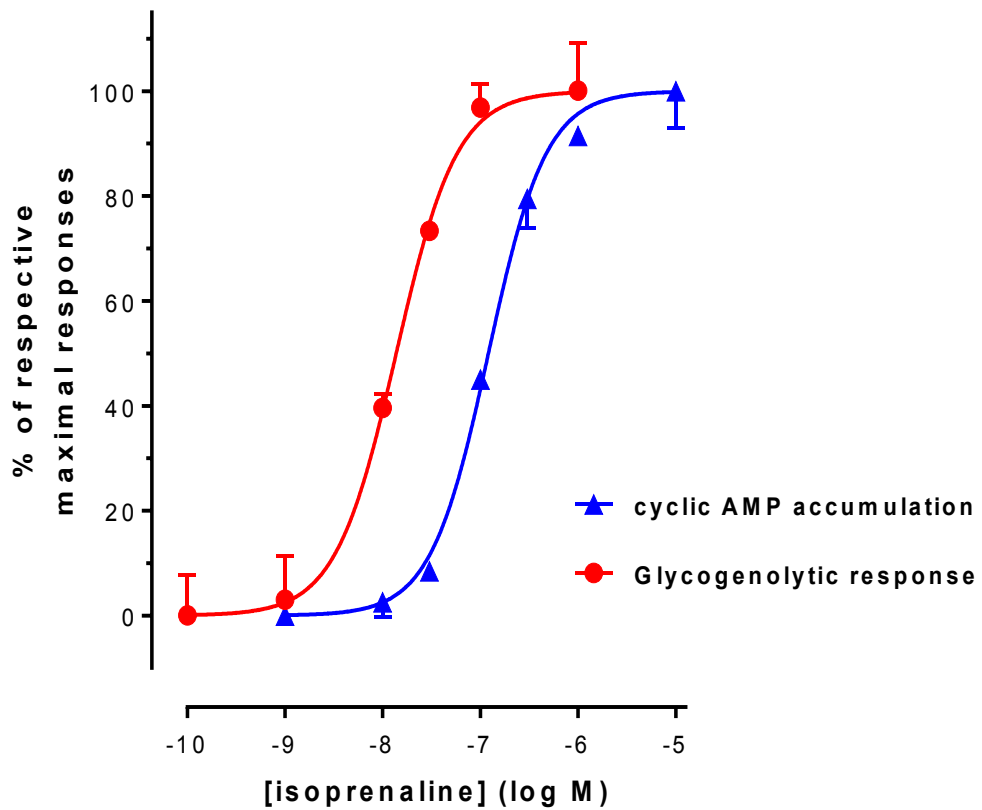
Figure 5.8.   Relationship between cAMP mobilization and glycogen turnover in rat cortical astrocytes. Confluent monolayers of cerebrocortical astrocytes were serum-starved for overnight prior to experiments. Concentration-dependency of isoprenaline mediated glycogenolytic response and cAMP accumulation was determined as described in *Methods*. Average values including cAMP and glycogen contents are indicated as percentages of those under maximal responses. All values are expressed as means ± S.E.M.

5.2.6. Effect of glycogen phosphorylase inhibition on agonist-induced glycogen breakdown

1,4-Dideoxy-1,4-imino-D-arabinitol (DAB) has already been shown to be an effective inhibitor of glucopenia-induced glycogen breakdown in astrocytes (see Figure 5.1); here I investigated how effective DAB is in blocking receptor-mediated glycogenolysis. Astrocyte cultures were pre-incubated with different concentrations of DAB (ranging from 30 nM to 300 μM) for 60 min prior to addition of isoprenaline (1 μM, 60 min). DAB concentration-dependently inhibited isoprenaline-mediated glycogenolysis (pIC_{50} (-log M) = 4.94 ± 0.35, n=3) causing complete inhibition of glycogenolysis at a sufficiently high concentration (control glycogen content, 11.49 ± 0.33; +isoprenaline, 3.88 ± 0.12; + isoprenaline + DAB (300 μM), 11.88 ± 0.52 μg/mg protein; n=3; Figure 5.9). It should also be noted that addition of DAB alone had no effect *per se* on the glycogen content in astrocytes (10.98 ± 0.30 μg/mg protein). Our results demonstrated pre-treatment with DAB (300 μM, 60 min) can completely suppress receptor-mediated glycogenolysis in astrocytes.
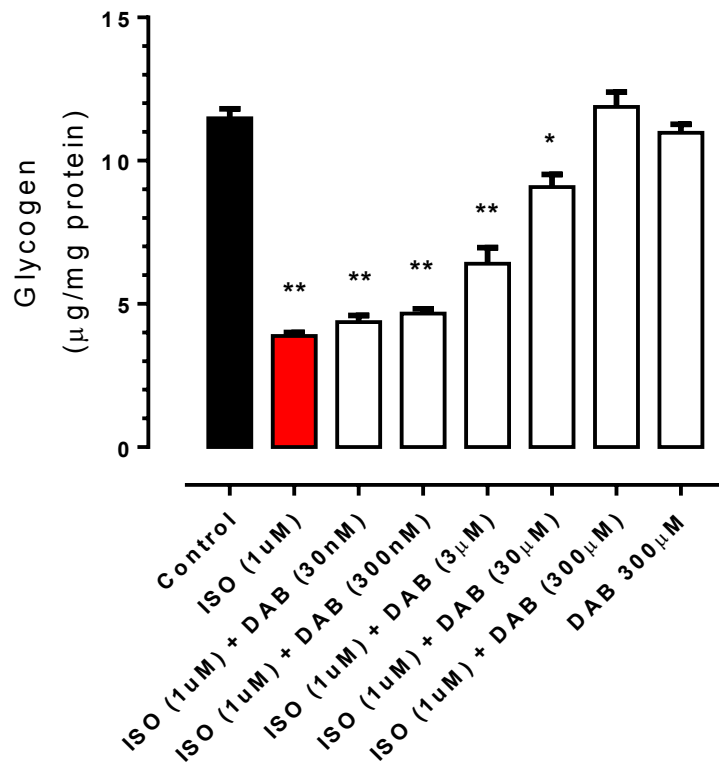
Figure 5.9. Inhibitory effects of glycogen phosphorylase inhibitor (DAB) on isoprenaline-stimulated glycogenolysis in rat cerebral astrocytes. Cultured rat cerebrocortical astrocytes were pre-incubated in the presence of different concentration of DAB for 1 h. The glycogen content was determined following the pre-incubation period and after subsequent exposure to isoprenaline (1 μM). Data are means ± S.E.M., n=3. Statistical analysis was performed using Bonferroni's multiple comparison following one-way ANOVA. *$p<0.05$, **$p<0.01$.

5.2.7. Net re-synthesis of glycogen following β-adrenoceptor blockade

My preliminary experiments have demonstrated that β-adrenoceptor stimulation can exert long-lasting glycogenolytic effects (Figure 5.3A), which has the potential to markedly deplete this energy reservoir in the CNS. To assess the rate of astrocytic glycogen re-synthesis following pharmacological stimulation (as opposed to glucopenic-induction of glycogen breakdown; Figure 5.2), time-course effects of isoprenaline (1 μM) or noradrenaline (1 μM) - stimulated astrocytic glycogen turnover were observed. After 30 min stimulation with the adrenoceptor agonist, a concentration of the non-selective β-adrenoceptor antagonist, timolol (10 μM), was added that could completely displace agonist binding (see Figure 5.10) and the time-course of recovery of astrocytic glycogen content followed.

Timolol addition to astrocytes stimulated by isoprenaline caused a complete recovery within 90 min (glycogen content at 120 min, 11.88 ± 0.63 versus a pre-stimulation level of 12.09 ± 0.43 μg/mg protein; n=3, Figure 5.10A) with no further change over the subsequent 2 h. In contrast, addition of timolol 30 min after noradrenaline challenge resulted in a faster recovery in glycogen level with a significant 'over-shoot' being observed (glycogen content at 120 min, 15.94 ± 0.33 versus a pre-stimulation level of 11.09 ± 0.19 μg/mg protein, n=4, $p<0.001$; Figure 5.10B). The rate of glycogen recovery following β-adrenoceptor blockade was 77 ng glucosyl equiv./mg protein/min where isoprenaline was the agonist and 123 ng glucosyl equiv./mg protein/min when glycogenolysis was stimulated by noradrenaline; both glycogen re-synthesis rates were substantially higher than obtained when glucose was re-added following a period of deprivation (Figure 5.2; 20 ng glucosyl equiv./mg protein/min).

5.2.8. α_2-Adrenoceptor activation has a glycogenic effect in rat astrocytes

As already demonstrated the key difference between the effects of maximally effective concentrations of noradrenaline in comparison with isoprenaline is that this agonist also stimulates astrocyte α-adrenoceptor populations and these actions will not be antagonized by timolol. Therefore, I next examined the potential effects of α-adrenoceptor activation on astrocytic glycogen turnover.

Addition of the α_2-adrenoceptor-selective agonist dexmedetomidine (100 nM) caused a time-dependent increase in astrocyte glycogen levels, with an approx. 50% increase in basal

glycogen content observed 120 min after agonist addition (basal, 10.0 ± 0.4; +dexmedetomidine, 15.4 ± 0.9 µg glycogen/mg protein; n=3; $p<0.01$; Figure 5.11).

5.2.9. Opposing effects of α_2-adrenoceptors and cAMP-elevating agents on glycogen turnover

I have previously shown that the α_2-adrenoceptor-selective agonist dexmedetomidine can concentration-dependently inhibit isoprenaline- or forskolin-stimulated cAMP accumulation in rat cortical astrocytes (Figure 3.8). These data are extended here. A fixed concentration of dexmedetomidine (300 nM) caused a marked suppression of cAMP accumulation stimulated by either isprenaline (Figure 5.13A) or PACAP (Figure 5.13B). Against each agonist dexmedetomidine has little effect on the potency of the cAMP-elevating ligand, but causes a ≥50% inhibition at maximally effective concentrations of either isoprenaline or PACAP. Against a lower concentration of forskolin (1 µM) than used previously (cf. Figure 3.8) it was notable that dexmedetomidine at high concentrations (≥100 nM) was able to suppress cAMP to near basal levels.

Having re-established the relationship between α_2-adrenoceptor activation in astrocytes and the cAMP-elevating effects of these agents, I next turned my attention to how such interactions alter glycogenolytic rates in astrocytes. At a maximally effective concentration of isoprenaline (1 µM), dexmedetomidine had little effect on the glycogenolysis caused by this agent, however, if a lower concentration of isoprenaline was used (10 nM; Figure 5.13A) dexmedetomidine could concentration-dependently inhibit the glycogenolytic response (pIC_{50} (-log M), 7.36 ± 0.25; n=3). Similar glycogen-sparing effects of dexmedetomidine were observed if forskolin was used (1 µM, Figure 5.13B; pIC_{50} (-log M), 8.01 ± 0.14, n=3).

PACAP concentration-dependently stimulated glycogenolysis (pEC_{50} (-log M), 9.93 ± 0.14, n=3; Figure 5.13C). Similar to isoprenaline, dexmedetomidine was ineffective in inhibiting glycogenolysis stimulated by a high concentration of PACAP (≥ 10 nM) but was highly effective in concentration-dependently reversing the glycogenolytic action of PACAP, this agent was added at a sub-maximally effective concentration (0.3 nM; Figure 5.13D). These data suggest that glycogenolysis stimulated by cAMP-elevating agents can be functionally antagonized by α_2-adrenoceptor activation in rat cortical astrocytes.
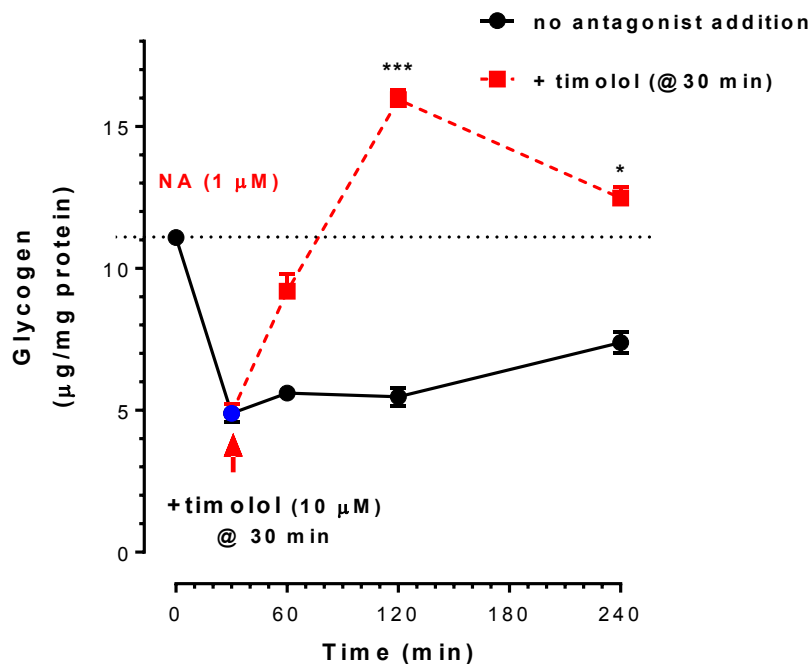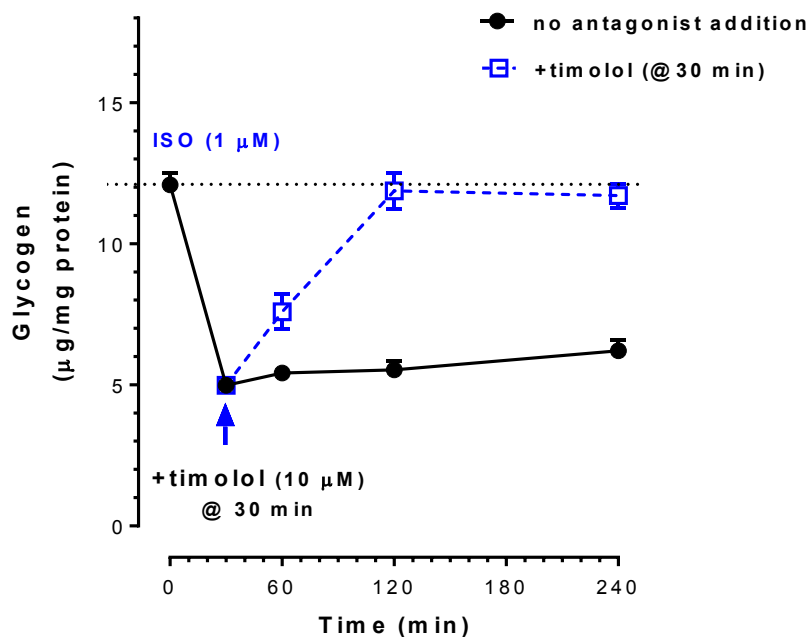
Figure 5.10.   **Time-courses of glycogen re-synthesis following adrenoceptor stimulation and antagonist (timolol) addition to cerebral cortex astrocytes.** Confluent monolayers of cerebrocortical astrocytes were serum-starved overnight prior to experiments. Cells were then challenged with either isoprenaline (1 µM, panel A) or noradrenaline (1 µM, panel B) for 30 min and followed by incubation with/without timolol (10 µM) treatment for the time-periods indicated.   Glycogen content was determined as described in *Methods*. Data are means ± S.E.M., n=3. Statistical analysis was performed using Bonferroni's multiple comparison following one-way ANOVA. *$p<0.05$, ***$p<0.001$.
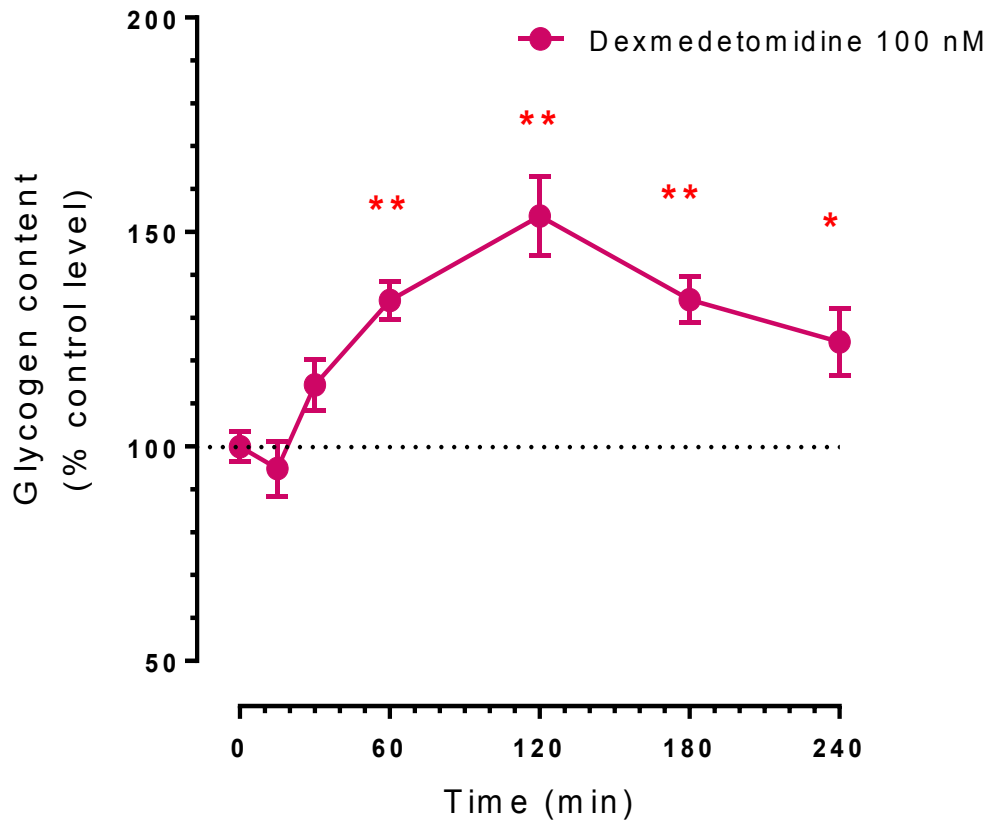
Figure 5.11. **Time-course of α_2-adrenoceptor-mediated glycogenic effect in rat cerebral cortex astrocytes.** Confluent monolayers of cerebrocortical astrocytes were serum-starved for overnight prior to experiments. Cells were treated with selective α_2-AR agonist dexmedetomidine (100 nM) as indicated time periods (15, 30, 60, 120, 180, 240 min). Glycogen content was determined as described in *Methods*. Data are means ± S.E.M., n=3. Statistical analysis was performed using Bonferroni's multiple comparison following one-way ANOVA. *$p<0.05$, **$p<0.01$.
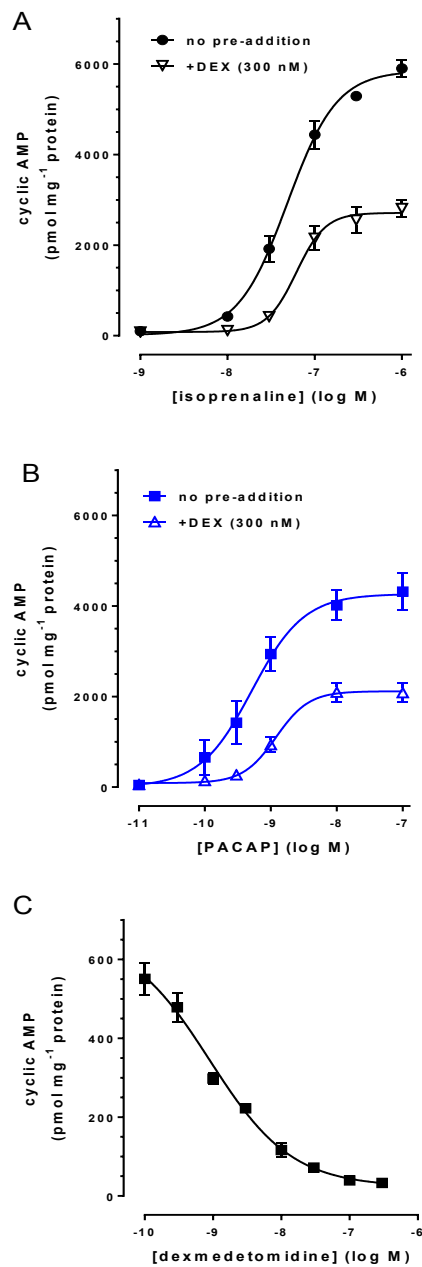
Figure 5.12   Inhibitory effects of the α₂-adrenoceptor agonist dexmedetomidine (Dex) on cAMP accumulations stimulated by either receptor-dependent or -independent cAMP-elevating agents in rat cortical astrocytes. The effects of a single concentration of dexmedetomidine (300 nM) on cAMP accumulation stimulated by different concentrations of isoprenaline (A) or PACAP (B). Dexmedetomidine concentration-dependently inhibited forskolin (1 μM) stimulated cAMP accumulation. cAMP values were determined as described in *Methods*. Data are means ± S.E.M. for at least 3 separate experiments.
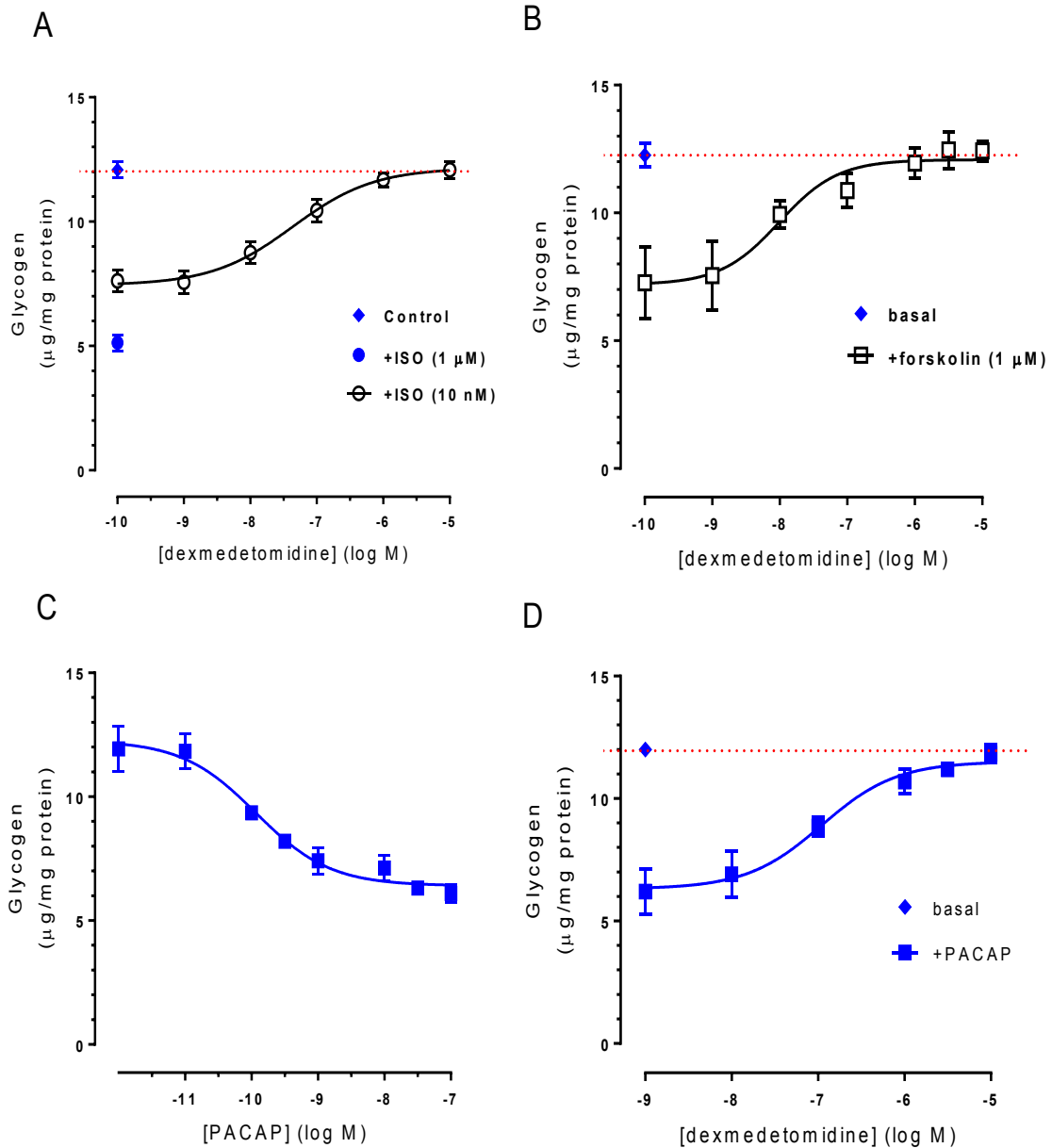
Figure 5.13. Concentration-dependent inhibitory effects of dexmedetomidine on glycogenolytic responses to isoprenaline, forskolin or PACAP in rat cerebral astrocytes. (A) showing increasing concentrations of dexmedetomidine pre-treatment with 10 min inhibited cAMP accumulation stimulated by isoprenaline (10 nM). Cells without treatment and challenged with 1 μM ISO are shown as negative and positive controls, respectively. Similar inhibitory effects were observed for forskolin- (1 μM; B) and PACAP (0.3 nM; D) -stimulated glycogenolytic effect and its inhibition by dexmedetomidine pre-treatment were shown in panel (C) and (D). Glycogen levels were determined as described in *Methods*. Data are means ± S.E.M.

5.2.10. Astrocytic glycogenolysis is triggered by store-operated Ca^{2+} entry (SOCE)

Increases in cytosolic Ca^{2+} concentration have been reported to activate phosphorylase kinase (PK) and consequently the rate-limiting enzyme glycogen phosphorylase (GP) (Muller, 2014, Obel et al., 2012) to increase glycogenolysis. Initial experiments focused on investigating the effects of α_1-adrenoceptor-stimulated intracellular Ca^{2+} mobilization on astrocyte glycogenolysis. As shown in Figure 5.14A, the selective α_1-adrenoceptor agonist, A61603 (100 nM) stimulated a Ca^{2+} response in rat cortical astrocytes (see also Chapter 3), which is considered to occur via activation of the PLC/IP_3/Ca^{2+} cascade, where Ca^{2+} is mobilized from the endoplasmic reticulum (ER) store (Piascik and Perez, 2001, Garcia-Sainz et al., 2000). Using a similar stimulation strategy A61603 at a range of concentrations failed to evoke a glycogenolytic response (Figure 5.14B).

Experiments were also performed using the SERCA inhibitor, thapsigargin (Tg). This agent blocks SERCA and promotes a passive depletion of ER Ca^{2+}-stores, triggering a sustained $[Ca^{2+}]_i$ elevation (see Figure 5.14A), which is sustained by the entry of extracellular Ca^{2+} ions by the mechanism of store-operated Ca^{2+} entry (SOCE) (Cahalan, 2009). Applying this strategy did cause significant glycogenolysis in astrocytes (control, 11.01 ± 0.34; +Tg (2 µM; 30 min), 6.81 ± 0.58 µg/mg protein, n=3; $p<0.01$; Figure 5.14C). These data suggest that changes in intracellular Ca^{2+} can regulate glycogenolysis in astrocytes, however, sustained SOCE may be required.

5.2.11. Glycogenolysis is required upon the extracellular K^+ increase

Extracellular potassium concentrations ($[K^+]_o$) in the mammalian central nervous system (CNS) increase during neuronal firing, and under some pathological conditions (Subbarao *et al.*, 1995). I next investigated whether changes in $[K^+]_o$ affect glycogen stores in astrocytes. To achieve this the medium $[K^+]$ was increased from the normal level of 5.4 mM. Increasing the $[K^+]_o$ to either 10 or 25 mM caused a marked and sustained decrease in astrocyte glycogen the store (Figure 5.15A). The concentration-dependency of the $[K^+]_o$ effect on glycogen content was also assessed (Figure 5.15B). At high $[K^+]_o$ (45 mM) the glycogenolysis elicited approached that seen in response to β-adrenoceptor activation (ISO; 1 µM); in addition, addition of the Ca^{2+} chelator EGTA (3 mM, 10 min) prior to elevation of $[K^+]_o$

completely annulled the glycogenolytic effect of hyperkalaemia (Figure 5.15B) suggesting that the effect of K^+ is secondary to Ca^{2+} entry, likely via L-type VOCCs.
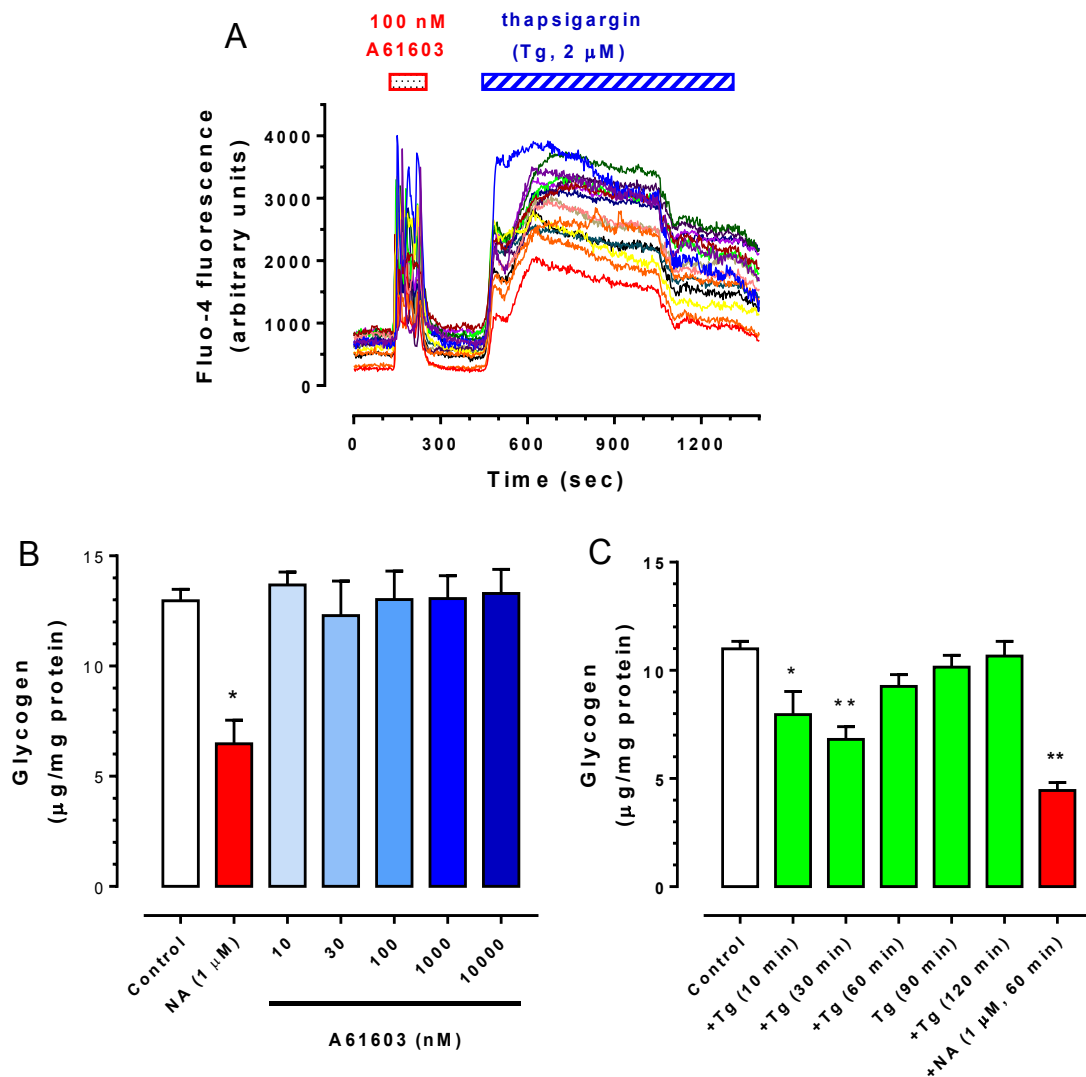
Figure 5.14. Effect of different modes of Ca^{2+} response on glycogenolysis in rat cortical astrocytes. α_1-adrenoceptor agonist A61603 and thapsigargin-induced intracellular Ca^{2+} mobilization in different mechanism, one of three individual experiments is represented in (panel A). Panel (B) shows concentration-dependent isoprenaline stimulation on the change of glycogen content in astrocytes. Panel (C) shows the time course effect of thapsigargin (2 μM) treatment on glycogen metabolism. Glycogen values were measured as described in *Methods*. Data are mean ± S.E.M., n=3. Statistical analysis was performed using one-way ANOVA followed by Bonferroni's multiple comparison test: *$p<0.05$, **$p<0.01$.
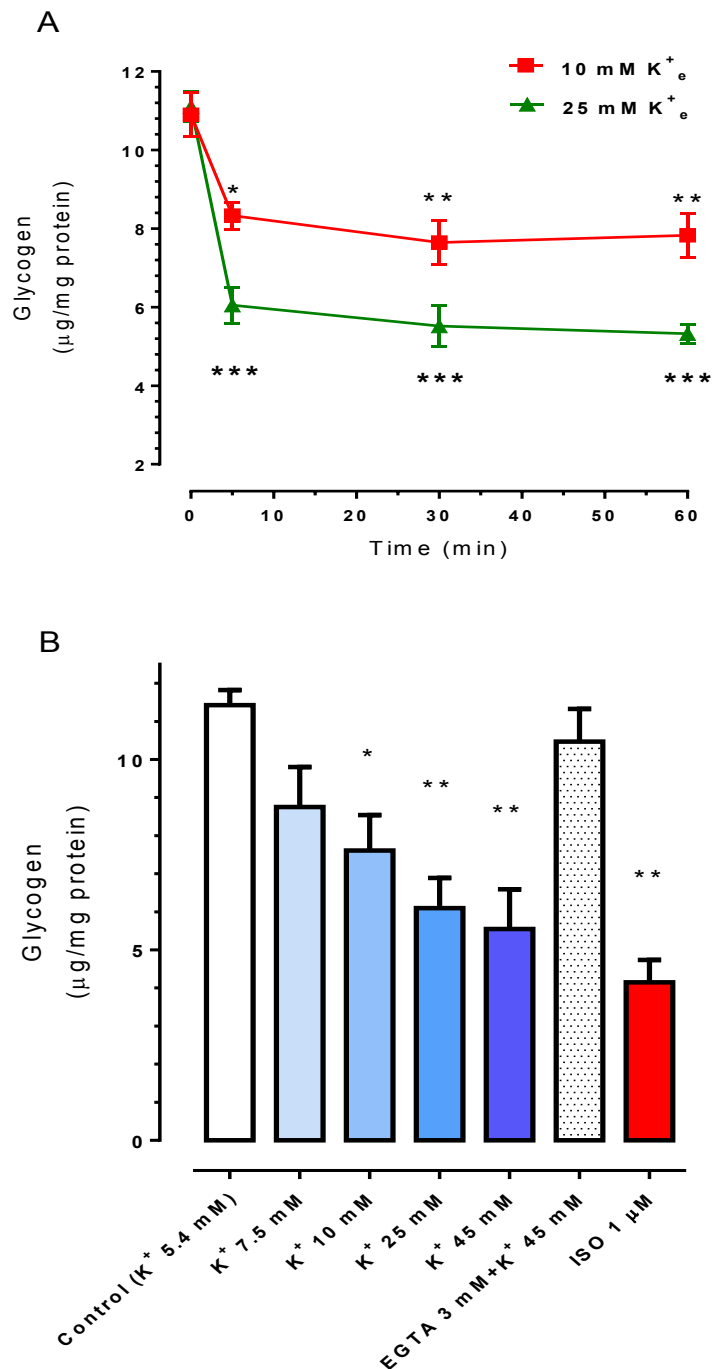
Figure 5.15. **Time-course and concentration-dependent effect of raising extracellular [K⁺] on glycogen content of rat cerebral cortex astrocytes.** Confluent monolayers of cells were serum-starved for 24 h prior to challenge with KCl (final concentration ranging from 7.5 - 45 mM) for 60 min, EGTA pre-treatment for 10 min following 45 mM KCl, isoprenaline (ISO; 1 µM) as a positive control. Glycogen content was determined (see *Methods*). Results are shown as means ± s.e.m. of 4 independent experiments performed in triplicate. Statistically significant differences (*$p<0.05$, **$p<0.01$) determined by one-way ANOVA followed by Bonferroni's multiple comparison test.

5.2.12 Dynamics of β-adrenoceptor activated morphological changes in rat cerebrocortical astrocytes

Morphological plasticity in astrocytes has been recognized for decades (Hatten, 1985, Ramakers and Moolenaar, 1998, Won and Oh, 2000, Rodnight and Gottfried, 2013). Cultured astrocytes from neonatal rodent brain usually exhibit more flat and polygonal shape (Won and Oh, 2000), however, many factors have been found to influence astrocyte phenotype, such as co-culture with neurons (Matsutani and Yamamoto, 1998, Matsutani and Yamamoto, 1997), as well as a number of pharmacological stimuli, which can cause cultured astrocytes to display a more process-bearing (stellate) morphology (Rodnight and Gottfried, 2013). In this latter regard, β-adrenoceptor/cAMP pathway activation has been shown to alter astrocyte morphology, however, the molecular mechanisms under this morphological plasticity and its functional consequences are not yet fully clear.

To observe the real-time dynamics of β-adrenoceptor-mediated morphological changes in a single living astrocytes, cells were transfected with a plasmid allowing expression of enhanced-green fluorescent protein (GFP). Fluorescence could be visualized distributing throughout the cytosol of individual astrocytes, 24 h after transfection (Figure.5.16). The decrease in cell cross-sectional area and the appearance of new, elongated cell processes evidenced astrocyte stellation (Vardjan *et al.*, 2014). To provide a quantification of the morphological changes induced with isoprenaline (1 μM) I analysed the change in cell cross-sectional area. A decrease in cell cross-sectional area was evident at the earliest time-point (5 min) after isoprenaline addition (16.9 ± 2.6% decrease versus control; $p<0.05$; Figure 5.16C) with greater changes in cell cross-sectional area observed at longer time-periods in the presence of the agonist (e.g. at 60 min: 58.8 ± 4.0% decrease versus control; $p<0.01$; Figure 5.16C). Similar changes in astrocyte morphological could be observed following addition of forskolin. These data indicate the receptor-dependent or -independent increases in cAMP are likely responsible for the observed changes in astrocyte morphology. Morphological change *in vitro* is rapid with maximal stellation occurring within a 60-120 min time-frame.

To assess another feature of cell stellation, a set of experiments was performed using an antibody raised against glial fibrillary acidic protein (GFAP; to identify astrocytes), phalloidin (to identify the actin cytoskeleton) and Hoechst stain (to identify nuclei). Addition of

isoprenaline (1 µM; for 60 min) caused a very marked astrocytic stellation (GFAP immunostaining; Figure 5.17A) and actin reorganization (phalloidin staining; Figure 5.17B; (Cui et al., 2014).

To investigate whether noradrenaline-mediated astrocyte stellation occurs exclusively via β-adrenoceptor activation it was shown that the marked changes in cell-shape evoked by addition of noradrenaline (1 µM, 60 min; Figure 5.18A, B) were completely prevented by pre-treatment with the β-adrenoceptor antagonist, timolol (10 µM added 30 min before noradrenaline; Figure 5.18C). Furthermore, the selective PKA inhibitor, KT5720 (5 µM, added 30 min before noradrenaline; Figure 5.18D) and glycogen phosphorylase inhibitor DAB (300 µM added 60 min before noradrenaline; Figure 5.18E) each inhibited agonist-stimulated morphological changes. I also provide some preliminary evidence for the reversibility of the morphological effects of β-adrenoceptor activation – thus when timolol (10 µM) was added 60 min after noradrenaline a progressive (and complete) reversal of the induced stellate astrocyte morphology had occurred 60 + 120 min after addition of timolol (Figure 5.18F, G).

In order to quantify the effects of noradrenaline and the different inhibitors used in Figure 5.18, the change in cell cross-sectional area and the percentage of cells displaying a stellate morphology was determined under each condition. The latter criterion was defined by examining astrocytes to identify processes longer than their perinuclear diameters (defined as 'stellate' cells) according to previous studies (Shao et al., 1994, Won and Oh, 2000). As shown in Figure 5.19, noradrenaline (1 µM, 60 min) was shown to cause a significant decrease in cell cross-sectional area ($p<0.01$; Figure 5.19A) and increase in astrocyte stellation (from $6.7 \pm 1.9\%$ of control cells to $98.7 \pm 7.2\%$ following agonist addition; $p<0.001$; Figure 5.19B). Timolol pre-treatment completely prevented both morphologic changes. Interestingly, either KT5720 or DAB pre-treatment markedly reduced noradrenaline-evoked morphological changes. For example, DAB reduced the proportion of cells exhibiting a 'stellate' morphology in the presence of noradrenaline from ($98.7 \pm 7.2\%$ to $20.0 \pm 3.3\%$ in the absence and presence of DAB, respectively; Figure 5.19B). These data indicate that astrocyte morphology is markedly altered via β-adrenoceptor/cAMP/PKA signalling pathway activation. In addition, it appears that disrupting the ability of noradrenaline to activate glycogenolysis also impacts on astrocyte stellation indicating perhaps that activation of this metabolic pathway is necessary for astrocyte morphological plasticity.
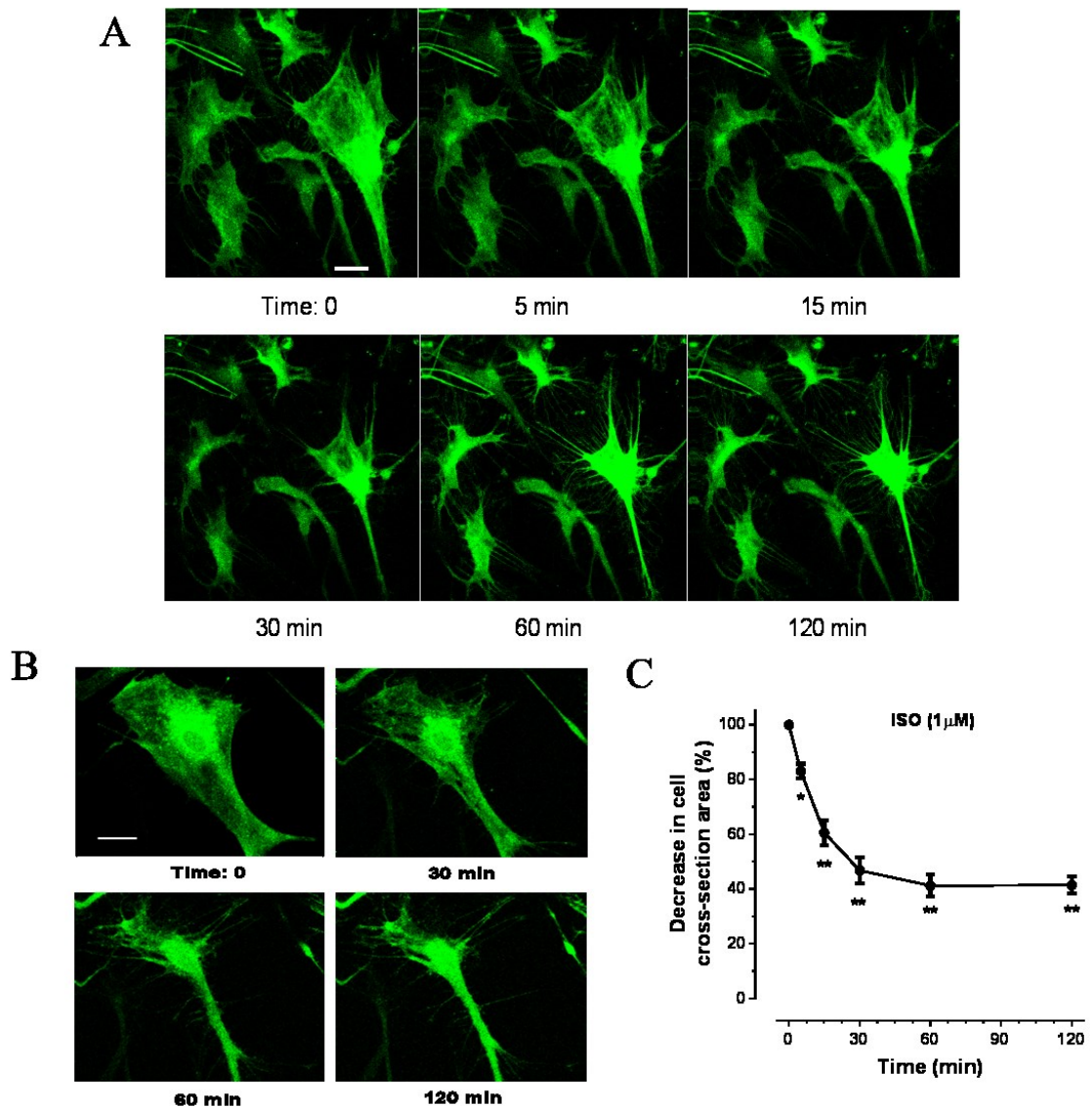
Figure 5.16. Time-course of isoprenaline-stimulated morphologic changes in astrocytes transfected with eGFP. Primary cultured astrocytes were transfected with enhanced green fluorescent protein (eGFP) and grew on coverslip for 3 days. Then cells were washed by KHB buffer twice and cultures were placed in a standard recording chamber in KHB buffer at 37°C and treated with isoprenaline (ISO; 1 μM) for the indicated time-periods. Representative fluorescent images of astrocytes were acquired using a confocal microscope, panel A shows a group of astrocytes and panel B focus on one specific astrocytes. Panel C shows ISO-stimulated morphological changes quantified by the change in cell cross-sectional area (%). At least 30 cells from 3 different batches of astrocytes were counted. Scale bar = 50 μm.
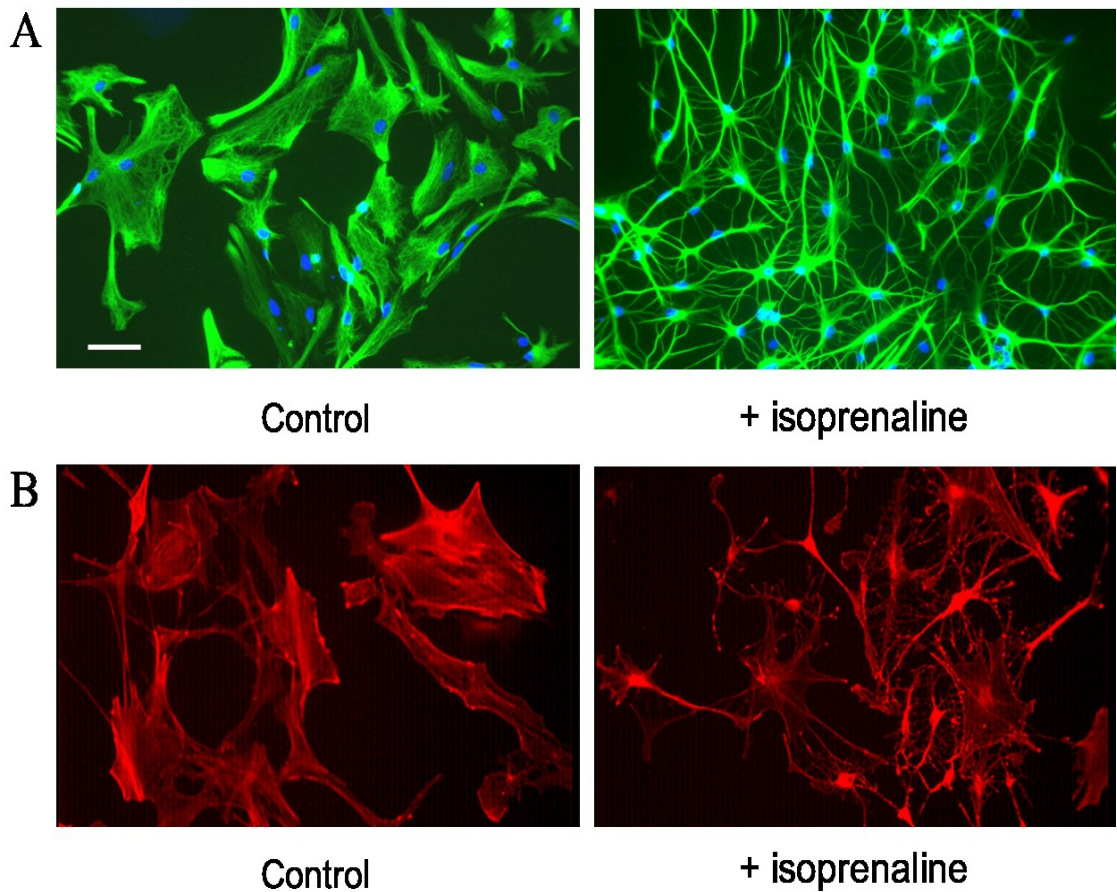
Figure 5.17. **β-adrenoceptor stimulation with isoprenaline stimulates marked morphological changes.** Primary cultured rat cerebral cortex astrocytes were grown in FCS medium until sub-confluent, then cells were treated with/without isoprenaline (1 µM, 60 min) in medium. Fluorescence microscopy detected astrocytes visualized either by GFAP (green, panel A) and the same field stained with the Hoechst dye to reveal nuclei (blue), or by actin (phalloidin, red, panel B) staining. At least 100 cells from 3 different batches of astrocytes were counted. Scale bar = 50 µm.
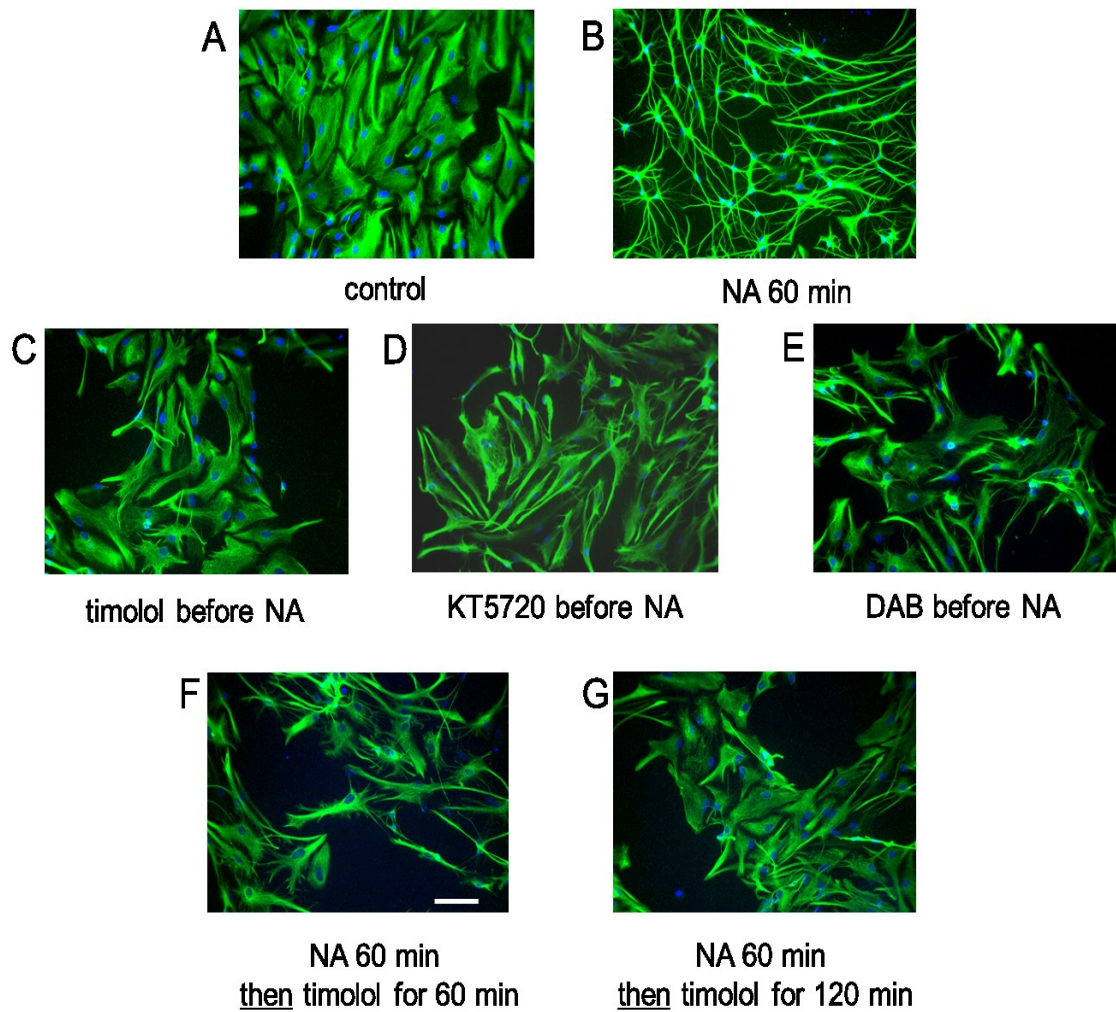
Figure 5.18. **Noradrenaline-stimulated astrocyte morphological changes are inhibited by a β-adrenoceptor antagonist and other inhibitors.** Primary cultured rat cerebral cortex astrocytes were grown in FCS medium until sub-confluency. (A) and (B) shows the shape of cells incubated in the absence or presence of noradrenaline (1 µM, 60 min). Pre-treatment with β-adrenoceptor antagonist timolol (10 µM, -30 min, C), selective protein kinase A inhibitor, KT5720 (5 µM, -30min, D) and glycogen phosphorylase inhibitor DAB (300 µM, -60 min, E) caused different effects in preventing NA (1 µM)-induced stellation. Astrocyte morphological changes caused by NA (1 µM, 60 min) stimulation were reversible followed timolol post-treatment (10 µM, 60 min, F) and (10 µM, 120 min, G). Scale bar = 50 µm.
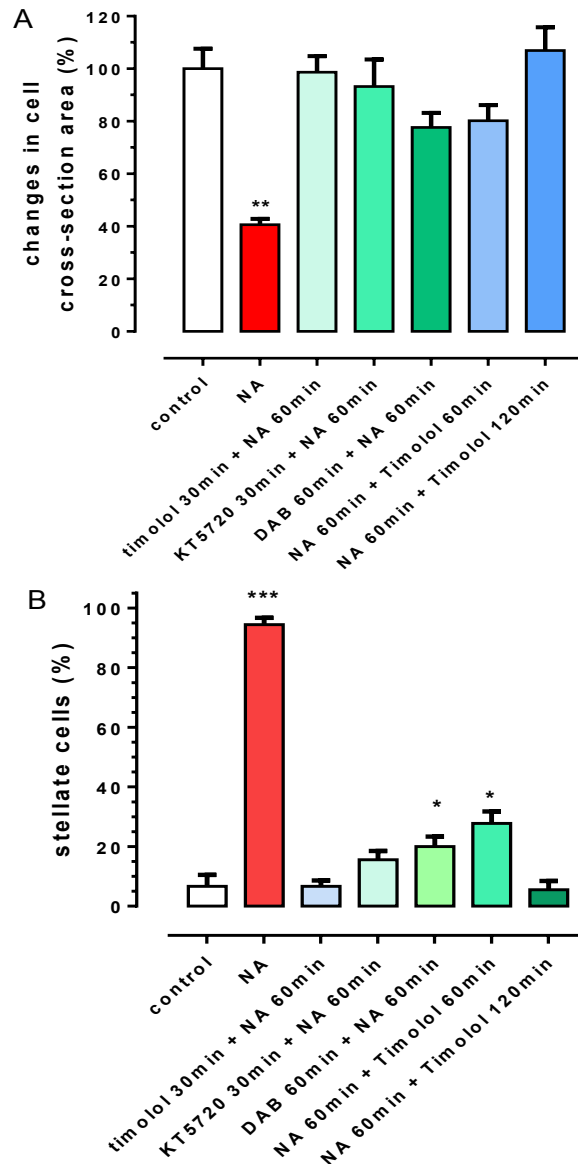
Figure 5.19. Quantitative analysis of astrocyte stellation induced by noradrenaline and the effects of different inhibitors. Cells were grown in FCS medium until sub-confluency, and then the cells were treated with noradrenaline (1 µM) in the presence or absence of different antagonist and inhibitor as indicated. Panel (A) shows the changes in cell cross-section area upon different pharmacologic stimuli, panel (B) shows the relative percentage of stellate astrocytes upon the same challenges. Data are means ± S.E.M. for at least 50 cells from 3 separate experiments. Significance values were determined using one-way ANOVA followed by Dunnett's multiple comparison test (versus appropriate control), where *$p<0.05$, **$p<0.01$, ***$p<0.001$.

5.3 Discussion

In the present Chapter, I have investigated the functional significance of astrocytic glycogen under a variety of conditions, including hypoglycaemia, hyperkalaemia, as well as in response to neurotransmitters. In common with a major theme of my research, attention has been focused on the roles of the different adrenoceptor subtypes expressed by astrocytes in regulating this metabolic response. In a final series of experiments, I have also extended my work to observe adrenoceptor-mediated changes in astrocyte morphology and provide preliminary evidence for a potential link between the ability of astrocytes to mobilize glycogen and undergo noradrenaline-induced morphological change.

Blood-derived glucose is considered to be the principal substrate for brain energy metabolism (Oz *et al.*, 2009), however, how the brain attempts to fulfil its energy requirement during hypoglycaemia is not yet fully understood. Under normal circumstances (euglycaemia, normoxia) glucose is taken up by astrocytes and can be anabolized into glycogen (Prebil *et al.*, 2011). This carbohydrate 'reserve' can supply neurons with glycolytic products (lactate, pyruvate) during times of metabolic stress, such as periods of glucose deprivation. Under normal physiological conditions, experimental evidence indicates that neurons and astrocytes both take up glucose, and astrocyte glycogen content is determined by a dynamic balance between glycogenolysis and glycogen synthesis. In resting situations, neuronal energy metabolism mainly depends on glucose oxidation and to a much lesser degree astrocytic glycolysis-derived lactate (Figure 5.20A). However, during glucose deprivation, astrocytic glycogen breaks down to a lactate/pyruvate, which via an astrocyte-neuron shuttle mechanism involving different types of monocarboxylate transporters, can sustain neurons during the periods of hypoglycaemia, or intense physiological activity (Brown *et al.*, 2003) (Figure 5.20B). The present experiments have demonstrated that switching astrocytes from medium containing 5 mM glucose to glucose-free conditions, immediately causes astrocyte glycogen content to decrease. During glucopenia (for up to 180 min), almost the entire astrocyte glycogen reserve is depleted, findings consistent with previous studies (Gruetter, 2003), which have estimated that brain glycogen can maintain energy metabolism for extended periods of time during hypoglycaemia conditions by using glycogen derived lactate to maintain neuronal function in the absence of glucose.
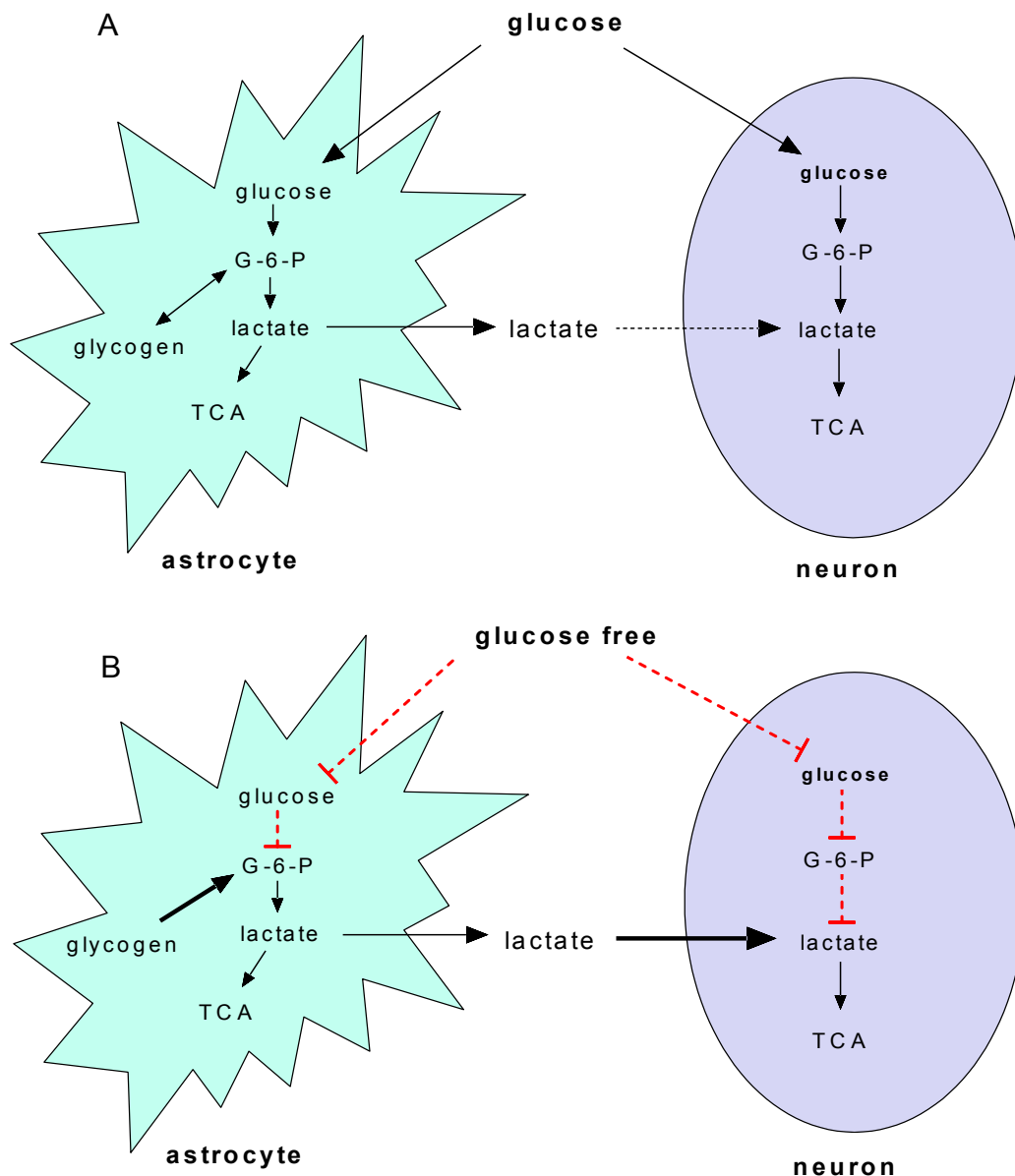
Figure 5.20. Astrocyte glycogenolysis and its contribution to neuron energy supply. (A) Under normal physiological conditions, neuronal energy requirements are satisfied by uptake of extracellular glucose, while astrocytes also take up glucose, some of which it utilized to build up a carbohydrate 'reserve' in the form of glycogen. Astrocytes are believed to be net lactate releasers; released lactate can be taken up by neurons to supply a proportion of their energy requirement. (B) When there is a deficit in extracellular glucose, CNS energy metabolism becomes highly dependent on astrocyte glycogenolysis, and the "astrocyte-to-neuron lactate shuttle" pathway, which can produce neuronal ATP via the tricarboxylic cycle (TCA).

Following glucopenia, re-establishing euglycaemic conditions results in immediate re-synthesis of glycogen (Hertz *et al.*, 2004) that in astrocytes in primary culture occurs over a sustained period (>3 h) and a near constant rate (~20 ng glucose equiv incorporated into glycogen per mg of cellular protein per minute; see Figure 5.2).

Glycogen mobilization is not only triggered by hypoglycaemia, but also by increased rates of neural firing. Upon increases in neuronal activity, there are a myriad of neurotransmitters (and neuromodulators) released that can exert actions on astrocytic glycogen metabolism (Hertz *et al.*, 2015b). In this regard, the role of noradrenaline as a glycogenolytic neurotransmitter has been examined in a large number of studies utilizing a variety of CNS preparations, including cultured astrocytoma cells, rat, mouse and/or chick primary astrocytes from different brain regions including cerebral cortex, thalamus and cerebellum. The specific signalling cascades and relative contribution of the different adrenoceptor subtypes continue to be debated, with conflicting evidence appearing to result from dependences in the species, developmental stage and experimental conditions used (Muller, 2014, Obel et al., 2012, Subbarao and Hertz, 1990a). For example, it has been shown that glycogenolytic responses of astrocytes to noradrenaline change throughout development (Odowd et al., 1995).

Regulation of glycogenolysis by adrenoceptors in astrocytes has been recognized for at least 30 years (Magistretti, 1987, Subbarao and Hertz, 1990a, Sorg and Magistretti, 1991a, Sorg and Magistretti, 1992). β-adrenoceptor-stimulated cAMP accumulation is regarded as a primary mechanism of glycogenolysis (Brown *et al.*, 2004), with the β_2-adrenoceptor being pharmacologically identified as dominant in stimulating astrocytic glycogenolysis in cells isolated from day-old chicks (Gibbs *et al.*, 2008), while β_1-adrenoceptors are the principal subtype expressed in the mammalian brain (Quach et al., 1978) (Quach et al., 1988). My own work using isolated rat neonatal astrocytes, clearly indicates an involvement of β-adrenoceptors in the glycogenolytic response to noradrenaline, with the β_1-adrenoceptor subtype being functionally dominant (Figure 5.5).

Evidence supports differences in the regulation of hepatic glycogenolysis between male and female rats upon catecholamine stimulation (Studer and Borle, 1982); however, in common with the data in Chapter 3 on cAMP accumulation profiles, no significant differences in glycogenolytic responses to noradrenaline were observed in astrocytes isolated from either

male and female donor neonates. In addition, β-adrenoceptor activation in astrocytes derived from either cerebral cortex or cerebellum caused similar glycogenolytic effects, although the proportion of glycogen present in cerebellar astrocytes that was susceptible to breakdown in the presence of the neurotransmitter may be lower (see Figure 5.4).

In my study I have also investigated the relationship between cAMP accumulation and the glycogenolytic response in astrocytes. It was found in early experiments that addition of a phosphodiesterase (PDE) inhibitor (IBMX) had highly variable effects in different batches of astrocytes (see Figure 5.7), where the presence of IBMX might cause a glycogenolytic effect that was as great as noradrenaline addition, or have little or no effect *per se*, but 'left-shift' the concentration-response curve for noradrenaline-mediated glycogenolysis. It was consistently shown that addition of the PDE inhibitor alone (IBMX, 300 µM) has only a modest effect on cAMP accumulation, causing at most a ~2-fold increase-over-basal. These data are best reconciled by invoking a large degree of signal amplification between the cAMP and glycogenolytic responses, essentially with a threshold change in cAMP accumulation being sufficient to evoke substantial glycogenolysis. Evidence for this was more systematically obtained by directly comparing these two responses (Figure 5.8) which clearly showed a 10 times lower EC_{50} for isoprenaline-stimulated glycogenolysis compared to cAMP accumulation. These data indicate that modest changes *in vivo* in extra-synaptic noradrenaline concentration (in the 1-30 nM range) are sufficient to mobilize astrocyte glycogen reserve and the concentrations of this transmitter necessary to cause such effects are within the physiological (Staiti et al., 2011) and pathophysiological (Carboni et al., 2010) range. In the future it would be informative to investigate this relationship at a sub-cellular level in astrocytes, as it is possible that different mechanisms (e.g. β-adrenoceptor activation versus PDE inhibition) have different efficiencies in converting a cAMP signal into glycogenolysis as has been shown in other cell-types (Fu et al., 2013, Lefkimmiatis and Zaccolo, 2014).

Astrocyte α_1-adrenoceptors are G_q-coupled receptors that can increase intracellular Ca^{2+} (Piascik and Perez, 2001, Pankratov and Lalo, 2015a). Previous studies have reported that increases in $[Ca^{2+}]_i$ can lead to the activation of glycogen phosphorylase (GP) activity (Obel et al., 2012, Muller et al., 2014). This likely is dependent on phosphorylase kinase (PhK) activity that can be regulated by Ca^{2+} ions. The ability of Ca^{2+} ions to regulate PhK can occur through calmodulin, a calcium binding protein known to bind to PhK to regulate its catalytic activity.

The precise mechanism(s) involving Ca^{2+} in activation of astrocytic GP, as well as the functional significance of this regulation in the brain is rather complicated and has been discussed in some detail previously (Obel *et al.*, 2012). Here I have reported that α_1-adrenoceptor-mediated intracellular Ca^{2+} increase, activated by the potent and selective agonist A61603, failed to exert a significant glycogenolytic effect in astrocytes (Figure 5.14). This experimental finding appears to exclude a role for Ca^{2+} in regulating glycogenolysis in rat cortex astrocytes, however, in hindsight, this finding should have been corroborated using noradrenaline in the absence and presence of β- (and α_2-) adrenoceptor antagonists.

Previous research has also reported that removal of Ca^{2+} from the medium is sufficient to abolish the glycogenolytic response to noradrenaline in mouse cortex astrocytes (Ververken *et al.*, 1982). Therefore, I also used the SERCA inhibitor thapsigargin to deplete ER Ca^{2+} stores and thus activate store-operated Ca^{2+} entry (SOCE), similar to a previously reported study (Muller *et al.*, 2014). Thapsigargin addition caused astrocytic glycogenolysis, indicating that Ca^{2+} can regulate glycogenolysis in this cell background (Figure 5.14). The contrasting effects of thapsigargin and A61603 lead me to speculate that mobilization of different sources (and perhaps different extents) of intracellular/extracellular Ca^{2+} have distinct metabolic consequences. Refilling of endoplasmic reticulum (ER) following depletion of this internal Ca^{2+} stores occurs via SOCE mechanism, which is controlled by sarco/endoplasmic reticulum Ca^{2+}-ATPase (SERCA) pumps, and regarded to be energy dependent process (Muller *et al.*, 2014). It is also well known that transient receptor potential (TRP) channels and Orai proteins are the basic components of a highly complex in regulating Ca^{2+} entry into the cell by the mechanism of SOCE (Salido et al., 2009, Kraft, 2015, Verkhratsky et al., 2012b, Pacheco and Vaca, 2013). Besides, it has been wide accepted that Ca^{2+}-regulated adenylyl cyclases (AC5, AC6, and AC8) are concentrated in caveolae (Smith et al., 2002, Mons et al., 1998, Rizzuto and Pozzan, 2006), acting as key integrators of cellular signalling. Research has also found these Ca^{2+}-regulated ACs show a marked selectivity for SOCE over other modes of elevating cytosolic Ca^{2+}, such as Ca^{2+} release from the ER (Willoughby et al., 2010, Skroblin et al., 2012). Recent work has also identified functional communication between Orai1 and AC8, which evolves dynamic, coordinated changes in the concentrations of Ca^{2+} and cAMP and integrated downstream consequences (Skroblin *et al.*, 2012). Therefore, it is likely that SOCE-mediated glycogenolysis in astrocytes attributed to the signal complex of AC8 and Orai1, along with STIM1, and their subsequent cAMP activation. Clearly further work is

needed to resolve whether the transient glycogenolysis seen following thapsigargin addition is directly attributable to Ca^{2+} acting on glycogenolytic enzymes or a more indirect, cAMP-dependent pathway plays an essential role.

The influence of α_2-adrenoceptors on astrocyte glycogen metabolism was also investigated. Addition of a selective α_2-adrenoceptor agonist (dexmedetomidine) caused an increase in astrocytic glycogen content, consistent with some previous research (Hertz et al., 2007, Hutchinson et al., 2011, Gibbs and Hutchinson, 2012), although results from another study reported that α_2-adrenoceptor activation induced glycogen breakdown (Subbarao and Hertz, 1990a). A potential physiological significance of astrocyte co-expression of β- and α_2-adrenoceptors was hinted at by experiments where the actions of noradrenaline were compared to those of a selective β-adrenoceptor agonist (isoprenaline). Addition of each agent caused an initial glycogenolysis. If β-adrenoceptor signalling was then completely blocked by a high concentration of an antagonist (timolol) it was notable that the recovery profiles of glycogen differed. The isoprenaline/timolol combination presumably completely annuls all adrenoceptor-mediated effects on glycogen re-synthesis and therefore re-synthesis precedes at a rate of 77 ng glucosyl equiv/mg protein/min with restoration of the pre-stimulation glycogen level within ~90 min. In contrast, the noradrenaline/timolol combination annuls the β-component, but does not alter α_2-adrenoceptor stimulation – under these conditions glycogen re-synthesis occurs at a 60% faster rate (123 ng glucosyl equiv/mg protein/min) and proceeds to 'load' the astrocytes with a level of glycogen that is greater than the pre-stimulation value (Figure 5.10). Finally, my study has also shown that selective activation of α_2-adrenoceptors in astrocytes stimulated with three different cAMP-elevating agents (isoprenaline, PACAP, forskolin) has the potential to completely ablate the ability of each agent to stimulate glycogenolysis (Figure 5.13). However, this metabolic effect of α_2-adrenoceptor activation only operates over a fairly narrow concentration range of the cAMP elevating agent. At higher concentrations of isoprenaline, PACAP or forskolin than were used in Figure 5.13, dexmedetomidine was ineffective as an anti-glycogenolytic agent. This is because in rat cortex astrocytes only modest increases in cAMP are required to maximally activate glycogenolysis (i.e. there is amplification of the signal between cAMP and glycogenolysis) and at higher concentrations of the cAMP-elevating agents α_2-adrenoceptor stimulation is only partially effective in suppressing cAMP accumulation (see Figure 5.12).

The inhibitory effects of a glycogen phosphorylase inhibitor (1, 4-dideoxy-1,4-imino-D-arabinitol; DAB;) (Andersen et al., 1999) on β-adrenoceptor-induced glycogenolysis has examined in this Chapter. My results show that DAB concentration-dependently inhibited receptor-driven glycogen degradation with complete inhibition occurring at a DAB concentration of 300 µM (Figure 5.9). It was also shown that astrocyte glycogen breakdown caused by complete glucose removal from the medium was also prevented by pre-addition of this concentration of DAB (Figure 5.1). In agreement with the present findings, DAB has previously been shown to inhibit glycogenolysis in liver preparations (Fosgerau et al., 2000; Latsis et al., 2002), as well as in cultured astrocytes (Walls et al., 2008; Hertz and Gibbs, 2009). However, the effective DAB concentration needed to inhibit glycogen phosphorylase activity differs considerably in the different reports. For example, DAB at the concentration of 3 mM was required to fully block glycogen breakdown induced by hypoglycaemia (Suh et al., 2007). Such discrepancies might be due to variation in glycogen phosphorylase isoenzymic composition (Newgard et al., 1989) and/or the relatively complex mechanism of action of this agent (Walls et al., 2008). In addition to this, poor membrane penetration of DAB should be kept in mind, which means different incubation periods with DAB might also affect its inhibitory effect and apparent potency. Overall, my experiments have validated the inhibitory action of DAB on astrocytic glycogenolysis.

Glycogen turnover in rat cortical astrocytes can be evoked not only by β-adrenoceptor stimulation and possibly store-operated Ca^{2+} entry, but also by an elevation of extracellular K^+ concentration. Small increases in $[K^+]_o$ concentration, within the pathophysiological range, could trigger glycogenolysis in astrocytes. Previous studies have shown that K^+ released into the extracellular space upon neuronal action potential firing can trigger glycogenolysis in astrocytes (Hertz et al., 2007, Xu et al., 2013). From time-course experiments it could be shown that maximal glycogenolysis occurred within 10 min of elevating medium K^+ and was concentration-dependently affected by the extent to which $[K^+]_o$ was raised (Figure 5.15). Similar data have been reported previously (Hof *et al.*, 1988b) but not fully mechanistically explained (Hertz et al., 2015a, DiNuzzo et al., 2013b, Macaulay and Zeuthen, 2012).

One possible explanation is that the increases in $[K^+]_o$ are sufficient to cause the opening of voltage-gated Ca^{2+} channels, known to be present in astrocytes (MacVicar, 1984, Latour et al., 2003) to stimulate glycogenolysis. Supportive of this, is the finding that addition of EGTA,

to chelate extracellular Ca^{2+}, effectively blocked K^+-evoked glycogenolysis (Figure 5.15). Research has already found that L-type voltage-operated Ca^{2+} channels can be evoked by excess extracellular K^+ (Hof *et al.*, 1988a). However, increases in glycogenolysis occur at increases in $[K^+]_o$ that are likely to only modestly affect resting membrane potential. Therefore if this mechanism wholly accounts for the observed K^+-evoked glycogenolysis then the glycogenolytic machinery must be especially sensitive to small sub-plasmalemmal increases in $[Ca^{2+}]_i$. It is possible that other mechanisms, such as effects of $[K^+]_o$ on Na^+/K^+ - ATPase, $K_{ir}4.1$ (Larsen *et al.*, 2014), $Na^+/K^+/Cl^-$ co-transporter 1 (NKCC1)(Walz, 1992, DiNuzzo et al., 2013b) also have potentially contributory actions to regulate the astrocyte glycogen store (Figure 5.21). Another pathway also has been proposed to potentially play a role: at high $[K^+]_o$, the Na^+/HCO_3^- cotransporter (NBC) can be activated and promote the influx of HCO_3^- ions (Brookes and Turner, 1994). The subsequent alkalization is a recognised stimulus of soluble adenylyl cyclase (sAC)(Choi et al., 2012b).
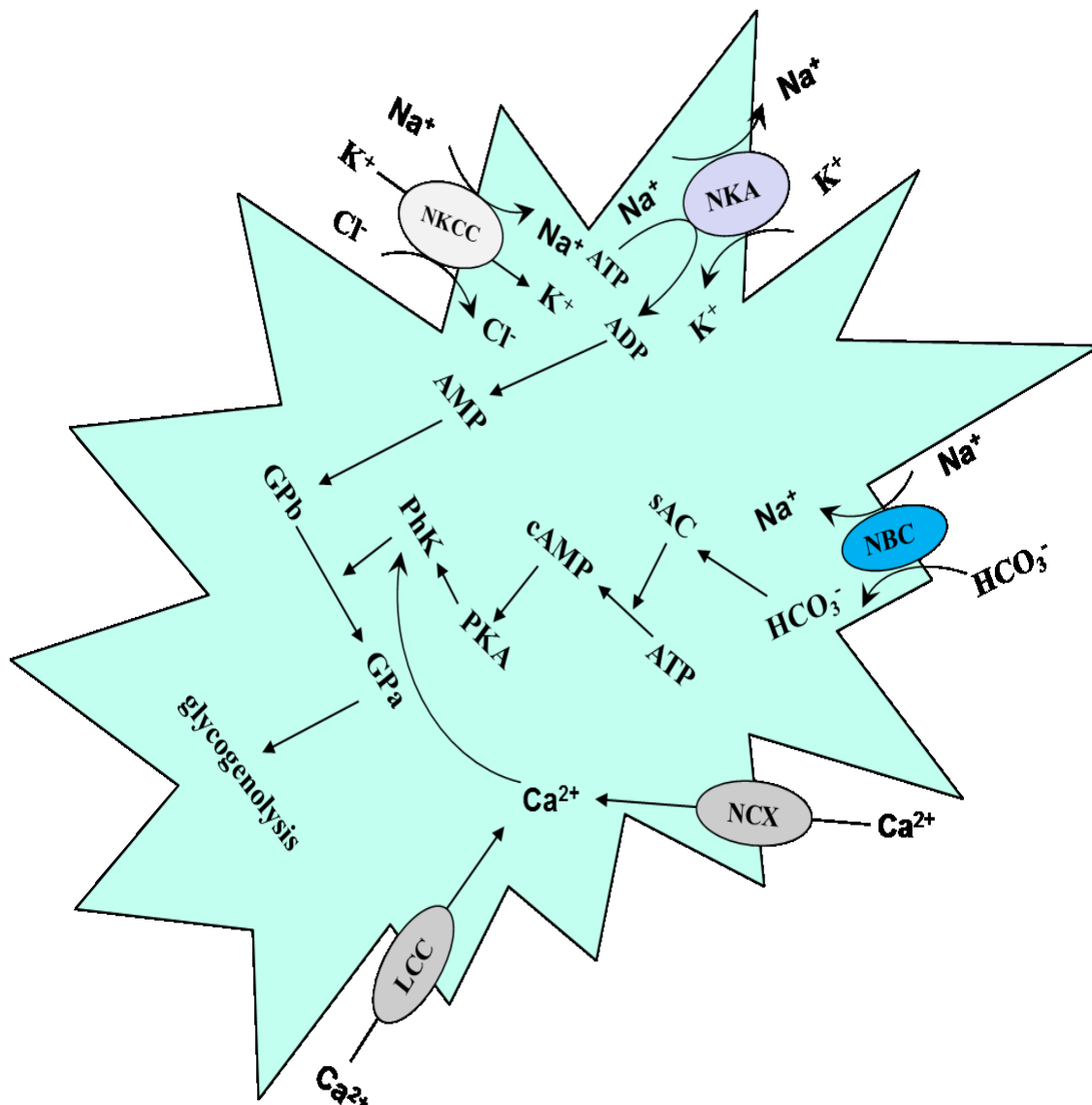
Figure 5.21. **Hypothetical pathways for extracellular K$^+$-induced glycogenolysis in rat cortical astrocytes.** Increases in extracellular potassium $[K^+]_o$ stimulates Na$^+$/K$^+$ ATPase (NKA), requiring ATP hydrolysis to ADP, which can be metabolized to 5'-AMP, which can allosterically stimulate glycogen phosphorylase b (GPb) and the glycogenolytic cascade. Elevated $[K^+]_o$ can also activate the Na$^+$/K$^+$/2Cl$^-$ co-transporter (NKCC1), and indirectly, NKA. Increased $[K^+]_o$ causes depolarization which can stimulate HCO$_3^-$ uptake by Na$^+$/HCO$_3^-$ cotransporters (NBC), leading to activation of the soluble adenylyl cyclase (sAC) isoenzyme and downstream cAMP/PKA and glycogen phosphorylase (GP) activation. Depolarization can also increase the opening of voltage-gated Ca^{2+} channels, such as L-type channel (LCC). Under some circumstances the Na$^+$/Ca^{2+} exchanger (NCX) can also allow the entry of Ca^{2+} which can activate PhK, GP phosphorylation and consequent glycogenolysis.

Astrocyte morphology is heterogeneous and can change in response to interactions with neurons, or the influence of a variety of pharmacological stimuli. An example of morphological change is stellation, where the cell body rounds up and fine processes form, accompanied by disassembly of the actin cytoskeleton (Fitch et al., 1999, Rodnight and Gottfried, 2013, Ramakers and Moolenaar, 1998). The neurotransmitter, noradrenaline, the β-adrenoceptor-selective agonist, isoprenaline, and the cAMP activator forskolin, can drive cell morphological transition from a flattened, polygonal shape to a stellate, process-bearing appearance, in agreement with a previous study (Vardjan et al., 2014). Moreover, noradrenaline stimulated astrocyte shape change could be completely prevented by pre-treatment with the β-adrenoceptor-selective antagonist timolol, and significantly attenuated by the PKA inhibitor KT5720, suggesting that noradrenaline mediates cell stellation via a pathway involving β-adrenoceptor/cAMP/PKA signalling. The morphological changes occurred rapidly upon receptor activation with significant cell membrane retraction, demonstrated as a reduction in cross-sectional area, seen as little as 5 min after isoprenaline addition (Figure 5.16). The maximum effect is achieved within 1 h, concomitant with the formation of fine processes, again consistent with previous research (Gharami and Das, 2004, Vardjan et al., 2014). These marked morphological changes in response to agonist stimulation were shown to be readily reversible. Much research effort has been devoted to understanding the molecular mechanisms and corresponding functional consequences of astrocytes morphological change. For example, a role for cAMP/PKA-dependent Rho family GTPases has been proposed (Racchetti et al., 2012, Ramakers and Moolenaar, 1998, Chen et al., 2005).

Finally, preliminary experiments were performed to assess whether any link exists between the ability of noradrenaline, via β-adrenoceptors, to regulate glycogen metabolism and cell morphology occurring as they do on similar timescales. My initial experiments showed that pre-treating astrocytes with a glycogen phosphorylase inhibitor (DAB), not only inhibits glycogenolysis, but also reduces the cell stellation response. Taken together, these data provide new insights into the signalling pathways controlling astrocyte morphology and a potential requirement for glycogen breakdown as a requirement for β-adrenoceptor-mediated morphological change in rat astrocytes.

Chapter 6

Final Discussion

6.1 Adrenoceptor-signalling in astrocytes

G protein-coupled receptors (GPCRs) are a primary mechanism through which non-excitable cells, such as astrocytes, can transduce extracellular information to intracellular signalling cascades. By responding to stimuli in the extracellular environment, especially to neurotransmitters released from neurons, astrocytes can dynamically contribute to the regulation of both glial and neuronal functions. Since astrocytes are recognized as a key cell-type in the central nervous system and play important roles in assisting neuronal function and network activity, interest in all aspects of astrocyte function has continued to increase in recent years. Perhaps most importantly, due to our need to better understand the diseases of an aging worldwide population, a growing body of research has indicated an involvement of astrocytes in a number of neurodegenerative diseases, including Parkinson's disease (Niranjan, 2014), Huntington's disease (Khakh and Sofroniew, 2014), Alzheimer's disease (Hol, 2015), as well as in hypoxic-ischemic encephalopathy-like stroke (Gleichman et al., 2015). The importance of astrocyte GPCR families has also been a focus due the fact that this receptor superfamily has been successfully targeted therapeutically to treat a large number of CNS and other diseases.

To date, the emphasis in astrocyte GPCR signalling activity has been focused on the regulation of the second messengers cAMP and Ca^{2+}, as well as MAPK signalling, which is not surprising given that these intracellular signals play such important roles in regulating biological processes (Vardjan and Zorec, 2015, Du et al., 2010a). Noradrenergic cell bodies within the locus coeruleus project axonal processes to release noradrenaline throughout the brain, including cerebral cortex and cerebellum (Gibbs et al., 2010). Astrocytes have been shown previously to express α_1-, α_2-, β_1-, and β_2-adrenoceptors (Hertz et al., 2010) and adrenergic signalling has found to regulate astrocyte-neuron communication through activating α- and β-adrenoceptors expressed in astrocytes, leading to regulation of various downstream cellular signalling pathways (O'Donnell et al., 2012). Moreover, noradrenaline has been shown to influence astrocytic and vascular functions related to the regulation of local blood flow, and blood-brain barrier permeability (Cohen et al., 1997a). Adrenoceptor

stimulation of astrocytes also has been linked to glycogen metabolism (Dong et al., 2012, Subbarao and Hertz, 1990b), neurotransmitter uptake (Stobart and Anderson, 2013) and gliotransmitter release (Vardjan et al., 2014), as well as gene transcription (Hertz et al., 2010) and changes in astrocyte morphology (Vardjan et al., 2014). It also has been reported that increases in astrocytic Ca^{2+} can trigger exocytotic release of gliotransmitters, including glutamate (Vardjan and Zorec, 2015, Zhang et al., 2004, Pasti et al., 2001), ATP and D-serine (Mothet et al., 2005, Rasooli-Nejad et al., 2014, Frenguelli et al., 2007). In addition, there is growing recognition that adrenoceptor-mediated information processing in the brain is coordinated by neuronal-glial network, and therefore astrocytes have been regarded as the primary target of noradrenergic neurons (Paukert et al., 2014b, Ding et al., 2013b). Consequently, astrocytic adrenoceptors are considered to play pivotal roles in a coordinated widespread manner to receive, integrate and transmit widespread adrenergic input information from remote adrenergic neurons to local environment, constituting the brain CNS network.

In agreement with previous research, this study has found evidence for all the different major adrenoceptor subtypes in rat cortical astrocytes. Adrenoceptor subtype-selective antagonists, CGP 20712A (β_1-selective) and ICI 118,551 (β_2-selective) were used to illustrate that β-adrenoceptor evoked cAMP responses are mediated almost exclusively by β_1-, not β_2-adrenoceptors (Figure 3.5). These functional data are somewhat at odds with PCR results that showed roughly equivalent mRNA expression levels of both β_1-, β_2-adrenoceptor subtypes in astrocytes. Other studies have also provided supportive opinions showing that there are differences among β-adrenoceptor subtypes in activating downstream signalling and functional consequences (Evans et al., 2010), including (i) the different profiles of β_1-/β_2-subtype selectivity of ligand for the two receptor–transducer interactions, resulting in directional diversity of downstream signalling (Communal et al., 1999, Evans et al., 2010); (ii) a difference in ligand-receptor affinity and potency between β_1-/β_2-adrenoceptors remains possible. Research has found β_2-adrenoceptors in rodents are more locally restricted, compared to β_1-adrenoceptors (Nikolaev et al., 2006, Baker, 2010); (iii) differential compartmentation of β_1- and β_2-adrenoceptor-mediated cAMP signalling presents the possibility that localized control of cAMP degradation through phosphodiesterases (PDEs) (Nikolaev et al., 2006). Research has also demonstrated that stimulation of β_1- and β_2-adrenoceptors have opposing effects on PDE4D recruitment in the membrane subdomain,

with β_1-adrenoceptor occupancy causing a local decrease, whereas β_2-adrenoceptor occupancy produces a local increase in PDE4 (Richter et al., 2008); (iv) dual coupling of β_2-, but not β_1-adrenoceptors, to G_s and G_i proteins has been observed in different cell backgrounds (Xiao, 2001, Hutchinson et al., 2007); G_s- and G_i-dependent pathways can have opposing functional consequences, and this could be a factor. However, it should be noted that in some instances β_2-adrenoceptors can have physiological important effects in astrocytes (Catus et al., 2011b, Day et al., 2014, Hutchinson et al., 2007). Further studies will be needed to determine whether β_2- (or indeed β_3-) adrenoceptors play any roles in primary rat cerebral cortex astrocytes.

There is an accumulating evidence that Ca^{2+} signalling in astrocytes can be elicited by synaptically-derived neurotransmitters (Lalo et al., 2014, Pankratov and Lalo, 2015a), and α_1-adrenoreceptors have been shown to be important participants in Ca^{2+} signalling through activation of the $PLC/IP_3/Ca^{2+}$ signalling pathway. This has been corroborated in the present work, since noradrenaline was shown to stimulate a robust Ca^{2+} response that was abolished by the selective α_1-adrenoceptor antagonist prazosin. In addition, selective α_1-adrenoceptor agonists (e.g. A61603) were shown to concentration-dependently increase $[Ca^{2+}]_i$. In contrast, selective activation of either α_2- or β-adrenoceptor populations failed to elicit intracellular Ca^{2+} responses. These data suggest that the Ca^{2+} response, observed following addition of noradrenaline to astrocytes, is primarily α_1-adrenoceptor-mediated with no evident contributions coming from α_2- or β-adrenoceptors.

In the current study α_2-adrenoceptors have also been functionally identified as being expressed on astrocytes through their ability to attenuate cAMP responses evoked by noradrenaline or the direct adenylyl cyclase activator (forskolin). The inhibitory actions of noradrenaline mediated by α_2-adrenoceptors were completely prevented by pertussis toxin pre-treatment (Ghanemi and Hu, 2015). I was interested to investigate how the dual regulation of cAMP accumulation by β_1- and α_2-adrenoceptors was translated into the ability of noradrenaline to regulate the astrocyte glycogen store. This was achieved through the use of adrenoceptor subtype-selective agonists and/or antagonists.

Comparisons of noradrenaline potency with respect to causing cAMP accumulation and glycogenolysis demonstrated that amplification occurs between the two steps (see Figure 5.8). Thus, a relatively modest increase in cAMP accumulation (≤5% of that caused by

maximal activation of the β_1-adrenoceptor population) is sufficient to cause a robust increase in glycogenolysis (≥90% of maximal response). This relationship was also evidenced by the effect of PDE inhibitor addition. Incubation of astrocytes with IBMX (300 µM), which caused a modest (<2-fold) increase in [cAMP], either was sufficient to activate glycogenolysis alone or to markedly potentiate the effect of noradrenaline (Figure 5.7). Thus, because only very modest increases in [cAMP] can lead to significant glycogenolysis, the ability of G_i-coupled GPCRs to attenuate the glycogenolytic response to G_s-coupled GPCRs is only observed over a narrow range (see Figure 5.13). Nevertheless, it might be argued that this is of considerable physiological significant as the range of concentrations where G_i-coupled GPCR/G_s-coupled GPCR "cross-talk" (Selbie and Hill, 1998, Hur and Kim, 2002) occurs may lie within the physiological neurotransmitter range *in vivo*.

6.2 Critique and future directions

The studies reported here have exclusively utilized a well-characterized *in vitro* preparations of primary astrocytes. These cells are prepared from new born rats (1-2 days-old) and are grown in culture for 10-15 days before experimentation. It is likely that such cells have lost many of the properties of astrocytes *in vivo* and, additionally, the neonatal origin of the cell preparation should also be kept in mind. Recent progress with membrane-targeted and genetically-encoded Ca^{2+} indicators (GECIs) could be useful tools to measure near membrane and cytosolic Ca^{2+} signals (Shigetomi et al., 2013a), to monitor various types of Ca^{2+} signals (waves, restricted signalling within microdomains, etc.), and feasibly allow *in vivo* investigation of the molecular mechanisms of Ca^{2+} signalling within entire astrocytes, including their fine distal processes that interact spatially with neurons and blood vessels (Khakh and McCarthy, 2015), although methods may need to be further optimized to deliver GECIs specifically to astrocytes. While it is feasible to advocate similar methods to assess real-time changes in cAMP *in vivo* (Vardjan et al., 2014), it is harder to see how changes in astrocyte glycogen levels might be quantified *in vivo*.

Although it's become clear that some neuronal functions are dependent on the activity of astrocytes and more specifically astrocyte glycogen mobilization, it remains unclear to what extent energy derived from glycogen is consumed by the astrocytes themselves, and how much substrate is transferred to neurons in the form of lactate. My current study of glycogen turnover in primary astrocytes can provide further insights into this intriguing

question about the functional importance of glycogen in response to neurotransmitter stimulation and in the presence of high extracellular K^+ and hypoglycaemia condition, which shows that brain energy metabolism involves more complicated mechanisms that were previously thought. A significant advance in my studies might be achieved by using co-culture systems where glial and neuronal activity could be simultaneously studied.

Research should be continued to study further a variety of physiological and pathological properties of astrocyte adrenoceptor subtypes and how these contribute to a variety of CNS disorders. One approach here would be to utilize a variety of animal models, for example a transgenic rat model of amyotrophic lateral sclerosis (Vermeiren et al., 2006), to generate primary astrocyte cultures and to assess whether astrocyte glycogen regulation either contributes to the disease state, or manipulation of this metabolic pathway has the potential to ameliorate either the underlying causes, or the symptoms of different diseases.

REFERENCES

ABBOTT, N. J., RONNBACK, L. & HANSSON, E. 2006. Astrocyte-endothelial interactions at the blood-brain barrier. *Nature Reviews Neuroscience,* 7**,** 41-53.

ABE, K. & MISAWA, M. 2003. Astrocyte stellation induced by Rho kinase inhibitors in culture. *Developmental Brain Research,* 143**,** 99-104.

ABRAMS, C. S. 2005. Intracellular signaling in platelets. *Current Opinion in Hematology,* 12**,** 401-405.

AGELL, N., BACHS, O., ROCAMORA, N. & VILLALONGA, P. 2002. Modulation of the Ras/Raf/MEK/ERK pathway by Ca2+, and calmodulin. *Cellular Signalling,* 14**,** 649-654.

AGULHON, C., PETRAVICZ, J., MCMULLEN, A. B., SWEGER, E. J., MINTON, S. K., TAVES, S. R., CASPER, K. B., FIACCO, T. A. & MCCARTHY, K. D. 2008. What is the role of astrocyte calcium in neurophysiology? *Neuron,* 59**,** 932-946.

AKINAGA, J., LIMA, V., KIGUTI, L. R. D., HEBELER-BARBOSA, F., ALCANTARA-HERNANDEZ, R., GARCIA-SAINZ, J. A. & PUPO, A. S. 2013. Differential Phosphorylation, Desensitization, and Internalization of alpha 1A-Adrenoceptors Activated by Norepinephrine and Oxymetazoline. *Molecular Pharmacology,* 83**,** 870-881.

ALESSANDRINI, A., CREWS, C. M. & ERIKSON, R. L. 1992. Phorbol ester stimulates a protein-tyrosine/threonine kinase that phosphorylates and activates the Erk-1 gene product. *Proc Natl Acad Sci U S A,* 89**,** 8200-4.

ALLEN, N. J. & BARRES, B. A. 2009a. NEUROSCIENCE Glia - more than just brain glue. *Nature,* 457**,** 675-677.

ALLEN, N. J. & BARRES, B. A. 2009b. Neuroscience: Glia - more than just brain glue. *Nature,* 457**,** 675-7.

AMIRY-MOGHADDAM, M., OTSUKA, T., HURN, P. D., TRAYSTMAN, R. J., HAUG, F.-M., FROEHNER, S. C., ADAMS, M. E., NEELY, J. D., AGRE, P. & OTTERSEN, O. P. 2003. An α-syntrophin-dependent pool of AQP4 in astroglial end-feet confers bidirectional water flow between blood and brain. *Proceedings of the National Academy of Sciences,* 100**,** 2106-2111.

AN, S., YANG, Y., WARD, R., LIU, Y., GUO, X. X. & XU, T. R. 2015. Raf-interactome in tuning the complexity and diversity of Raf function. *Febs Journal,* 282**,** 32-53.

ANDERSEN, B., RASSOV, A., WESTERGAARD, N. & LUNDGREN, K. 1999. Inhibition of glycogenolysis in primary rat hepatocytes by 1, 4-dideoxy-1,4-imino-D-arabinitol. *Biochem J,* 342 Pt 3**,** 545-50.

ARAQUE, A., CARMIGNOTO, G., HAYDON, P. G., OLIET, S. H., ROBITAILLE, R. & VOLTERRA, A. 2014a. Gliotransmitters travel in time and space. *Neuron,* 81**,** 728-39.

ARAQUE, A., CARMIGNOTO, G., HAYDON, PHILIP G., OLIET, STÉPHANE H. R., ROBITAILLE, R. & VOLTERRA, A. 2014b. Gliotransmitters Travel in Time and Space. *Neuron,* 81**,** 728-739.

ARAQUE, A., PARPURA, V., SANZGIRI, R. P. & HAYDON, P. G. 1999. Tripartite synapses: glia, the unacknowledged partner. *Trends Neurosci,* 22**,** 208-15.

BAKER, J. G. 2010. The selectivity of β‐adrenoceptor agonists at human β1‐, β2‐ and β3‐adrenoceptors. *British journal of pharmacology,* 160**,** 1048-1061.

BALLABH, P., BRAUN, A. & NEDERGAARD, M. 2004. The blood-brain barrier: an overview - Structure, regulation, and clinical implications. *Neurobiology of Disease,* 16**,** 1-13.

BAPAT, S., VERKLEIJ, A. & POST, J. A. 2001. Peroxynitrite activates mitogen-activated protein kinase (MAPK) via a MEK-independent pathway: a role for protein kinase C. *FEBS Lett,* 499**,** 21-6.

BARRES, B. A. 2008. The mystery and magic of glia: a perspective on their roles in health and disease. *Neuron,* 60**,** 430-40.

BARTLETT, J. M. & STIRLING, D. 2003. A short history of the polymerase chain reaction. *Methods Mol Biol,* 226**,** 3-6.

BEKAR, L. K., HE, W. & NEDERGAARD, M. 2008a. Locus Coeruleus alpha-Adrenergic-Mediated Activation of Cortical Astrocytes In Vivo. *Cerebral Cortex,* 18**,** 2789-2795.

BEKAR, L. K., HE, W. & NEDERGAARD, M. 2008b. Locus coeruleus alpha-adrenergic-mediated activation of cortical astrocytes in vivo. *Cereb Cortex,* 18**,** 2789-95.

BELANGER, M., ALLAMAN, I. & MAGISTRETTI, P. J. 2011. Brain energy metabolism: focus on astrocyte-neuron metabolic cooperation. *Cell Metab,* 14**,** 724-38.

BERG, J. M., TYMOCZKO, J. L. & STRYER, L. 2002. Biochemistry, ; W. H. Freeman and Company: New York.

BERRIDGE, M. J. 2014. Module 2: Cell Signalling Pathways. *Cell Signalling Biology,* 6**,** csb0001002.

BEZZI, P., GUNDERSEN, V., GALBETE, J. L., SEIFERT, G., STEINHAUSER, C., PILATI, E. & VOLTERRA, A. 2004. Astrocytes contain a vesicular compartment that is competent for regulated exocytosis of glutamate. *Nat Neurosci,* 7**,** 613-20.

BIRD, G. S., BURGESS, G. M. & PUTNEY, J. W. 1993. Sulfhydryl-Reagents and Camp-Dependent Kinase Increase the Sensitivity of the Inositol 1,4,5-Trisphosphate Receptor in Hepatocytes. *Journal of Biological Chemistry,* 268**,** 17917-17923.

BIRD, G. S. J. & PUTNEY, J. W. 2005. Capacitative calcium entry supports calcium oscillations in human embryonic kidney cells. *The Journal of physiology,* 562**,** 697-706.

BISCARDI, J. S., MAA, M. C., TICE, D. A., COX, M. E., LEU, T. H. & PARSONS, S. J. 1999. c-Src-mediated phosphorylation of the epidermal growth factor receptor on Tyr(845) and Tyr(1101) is associated with modulation of receptor function. *Journal of Biological Chemistry,* 274**,** 8335-8343.

BLAUKAT, A., BARAC, A., CROSS, M. J., OFFERMANNS, S. & DIKIC, I. 2000. G protein-coupled receptor-mediated mitogen-activated protein kinase activation through cooperation of G alpha(q), and G alpha(i) signals. *Molecular and Cellular Biology,* 20**,** 6837-6848.

BLOBEL, C. P. 2005. ADAMs: key components in EGFR signalling and development. *Nat Rev Mol Cell Biol,* 6**,** 32-43.

BOWER, D. M. & PRATHER, K. L. J. 2009. Engineering of bacterial strains and vectors for the production of plasmid DNA. *Applied Microbiology and Biotechnology,* 82**,** 805-813.

BRADLEY, S. & CHALLISS, R. 2011. Defining protein kinase/phosphatase isoenzymic regulation of mGlu5 receptor‐stimulated phospholipase C and Ca2+ responses in astrocytes. *British journal of pharmacology,* 164**,** 755-771.

BRADLEY, S. J. & CHALLISS, R. A. 2012. G protein-coupled receptor signalling in astrocytes in health and disease: a focus on metabotropic glutamate receptors. *Biochem Pharmacol,* 84**,** 249-59.

BRADLEY, S. J., WATSON, J. M. & CHALLISS, R. A. J. 2009. Effects of Positive Allosteric Modulators on Single-Cell Oscillatory Ca2+ Signaling Initiated by the Type 5 Metabotropic Glutamate Receptor. *Molecular Pharmacology,* 76**,** 1302-1313.

BRAUN, D., MADRIGAL, J. L. & FEINSTEIN, D. L. 2014. Noradrenergic regulation of glial activation: molecular mechanisms and therapeutic implications. *Curr Neuropharmacol,* 12**,** 342-52.

BROOKES, N. & TURNER, R. J. 1994. K (+)-induced alkalinization in mouse cerebral astrocytes mediated by reversal of electrogenic Na (+)-HCO3-cotransport. *American Journal of Physiology-Cell Physiology,* 267**,** C1633-C1640.

BROWN, A. 2013. Glycogen and energy metabolism. *Neuroglia, 3rd Edition (Ransom BR, Kettenmann H, eds)***,** 457-469.

BROWN, A. M. 2004. Brain glycogen re-awakened. *J Neurochem,* 89**,** 537-52.

BROWN, A. M., BALTAN TEKKOK, S. & RANSOM, B. R. 2004. Energy transfer from astrocytes to axons: the role of CNS glycogen. *Neurochem Int,* 45**,** 529-36.

BROWN, A. M. & RANSOM, B. R. 2007. Astrocyte glycogen and brain energy metabolism. *Glia,* 55**,** 1263-1271.

BROWN, A. M. & RANSOM, B. R. 2015a. Astrocyte glycogen as an emergency fuel under conditions of glucose deprivation or intense neural activity. *Metab Brain Dis,* 30**,** 233-9.

BROWN, A. M. & RANSOM, B. R. 2015b. Astrocyte glycogen as an emergency fuel under conditions of glucose deprivation or intense neural activity. *Metabolic brain disease,* 30**,** 233-239.

BROWN, A. M., SICKMANN, H. M., FOSGERAU, K., LUND, T. M., SCHOUSBOE, A., WAAGEPETERSEN, H. S. & RANSOM, B. R. 2005. Astrocyte glycogen metabolism is required for neural activity during aglycemia or intense stimulation in mouse white matter. *J Neurosci Res,* 79**,** 74-80.

BROWN, A. M., TEKKOK, S. B. & RANSOM, B. R. 2003. Glycogen regulation and functional role in mouse white matter. *J Physiol,* 549**,** 501-12.

BROWN, B. L., ALBANO, J. D., EKINS, R. P. & SGHERZI, A. M. 1971. A simple and sensitive saturation assay method for the measurement of adenosine 3':5'-cyclic monophosphate. *Biochem J,* 121**,** 561-2.

BUERKLE, H. & YAKSH, T. L. 1998. Pharmacological evidence for different alpha(2)-adrenergic receptor sites mediating analgesia and sedation in the rat. *British Journal of Anaesthesia,* 81**,** 208-215.

BURDA, J. E. & SOFRONIEW, M. V. 2014. Reactive Gliosis and the Multicellular Response to CNS Damage and Disease. *Neuron,* 81**,** 229-248.

BURRIDGE, K. & DOUGHMAN, R. 2006. Front and back by Rho and Rac. *Nature Cell Biology,* 8**,** 781-782.

BUSHONG, E. A., MARTONE, M. E., JONES, Y. Z. & ELLISMAN, M. H. 2002. Protoplasmic astrocytes in CA1 stratum radiatum occupy separate anatomical domains. *Journal of Neuroscience,* 22**,** 183-192.

BYLUND, D. B., EIKENBERG, D. C., HIEBLE, J. P., LANGER, S. Z., LEFKOWITZ, R. J., MINNEMAN, K. P., MOLINOFF, P. B., RUFFOLO, R. R. & TRENDELENBURG, U. 1994. International Union of Pharmacology Nomenclature of Adrenoceptors. *Pharmacological Reviews,* 46**,** 121-136.

CAHALAN, M. D. 2009. STIMulating store-operated Ca(2+) entry. *Nat Cell Biol,* 11**,** 669-77.

CARBONI, E., BARROS, V. G., IBBA, M., SILVAGNI, A., MURA, C. & ANTONELLI, M. C. 2010. Prenatal restraint stress: an in vivo microdialysis study on catecholamine release in the rat prefrontal cortex. *Neuroscience,* 168**,** 156-66.

CARR, R., KOZIOL-WHITE, C., ZHANG, J., LAM, H., AN, S. S., TALL, G. G., PANETTIERI, R. A. & BENOVIC, J. L. 2016. Interdicting G(q) Activation in Airway Disease by Receptor-Dependent and Receptor-Independent Mechanisms. *Molecular Pharmacology,* 89**,** 94-104.

CATUS, S. L., GIBBS, M. E., SATO, M., SUMMERS, R. J. & HUTCHINSON, D. S. 2011a. Role of beta-adrenoceptors in glucose uptake in astrocytes using beta-adrenoceptor knockout mice. *Br J Pharmacol,* 162**,** 1700-15.

CATUS, S. L., GIBBS, M. E., SATO, M., SUMMERS, R. J. & HUTCHINSON, D. S. 2011b. Role of β - adrenoceptors in glucose uptake in astrocytes using β - adrenoceptor knockout mice. *British journal of pharmacology,* 162**,** 1700-1715.

CERVANTES, D., CROSBY, C. & XIANG, Y. 2010. Arrestin Orchestrates Crosstalk Between G Protein-Coupled Receptors to Modulate the Spatiotemporal Activation of ERK MAPK. *Circulation Research,* 106**,** 79-U126.

CHARLES, A. 2013. Migraine: a brain state. *Current opinion in neurology,* 26**,** 235-239.

CHAUDHRY, F. A., LEHRE, K. P., VAN LOOKEREN CAMPAGNE, M., OTTERSEN, O. P., DANBOLT, N. C. & STORM-MATHISEN, J. 1995. Glutamate transporters in glial plasma membranes: highly differentiated localizations revealed by quantitative ultrastructural immunocytochemistry. *Neuron,* 15**,** 711-20.

CHEN, C.-J., LIAO, S.-L., HUANG, Y.-S. & CHIANG, A.-N. 2005. RhoA inactivation is crucial to manganese-induced astrocyte stellation. *Biochemical and biophysical research communications,* 326**,** 873-879.

CHEN, Y., ZHAO, Z., CODE, W. E. & HERTZ, L. 2000. A correlation between dexmedetomidine-induced biphasic increases in free cytosolic calcium concentration and energy metabolism in astrocytes. *Anesthesia and Analgesia,* 91**,** 353-357.

CHENG, P. P., ALBERTS, I. & LI, X. H. 2013. The role of ERK1/2 in the regulation of proliferation and differentiation of astrocytes in developing brain. *International Journal of Developmental Neuroscience,* 31**,** 783-789.

CHIN, E. R. 2010. Intracellular Ca2+ signaling in skeletal muscle: decoding a complex message. *Exercise and sport sciences reviews,* 38**,** 76-85.

CHIU, F. C., NORTON, W. T. & FIELDS, K. L. 1981. The Cytoskeleton of Primary Astrocytes in Culture Contains Actin, Glial Fibrillary Acidic Protein, and the Fibroblast-Type Filament Protein, Vimentin. *Journal of Neurochemistry,* 37**,** 147-155.

CHOI, H. B., GORDON, G. R., ZHOU, N., TAI, C., RUNGTA, R. L., MARTINEZ, J., MILNER, T. A., RYU, J. K., MCLARNON, J. G. & TRESGUERRES, M. 2012a. Metabolic communication between astrocytes and neurons via bicarbonate-responsive soluble adenylyl cyclase. *Neuron,* 75**,** 1094-1104.

CHOI, H. B., GORDON, G. R. J., ZHOU, N., TAI, C., RUNGTA, R. L., MARTINEZ, J., MILNER, T. A., RYU, J. K., MCLARNON, J. G., TRESGUERRES, M., LEVIN, L. R., BUCK, J. & MACVICAR, B. A. 2012b. Metabolic Communication between Astrocytes and Neurons via Bicarbonate-Responsive Soluble Adenylyl Cyclase. *Neuron,* 75**,** 1094-1104.

CLOIX, J. F., TAHI, Z., BOISSONNET, A. & HEVOR, T. 2010. Brain glycogen and neurotransmitter levels in fast and slow methionine sulfoximine-selected mice. *Exp Neurol,* 225**,** 274-83.

COFFA, S., BREITMAN, M., HANSON, S. M., CALLAWAY, K., KOOK, S., DALBY, K. N. & GUREVICH, V. V. 2011. The effect of arrestin conformation on the recruitment of c-Raf1, MEK1, and ERK1/2 activation. *PLoS One,* 6**,** e28723.

COHEN, Z., MOLINATTI, G. & HAMEL, E. 1997a. Astroglial and vascular interactions of noradrenaline terminals in the rat cerebral cortex. *J Cereb Blood Flow Metab,* 17**,** 894-904.

COHEN, Z., MOLINATTI, G. & HAMEL, E. 1997b. Astroglial and vascular interactions of noradrenaline terminals in the rat cerebral cortex. *Journal of Cerebral Blood Flow and Metabolism,* 17**,** 894-904.

COMMUNAL, C., SINGH, K., SAWYER, D. B. & COLUCCI, W. S. 1999. Opposing effects of beta(1)- and beta(2)-adrenergic receptors on cardiac myocyte apoptosis : role of a pertussis toxin-sensitive G protein. *Circulation,* 100**,** 2210-2.

COOK, S. J. & MCCORMICK, F. 1993. Inhibition by cAMP of Ras-dependent activation of Raf. *Science,* 262**,** 1069-72.

CORNELL-BELL, A. H., FINKBEINER, S. M., COOPER, M. S. & SMITH, S. J. 1990. Glutamate induces calcium waves in cultured astrocytes: long-range glial signaling. *Science,* 247**,** 470-473.

CRESPO, P., XU, N. Z., SIMONDS, W. F. & GUTKIND, J. S. 1994. Ras-Dependent Activation of Map Kinase Pathway Mediated by G-Protein Beta-Gamma-Subunits. *Nature,* 369**,** 418-420.

CREWS, C. M., ALESSANDRINI, A. & ERIKSON, R. L. 1992. The primary structure of MEK, a protein kinase that phosphorylates the ERK gene product. *Science,* 258**,** 478-80.

CRUZ, N. F. & DIENEL, G. A. 2002. High glycogen levels in brains of rats with minimal environmental stimuli: Implications for metabolic contributions of working astrocytes. *Journal of Cerebral Blood Flow and Metabolism,* 22**,** 1476-1489.

CUI, X., ZHANG, X., YIN, Q., MENG, A., SU, S., JING, X., LI, H., GUAN, X., LI, X. & LIU, S. 2014. F‑actin cytoskeleton reorganization is associated with hepatic stellate cell activation. *Molecular medicine reports,* 9**,** 1641-1647.

CULLEN, P. J. & LOCKYER, P. J. 2002. Integration of calcium and Ras signalling. *Nature Reviews Molecular Cell Biology,* 3**,** 339-348.

CUMMINS, C., LUST, W. D. & PASSONNEAU, J. 1983. Regulation of glycogen metabolism in primary and transformed astrocytes in vitro. *Journal of neurochemistry,* 40**,** 128-136.

DALLÉRAC, G., CHEVER, O. & ROUACH, N. 2014. How do astrocytes shape synaptic transmission? Insights from electrophysiology. *Frontiers in cellular neuroscience,* 7.

DAY, J. S., O'NEILL, E., CAWLEY, C., ARETZ, N. K., KILROY, D., GIBNEY, S. M., HARKIN, A. & CONNOR, T. J. 2014. Noradrenaline acting on astrocytic beta(2)-adrenoceptors induces neurite outgrowth in primary cortical neurons. *Neuropharmacology,* 77**,** 234-48.

DE LEAN, A., STADEL, J. M. & LEFKOWITZ, R. J. 1980. A ternary complex model explains the agonist-specific binding properties of the adenylate cyclase-coupled beta-adrenergic receptor. *J Biol Chem,* 255**,** 7108-17.

DELLAROCCA, G. J., VANBIESEN, T., DAAKA, Y., LUTTRELL, D. K., LUTTRELL, L. M. & LEFKOWITZ, R. J. 1997. Ras-dependent mitogen-activated protein kinase activation by G protein-coupled receptors - Convergence of G(i)- and G(q)-mediated pathways on calcium/calmodulin, Pyk2, and Src kinase. *Journal of Biological Chemistry,* 272**,** 19125-19132.

DEMETRIUS, L. A., MAGISTRETTI, P. J. & PELLERIN, L. 2015. Alzheimer's disease: the amyloid hypothesis and the Inverse Warburg effect. *Frontiers in Physiology,* 5.

DESSY, C., KIM, E., SOUGNEZ, C. L., LAPORTE, R. & MORGAN, K. G. 1998. A role for MAP kinase in differentiated smooth muscle contraction evoked by alpha-adrenoceptor stimulation. *American Journal of Physiology-Cell Physiology,* 275**,** C1081-C1086.

DEWIRE, S. M., AHN, S., LEFKOWITZ, R. J. & SHENOY, S. K. 2007. beta-arrestins and cell signaling. *Annual Review of Physiology,* 69**,** 483-510.

DHILLON, A. S., POLLOCK, C., STEEN, H., SHAW, P. E., MISCHAK, H. & KOLCH, W. 2002. Cyclic AMP-dependent kinase regulates Raf-1 kinase mainly by phosphorylation of serine 259. *Molecular and Cellular Biology,* 22**,** 3237-3246.

DIENEL, G. A., BALL, K. K. & CRUZ, N. F. 2007. A glycogen phosphorylase inhibitor selectively enhances local rates of glucose utilization in brain during sensory stimulation of conscious rats: implications for glycogen turnover. *J Neurochem,* 102**,** 466-78.

DIENEL, G. A. & CRUZ, N. F. 2014. Contributions of glycogen to astrocytic energetics during brain activation. *Metabolic Brain Disease***,** 1-18.

DIKIC, I., TOKIWA, G., LEV, S., COURTNEIDGE, S. A. & SCHLESSINGER, J. 1996. A role for Pyk2 and Src in linking G-protein-coupled receptors with MAP kinase activation. *Nature,* 383**,** 547-550.

DING, F., O'DONNELL, J., THRANE, A. S., ZEPPENFELD, D., KANG, H., XIE, L., WANG, F. & NEDERGAARD, M. 2013a. alpha1-Adrenergic receptors mediate coordinated Ca2+ signaling of cortical astrocytes in awake, behaving mice. *Cell Calcium,* 54**,** 387-94.

DING, F. F., O'DONNELL, J., THRANE, A. S., ZEPPENFELD, D., KANG, H. Y., XIE, L. L., WANG, F. S. & NEDERGAARD, M. 2013b. alpha(1)-Adrenergic receptors mediate coordinated Ca2+ signaling of cortical astrocytes in awake, behaving mice. *Cell Calcium,* 54**,** 387-394.

DINUZZO, M., MANGIA, S., MARAVIGLIA, B. & GIOVE, F. 2013a. Regulatory mechanisms for glycogenolysis and K+ uptake in brain astrocytes. *Neurochem Int,* 63**,** 458-64.

DINUZZO, M., MANGIA, S., MARAVIGLIA, B. & GIOVE, F. 2013b. Regulatory mechanisms for glycogenolysis and K+ uptake in brain astrocytes. *Neurochemistry International,* 63**,** 458-464.

DISTLER, C., DREHER, Z. & STONE, J. 1991. Contact spacing among astrocytes in the central nervous system: an hypothesis of their structural role. *Glia,* 4**,** 484-94.

DITYATEV, A. & RUSAKOV, D. A. 2011. Molecular signals of plasticity at the tetrapartite synapse. *Curr Opin Neurobiol,* 21**,** 353-9.

DONG, J. H., CHEN, X., CUI, M., YU, X., PANG, Q. & SUN, J. P. 2012. Beta2-Adrenergic Receptor and Astrocyte Glucose Metabolism. *Journal of Molecular Neuroscience,* 48**,** 456-463.

DONG, J. M., LEUNG, T., MANSER, E. & LIM, L. 1998. cAMP-induced morphological changes are counteracted by the activated RhoA small GTPase and the Rho kinase ROK alpha. *Journal of Biological Chemistry,* 273**,** 22554-22562.

DOSSANTOS, M. F., HOLANDA-AFONSO, R. C., LIMA, R. L., DASILVA, A. F. & MOURA-NETO, V. 2015. The role of the blood–brain barrier in the development and treatment of migraine and other pain disorders. *Cerebral endothelial and glial cells are more than bricks in the Great Wall of the brain: insights into the way the blood-brain barrier actually works (Celebrating the centenary of Goldman's experiments).*

DU, T., LI, B., LI, H., LI, M., HERTZ, L. & PENG, L. 2010a. Signaling pathways of isoproterenol‐induced ERK1/2 phosphorylation in primary cultures of astrocytes are concentration‐dependent. *Journal of neurochemistry,* 115**,** 1007-1023.

DU, T., LI, B. M., LI, H. M., LI, M., HERTZ, L. & PENG, L. A. 2010b. Signaling pathways of isoproterenol-induced ERK1/2 phosphorylation in primary cultures of astrocytes are concentration-dependent. *Journal of Neurochemistry,* 115**,** 1007-1023.

DUDLEY, D. T., PANG, L., DECKER, S. J., BRIDGES, A. J. & SALTIEL, A. R. 1995. A synthetic inhibitor of the mitogen-activated protein kinase cascade. *Proc Natl Acad Sci U S A,* 92**,** 7686-9.

DUFFY, S. & MACVICAR, B. A. 1995. Adrenergic Calcium Signaling in Astrocyte Networks within the Hippocampal Slice. *Journal of Neuroscience,* 15**,** 5535-5550.

DUGAN, L. L., KIM, J. S., ZHANG, Y. J., BART, R. D., SUN, Y. L., HOLTZMAN, D. M. & GUTMANN, D. H. 1999. Differential effects of cAMP in neurons and astrocytes - Role of B-raf. *Journal of Biological Chemistry,* 274**,** 25842-25848.

DUPONT, G., COMBETTES, L., BIRD, G. S. & PUTNEY, J. W. 2011. Calcium Oscillations. *Cold Spring Harbor Perspectives in Biology,* 3.

EDAMATSU, H., KAZIRO, Y. & ITOH, H. 1998. Expression of an oncogenic mutant G α i2 activates Ras in Rat‐1 fibroblast cells. *FEBS letters,* 440**,** 231-234.

EDDLESTON, M. & MUCKE, L. 1993. Molecular Profile of Reactive Astrocytes - Implications for Their Role in Neurologic Disease. *Neuroscience,* 54**,** 15-36.

EICHMANN, T., LORENZ, K., HOFFMANN, M., BROCKMANN, J., KRASEL, C., LOHSE, M. J. & QUITTERER, U. 2003. The amino-terminal domain of G-protein-coupled receptor kinase 2 is a regulatory Gbeta gamma binding site. *J Biol Chem,* 278**,** 8052-7.

EMSLEY, J. G. & MACKLIS, J. D. 2006. Astroglial heterogeneity closely reflects the neuronal-defined anatomy of the adult murine CNS. *Neuron Glia Biol,* 2**,** 175-86.

ESPINOZA-ROJO, M., IVONNE ITURRALDE-RODRIGUEZ, K., ELENA CHANEZ-CARDENAS, M., EUGENIA RUIZ-TACHIQUIN, M. & AGUILERA, P. 2010. Glucose transporters regulation on ischemic brain: possible role as therapeutic target. *Central Nervous System Agents in Medicinal Chemistry (Formerly Current Medicinal Chemistry-Central Nervous System Agents),* 10**,** 317-325.

EVANS, B. A., SATO, M., SARWAR, M., HUTCHINSON, D. S. & SUMMERS, R. J. 2010. Ligand‐directed signalling at β‐adrenoceptors. *British journal of pharmacology,* 159**,** 1022-1038.

FABBRI, E., GAMBAROTTA, A. & MOON, T. W. 1995. Adrenergic signaling and second messenger production in hepatocytes of two fish species. *Gen Comp Endocrinol,* 99**,** 114-24.

FABJAN, A., ZALETEL, M. & ŽVAN, B. 2015. Is there a persistent dysfunction of neurovascular coupling in migraine? *BioMed research international,* 2015.

FAVATA, M. F., HORIUCHI, K. Y., MANOS, E. J., DAULERIO, A. J., STRADLEY, D. A., FEESER, W. S., VAN DYK, D. E., PITTS, W. J., EARL, R. A., HOBBS, F., COPELAND, R. A., MAGOLDA, R. L., SCHERLE, P. A. & TRZASKOS, J. M. 1998. Identification of a novel inhibitor of mitogen-activated protein kinase kinase. *Journal of Biological Chemistry,* 273**,** 18623-18632.

FAVERO, C. B. & MANDELL, J. W. 2007. A pharmacological activator of AMP-activated protein kinase (AMPK) induces astrocyte stellation. *Brain Res,* 1168**,** 1-10.

FELLIN, T. 2009. Communication between neurons and astrocytes: relevance to the modulation of synaptic and network activity. *J Neurochem,* 108**,** 533-44.

FITCH, M. T., DOLLER, C., COMBS, C. K., LANDRETH, G. E. & SILVER, J. 1999. Cellular and molecular mechanisms of glial scarring and progressive cavitation: in vivo and in vitroanalysis of inflammation-induced secondary injury after CNS trauma. *Journal of Neuroscience,* 19**,** 8182-8198.

FREEDMAN, N. J. & LEFKOWITZ, R. J. 1996. Desensitization of G protein-coupled receptors. *Recent Prog Horm Res,* 51**,** 319-51; discussion 352-3.

FRENGUELLI, B. G., WIGMORE, G., LLAUDET, E. & DALE, N. 2007. Temporal and mechanistic dissociation of ATP and adenosine release during ischaemia in the mammalian hippocampus. *J Neurochem,* 101**,** 1400-13.

FRIER, B. M. 2014. Hypoglycaemia in diabetes mellitus: epidemiology and clinical implications. *Nature Reviews Endocrinology,* 10**,** 711-722.

FU, Q., CHEN, X. & XIANG, Y. K. 2013. Compartmentalization of beta-adrenergic signals in cardiomyocytes. *Trends Cardiovasc Med,* 23**,** 250-6.

FUKUNAGA, K. & MIYAMOTO, E. 1998. Role of MAP kinase in neurons. *Mol Neurobiol,* 16**,** 79-95.

GALLAGHER, C. J. & SALTER, M. W. 2003. Differential properties of astrocyte calcium waves mediated by P2Y1 and P2Y2 receptors. *Journal of Neuroscience,* 23**,** 6728-6739.

GARCIA-SAINZ, J. A., VAZQUEZ-PRADO, J. & MEDINA, L. D. 2000. alpha(1)-adrenoceptors: function and phosphorylation. *European Journal of Pharmacology,* 389**,** 1-12.

GAVI, S., SHUMAY, E., WANG, H. Y. & MALBON, C. C. 2006. G-protein-coupled receptors and tyrosine kinases: crossroads in cell signaling and regulation. *Trends in Endocrinology and Metabolism,* 17**,** 46-52.

GHANDOUR, M. S., PARKKILA, A. K., PARKKILA, S., WAHEED, A. & SLY, W. S. 2000. Mitochondrial Carbonic Anhydrase in the Nervous System. *Journal of neurochemistry,* 75**,** 2212-2220.

GHANEMI, A. & HU, X. 2015. Elements toward novel therapeutic targeting of the adrenergic system. *Neuropeptides,* 49**,** 25-35.

GHARAMI, K. & DAS, S. 2004. Delayed but sustained induction of mitogen‐activated protein kinase activity is associated with β‐adrenergic receptor‐mediated morphological differentiation of astrocytes. *Journal of neurochemistry,* 88**,** 12-22.

GHOSH, M. & DAS, S. 2007. Increased beta(2)-adrenergic receptor activity by thyroid hormone possibly leads to differentiation and maturation of astrocytes in culture. *Cell Mol Neurobiol,* 27**,** 1007-21.

GIAUME, C. & VENANCE, L. 1998. Intercellular calcium signaling and gap junctional communication in astrocytes. *Glia,* 24**,** 50-64.

GIBBS, M. E. 2015. Role of Glycogenolysis in Memory and Learning: Regulation by Noradrenaline, Serotonin and ATP. *Frontiers in integrative neuroscience,* 9.

GIBBS, M. E., ANDERSON, D. G. & HERTZ, L. 2006. Inhibition of glycogenolysis in astrocytes interrupts memory consolidation in young chickens. *Glia,* 54**,** 214-22.

GIBBS, M. E. & HUTCHINSON, D. S. 2012. Rapid Turnover of Glycogen in Memory Formation. *Neurochemical Research,* 37**,** 2456-2463.

GIBBS, M. E., HUTCHINSON, D. S. & SUMMERS, R. J. 2008. Role of β-adrenoceptors in memory consolidation: β3-adrenoceptors act on glucose uptake and β2-adrenoceptors on glycogenolysis. *Neuropsychopharmacology,* 33**,** 2384-2397.

GIBBS, M. E., HUTCHINSON, D. S. & SUMMERS, R. J. 2010. Noradrenaline release in the locus coeruleus modulates memory formation and consolidation; roles for alpha- and beta-adrenergic receptors. *Neuroscience,* 170**,** 1209-22.

GIOVANNITTI, J. A., JR., THOMS, S. M. & CRAWFORD, J. J. 2015. Alpha-2 adrenergic receptor agonists: a review of current clinical applications. *Anesth Prog,* 62**,** 31-9.

GLEICHMAN, A., KAWAGUCHI, R., GUO, Z., SOFRONIEW, M., YU, P., COPPOLA, G. & CARMICHAEL, S. T. 2015. Astrocyte diversity in response to stroke. *Glia,* 63**,** E259-E260.

GOLD, P. E. 2016. Balancing the Contributions of Multiple Neural Systems During Learning and Memory. *The Neurobiological Basis of Memory.* Springer.

GOLDSMITH, Z. G. & DHANASEKARAN, D. N. 2007. G protein regulation of MAPK networks. *Oncogene,* 26**,** 3122-3142.

GOMES, F. C., PAULIN, D. & MOURA NETO, V. 1999. Glial fibrillary acidic protein (GFAP): modulation by growth factors and its implication in astrocyte differentiation. *Braz J Med Biol Res,* 32**,** 619-31.

GONG, H., SUN, H., KOCH, W. J., RAU, T., ESCHENHAGEN, T., RAVENS, U., HEUBACH, J. F., ADAMSON, D. L. & HARDING, S. E. 2002. Specific β2AR blocker ICI 118,551 actively decreases contraction through a Gi-coupled form of the β2AR in myocytes from failing human heart. *Circulation,* 105**,** 2497-2503.

GONZALEZ-PEREZ, O., LOPEZ-VIRGEN, V. & QUINONES-HINOJOSA, A. 2015. Astrocytes: Everything but the glue. *Neuroimmunol Neuroinflamm,* 2**,** 115-117.

GORDON, G. R., IREMONGER, K. J., KANTEVARI, S., ELLIS-DAVIES, G. C., MACVICAR, B. A. & BAINS, J. S. 2009. Astrocyte-mediated distributed plasticity at hypothalamic glutamate synapses. *Neuron,* 64**,** 391-403.

GORDON, G. R. J., BAIMOUKHAMETOVA, D. V., HEWITT, S. A., RAJAPAKSHA, W. R. A. K. J. S., FISHER, T. E. & BAINS, J. S. 2005. Norepinephrine triggers release of glial ATP to increase postsynaptic efficacy. *Nature Neuroscience,* 8**,** 1078-1086.

GRUETTER, R. 2003. Glycogen: the forgotten cerebral energy store. *J Neurosci Res,* 74**,** 179-83.

HALASSA, M. M., FELLIN, T., TAKANO, H., DONG, J. H. & HAYDON, P. G. 2007. Synaptic islands defined by the territory of a single astrocyte. *J Neurosci,* 27**,** 6473-7.

HALASSA, M. M. & HAYDON, P. G. 2010. Integrated brain circuits: astrocytic networks modulate neuronal activity and behavior. *Annual review of physiology,* 72**,** 335.

HAMILTON, N., VAYRO, S., KIRCHHOFF, F., VERKHRATSKY, A., ROBBINS, J., GORECKI, D. C. & BUTT, A. M. 2008. Mechanisms of ATP- and glutamate-mediated calcium signaling in white matter astrocytes. *Glia,* 56**,** 734-749.

HAMILTON, N. B. & ATTWELL, D. 2010. Do astrocytes really exocytose neurotransmitters? *Nat Rev Neurosci,* 11**,** 227-38.

HAN, C. C., MA, Y., LI, Y., WANG, Y. & WEI, W. 2016. Regulatory effects of GRK2 on GPCRs and non-GPCRs and possible use as a drug target (Review). *Int J Mol Med,* 38**,** 987-94.

HANKE, J. H., GARDNER, J. P., DOW, R. L., CHANGELIAN, P. S., BRISSETTE, W. H., WERINGER, E. J., POLLOK, B. A. & CONNELLY, P. A. 1996. Discovery of a novel, potent, and Src family-selective tyrosine kinase inhibitor. Study of Lck- and FynT-dependent T cell activation. *J Biol Chem,* 271**,** 695-701.

HARRIS, J. J., JOLIVET, R. & ATTWELL, D. 2012. Synaptic energy use and supply. *Neuron,* 75**,** 762-77.

HATTEN, M. E. 1985. Neuronal Regulation of Astroglial Morphology and Proliferation Invitro. *Journal of Cell Biology,* 100**,** 384-396.

HAYDON, P. G. & CARMIGNOTO, G. 2006. Astrocyte control of synaptic transmission and neurovascular coupling. *Physiological Reviews,* 86**,** 1009-1031.

HELLER, J. P. & RUSAKOV, D. A. 2015. Morphological plasticity of astroglia: Understanding synaptic microenvironment. *Glia,* 63**,** 2133-51.

HENEKA, M. T., GALEA, E., GAVRILUYK, V., DUMITRESCU-OZIMEK, L., DAESCHNER, J., O'BANION, M. K., WEINBERG, G., KLOCKGETHER, T. & FEINSTEIN, D. L. 2002. Noradrenergic depletion potentiates beta-amyloid-induced cortical inflammation: implications for Alzheimer's disease. *Journal of Neuroscience,* 22**,** 2434-2442.

HERTZ, L., CHEN, Y., GIBBS, M. E., ZANG, P. & PENG, L. 2004. Astrocytic adrenoceptors: a major drug target in neurological and psychiatric disorders? *Curr Drug Targets CNS Neurol Disord,* 3**,** 239-67.

HERTZ, L., GERKAU, N. J., XU, J. N., DURRY, S., SONG, D., ROSE, C. R. & PENG, L. 2015a. Roles of astrocytic Na+,K+-ATPase and glycogenolysis for K+ homeostasis in mammalian brain. *Journal of Neuroscience Research,* 93**,** 1019-1030.

HERTZ, L., LOVATT, D., GOLDMAN, S. A. & NEDERGAARD, M. 2010. Adrenoceptors in brain: cellular gene expression and effects on astrocytic metabolism and [Ca(2+)]i. *Neurochem Int,* 57**,** 411-20.

HERTZ, L., PENG, L. & DIENEL, G. A. 2007. Energy metabolism in astrocytes: high rate of oxidative metabolism and spatiotemporal dependence on glycolysis/glycogenolysis. *Journal of Cerebral Blood Flow & Metabolism,* 27**,** 219-249.

HERTZ, L., XU, J., SONG, D., DU, T., LI, B., YAN, E. & PENG, L. 2015b. Astrocytic glycogenolysis: mechanisms and functions. *Metabolic brain disease,* 30**,** 317-333.

HERTZ, L., XU, J., SONG, D., DU, T., YAN, E. & PENG, L. 2013. Brain glycogenolysis, adrenoceptors, pyruvate carboxylase, Na(+),K(+)-ATPase and Marie E. Gibbs' pioneering learning studies. *Front Integr Neurosci,* 7**,** 20.

HOF, P., PASCALE, E. & MAGISTRETTI, P. J. 1988a. K+ at concentrations reached in the extracellular space during neuronal activity promotes a Ca2+-dependent glycogen hydrolysis in mouse cerebral cortex. *Journal of Neuroscience,* 8**,** 1922-1928.

HOF, P. R., PASCALE, E. & MAGISTRETTI, P. J. 1988b. K+ at concentrations reached in the extracellular space during neuronal activity promotes a Ca2+-dependent glycogen hydrolysis in mouse cerebral cortex. *J Neurosci,* 8**,** 1922-8.

HOL, E. 2015. Astrocytes in the aging brain and in Alzheimer's disease. *Glia,* 63**,** E69-E70.

HOL, E. M. & PEKNY, M. 2015. Glial fibrillary acidic protein (GFAP) and the astrocyte intermediate filament system in diseases of the central nervous system. *Current Opinion in Cell Biology,* 32**,** 121-130.

HOUSLAY, M. D. 2006. A RSK (y) relationship with promiscuous PKA. *Science Signaling,* 2006**,** pe32-pe32.

HSIEH, H. L., TUNG, W. H., WU, C. Y., WANG, H. H., LIN, C. C., WANG, T. S. & YANG, C. M. 2009. Thrombin induces EGF receptor expression and cell proliferation via a PKC(delta)/c-Src-dependent pathway in vascular smooth muscle cells. *Arterioscler Thromb Vasc Biol,* 29**,** 1594-601.

HU, Z. W., SHI, X. Y., LIN, R. Z. & HOFFMAN, B. B. 1996. alpha(1) Adrenergic receptors activate phosphatidylinositol 3-kinase in human vascular smooth muscle cells - Role in mitogenesis. *Journal of Biological Chemistry,* 271**,** 8977-8982.

HUGHES, E. G., ELMARIAH, S. B. & BALICE-GORDON, R. J. 2010. Astrocyte secreted proteins selectively increase hippocampal GABAergic axon length, branching, and synaptogenesis. *Molecular and Cellular Neuroscience,* 43**,** 136-145.

HUNEYCUTT, B. S. & BENVENISTE, E. N. 1995. Regulation of astrocyte cell biology by the cAMP/protein kinase A signaling pathway. *Advances in Neuroimmunology,* 5**,** 261-269.

HUR, E. M. & KIM, K. T. 2002. G protein-coupled receptor signalling and cross-talk - Achieving rapidity and specificity. *Cellular Signalling,* 14**,** 397-405.

HUTCHINSON, D. S., CATUS, S. L., MERLIN, J., SUMMERS, R. J. & GIBBS, M. E. 2011. α2‐Adrenoceptors activate noradrenaline‐mediated glycogen turnover in chick astrocytes. *Journal of neurochemistry,* 117**,** 915-926.

HUTCHINSON, D. S., SUMMERS, R. J. & GIBBS, M. E. 2007. Beta2- and beta3-adrenoceptors activate glucose uptake in chick astrocytes by distinct mechanisms: a mechanism for memory enhancement? *J Neurochem,* 103**,** 997-1008.

HYNES, N. E., INGHAM, P. W., LIM, W. A., MARSHALL, C. J., MASSAGUE, J. & PAWSON, T. 2013. Signalling change: signal transduction through the decades. *Nat Rev Mol Cell Biol,* 14**,** 393-8.

IADECOLA, C. & NEDERGAARD, M. 2007. Glial regulation of the cerebral microvasculature. *Nature Neuroscience,* 10**,** 1369-1376.

INAMDAR, V., PATEL, A., MANNE, B. K., DANGELMAIER, C. & KUNAPULI, S. P. 2015. Characterization of UBO-QIC as a G alpha(q) inhibitor in platelets. *Platelets,* 26**,** 771-778.

ITO, A., SATOH, T., KAZIRO, Y. & ITOH, H. 1995. G-Protein Beta-Gamma Subunit Activates Ras, Raf, and Map Kinase in Hek-293 Cells. *Febs Letters,* 368**,** 183-187.

JOYCE, J. N., LEXOW, N., KIM, S. J., ARTYMYSHYN, R., SENZON, S., LAWRENCE, D., CASSANOVA, M. F., KLEINMAN, J. E., BIRD, E. D. & WINOKUR, A. 1992. Distribution of beta-adrenergic receptor subtypes in human post-mortem brain: alterations in limbic regions of schizophrenics. *Synapse,* 10**,** 228-46.

JOZWIAK-BEBENISTA, M., WIKTOROWSKA-OWCZAREK, A. & KOWALCZYK, E. 2016. [Beta-adrenoceptor-mediated cyclic AMP signal in different types of cultured nerve cells in normoxic and hypoxic conditions]. *Mol Biol (Mosk),* 50**,** 838-846.

JUNKER, V., BECKER, A., HUHNE, R., ZEMBATOV, M., RAVATI, A., CULMSEE, C. & KRIEGLSTEIN, J. 2002a. Stimulation of beta-adrenoceptors activates astrocytes and provides neuroprotection. *Eur J Pharmacol,* 446**,** 25-36.

JUNKER, V., BECKER, A., HUHNE, R., ZEMBATOV, M., RAVATI, A., CULMSEE, C. & KRIEGLSTEIN, J. 2002b. Stimulation of beta-adrenoceptors activates astrocytes and provides neuroprotection. *European Journal of Pharmacology,* 446**,** 25-36.

KANG, K., LEE, S. W., HAN, J. E., CHOI, J. W. & SONG, M. R. 2014. The Complex Morphology of Reactive Astrocytes Controlled by Fibroblast Growth Factor Signaling. *Glia,* 62**,** 1328-1344.

KATZ, A., WU, D. Q. & SIMON, M. I. 1992. Subunits-Beta-Gamma of Heterotrimeric G-Protein Activate Beta-2 Isoform of Phospholipase-C. *Nature,* 360**,** 686-689.

KAWAMURA, M. & KAWAMURA, M. 2011. Long-term facilitation of spontaneous calcium oscillations in astrocytes with endogenous adenosine in hippocampal slice cultures. *Cell Calcium,* 49**,** 249-258.

KAYA, A. I., ONARAN, H. O., OZCAN, G., AMBROSIO, C., COSTA, T., BALLI, S. & UGUR, O. 2012. Cell Contact-dependent Functional Selectivity of beta(2)-Adrenergic Receptor Ligands in Stimulating cAMP Accumulation and Extracellular Signal-regulated Kinase Phosphorylation. *Journal of Biological Chemistry,* 287**,** 6362-6374.

KHAKH, B. S. & MCCARTHY, K. D. 2015. Astrocyte calcium signaling: from observations to functions and the challenges therein. *Cold Spring Harbor perspectives in biology,* 7**,** a020404.

KHAKH, B. S. & SOFRONIEW, M. V. 2014. Astrocytes and Huntington's Disease. *Acs Chemical Neuroscience,* 5**,** 494-496.

KHAKH, B. S. & SOFRONIEW, M. V. 2015. Diversity of astrocyte functions and phenotypes in neural circuits. *Nature Neuroscience,* 18**,** 942-952.

KIMELBERG, H. K. 2007. Supportive or information-processing functions of the mature protoplasmic astrocyte in the mammalian CNS? A critical appraisal. *Neuron Glia Biol,* 3**,** 181-9.

KIRISCHUK, S., TUSCHICK, S., VERKHRATSKY, A. & KETTENMANN, H. 1996. Calcium signalling in mouse Bergmann glial cells mediated by alpha1-adrenoreceptors and H1 histamine receptors. *Eur J Neurosci,* 8**,** 1198-208.

KOCH, W. J., HAWES, B. E., ALLEN, L. F. & LEFKOWITZ, R. J. 1994a. Direct Evidence That G(I)-Coupled Receptor Stimulation of Mitogen-Activated Protein-Kinase Is Mediated by G(Beta-Gamma) Activation of P21(Ras). *Proceedings of the National Academy of Sciences of the United States of America,* 91**,** 12706-12710.

KOCH, W. J., HAWES, B. E., INGLESE, J., LUTTRELL, L. M. & LEFKOWITZ, R. J. 1994b. Cellular Expression of the Carboxyl-Terminus of a G-Protein-Coupled Receptor Kinase Attenuates G(Beta-Gamma)-Mediated Signaling. *Journal of Biological Chemistry,* 269**,** 6193-6197.

KOENIG, J. A. & EDWARDSON, J. M. 1997. Endocytosis and recycling of G protein-coupled receptors. *Trends Pharmacol Sci,* 18**,** 276-87.

KRAFT, R. 2015. STIM and ORAI proteins in the nervous system. *Channels (Austin),* 9**,** 245-52.

KRANENBURG, O. & MOOLENAAR, W. H. 2001. Ras-MAP kinase signaling by lysophosphatidic acid and other G protein-coupled receptor agonists. *Oncogene,* 20**,** 1540-6.

KWON, H. B. & SABATINI, B. L. 2011. Glutamate induces de novo growth of functional spines in developing cortex. *Nature,* 474**,** 100-104.

LALO, U., RASOOLI-NEJAD, S. & PANKRATOV, Y. 2014. Exocytosis of gliotransmitters from cortical astrocytes: implications for synaptic plasticity and aging. *Biochemical Society Transactions,* 42**,** 1275-1281.

LARSEN, B. R., ASSENTOFT, M., COTRINA, M. L., HUA, S. Z., NEDERGAARD, M., KAILA, K., VOIPIO, J. & MACAULAY, N. 2014. Contributions of the Na(+)/K(+)-ATPase, NKCC1, and Kir4.1 to hippocampal K(+) clearance and volume responses. *Glia,* 62**,** 608-22.

LASKEY, A. D., ROTH, B. J., SIMPSON, P. B. & RUSSELL, J. T. 1998. Images of Ca2+ flux in astrocytes: evidence for spatially distinct sites of Ca2+ release and uptake. *Cell Calcium,* 23**,** 423-432.

LATOUR, I., HAMID, J., BEEDLE, A. M., ZAMPONI, G. W. & MACVICAR, B. A. 2003. Expression of voltage-gated Ca2+ channel subtypes in cultured astrocytes. *Glia,* 41**,** 347-53.

LAUGWITZ, K. L., ALLGEIER, A., OFFERMANNS, S., SPICHER, K., VANSANDE, J., DUMONT, J. E. & SCHULTZ, G. 1996. The human thyrotropin receptor: A heptahelical receptor capable of stimulating members of all four G protein families. *Proceedings of the National Academy of Sciences of the United States of America,* 93**,** 116-120.

LEE, K., MAKINO, S., IMAGAWA, T., KIM, M. & UEHARA, M. 2001. Effects of adrenergic agonists on glycogenolysis in primary cultures of glycogen body cells and telencephalon astrocytes of the chick. *Poultry science,* 80**,** 1736-1742.

LEFKIMMIATIS, K. & ZACCOLO, M. 2014. cAMP signaling in subcellular compartments. *Pharmacol Ther,* 143**,** 295-304.

LEV, S., MORENO, H., MARTINEZ, R., CANOLL, P., PELES, E., MUSACCHIO, J. M., PLOWMAN, G. D., RUDY, B. & SCHLESSINGER, J. 1995. Protein-Tyrosine Kinase Pyk2 Involved in Ca2+-Induced Regulation of Ion-Channel and Map Kinase Functions. *Nature,* 376**,** 737-745.

LEVY, F. O., ZHU, X., KAUMANN, A. J. & BIRNBAUMER, L. 1993. Efficacy of beta 1-adrenergic receptors is lower than that of beta 2-adrenergic receptors. *Proc Natl Acad Sci U S A,* 90**,** 10798-802.

LI, D., AGULHON, C., SCHMIDT, E., OHEIM, M. & ROPERT, N. 2013. New tools for investigating astrocyte-to-neuron communication. *Front Cell Neurosci,* 7**,** 193.

LIN, C. H., YOU, J. R., WEI, K. C. & GEAN, P. W. 2014. Stimulating ERK/PI3K/NF κ B signaling pathways upon activation of mGluR2/3 restores OGD‐induced impairment in glutamate clearance in astrocytes. *European Journal of Neuroscience,* 39**,** 83-96.

LIPPS, G. 2008. *Plasmids: current research and future trends*, Horizon Scientific Press.

LITOSCH, I. 2002. Novel Mechanisms for Feedback Regulation of Phospholipase C‐β Activity. *IUBMB life,* 54**,** 253-260.

LIU, N., STOICA, G., YAN, M. S., SCOFIELD, V. L., QIANG, W. N., LYNN, W. S. & WONG, P. K. Y. 2005. ATM deficiency induces oxidative stress and endoplasmic reticulum stress in astrocytes. *Laboratory Investigation,* 85**,** 1471-1480.

LOPEZILASACA, M., CRESPO, P., PELLICI, P. G., GUTKIND, J. S. & WETZKER, R. 1997. Linkage of G protein-coupled receptors to the MAPK signaling pathway through PI 3-kinase gamma. *Science,* 275**,** 394-397.

LUTTRELL, L. M. 2003. 'Location, location, location': activation and targeting of MAP kinases by G protein-coupled receptors. *J Mol Endocrinol,* 30**,** 117-26.

LUTTRELL, L. M., DAAKA, Y. & LEFKOWITZ, R. J. 1999. Regulation of tyrosine kinase cascades by G-protein-coupled receptors. *Current Opinion in Cell Biology,* 11**,** 177-183.

MACAULAY, N. & ZEUTHEN, T. 2012. Glial K(+) clearance and cell swelling: key roles for cotransporters and pumps. *Neurochem Res,* 37**,** 2299-309.

MACDONALD, S. G., CREWS, C. M., WU, L., DRILLER, J., CLARK, R., ERIKSON, R. L. & MCCORMICK, F. 1993. Reconstitution of the Raf-1-Mek-Erk Signal-Transduction Pathway in-Vitro. *Molecular and Cellular Biology,* 13**,** 6615-6620.

MACVICAR, B. A. 1984. Voltage-dependent calcium channels in glial cells. *Science,* 226**,** 1345-7.

MACVICAR, B. A. & NEWMAN, E. A. 2015. Astrocyte regulation of blood flow in the brain. *Cold Spring Harb Perspect Biol,* 7.

MADERSPACH, K. & FAJSZI, C. 1982. Beta-Adrenergic Receptors of Brain-Cells - Membrane Integrity Implies Apparent Positive Cooperativity and Higher Affinity. *Biochimica Et Biophysica Acta,* 692**,** 469-478.

MADRY, C. & ATTWELL, D. 2015. Receptors, Ion Channels, and Signaling Mechanisms Underlying Microglial Dynamics. *Journal of Biological Chemistry,* 290**,** 12443-12450.

MAGISTRETTI, P. 1987. Regulation of glycogenolysis by neurotransmitters in the central nervous system. *Diabete & metabolisme,* 14**,** 237-246.

MAGISTRETTI, P. J. & PELLERIN, L. 1999. Astrocytes couple synaptic activity to glucose utilization in the brain. *Physiology,* 14**,** 177-182.

MANGIA, S., GIOVE, F. & DINUZZO, M. 2013. K+ homeostasis in the brain: a new role for glycogenolysis. *Neurochemical research,* 38**,** 470-471.

MARAGAKIS, N. J. & ROTHSTEIN, J. D. 2006. Mechanisms of Disease: astrocytes in neurodegenerative disease. *Nat Clin Pract Neurol,* 2**,** 679-89.

MARINISSEN, M. J. & GUTKIND, J. S. 2001. G-protein-coupled receptors and signaling networks: emerging paradigms. *Trends in Pharmacological Sciences,* 22**,** 368-376.

MARTIN, N. P., WHALEN, E. J., ZAMAH, M. A., PIERCE, K. L. & LEFKOWITZ, R. J. 2004. PKA-mediated phosphorylation of the beta(1)-adrenergic receptor promotes G(s)/G(i) switching. *Cellular Signalling,* 16**,** 1397-1403.

MATHUR, D., LOPEZ-RODAS, G., CASANOVA, B. & MARTI, M. B. 2014. Perturbed glucose metabolism: insights into multiple sclerosis pathogenesis. *Frontiers in Neurology,* 5.

MATSUTANI, S. & YAMAMOTO, N. 1997. Neuronal regulation of astrocyte morphology in vitro is mediated by GABAergic signaling. *Glia,* 20**,** 1-9.

MATSUTANI, S. & YAMAMOTO, N. 1998. GABAergic neuron-to-astrocyte signaling regulates dendritic branching in coculture. *Journal of Neurobiology,* 37**,** 251-264.

MATYASH, V. & KETTENMANN, H. 2010. Heterogeneity in astrocyte morphology and physiology. *Brain Res Rev,* 63**,** 2-10.

MAVROPOULOS, G., MINGUET, G. & BRICHANT, J. F. 2014. [Alpha-2 adrenoreceptor agonists in anaesthesia and intensive care medicine]. *Rev Med Liege,* 69**,** 97-101.

MAY, V., CLASON, T. A., BUTTOLPH, T. R., GIRARD, B. M. & PARSONS, R. L. 2014. Calcium Influx, But Not Intracellular Calcium Release, Supports PACAP-Mediated ERK Activation in HEK PAC1 Receptor Cells. *Journal of Molecular Neuroscience,* 54**,** 342-350.

MCCARTHY, K. D. & DE VELLIS, J. 1980. Preparation of separate astroglial and oligodendroglial cell cultures from rat cerebral tissue. *J Cell Biol,* 85**,** 890-902.

MIDDELDORP, J., BOER, K., SLUIJS, J. A., DE FILIPPIS, L., ENCHA-RAZAVI, F., VESCOVI, A. L., SWAAB, D. F., ARONICA, E. & HOL, E. M. 2010. GFAP delta in radial glia and subventricular zone progenitors in the developing human cortex. *Development,* 137**,** 313-321.

MIDDELDORP, J. & HOL, E. M. 2011. GFAP in health and disease. *Progress in Neurobiology,* 93**,** 421-443.

MILLS, S. 2002. Implications of feedback regulation of beta-adrenergic signaling. *Journal of Animal Science,* 80**,** E30-E35.

MILNER, T. A., LEE, A., AICHER, S. A. & ROSIN, D. L. 1998. Hippocampal alpha(2A)-adrenergic receptors are located predominantly presynaptically but are also found postsynaptically and in selective astrocytes. *Journal of Comparative Neurology,* 395**,** 310-327.

MINNEMAN, K. P. & ESBENSHADE, T. A. 1994. Alpha(1)-Adrenergic Receptor Subtypes. *Annual Review of Pharmacology and Toxicology,* 34**,** 117-133.

MOCHIZUKI, N., OHBA, Y., KIYOKAWA, E., KURATA, T., MURAKAMI, T., OZAKI, T., KITABATAKE, A., NAGASHIMA, K. & MATSUDA, M. 1999. Activation of the ERK/MAPK pathway by an isoform of rap1GAP associated with Gαi. *Nature,* 400**,** 891-894.

MONS, N., DECORTE, L., JAFFARD, R. & COOPER, D. M. 1998. Ca2+-sensitive adenylyl cyclases, key integrators of cellular signalling. *Life Sci,* 62**,** 1647-52.

MONTIEL, M., QUESADA, J. & JIMENEZ, E. 2007. Activation of calcium-dependent kinases and epidermal growth factor receptor regulate muscarinic acetylcholine receptor-mediated MAPK/ERK activation in thyroid epithelial cells. *Cell Signal,* 19**,** 2138-46.

MORI, K., OZAKI, E., ZHANG, B., YANG, L. H., YOKOYAMA, A., TAKEDA, I., MAEDA, N., SAKANAKA, M. & TANAKA, J. 2002. Effects of norepinephrine on rat cultured microglial cells that express alpha 1, alpha 2, beta 1 and beta 2 adrenergic receptors. *Neuropharmacology,* 43**,** 1026-1034.

MOSS, J. & VAUGHAN, M. 1988. Adp-Ribosylation of Guanyl Nucleotide-Binding Regulatory Proteins by Bacterial Toxins. *Advances in Enzymology and Related Areas of Molecular Biology,* 61**,** 303-379.

MOTHET, J. P., POLLEGIONI, L., OUANOUNOU, G., MARTINEAU, M., FOSSIER, P. & BAUX, G. 2005. Glutamate receptor activation triggers a calcium-dependent and SNARE protein-dependent release of the gliotransmitter D-serine. *Proc Natl Acad Sci U S A,* 102**,** 5606-11.

MULLER, M. S. 2014. Functional impact of glycogen degradation on astrocytic signalling. *Biochemical Society Transactions,* 42**,** 1311-1315.

MULLER, M. S., FOX, R., SCHOUSBOE, A., WAAGEPETERSEN, H. S. & BAK, L. K. 2014. Astrocyte glycogenolysis is triggered by store-operated calcium entry and provides metabolic energy for cellular calcium homeostasis. *Glia,* 62**,** 526-34.

NASH, M. S., SCHELL, M. J., ATKINSON, P. J., JOHNSTON, N. R., NAHORSKI, S. R. & CHALLISS, R. J. 2002. Determinants of Metabotropic Glutamate Receptor-5-mediated Ca2+ and Inositol 1, 4, 5-Trisphosphate Oscillation Frequency RECEPTOR DENSITY VERSUS AGONIST CONCENTRATION. *Journal of Biological Chemistry,* 277**,** 35947-35960.

NAVARRETE, M., PEREA, G., MAGLIO, L., PASTOR, J., DE SOLA, R. G. & ARAQUE, A. 2012. Astrocyte calcium signal and gliotransmission in human brain tissue. *Cerebral Cortex***,** bhs122.

NEDERGAARD, M., RODRIGUEZ, J. J. & VERKHRATSKY, A. 2010. Glial calcium and diseases of the nervous system. *Cell Calcium,* 47**,** 140-149.

NEWGARD, C. B., HWANG, P. K. & FLETTERICK, R. J. 1989. The family of glycogen phosphorylases: structure and function. *Crit Rev Biochem Mol Biol,* 24**,** 69-99.

NEWMAN, L. A., KOROL, D. L. & GOLD, P. E. 2011. Lactate produced by glycogenolysis in astrocytes regulates memory processing. *PLoS One,* 6**,** e28427.

NICHOLAS, A. P., PIERIBONE, V. A. & HOKFELT, T. 1993. Cellular-Localization of Messenger-Rna for Beta-1 and Beta-2-Adrenergic Receptors in Rat-Brain - an in-Situ Hybridization Study. *Neuroscience,* 56**,** 1023-1039.

NICHOLS, N. R., DAY, J. R., LAPING, N. J., JOHNSON, S. A. & FINCH, C. E. 1993. Gfap Messenger-Rna Increases with Age in Rat and Human Brain. *Neurobiology of Aging,* 14**,** 421-429.

NIKOLAEV, V. O., BUNEMANN, M., SCHMITTECKERT, E., LOHSE, M. J. & ENGELHARDT, S. 2006. Cyclic AMP imaging in adult cardiac myocytes reveals far-reaching beta1-adrenergic but locally confined beta2-adrenergic receptor-mediated signaling. *Circ Res,* 99**,** 1084-91.

NIRANJAN, R. 2014. The Role of Inflammatory and Oxidative Stress Mechanisms in the Pathogenesis of Parkinson's Disease: Focus on Astrocytes. *Molecular Neurobiology,* 49**,** 28-38.

O'DONNELL, J., ZEPPENFELD, D., MCCONNELL, E., PENA, S. & NEDERGAARD, M. 2012. Norepinephrine: A Neuromodulator That Boosts the Function of Multiple Cell Types to Optimize CNS Performance. *Neurochemical Research,* 37**,** 2496-2512.

OBEL, L. F., MULLER, M. S., WALLS, A. B., SICKMANN, H. M., BAK, L. K., WAAGEPETERSEN, H. S. & SCHOUSBOE, A. 2012. Brain glycogen-new perspectives on its metabolic function and regulation at the subcellular level. *Front Neuroenergetics,* 4**,** 3.

OBERHEIM, N. A., GOLDMAN, S. A. & NEDERGAARD, M. 2012. Heterogeneity of astrocytic form and function. *Astrocytes: Methods and Protocols***,** 23-45.

OBERHEIM, N. A., WANG, X., GOLDMAN, S. & NEDERGAARD, M. 2006. Astrocytic complexity distinguishes the human brain. *Trends Neurosci,* 29**,** 547-53.

ODOWD, B. S., BARRINGTON, J., NG, K. T., HERTZ, E. & HERTZ, L. 1995. Glycogenolytic Response of Primary Chick and Mouse Cultures of Astrocytes to Noradrenaline across Development. *Developmental Brain Research,* 88**,** 220-223.

OFFERMANNS, S., WIELAND, T., HOMANN, D., SANDMANN, J., BOMBIEN, E., SPICHER, K., SCHULTZ, G. & JAKOBS, K. H. 1994. Transfected Muscarinic Acetylcholine-Receptors Selectively Couple to G(I)-Type G-Proteins and G(Q/11). *Molecular Pharmacology,* 45**,** 890-898.

OISHI, A., MAKITA, N., SATO, J. & IIRI, T. 2012. Regulation of RhoA signaling by the cAMP-dependent phosphorylation of RhoGDIalpha. *J Biol Chem,* 287**,** 38705-15.

OTA, Y., ZANETTI, A. T. & HALLOCK, R. M. 2013. The role of astrocytes in the regulation of synaptic plasticity and memory formation. *Neural plasticity,* 2013.

OZ, G., KUMAR, A., RAO, J. P., KODL, C. T., CHOW, L., EBERLY, L. E. & SEAQUIST, E. R. 2009. Human brain glycogen metabolism during and after hypoglycemia. *Diabetes,* 58**,** 1978-85.

PACE, A., FAURE, M. & BOURNE, H. 1995. Gi2-mediated activation of the MAP kinase cascade. *Molecular biology of the cell,* 6**,** 1685-1695.

PACHECO, J. & VACA, L. 2013. A Microscopic View of the Store-Operated Calcium Entry-Pathway. *ISRN Cell Biology,* 2013.

PANATIER, A. & ROBITAILLE, R. 2016. Astrocytic mGluR5 and the tripartite synapse. *Neuroscience,* 323**,** 29-34.

PANATIER, A., VALLÉE, J., HABER, M., MURAI, K. K., LACAILLE, J.-C. & ROBITAILLE, R. 2011. Astrocytes are endogenous regulators of basal transmission at central synapses. *Cell,* 146**,** 785-798.

PANGRSIC, T., POTOKAR, M., HAYDON, P. G., ZOREC, R. & KREFT, M. 2006. Astrocyte swelling leads to membrane unfolding, not membrane insertion. *Journal of Neurochemistry,* 99**,** 514-523.

PANKRATOV, Y. & LALO, U. 2015a. Role for astroglial alpha 1-adrenoreceptors in gliotransmission and control of synaptic plasticity in the neocortex. *Frontiers in Cellular Neuroscience,* 9.

PANKRATOV, Y. & LALO, U. 2015b. Role for astroglial α1-adrenoreceptors in gliotransmission and control of synaptic plasticity in the neocortex. *Frontiers in cellular neuroscience,* 9.

PARPURA, V., HENEKA, M. T., MONTANA, V., OLIET, S. H., SCHOUSBOE, A., HAYDON, P. G., STOUT, R. F., JR., SPRAY, D. C., REICHENBACH, A., PANNICKE, T., PEKNY, M., PEKNA, M., ZOREC, R. & VERKHRATSKY, A. 2012. Glial cells in (patho)physiology. *J Neurochem,* 121**,** 4-27.

PASCHALIS, A., CHURCHILL, L., MARINA, N., KASYMOV, V., GOURINE, A. & ACKLAND, G. 2009. beta1-Adrenoceptor distribution in the rat brain: an immunohistochemical study. *Neurosci Lett,* 458**,** 84-8.

PASTI, L., ZONTA, M., POZZAN, T., VICINI, S. & CARMIGNOTO, G. 2001. Cytosolic calcium oscillations in astrocytes may regulate exocytotic release of glutamate. *J Neurosci,* 21**,** 477-84.

PAUKERT, M., AGARWAL, A., CHA, J., DOZE, V. A., KANG, J. U. & BERGLES, D. E. 2014a. Norepinephrine controls astroglial responsiveness to local circuit activity. *Neuron,* 82**,** 1263-70.

PAUKERT, M., AGARWAL, A., CHA, J., DOZE, V. A., KANG, J. U. & BERGLES, D. E. 2014b. Norepinephrine Controls Astroglial Responsiveness to Local Circuit Activity. *Neuron, 82*, 1263-1270.

PEARCE, B. & MURPHY, S. 1993. Protein kinase C down-regulation in astrocytes: differential effects on agonist-stimulated inositol phosphate accumulation. *Neurochem Int, 23*, 407-12.

PEAVY, R. D., CHANG, M. S. S., SANDERS-BUSH, E. & CONN, P. J. 2001. Metabotropic glutamate receptor 5-induced phosphorylation of extracellular signal-regulated kinase in astrocytes depends on transactivation of the epidermal growth factor receptor. *Journal of Neuroscience, 21*, 9619-9628.

PEKNY, M. & NILSSON, M. 2005. Astrocyte activation and reactive gliosis. *Glia, 50*, 427-434.

PEKNY, M. & PEKNA, M. 2014. Astrocyte Reactivity and Reactive Astrogliosis: Costs and Benefits. *Physiological Reviews, 94*, 1077-1098.

PELLERIN, L. & MAGISTRETTI, P. J. 1994. Glutamate Uptake into Astrocytes Stimulates Aerobic Glycolysis - a Mechanism Coupling Neuronal-Activity to Glucose-Utilization. *Proceedings of the National Academy of Sciences of the United States of America, 91*, 10625-10629.

PENG, L., LI, B., DU, T., KONG, E. K., HU, X., ZHANG, S., SHAN, X. & ZHANG, M. 2010a. Astrocytic transactivation by alpha2A-adrenergic and 5-HT2B serotonergic signaling. *Neurochem Int, 57*, 421-31.

PENG, L., LI, B., DU, T., KONG, E. K., HU, X., ZHANG, S., SHAN, X. & ZHANG, M. 2010b. Astrocytic transactivation by α 2A-adrenergic and 5-HT 2B serotonergic signaling. *Neurochemistry international, 57*, 421-431.

PEREA, G., NAVARRETE, M. & ARAQUE, A. 2009. Tripartite synapses: astrocytes process and control synaptic information. *Trends Neurosci, 32*, 421-31.

PEREZ, V., BOUSCHET, T., FERNANDEZ, C., BOCKAERT, J. & JOURNOT, L. 2005. Dynamic reorganization of the astrocyte actin cytoskeleton elicited by cAMP and PACAP: a role for phosphatidyllnositol 3-kinase inhibition. *European Journal of Neuroscience, 21*, 26-32.

PHILIP, F., KADAMUR, G., SILOS, R., WOODSON, J. & ROSS, E. M. 2010. Synergistic Activation of Phospholipase C-beta 3 by G alpha(q) and G beta gamma Describes a Simple Two-State Coincidence Detector. *Current Biology, 20*, 1327-1335.

PIASCIK, M. T. & PEREZ, D. M. 2001. Alpha1-adrenergic receptors: new insights and directions. *J Pharmacol Exp Ther, 298*, 403-10.

PIERCE, K. L., TOHGO, A., AHN, S., FIELD, M. E., LUTTRELL, L. M. & LEFKOWITZ, R. J. 2001. Epidermal growth factor (EGF) receptor-dependent ERK activation by G protein-coupled receptors - A co-culture system for identifying intermediates upstream and downstream of heparin-binding EGF shedding. *Journal of Biological Chemistry, 276*, 23155-23160.

PINTO, L. & GOTZ, M. 2007. Radial glial cell heterogeneity--the source of diverse progeny in the CNS. *Prog Neurobiol, 83*, 2-23.

PIRTTIMAKI, T. M., HALL, S. D. & PARRI, H. R. 2011. Sustained Neuronal Activity Generated by Glial Plasticity. *Journal of Neuroscience, 31*, 7637-7647.

PIRTTIMAKI, T. M. & PARRI, H. R. 2013. Astrocyte plasticity: implications for synaptic and neuronal activity. *Neuroscientist, 19*, 604-15.

PITCHER, J., LOHSE, M. J., CODINA, J., CARON, M. G. & LEFKOWITZ, R. J. 1992. Desensitization of the Isolated Beta-2-Adrenergic Receptor by Beta-Adrenergic-Receptor Kinase, Camp-Dependent Protein-Kinase, and Protein-Kinase-C Occurs Via Distinct Molecular Mechanisms. *Biochemistry, 31*, 3193-3197.

POLITI, A., GASPERS, L. D., THOMAS, A. P. & HOFER, T. 2006. Models of IP3 and Ca2+ oscillations: frequency encoding and identification of underlying feedbacks. *Biophys J, 90*, 3120-33.

PREBIL, M., JENSEN, J., ZOREC, R. & KREFT, M. 2011. Astrocytes and energy metabolism. *Arch Physiol Biochem, 117*, 64-9.

PRENZEL, N., ZWICK, E., DAUB, H., LESERER, M., ABRAHAM, R., WALLASCH, C. & ULLRICH, A. 1999. EGF receptor transactivation by G-protein-coupled receptors requires metalloproteinase cleavage of proHB-EGF. *Nature, 402*, 884-888.

QIAGEN 2012. HiSpeed Plasmid Purification Handbook.

QUACH, T. T., DUCHEMIN, A. M., ROSE, C. & SCHWARTZ, J. C. 1988. [3H]glycogenolysis in brain slices mediated by beta-adrenoceptors: comparison of physiological response and [3H]dihydroalprenolol binding parameters. *Neuropharmacology,* 27**,** 629-35.

QUACH, T. T., ROSE, C. & SCHWARTZ, J. C. 1978. [3H]Glycogen hydrolysis in brain slices: responses to neurotransmitters and modulation of noradrenaline receptors. *J Neurochem,* 30**,** 1335-41.

RACCHETTI, G., D'ALESSANDRO, R. & MELDOLESI, J. 2012. Astrocyte stellation, a process dependent on Rac1 is sustained by the regulated exocytosis of enlargeosomes. *Glia,* 60**,** 465-475.

RADHIKA, V. & DHANASEKARAN, N. 2001. Transforming G proteins. *Oncogene,* 20.

RAINBOW, T. C., PARSONS, B. & WOLFE, B. B. 1984. Quantitative autoradiography of beta 1- and beta 2-adrenergic receptors in rat brain. *Proc Natl Acad Sci U S A,* 81**,** 1585-9.

RAMAKERS, G. J. & MOOLENAAR, W. H. 1998. Regulation of astrocyte morphology by RhoA and lysophosphatidic acid. *Experimental cell research,* 245**,** 252-262.

RANG, H. P. 2006. The receptor concept: pharmacology's big idea. *British Journal of Pharmacology,* 147**,** S9-S16.

RASMUSSEN, H. & BARRETT, P. Q. 1984. Calcium Messenger System - an Integrated View. *Physiological Reviews,* 64**,** 938-984.

RASOOLI-NEJAD, S., PALYGIN, O., LALO, U. & PANKRATOV, Y. 2014. Cannabinoid receptors contribute to astroglial Ca(2)(+)-signalling and control of synaptic plasticity in the neocortex. *Philos Trans R Soc Lond B Biol Sci,* 369**,** 20140077.

REUTTER, M. A., RICHARDS, E. M. & SUMNERS, C. 1998. Regulation of alpha2A-adrenergic receptor expression by epinephrine in cultured astroglia from rat brain. *J Neurochem,* 70**,** 86-95.

RICHTER, W., DAY, P., AGRAWAL, R., BRUSS, M. D., GRANIER, S., WANG, Y. L., RASMUSSEN, S. G. F., HOMER, K., WANG, P., LEI, T., PATTERSON, A. J., KOBILKA, B. & CONTI, M. 2008. Signaling from beta 1-and beta 2-adrenergic receptors is defined by differential interactions with PDE4. *Faseb Journal,* 22.

RIZZUTO, R. & POZZAN, T. 2006. Microdomains of intracellular Ca2+: Molecular determinants and functional consequences. *Physiological Reviews,* 86**,** 369-408.

ROBEL, S., BERNINGER, B. & GOTZ, M. 2011. The stem cell potential of glia: lessons from reactive gliosis. *Nature Reviews Neuroscience,* 12**,** 88-104.

RODNIGHT, R. B. & GOTTFRIED, C. 2013. Morphological plasticity of rodent astroglia. *Journal of Neurochemistry,* 124**,** 263-275.

ROSE, C. R. & RANSOM, B. R. 1997. Gap junctions equalize intracellular Na+ concentration in astrocytes. *Glia,* 20**,** 299-307.

ROSS, E. M. 2008. Coordinating speed and amplitude in G-protein signaling. *Current Biology,* 18**,** R777-R783.

ROUACH, N., KOULAKOFF, A., ABUDARA, V., WILLECKE, K. & GIAUME, C. 2008. Astroglial metabolic networks sustain hippocampal synaptic transmission. *Science,* 322**,** 1551-5.

ROYBON, L., LAMAS, N. J., GARCIA-DIAZ, A., YANG, E. J., SATTLER, R., JACKSON-LEWIS, V., KIM, Y. A., KACHEL, C. A., ROTHSTEIN, J. D., PRZEDBORSKI, S., WICHTERLE, H. & HENDERSON, C. E. 2013. Human Stem Cell-Derived Spinal Cord Astrocytes with Defined Mature or Reactive Phenotypes. *Cell Reports,* 4**,** 1035-1048.

ROZENGURT, E. 2007. Mitogenic signaling pathways induced by G protein-coupled receptors. *Journal of Cellular Physiology,* 213**,** 589-602.

SAFAVI-ABBASI, S., WOLFF, J. R. & MISSLER, M. 2001. Rapid morphological changes in astrocytes are accompanied by redistribution but not by quantitative changes of cytoskeletal proteins. *Glia,* 36**,** 102-115.

SAINI, D. K., KALYANARAMAN, V., CHISARI, M. & GAUTAM, N. 2007. A family of G protein betagamma subunits translocate reversibly from the plasma membrane to endomembranes on receptor activation. *J Biol Chem,* 282**,** 24099-108.

SALIDO, G. M., SAGE, S. O. & ROSADO, J. A. 2009. TRPC channels and store-operated Ca2+ entry. *Biochimica Et Biophysica Acta-Molecular Cell Research,* 1793**,** 223-230.

SAMBROOK, J. & RUSSELL, D. 2001. Gel electrophoresis of DNA and pulsed-field agarose gel electrophoresis. *Molecular cloning: a laboratory manual,* 1**,** 3.

SAPENA, R., MORIN, D., ZINI, R., MORIN, C. & TILLEMENT, J. P. 1996. Desipramine treatment differently down-regulates beta-adrenoceptors of freshly isolated neurons and astrocytes. *European Journal of Pharmacology,* 300**,** 159-162.

SASSONE-CORSI, P. 2012. The Cyclic AMP Pathway. *Cold Spring Harbor Perspectives in Biology,* 4.

SATO, M., HUTCHINSON, D. S., EVANS, B. A. & SUMMERS, R. J. 2007. Functional domains of the mouse beta(3)-adrenoceptor associated with differential G-protein coupling. *Biochem Soc Trans,* 35, 1035-7.

SCHMITT, J. M. & STORK, P. J. S. 2001. Cyclic AMP-mediated inhibition of cell growth requires the small G protein Rap1. *Molecular and Cellular Biology,* 21**,** 3671-3683.

SCHONWASSER, D. C., MARAIS, R. M., MARSHALL, C. J. & PARKER, P. J. 1998. Activation of the mitogen-activated protein kinase/extracellular signal-regulated kinase pathway by conventional, novel, and atypical protein kinase C isotypes. *Molecular and Cellular Biology,* 18**,** 790-798.

SCHOUSBOE, A. 2000. Pharmacological and functional characterization of astrocytic GABA transport: a short review. *Neurochem Res,* 25**,** 1241-4.

SCHOUSBOE, A., SICKMANN, H. M., WALLS, A. B., BAK, L. K. & WAAGEPETERSEN, H. S. 2010. Functional importance of the astrocytic glycogen-shunt and glycolysis for maintenance of an intact intra/extracellular glutamate gradient. *Neurotoxicity research,* 18**,** 94-99.

SCHRAGE, R., SCHMITZ, A. L., GAFFAL, E., ANNALA, S., KEHRAUS, S., WENZEL, D., BULLESBACH, K. M., BALD, T., INOUE, A., SHINJO, Y., GALANDRIN, S., SHRIDHAR, N., HESSE, M., GRUNDMANN, M., MERTEN, N., CHARPENTIER, T. H., MARTZ, M., BUTCHER, A. J., SLODCZYK, T., ARMANDO, S., EFFERN, M., NAMKUNG, Y., JENKINS, L., HORN, V., STOSSEL, A., DARGATZ, H., TIETZE, D., IMHOF, D., GALES, C., DREWKE, C., MULLER, C. E., HOLZEL, M., MILLIGAN, G., TOBIN, A. B., GOMEZA, J., DOHLMAN, H. G., SONDEK, J., HARDEN, T. K., BOUVIER, M., LAPORTE, S. A., AOKI, J., FLEISCHMANN, B. K., MOHR, K., KONIG, G. M., TUTING, T. & KOSTENIS, E. 2015. The experimental power of FR900359 to study Gq-regulated biological processes. *Nat Commun,* 6**,** 10156.

SELBIE, L. A. & HILL, S. J. 1998. G protein-coupled-receptor cross-talk: the fine-tuning of multiple receptor-signalling pathways. *Trends in Pharmacological Sciences,* 19**,** 87-93.

SHAH, B. H., SHAH, F. B. & CATT, K. J. 2006. Role of metalloproteinase-dependent EGF receptor activation in alpha(1)-adrenoceptor-stimulated MAP kinase phosphorylation in GT1-7 neurons. *Journal of Neurochemistry,* 96**,** 520-532.

SHAH, B. H., SIDDIQUI, A., QURESHI, K. A., KHAN, M., RAFI, S., UJAN, V. A., YAQUB, Y., RASHEED, H. & SAEED, S. A. 1999. Co-activation of Gi and Gq proteins exerts synergistic effect on human platelet aggregation through activation of phospholipase C and Ca2+ signalling pathways. *Experimental and Molecular Medicine,* 31**,** 42-46.

SHAO, Y., ENKVIST, M. & MCCARTHY, K. D. 1994. Glutamate blocks astroglial stellation: effect of glutamate uptake and volume changes. *Glia,* 11**,** 1-10.

SHENOY, S. K. & LEFKOWITZ, R. J. 2003. Multifaceted roles of beta-arrestins in the regulation of seven-membrane-spanning receptor trafficking and signalling. *Biochemical Journal,* 375**,** 503-515.

SHIGETOMI, E., BUSHONG, E. A., HAUSTEIN, M. D., TONG, X., JACKSON-WEAVER, O., KRACUN, S., XU, J., SOFRONIEW, M. V., ELLISMAN, M. H. & KHAKH, B. S. 2013a. Imaging calcium microdomains within entire astrocyte territories and endfeet with GCaMPs expressed using adeno-associated viruses. *The Journal of general physiology,* 141**,** 633-647.

SHIGETOMI, E., BUSHONG, E. A., HAUSTEIN, M. D., TONG, X. P., JACKSON-WEAVER, O., KRACUN, S., XU, J., SOFRONIEW, M. V., ELLISMAN, M. H. & KHAKH, B. S. 2013b. Imaging calcium microdomains within entire astrocyte territories and endfeet with GCaMPs expressed using adeno-associated viruses. *Journal of General Physiology,* 141**,** 633-647.

SHUTTLEWORTH, T. 1999. What drives calcium entry during [Ca 2+] i oscillations?–challenging the capacitative model. *Cell calcium,* 25**,** 237-246.

SIMARD, M., ARCUINO, G., TAKANO, T., LIU, Q. S. & NEDERGAARD, M. 2003. Signaling at the gliovascular interface. *J Neurosci,* 23**,** 9254-62.

SIMARD, M. & NEDERGAARD, M. 2004. The neurobiology of glia in the context of water and ion homeostasis. *Neuroscience,* 129**,** 877-896.

SKROBLIN, L. V., KLUSSMANN, E. & COOPER, D. M. 2012. Direct Binding Between Orai1 and AC8 Mediates Dynamic Interplay.

SMITH, K. E., GU, C., FAGAN, K. A., HU, B. & COOPER, D. M. F. 2002. Residence of adenylyl cyclase type 8 in caveolae is necessary but not sufficient for regulation by capacitative Ca2+ entry. *Journal of Biological Chemistry,* 277**,** 6025-6031.

SOFRONIEW, M. V. 2009. Molecular dissection of reactive astrogliosis and glial scar formation. *Trends in Neurosciences,* 32**,** 638-647.

SOFRONIEW, M. V. & VINTERS, H. V. 2010a. Astrocytes: biology and pathology. *Acta Neuropathologica,* 119**,** 7-35.

SOFRONIEW, M. V. & VINTERS, H. V. 2010b. Astrocytes: biology and pathology. *Acta Neuropathol,* 119**,** 7-35.

SORG, O. & MAGISTRETTI, P. J. 1991a. Characterization of the glycogenolysis elicited by vasoactive intestinal peptide, noradrenaline and adenosine in primary cultures of mouse cerebral cortical astrocytes. *Brain research,* 563**,** 227-233.

SORG, O. & MAGISTRETTI, P. J. 1991b. Characterization of the glycogenolysis elicited by vasoactive intestinal peptide, noradrenaline and adenosine in primary cultures of mouse cerebral cortical astrocytes. *Brain Res,* 563**,** 227-33.

SORG, O. & MAGISTRETTI, P. J. 1992. Vasoactive intestinal peptide and noradrenaline exert long-term control on glycogen levels in astrocytes: blockade by protein synthesis inhibition. *The Journal of neuroscience,* 12**,** 4923-4931.

STAITI, A. M., MORGANE, P. J., GALLER, J. R., GRIVETTI, J. Y., BASS, D. C. & MOKLER, D. J. 2011. A microdialysis study of the medial prefrontal cortex of adolescent and adult rats. *Neuropharmacology,* 61**,** 544-9.

STEINMAN, M. Q., GAO, V. & ALBERINI, C. M. 2016. The role of lactate-mediated metabolic coupling between astrocytes and neurons in long-term memory formation. *Frontiers in integrative neuroscience,* 10.

STOBART, J. L. & ANDERSON, C. M. 2013. Multifunctional role of astrocytes as gatekeepers of neuronal energy supply. *Frontiers in Cellular Neuroscience,* 7.

STORK, P. J. S. & SCHMITT, J. M. 2002. Crosstalk between cAMP and MAP kinase signaling in the regulation of cell proliferation. *Trends in Cell Biology,* 12**,** 258-266.

STUDER, R. K. & BORLE, A. 1982. Differences between male and female rats in the regulation of hepatic glycogenolysis. The relative role of calcium and cAMP in phosphorylase activation by catecholamines. *Journal of Biological Chemistry,* 257**,** 7987-7993.

SU, C., UNDERWOOD, W., RYBALCHENKO, N. & SINGH, M. 2011. ERK1/2 and ERK5 Have Distinct Roles in the Regulation of Brain-Derived Neurotrophic Factor Expression. *Journal of Neuroscience Research,* 89**,** 1542-1550.

SUBBARAO, K. V. & HERTZ, L. 1990a. Effect of adrenergic agonists on glycogenolysis in primary cultures of astrocytes. *Brain research,* 536**,** 220-226.

SUBBARAO, K. V. & HERTZ, L. 1990b. Effect of Adrenergic Agonists on Glycogenolysis in Primary Cultures of Astrocytes. *Brain Research,* 536**,** 220-226.

SUBBARAO, K. V., STOLZENBURG, J. U. & HERTZ, L. 1995. Pharmacological Characteristics of Potassium-Induced, Glycogenolysis in Astrocytes. *Neuroscience Letters,* 196**,** 45-48.

SUN, D. & JAKOBS, T. C. 2012. Structural Remodeling of Astrocytes in the Injured CNS. *Neuroscientist,* 18**,** 567-588.

SUZUKI, A., STERN, S. A., BOZDAGI, O., HUNTLEY, G. W., WALKER, R. H., MAGISTRETTI, P. J. & ALBERINI, C. M. 2011. Astrocyte-Neuron Lactate Transport Is Required for Long-Term Memory Formation. *Cell,* 144**,** 810-823.

TAKAHASHI, M., LI, Y., DILLON, T. J. & STORK, P. J. 2016. Phosphorylation of Rap1 by cAMP-dependent protein kinase (PKA) creates a binding site for KSR to sustain ERK activation by cAMP. *J Biol Chem*.

TAKANO, T., TIAN, G. F., PENG, W., LOU, N., LIBIONKA, W., HAN, X. & NEDERGAARD, M. 2006. Astrocyte-mediated control of cerebral blood flow. *Nat Neurosci,* 9**,** 260-7.

TAPINOS, N. & RAMBUKKANA, A. 2005. Insights into regulation of human Schwann cell proliferation by Erk1/2 via a MEK-independent and p56Lck-dependent pathway from leprosy bacilli. *Proc Natl Acad Sci U S A,* 102**,** 9188-93.

TAS, P. W., GAMBARYAN, S. & ROEWER, N. 2007. Volatile anesthetics affect the morphology of rat glioma C6 cells via RhoA, ERK, and Akt activation. *Journal of cellular biochemistry,* 102**,** 368-376.

TAYLOR, S. S., KIM, C., CHENG, C. Y., BROWN, S. H. J., WU, H. & KANNAN, N. 2008. Signaling through cAMP and cAMP-dependent protein kinase: Diverse strategies for drug design. *Biochimica Et Biophysica Acta-Proteins and Proteomics,* 1784**,** 16-26.

TEKKOK, S. B., BROWN, A. M. & RANSOM, B. R. 2003. Axon function persists during anoxia in mammalian white matter. *J Cereb Blood Flow Metab,* 23**,** 1340-7.

TEKKOK, S. B., BROWN, A. M., WESTENBROEK, R., PELLERIN, L. & RANSOM, B. R. 2005. Transfer of glycogen-derived lactate from astrocytes to axons via specific monocarboxylate transporters supports mouse optic nerve activity. *Journal of Neuroscience Research,* 81**,** 644-652.

THANDI, S., BLANK, J. L. & CHALLISS, R. A. 2002. Group-I metabotropic glutamate receptors, mGlu1a and mGlu5a, couple to extracellular signal-regulated kinase (ERK) activation via distinct, but overlapping, signalling pathways. *J Neurochem,* 83**,** 1139-53.

THORE, S., DYACHOK, O. & TENGHOLM, A. 2004. Oscillations of phospholipase C activity triggered by depolarization and Ca2+ influx in insulin-secreting cells. *J Biol Chem,* 279**,** 19396-400.

TOHGO, A., PIERCE, K. L., CHOY, E. W., LEFKOWITZ, R. J. & LUTTRELL, L. M. 2002. beta-Arrestin scaffolding of the ERK cascade enhances cytosolic ERK activity but inhibits ERK-mediated transcription following angiotensin AT1a receptor stimulation. *J Biol Chem,* 277**,** 9429-36.

ULU, N., GURDAL, H., LANDHEER, S. W., DUIN, M., GUC, M. O., BUIKEMA, H. & HENNING, R. H. 2010. alpha(1)-Adrenoceptor-mediated contraction of rat aorta is partly mediated via transactivation of the epidermal growth factor receptor. *British Journal of Pharmacology,* 161**,** 1301-1310.

VAN HALL, G., STROMSTAD, M., RASMUSSEN, P., JANS, O., ZAAR, M., GAM, C., QUISTORFF, B., SECHER, N. H. & NIELSEN, H. B. 2009. Blood lactate is an important energy source for the human brain. *Journal of Cerebral Blood Flow and Metabolism,* 29**,** 1121-1129.

VARDJAN, N., KREFT, M. & ZOREC, R. 2014. Dynamics of β‐adrenergic/cAMP signaling and morphological changes in cultured astrocytes. *Glia,* 62**,** 566-579.

VARDJAN, N. & ZOREC, R. 2015. Excitable Astrocytes: Ca(2+)- and cAMP-Regulated Exocytosis. *Neurochem Res,* 40**,** 2414-24.

VENTURA, R. & HARRIS, K. M. 1999. Three-dimensional relationships between hippocampal synapses and astrocytes. *The Journal of Neuroscience,* 19**,** 6897-6906.

VERKHRATSKY, A. & KIRCHHOFF, F. 2007. NMDA receptors in glia. *Neuroscientist,* 13**,** 28-37.

VERKHRATSKY, A., PARPURA, V. & RODRIGUEZ, J. J. 2011. Where the thoughts dwell: the physiology of neuronal-glial "diffuse neural net". *Brain Res Rev,* 66**,** 133-51.

VERKHRATSKY, A., RODRIGUEZ, J. J. & PARPURA, V. 2012a. Calcium signalling in astroglia. *Mol Cell Endocrinol,* 353**,** 45-56.

VERKHRATSKY, A., RODRIGUEZ, J. J. & PARPURA, V. 2012b. Calcium signalling in astroglia. *Molecular and Cellular Endocrinology,* 353**,** 45-56.

VERMEIREN, C., HEMPTINNE, I., VANHOUTTE, N., TILLEUX, S., MALOTEAUX, J. M. & HERMANS, E. 2006. Loss of metabotropic glutamate receptor-mediated regulation of glutamate transport in chemically activated astrocytes in a rat model of amyotrophic lateral sclerosis. *J Neurochem,* 96**,** 719-31.

VERVERKEN, D., VELDHOVEN, P., PROOST, C., CARTON, H. & WULF, H. 1982. On the role of calcium ions in the regulation of glycogenolysis in mouse brain cortical slices. *Journal of neurochemistry,* 38**,** 1286-1295.

VEZZOSI, D. & BERTHERAT, J. 2011. Phosphodiesterases in endocrine physiology and disease. *European Journal of Endocrinology,* 165**,** 177-188.

VOLTERRA, A., LIAUDET, N. & SAVTCHOUK, I. 2014. Astrocyte Ca(2)(+) signalling: an unexpected complexity. *Nat Rev Neurosci,* 15**,** 327-35.

WALLUKAT, G. 2002. The β-adrenergic receptors. *Herz,* 27**,** 683-690.

WALZ, W. 1992. Role of Na/K/Cl cotransport in astrocytes. *Can J Physiol Pharmacol,* 70 Suppl**,** S260-2.

WALZ, W. 2000. Role of astrocytes in the clearance of excess extracellular potassium. *Neurochem Int,* 36**,** 291-300.

WANG, D. D. & BORDEY, A. 2008. The astrocyte odyssey. *Prog Neurobiol,* 86**,** 342-67.

WANG, F., SMITH, N. A., XU, Q., FUJITA, T., BABA, A., MATSUDA, T., TAKANO, T., BEKAR, L. & NEDERGAARD, M. 2012. Astrocytes modulate neural network activity by Ca(2)+-dependent uptake of extracellular K+. *Sci Signal,* 5**,** ra26.

WANG, L., LIU, F. & ADAMO, M. L. 2001. Cyclic AMP inhibits extracellular signal-regulated kinase and phosphatidylinositol 3-kinase/Akt pathways by inhibiting Rap1. *Journal of Biological Chemistry,* 276**,** 37242-37249.

WANG, X., LOU, N., XU, Q., TIAN, G. F., PENG, W. G., HAN, X., KANG, J., TAKANO, T. & NEDERGAARD, M. 2006. Astrocytic Ca2+ signaling evoked by sensory stimulation in vivo. *Nat Neurosci,* 9**,** 816-23.

WENZEL-SEIFERT, K., LIU, H. Y. & SEIFERT, R. 2002. Similarities and differences in the coupling of human beta1- and beta2-adrenoceptors to Gs(alpha) splice variants. *Biochem Pharmacol,* 64**,** 9-20.

WERRY, T. D., WILKINSON, G. F. & WILLARS, G. B. 2003. Mechanisms of cross-talk between G-protein-coupled receptors resulting in enhanced release of intracellular Ca2+. *Biochem J,* 374**,** 281-96.

WETZKER, R. & BOHMER, F. D. 2003. Transactivation joins multiple tracks to the ERK/MAPK cascade. *Nature Reviews Molecular Cell Biology,* 4**,** 651-657.

WILLOUGHBY, D., WACHTEN, S., MASADA, N. & COOPER, D. M. 2010. Direct demonstration of discrete Ca2+ microdomains associated with different isoforms of adenylyl cyclase. *J Cell Sci,* 123**,** 107-117.

WOLOSKER, H., BALU, D. T. & COYLE, J. T. 2016. The rise and fall of the d-serine-mediated gliotransmission hypothesis. *Trends in Neurosciences,* 39**,** 712-721.

WON, C. K. & OH, Y. S. 2000. CAMP-induced stellation in primary astrocyte cultures with regional heterogeneity. *Brain Research,* 887**,** 250-258.

WOO, A. Y. H., WANG, T. B., ZENG, X. K., ZHU, W. Z., ABERNETHY, D. R., WAINER, I. W. & XIAO, R. P. 2009. Stereochemistry of an Agonist Determines Coupling Preference of beta(2)-Adrenoceptor to Different G Proteins in Cardiomyocytes. *Molecular Pharmacology,* 75**,** 158-165.

WOO, D. H., HAN, K. S., SHIM, J. W., YOON, B. E., KIM, E., BAE, J. Y., OH, S. J., HWANG, E. M., MARMORSTEIN, A. D., BAE, Y. C., PARK, J. Y. & LEE, C. J. 2012. TREK-1 and Best1 channels mediate fast and slow glutamate release in astrocytes upon GPCR activation. *Cell,* 151**,** 25-40.

XIAO, R.-P. 2001. Beta-adrenergic signaling in the heart: dual coupling of the beta2-adrenergic receptor to G (s) and G (i) proteins. *Sci Stke,* 104**,** re15.

XIAO, R.-P., AVDONIN, P., ZHOU, Y.-Y., CHENG, H., AKHTER, S. A., ESCHENHAGEN, T., LEFKOWITZ, R. J., KOCH, W. J. & LAKATTA, E. G. 1999. Coupling of β2-adrenoceptor to Gi proteins and its physiological relevance in murine cardiac myocytes. *Circulation research,* 84**,** 43-52.

XU, J., SONG, D., XUE, Z., GU, L., HERTZ, L. & PENG, L. 2013. Requirement of glycogenolysis for uptake of increased extracellular K+ in astrocytes: potential implications for K+ homeostasis and glycogen usage in brain. *Neurochem Res,* 38**,** 472-85.

YAN, X., LIU, J., ZHANG, Z., LI, W., SUN, S., ZHAO, J., DONG, X., QIAN, J. & SUN, H. 2016. Low-level laser irradiation modulates brain-derived neurotrophic factor mRNA transcription through calcium-dependent activation of the ERK/CREB pathway. *Lasers Med Sci*.

YOUNG, K. W., NASH, M. S., CHALLISS, R. A. & NAHORSKI, S. R. 2003. Role of Ca2+ feedback on single cell inositol 1,4,5-trisphosphate oscillations mediated by G-protein-coupled receptors. *J Biol Chem,* 278**,** 20753-60.

ZAFRA, F., ARAGON, C., OLIVARES, L., DANBOLT, N. C., GIMENEZ, C. & STORM-MATHISEN, J. 1995. Glycine transporters are differentially expressed among CNS cells. *J Neurosci,* 15**,** 3952-69.

ZAMANIAN, J. L., XU, L. J., FOO, L. C., NOURI, N., ZHOU, L., GIFFARD, R. G. & BARRES, B. A. 2012. Genomic Analysis of Reactive Astrogliosis. *Journal of Neuroscience,* 32**,** 6391-6410.

ZHANG, Q., PANGRSIC, T., KREFT, M., KRZAN, M., LI, N., SUL, J. Y., HALASSA, M., VAN BOCKSTAELE, E., ZOREC, R. & HAYDON, P. G. 2004. Fusion-related release of glutamate from astrocytes. *J Biol Chem,* 279**,** 12724-33.

ZHANG, Y., RODRIGUEZ, A. L. & CONN, P. J. 2005. Allosteric potentiators of metabotropic glutamate receptor subtype 5 have differential effects on different signaling pathways in cortical astrocytes. *J Pharmacol Exp Ther,* 315**,** 1212-9.

ZHONG, M., YANG, M. & SANBORN, B. M. 2003. Extracellular signal-regulated kinase 1/2 activation by myometrial oxytocin receptor involves G alpha(q)G beta gamma and epidermal growth factor receptor tyrosine kinase activation. *Endocrinology,* 144**,** 2947-2956.

ZHOU, M. & KIMELBERG, H. K. 2000. Freshly isolated astrocytes from rat hippocampus show two distinct current patterns and different [K+] ouptake capabilities. *Journal of neurophysiology,* 84**,** 2746-2757.

ZLOKOVIC, B. V. 2008. The blood-brain barrier in health and chronic neurodegenerative disorders. *Neuron,* 57**,** 178-201.

ZOREC, R., HORVAT, A., VARDJAN, N. & VERKHRATSKY, A. 2015. Memory formation shaped by astroglia. *Frontiers in integrative neuroscience,* 9.

ZSARNOVSZKY, A. & BELCHER, S. M. 2004. Spatial, temporal, and cellular distribution of the activated extracellular signal regulated kinases 1 and 2 in the developing and mature rat cerebellum. *Brain Res Dev Brain Res,* 150**,** 199-209.